

Long-Range Interactions in Complex Networks

Franck Kalala Mutombo

Department of Mathematics and Statistics

University of Strathclyde

Glasgow, UK

April 2012

This thesis is submitted to the University of Strathclyde for the
degree of Doctor of Philosophy in the Faculty of Science.

The copyright of this thesis belongs to the author under the terms of the United Kingdom Copyright Acts as qualified by University of Strathclyde Regulation 3.50. Due acknowledgement must always be made of the use of any material in, or derived from, this thesis.

Acknowledgements

I am heartily thankful to my advisor, Professor Ernesto Estrada, whose encouragement, guidance and support from the initial to the final level enabled me to develop an understanding of the subject. Without his guidance, support and encouragement, this thesis would never have come true, not to mention his advice and his knowledge of Complex Networks.

I offer my regards and blessings to all of those who supported me in any respect during the completion of the project.

Last but not the least, my family and the one above all of us, the omnipresent God, for answering my prayers for giving me the strength to plod on despite of all the difficulties encountered.

Abstract

An interaction in a complex network is any kind of information or process that can propagate between network units or components along network links. Complex networks, which represent the structural skeleton of our societal, technological and infrastructural systems, play a major role in the propagation of processes. These processes include for example the case of epidemic spreading, the diffusion process, synchronisation, the consensus process and many others. It is usually assumed that interactions in networks propagate only from a node to its nearest neighbours. This thesis is about interactions that can be transmitted from a node to others that are not directly connected to it. These types of interactions are here called long-range interactions (LRI). The thesis is about those long-range interactions in complex networks. We will focus on the case of infection or epidemic spreading in complex networks. An “infection”, understood here in a very broad sense, can be propagated through the network of social contacts among individuals. These social contacts include both “close” contacts and “casual” encounters among individuals in transport, leisure, shopping, etc. Knowing the first through the study of the social networks is not a difficult task, but having a clear picture of the network of casual contacts is a very hard problem in a society of increasing mobility. Here we assume, on the basis of several pieces of empirical evidence, that the casual contacts between two individuals are a function of their social

distance in the network of close contacts. Then, we assume that we know the network of close contacts and infer the casual encounters by means of nonrandom long-range (LR) interactions determined by the social proximity of the two individuals. This approach is then implemented in a susceptible-infected-susceptible (SIS) model accounting for the spread of infections in complex networks. A parameter called “conductance” controls the feasibility of those casual encounters. In a zero conductance network only contagion through close contacts is allowed. As the conductance increases the probability of having casual encounters also increases. We show here that as the conductance parameter increases, the rate of propagation increases dramatically and the infection is less likely to die out. This increment is particularly marked in networks with scale-free degree distributions, where infections easily become epidemics. We show that the epidemic threshold of the model is given by the inverse of the largest eigenvalue of the generalised graph matrix that represents all the social contacts in the network. We point out that, from a Statistical Mechanical point of view, the epidemic threshold is also seen as the negative of the inverse of the free energy of the network when the system is frozen at extremely low temperatures. The proposed model is able to reproduce the age-assortativity or homophily observed in many social networks. Our model provides a general framework for studying epidemic spreading in networks with arbitrary topology with and without casual contacts accounted for by means of LR interactions.

List of Figures

1	Illustration of graph representations	12
2	A digraph with 4 vertices and 5 edges	13
3	Two isomorphic graphs	14
4	Graph (a) and its subgraph (b), spanning graph (c) and induced graph (c).	18
5	Complete graph K_5 on 5 nodes (a), a star graph S_7 having 6 leaves (b), and a 4-regular graph on 8 nodes (c) and a comb graph (d). . .	23
6	Path P_4 (a) and cycle C_6 (b).	25
7	A $K_{4,4}$ bipartite graph	26
8	Weighted graph	28
9	A tree having 9 nodes.	30
1.1	Very simple networks, with node values and lines values.	33
1.2	Chess masters network containing all 685 World Chess Championship matches from 1886-1985. Each node is the last name of a chess master. Each edge is directed from white to black and contains selected game info. The network consisted of 25 players (nodes) and 685 edges (number of games). This network was produced using NetworkX [9] in Python.	34

1.3	Examples of networks (a) the Internet network, (b) The network of Protein Interaction, (c) Ego network of the largest hub in a Barabási-Albert network. An Ego network consist of a focal node (‘ego’) and the nodes to whom ego is directly connected to (these are called ‘alters’) plus the ties, if any, among the alters, and (d) the Friendship network.	35
1.4	Plots of the adjacency matrices of the Jazz musician network (a) and the network of the top 500 corporations in the USA (b).	36
1.5	Illustration of the degree distribution (b) for a simple network in (a).	36
1.6	A histogram of the degree distribution of the network of Jazz musicians (a) and the network of corporate directors in the USA (b).	38
1.7	Degree distributions in networks (a) Poisson distribution, (b) Gaussian distribution, (c) Power-law distribution, (d) Exponential distribution.	38
1.8	Probability (a) and cumulative distribution functions (b) for the version of the internet at autonomous system (AS) level displaying a power-law degree distribution.	44
1.9	Cumulative distribution functions for the version of the internet using logarithmic bins displaying a power-law degree distribution.	45
1.10	The CDFs of three small samples drawn from continuous distributions: a power law with $\alpha = 2.5$, a log normal with $\mu = 0.25$, $\sigma = 0.18$ and exponential with $\lambda = 0.125$. Visually these three CDF appear roughly straight on the logarithmic scales used, but only one is a true power-law.	46

1.11	Illustration of the definitions of the clustering coefficient C , using equation (1.52), this network has two triangles and six connected triples (three for each triangle), $C = 3 \times 2/6 = 1$ or if we use equation (1.53), the network has six closed triples and six connected triples, $C = 6/6 = 1$ and using equation (1.54), the network has two triangles and twelve closed path of length two, $C = 6 \times 2/12 = 1$. The individual vertices have local clustering coefficients $c_a = c_c = 1$ and $c_b = c_d = 2/3$ using equation (1.55) and for the mean value $\bar{C} = 5/6$ when using equation (1.56).	60
1.12	The orientation of arbitrary edges in (b) of the corresponding undirected graph in (a)	65
1.13	Illustrations of some realisations/configurations of Erdős-Rényi random networks with 20 nodes and different interlink probabilities (for each probability only one member of the ensemble $G(n, p)$ is shown).	71
1.14	Example of a random network obtained with the preferential attachment method of Barabási and Albert with $n = 20$ and $d = 4$. . .	75
1.15	Cumulative degree distribution (a) and probability distribution (b) for a SF with $n = 10000$, constructed according to the BA model. For each node entering the network, 2 new edges are placed.	76
2.1	Unique, globally stable, steady-state, equilibrium (monotonic convergence) (a), Unique, globally stable, steady-state equilibrium (oscillatory convergence) (b), two periodic cycles (c), Unique and unstable steady-state equilibrium (oscillatory divergence) (d), Continuum of unstable steady-state equilibrium (e), Continuum of unstable steady-state equilibrium (f).	84

2.2	Unique and globally stable steady-state equilibrium (a), Multiple locally stable steady-state equilibria (b).	89
2.3	Stable node (a), Saddle node (b), Focus (c), Source (d)	97
3.1	Evolution of the number of infected individuals in the SI Model. The rate of infection here is $\beta = 0.2$, the initial number of infected individuals is 20% of the total population $N = 1000$. The curve grows exponentially at the very beginning and the infected individuals infect more and more the susceptible ones. The curve saturates as the number of susceptible get reduced.	121
3.2	Illustration of the time evolution of the SIR model. The curves show the fractions of the population in the susceptible, infected and recovered states as a function of time. The values of the parameters used are $\beta = 0.3$, $\delta = 0.1$, $s_0 = 0.99$, $i_0 = 0.01$, and $r_0 = 0$	124
3.3	Illustration of the time evolution for the SIS model. The fraction of infected in the SIS model grows with time as for the SI model but in this model, the fraction of infected never reaches one, tending instead to a steady state at which the rate of infection and recovery are equal.	128
3.4	Evolution of the fraction of infected as a function of the average density of infected vertices θ and for different degrees.	140
3.5	Graphic solution of equation (3.78). If the slope of the function $h(\theta)$ is greater than or equal to 1 there is a non trivial solution (a) but if the slope of the function $h(\theta)$ is less than one we only have one trivial solution (b). The solution occurs at the intersection of the curves $h(\theta)$ and $y = \theta$ (see plot (a)).	141

4.1	Illustrations of the rewiring process, which is the basis of the Watts-Strogatz model for small networks. Starting from a regular lattice network with $n = 20$, $k = 4$ some links are rewiring with probability p	150
4.2	Structural evolution of the Watts-Strogatz model. Illustrations of the variation of the average path length and the clustering coefficient with the change of the rewiring probability for a network having $n = 1000$ nodes and $k = 10$. Each point is the average of 50 realisations. The values for the average path length and clustering coefficient are normalised by dividing them by the respective values obtained for $WS(1000, 10, 0)$	151
4.3	Three basic network types in the model of Watts and Strogatz. The leftmost network is a ring of 20 nodes ($n = 20$), where each vertex is connected to its four neighbours ($k = 4$). This is an ordered network which has a high clustering coefficient C and a long pathlength L . By choosing an edge at random, and reconnecting it to a randomly chosen vertex, networks with increasingly random structure can be generated for increasing rewiring probability p . In the case of $p = 1$, the network becomes completely random, and has a low clustering coefficient and a short pathlength. For small values of p so-called small-world networks arise, which combine the high clustering coefficient of ordered networks with the short pathlength of random networks.	151
4.4	A two-dimensional grid network with $n = 6$, $p = 1$, and $q = 1$ (a), and (b) the contacts of a node u with $p = 1$ and $q = 3$. The three long range contacts are v , z and t	154

4.5	The lower bound of the expected delivery time in a decentralised algorithm. The x -axis is the value of α ; the y -axis is the resulting exponent of n	156
4.6	Clustering coefficient in the Grindrod random network. The change in the average clustering coefficient in range-dependent random networks developed by Grindrod, with the change in the parameter η for three different average degrees: continuous line ($\bar{k} = 2.5$), line with stars ($\bar{k} = 3.5$) and line with circles ($\bar{k} = 2.5$).	157
4.7	Probability p of an edge linking two vertices as a function of the distance d separating these two vertices in the Cohen et al. model .	169
5.1	Graphs show data by (A) duration, (B) location, and (C) frequency of contact; the correlation between duration and frequency of contact is shown in (D). All correlations are highly significant ($p < 0.001$, χ^2 -test). The figures are based on pooled contact data from all eight countries and weighted according to sampling weights as explained in the methods (based on household size and age). Figure reproduced from [91] with the permission of the authors.	179
5.2	Smoothed contacts matrices for each country based on all reported contacts occurring in the home setting. White indicates high contact rates, green intermediate contact rates, and blue low contact rates. Figure reproduced from [91] with the permission of the authors.	180
5.3	Smoothed contacts matrices for each country based on physical contacts only occurring in the work setting. White indicates high contact rates, green intermediate contact rates, and blue low contact rates. Figure reproduced from [91] with the permission of the authors.	181

6.1 $G = (V, E)$, with $|V| = 5$ vertices and $|E| = 5$ edges 204

6.2 Multilayer representation of the $\Gamma(G, x)$. In (a) a social network with 5 nodes and 5 social connections is represented. In layers (b) and (c) the eventual proximity interactions between nodes are represented. Eventual proximity of nodes in (b) and (c) are given by $2x$ and $3x^2$, respectively. Layer (d) represents the superposition of the three previous layers and accounts for both direct and LR transmission of an infection by superposing the social and proximity networks. 206

6.3 Illustration of the evolution of the degree of the nodes in a network created with the BA model as the values of the conductance change. Here for a BA network with $n = 1000$ and $\bar{k} \approx 6$ we represent the values of the generalised degree $k(x)$ for every node for different values of $0 \leq x \leq 0.5$. Notice that there is an inversion of the centrality of the nodes as the values of the conductance increases. . . 213

6.4 Illustration of the evolution of the degree of the nodes in a network created with the BA model as the values of the conductance change. Here for a BA network with $n = 1000$ and $\bar{k} \approx 6$ we represent the values of the generalised degree $k(x)$ for every node for different values of $0.6 \leq x \leq 1$. Notice that there is an inversion of the centrality of the nodes as the values of the conductance increases. . . 214

6.5 Illustration of the evolution of the degree of the nodes in a network created with the ER model as the values of the conductance change. Here for a ER network with $n = 1000$ and $\bar{k} \approx 6$ we represent the values of the generalised degree $k(x)$ for every node for different values of x such that $0 \leq x \leq 0.5$ 215

6.6 Illustration of the evolution of the degree of the nodes in a network created with the ER model as the values of the conductance change. Here for a ER network with $n = 1000$ and $\bar{k} \approx 6$ we represent the values of the generalised degree $k(x)$ for every node for different values of x such that $0.6 \leq x \leq 1$ 216

6.7 Illustration of the Kendall rank correlation coefficient τ between the degree ($x = 0$) and the generalised degree ($x \neq 0$) for BA and ER networks having both $n = 1000$ nodes and average degree $\bar{k} \approx 6$. . . 218

6.8 Generalised subgraphs centrality measures in the BA network having 100 nodes and average degree $\bar{k} \approx 6$ and for different values of the conductance x 220

6.9 Generalised subgraphs centrality measures in the BA network having 100 nodes and average degree $\bar{k} \approx 6$ and for different values of the conductance x 223

6.10 Generalised subgraphs centrality measures in the ER network having 100 nodes and average degree $\bar{k} \approx 6$ and for different values of the conductance x 227

6.11 Illustrations of the mean subgraph centrality and variance for different values of the conductance in the BA and ER networks having both 100 nodes and average degree $\bar{k} \approx 6$ 228

6.12 Generalised subgraphs centrality measures in the ER network having 100 nodes and average degree $\bar{k} \approx 6$ and for different values of the conductance x 229

6.13 Rank correlations between subgraph centrality and generalised subgraph centrality for a BA network having $n = 100$ nodes and average degree $\bar{k} \approx 6$ and for different values of x 232

6.14 Rank correlations between subgraph centrality and generalised subgraph centrality for a BA network having $n = 100$ nodes and average degree $\bar{k} \approx 6$ and for different values of x 233

6.15 Rank correlations between subgraph centrality and generalised subgraph centrality for a ER network having $n = 100$ nodes and average degree $\bar{k} \approx 6$ and for different values of x 233

6.16 Rank correlations between subgraph centrality and generalised subgraph centrality for a ER network having $n = 100$ nodes and average degree $\bar{k} \approx 6$ and for different values of x 234

6.17 Evolution of the rank correlation coefficient ρ as a function of the conductance for BA and ER networks. The inversion point in the centrality measure is pretty much the same for both BA and ER networks, but in BA network this inversion point is reached much earlier than in ER network. 234

6.18 Generalised closeness centrality measures for each node in a BA network having $n = 100$ nodes and average degree $\bar{k} \approx 6$ and for different values of the conductance x 237

6.19 Generalised closeness centrality measures for each node in a BA network having $n = 100$ nodes and average degree $\bar{k} \approx 6$ and for different values of the conductance x 238

6.20 Rank correlations for the network of corporate directors of the top 500 corporations in the USA for different values of x 239

6.21 Rank correlations for the network measures for the jazz musicians for different values of x 239

6.22	In (a) individuals are placed on a WS-model starting from node labelled 1 to node labelled 100. Individual 1 has age 0, individual 2 has 0.757 and individual 100 has age 75. In (b) we are rewiring some edges at random. For example link (16, 15) has been rewired at random to link (15, 100) and link (10, 9) has been rewired at random to link (9, 20) and so on. In (c) the rewiring is not random, but depends on the distance between nodes. For instance the link (15, 16) is rewired to the link (15, 20) but taking into account the distance between the node 15 and 20 represented in red.	240
6.23	Average age of the nearest neighbour nodes in different age groups (see text) by using the WS model with node ages and a random rewiring of links. The ages are organised from top to bottom at probability 0.0 in the following groups: 0 – 5, 5 – 10, 10 – 15, 15 – 20, 20 – 30, 30 – 40, 40 – 50, 50 – 60, 60 – 70, and 70+.	241
6.24	Average age of the nearest neighbour nodes in different age groups (see text) by using the WS model with node ages in which the rewiring probability depends explicitly on the inter node distance. The ages are organised in groups as in Figure 6.23.	242
6.25	Characteristic average path length and average clustering coefficients in age-WS model with deterministic rewiring.	243

6.26	Age assortativity measure $A(x)$ in the deterministic rewiring and $A(p)$ in the random rewiring. As can be seen the assortativity measure in random rewiring is larger than the age assortativity measure in the deterministic rewiring. There is less variability in the age of nodes in deterministic rewiring than in random rewiring. This fact is in agreement with the age homophily observed by Mossong et al. [13]	245
7.1	Results for the simulations (dashed lines) and the NLDS (solid lines) for a path graph having $n = 200$ nodes. In both cases $\beta = 0.035$ and $\delta = 0.02$ (left) and $\delta = 0.075$ (right). As $\beta/\delta > \tau = 0.5$ (left plot) and also $\beta/\delta > \tau = 0.5$ (right plot), we see that the infection is growing and becomes an epidemic. The simulations are the averages of just 10 realisations.	256
7.2	Results for the simulations (dashed lines) and the NLDS (solid lines) for a path graph having $n = 200$ nodes. In both cases $\beta = 10^{-5}$ and $\delta = 0.024$ (left) and $\delta = 0.038$ (right). As $\beta/\delta < \tau = 0.5$ (left plot) and also $\beta/\delta < \tau = 0.5$ (right plot), we see that the infection dies out and as time is increasing the infection is going to zero.	256
7.3	Results for the simulations (dashed lines) and the NLDS (solid lines) for a cycle graph having $n = 200$ nodes. In the first case $\beta = 0.35$ and $\delta = 0.024$ (left) and in the second case $\beta = 10^{-5}$ and $\delta = 0.038$ (right). As $\beta/\delta < \tau = 0.5$ (left plot) the infection is growing and never dies out and as $\beta/\delta < \tau = 0.5$ (right plot), we see that the infection dies out and as time is increasing the number of infected nodes is going to zero.	258

- 7.4 Results for the simulations (dashed lines) and the NLDS (solid lines) for a star graph having $n = 1000$ nodes. In (a) and (b) we start with all nodes infected. As $\beta/\delta < \tau = 1/999$ we see that the infection dies out and as time is increasing the number of infected nodes is going to zero. In (c) and (d) we start with a small number of infected nodes, in this case 5, and as $\beta/\delta > \tau = 1/999$ we see that the epidemic is growing and never dies out and becomes an epidemic. The results are the average of just 15 realisations. 259
- 7.5 Results for the simulations (dashed lines) and the NLDS (solid lines) for a complete graph having $n = 200$ nodes. In the left plot we start with 10 infected nodes and $\beta = 0.0023$ and $\delta = 0.001$. As $\beta/\delta > \tau$ we see that the infection is growing and never dies out and becomes an epidemic. In the right plot we have $\beta = 10^{-6}$ and $\delta = 10^{-1}$ and we see that the infection dies out and as time is increasing the number of infected nodes is going to zero. The results are the average of just 10 realisations. 260
- 7.6 Results for the simulations (dashed lines) and the NLDS (solid lines) for a complete bipartite graph having $n_1 = 100$ and $n_2 = 100$. In the left plot we start with 10 infected and $\beta = 0.0023$ and $\delta = 0.001$. As $\beta/\delta > \tau$ we see that the epidemic is growing and never dies out and becomes an epidemic. In the right plot we have $\beta = 10^{-6}$ and $\delta = 10^{-1}$ and we see that the infection dies out and as time is increasing the number of infected nodes is going to zero. The results are the average of just 10 realisations. 261

7.7 Results for the simulations (dashed lines) and the NLDS (solid lines) for an ER network having $n = 1000$ nodes (a) and (c) (β is fixed and δ varies) and for a BA network (b) and (d) (β is fixed and δ varies) having the same number of nodes. Both networks have the same average degree $\bar{k} \approx 6$. In the two cases the simulations start with a small number of randomly infected nodes, here 20. 262

7.8 Results of the simulations (dashed lines) and NLDS (solid lines) for the Jazz musicians network (left) and for top 500 corporate directors in the USA (right). The results are averages of 100 realisations and $\beta = 0.02, \delta = 0.12$ 262

8.1 Results of the simulations (dashed lines) and the exact GNLDMMCA (solid lines) for a path graph (left) and cycle graph (right) with $n = 100$ nodes, where $\tau(0) = 0.5$ for both of them. Parameters in both plots are $\beta = 0.35, \delta = 0.0023$ and starting with about 10% of the nodes infected; since $\beta/\delta > \tau(0)$, the infection will become an epidemic for any value of the conductance x . The results are the average of 150 realizations. The values of the conductivity parameter are, from bottom to top, $x = 0, 0.1$ and 0.2 273

8.2 Results of the simulations (dashed lines) and the exact GNLDMMCA (solid lines) for a star graph with $n = 1000$ nodes, where $\tau = 1/999 \approx 0.0316$. Parameters in the left plot are $\beta = 0.002$, $\delta = 0.01$ and starting with about 20% of the nodes infected; since $\beta/\delta = 0.2 > \tau$, the infection will become an epidemic for any value of the conductance x . Parameters in the right plot are $\beta = 0.0002$ and $\delta = 0.024$; thus $\beta/\delta = 0.0083 < \tau$, and even when starting with all nodes infected, the epidemic dies out for all values of the parameter x . The results are the average of 100 realizations. The values of the conductivity parameter are, from bottom to top, 0.0, 0.03, 0.06, 0.09, 0.13, 0.20, 0.30, and 0.50. 275

8.3 Dependence of the epidemic threshold with the conductance for a star graph having $n = 1000$ nodes. 275

8.4 Results of the simulations (dashed lines) and the exact GNLDMMCA (solid lines) for (left) ER and (right) BA networks having $n = 1000$ nodes, $\bar{k} \approx 6$, with $\beta = 0.02$ and $\delta = 0.12$, and for different values of the parameter x . The results are the average of 250 realisations. The values of the conductivity parameters are, from bottom to top, 0.0, 0.03, 0.06, 0.09, and 0.13. 276

8.5	Illustration of the progress of an infection in an ER (first row) and a BA (second row) network. The first column represents the initial stage in which only 10% of the nodes are infected (marked in red) in ER and BA. In the second column we illustrate the progress of the infection for time $t = 25$ when only direct transmission is considered for both ER and BA. The last column represents the progress of the infection at the same time as before ($t = 25$) but now considering both direct and LR transmissions of the infection. Both networks have the same size ($n = 100$) and average degree ($\bar{k} = 12$). The value of the conductance for this snapshot is $x = 0.03$	277
8.6	Illustration of the evolution of $t_{1/2}$ as a function of the conductance in ER and BA random networks ($n = 1000$ nodes, $\bar{k} = 6$, $\beta = 0.02$ and $\delta = 0.12$).	279
8.7	Regular Networks having $n = 10$ nodes where each node has degree	3280
8.8	Regular Networks having $n = 10$ nodes where each node has degree	3281
8.9	Results of the simulations (dashed lines) and the exact GNLDS-MMCA (solid lines) for the first nine regular networks of Figure 8.7 which all have $n = 10$ nodes which each have degree 3, $\beta = 0.3$ and $\delta = 0.0001$. The values of conductance parameter are, from bottom to top, 0.0, 0.3. Simulations start with only one randomly infected node and are the average of 100 realisations.	282

8.10	Results of the simulations (dashed lines) and the exact GNLDMMCA (solid lines) for the last ten regular networks of Figure 8.7 which each have $n = 10$ nodes which each have degree 3, $\beta = 0.3$ and $\delta = 0.0001$ and for two different values of the conductance. The values of the conductivity parameter are, from bottom to top, 0.0, 0.3. Simulations start with only one randomly infected node and are the average of 100 realisations.	283
8.11	Results of the simulations (dashed lines) and the exact GNLDMMCA (solid lines) for networks with power-law degree distributions $p(k) \sim k^{-\gamma}$ with (left) $\gamma = 1.89$ and (right) $\gamma = 1.98$. The results are the average of 100 realisations for networks with $n = 1000$ nodes, $\beta = 0.02$, and $\delta = 0.12$ and for different values of the parameter x . The values of the conductivity parameter are, from bottom to top, 0.0, 0.03, 0.06, 0.09, 0.13, 0.15, and 0.20.	285
8.12	Rate of epidemic spreading measured by $t_{1/2}$, i.e., the time needed to infect 50% of the whole population, for different values of the power-law exponent γ and for different values of the conductance x .	286
8.13	Probability of infection $\bar{d}(k)x^{\bar{d}(k)-1}$ for different values of the conductance x for BA and ER networks having the same number of nodes, $n = 1000$, and the same average degree.	287
8.14	Illustration of the evolution of the cumulative degree distribution of the nodes for the network studied in Figure 6.3 and Figure 6.4 for $x = 0$, $x = 0.1$, $x = 0.2$, $x = 0.3$, $x = 0.4$ and $x = 0.5$. Notice that there is a change in the distribution from a power law at $x = 0$ to a Poissonian-like distribution as x increases.	288

8.15	Illustration of the evolution of the cumulative degree distribution of the nodes for the network studied in Figure 6.3 and Figure 6.4 for $x = 0.6$, $x = 0.7$, $x = 0.8$, $x = 0.9$ and $x = 1$. Notice that there is a change in the distribution from a power law at $x = 0$ to a Poissonian-like distribution as x increases.	289
8.16	(left) Change of the rank correlation between $k_i(x = 0)$ and $k_i(x \neq 0)$ as a function of the conductance x for scale-free (SF) networks with different exponents of the power law. (Right) Scaling of the conductance at which an inversion in the rank correlation occurs as a function of the exponent of the power law in SF networks (see text for explanations).	290
8.17	Results of the simulations and GNLDs-MMCA for the networks of collaboration among (left) jazz musicians and (right) for the corporate directors of the top 500 corporations in the United States. The results are the average of 250 realisations with $\beta = 0.02$, $\delta = 0.12$ and for different values of the conductance parameter x . The values of the conductivity parameter are, from bottom to top, 0.0, 0.03, 0.06, 0.09, 0.13, and 0.20.	291

List of Tables

1.1	Degree distribution of the simple network in Figure 1.5 (b).	36
6.1	First 10 most central nodes (left to right) for different values of x for a BA network having $n = 100$ nodes and average degree $\bar{k} \approx 6$. . .	231
6.2	First 10 less central nodes (left to right) for different values of x for a BA network having $n = 100$ nodes and average degree $\bar{k} \approx 6$	235
6.3	Top 10 most central nodes (left to right) for different values of x for an ER network having $n = 100$ nodes and average degree $\bar{k} \approx 6$. . .	236
8.1	Conductance x , largest eigenvalues $\lambda_1(x)$ and epidemic thresholds $1/\lambda_1(x)$ for the ER and BA random networks having $n = 1000$, $\bar{k} = 6$, $\beta = 0.02$ and $\delta = 0.12$. The threshold in the ER model is almost the double of the threshold in the BA model.	277
8.2	Time needed by an infection to infection 50% of the population for different values of the conductance, for an ER and a BA network having both $n = 1000$ nodes and $\bar{k} = 6$, $\beta = 0.02$ and $\delta = 0.12$	279
8.3	Conductance x , largest eigenvalues $\lambda_1(x)$, and epidemic threshold $1/\lambda_1(x)$ for two power-law distributions with $\gamma = 1.89$ and $\gamma = 1.89$, $\bar{k} = 6$, $\beta = 0.02$ and $\delta = 0.12$. The threshold for $\gamma = 1.89$ is always smaller than for $\gamma = 1.98$	284

Contents

0.1	A word on Complex Networks	1
0.2	Spreading in Complex Networks	6
0.3	Thesis Contributions	9
0.4	Thesis structure	10
0.5	Essentials of Graph Theory	11
0.5.1	Graph	11
0.5.2	Adjacency Matrix	16
0.5.3	Subgraphs	17
0.5.4	Degree of Vertices	19
0.5.5	Special Graphs	22
0.5.6	Paths and cycles	24
0.5.7	Walks	24
0.5.8	Shortest Paths	27
0.5.9	Tree	29
I	Theory	31
1	Networks Structure and Models	32
1.1	Some Example of Networks	33
1.2	Properties of Networks	34

1.3	Binomial Distribution	38
1.4	Poisson Distribution	40
1.5	Power-Law Degree Distribution	41
1.6	Small World Effect	55
1.7	Clustering Coefficient	57
1.8	Degree-degree Correlations and Assortativity	60
1.9	Laplacian of a Network	64
1.10	Network Spectrum	67
1.11	Random Models of Networks	70
1.11.1	Erdős-Rényi (ER) Model	70
1.11.2	Scale Free Networks	74
1.11.2.1	The Barabási-Albert (BA) Model	76
2	An Overview of Dynamical Systems	79
2.1	Dynamical Systems	79
2.1.1	One-Dimensional First-Order Discrete Dynamical Systems	80
2.2	Non-linear System	88
2.2.1	Multi-Dimensional First-Order Systems	90
2.2.2	Non-Linear System	102
2.3	Simple Dynamical System on a Network	105
2.3.1	Examples: The Diffusion and Synchronisation Processes on Networks	108
2.3.2	The Synchronisation Process	111
3	Epidemic Spreading in Complex Networks	115
3.1	Compartmental Models and the Homogeneous Assumption	116
3.2	The Susceptible-Infected (SI) Model	118

3.3	The Susceptible-Infected-Recovered Model (SIR)	122
3.4	The Susceptible-Infected-Susceptible Model	126
3.4.1	The Solution	127
3.5	The Susceptible-Infected-Recovered-Susceptible (SIRS) model	129
3.6	Epidemics in Heterogeneous Networks	130
3.6.1	The SI model on Heterogeneous Networks	131
3.6.2	The SIR and the SIS models in Heterogeneous networks	134
3.6.3	The case of the effect of mixing patterns	136
3.7	Large Time Limit of Epidemic Outbreaks	139
4	Long-Range Interactions in Networks	147
4.1	Random Long-Range Interactions	148
4.1.1	Watts-Strogatz Model(WSM)	148
4.1.1.1	Small world model	148
4.2	Kleinberg Model (KM)	152
4.3	Range Dependent Model (RDM)	156
4.4	Nonrandom Long-Range Interactions	158
4.4.1	The Jackson and Wolinsky Model (JWM)	158
4.4.2	Example 1: The Connections Model	161
4.4.3	Example 2: The Co-author Model	162
5	Social Contacts: Close and Casual Contacts. Empirical Evidence	171
5.1	Social Networks	171
5.2	Relevance of Social Network Interactions for the Spread of Infections	173
5.3	Role of Assortativity in Social Networks and its Implications on Long-Range Interactions	184
5.4	Attempts for Accounting for all Close Contacts	188

6 Accounting for Close and Casual Contacts in Complex Networks 195

6.1 The Network 196

6.1.1 Probability of establishing Short/Direct-Contacts 196

6.1.2 Probability of establishing Long-Range Contacts 196

6.1.3 Future Value (FV) of a piece of Information 197

6.1.4 Present Value (PV) of a piece of Information 198

6.2 Generalised Topological Index and the Generalised Graph Matrix . 202

6.2.1 Mathematical Definition 203

6.2.2 Properties of the Matrix $\Gamma(G, x)$ 205

6.3 Generalised Degree 209

6.3.1 Generalised Degree for Some Special Networks 210

6.3.2 Connection with Jackson and Wolinsky Model 212

6.3.3 The Study of the Generalised Degree for BA Network 213

6.3.4 The Study of the Generalised Degree for ER Network 215

6.3.5 Relationship between Degree and Generalised Degree 216

6.4 Extension of the concepts of Subgraph Centrality, Closeness, and
Betweenness Centrality 218

6.4.1 Subgraph Centrality in terms of the Generalised Graph Ma-
trix $\Gamma(G, x)$ 219

6.4.2 Communicability in terms of the Generalised Graph Matrix
 $\Gamma(G, x)$ 223

6.4.3 Closeness Centrality in terms of the Generalised Graph Ma-
trix $\Gamma(G, x)$ 225

6.4.4 Betweenness Centrality in terms of the Generalised Graph
Matrix 226

6.4.5	Influence of the Conductance on Centrality Measures	227
6.5	Age-Assortativity and the Modification of Watt-Strogatz Model . . .	236
6.5.1	Random Rewiring and Age Homophily	237
6.5.2	Deterministic Rewiring and Age Homophily	241
7	Non-Linear Dynamical System (NLDS)	246
7.1	Propagation of Computer Viruses	247
7.2	Model definition of NLDS	250
7.3	The Epidemic Threshold under NLDS	254
7.4	Numerical Experiment on NLDS	255
8	Generalised Non-Linear Dynamical System (GNLDS)	264
8.1	Model definition of GNLDS	264
8.2	Applications of the GNLDS-MMCA Model	271
8.2.1	Networks Generation	271
8.2.2	Simulations	272
8.2.3	Simulations and GNLDS Tests on a Path and Cycle Networks	272
8.2.4	Simulations and GNLDS Tests on a Star Network	273
8.3	Simulations and GNLDS Tests on ER and BA Random Networks .	276
8.3.1	Why epidemics spread faster in a BA than in an ER random networks as the conductance increases?	278
8.3.2	GNLDS on Regular Networks	279
8.3.3	Influence of the Network Heterogeneity on the Spreading of Infections	282
8.4	Influence of the force of infection $d_{ij}x^{d_{ij}-1}$ in BA and ER random networks	285
8.5	Epidemics Spreading in Real World Networks	291

8.6	Statistical Mechanics Interpretation of the Epidemic Threshold in the GNLDS Model	293
8.7	Programs Developed	296
8.7.1	closenessx.py	317
9	Conclusion	319
9.1	Future Work	321

Introduction

0.1 A word on Complex Networks

In an abstract way, a complex network is a collection of entities or components that represent its fundamental units and a set of links or connections that characterise any kind of relationship between these components. Networks are everywhere, ranging from social networks, technological networks and biological networks [52, 92–94]. Examples of social networks include the networks of acquaintances, networks of collaborations and phone-call networks. For instance the famous Erdős numbers in fact describe a social network where mathematicians are assigned numbers indicating their ‘collaboration distance’ to the well-known mathematician Paul Erdős who published nearly 1500 papers in his life, mostly co-authored with others. Technological networks include the internet, telephone networks, transportation networks and railway systems. The internet is one of the largest man-made networks and can be defined as a huge collection of thousands of millions of computers and routers connected by physical links, or at a more coarse-grain level, can be considered as consisting of thousands of administrative domains among which data are transferred. Biological networks include cellular networks, which is an ensemble of genes, proteins and other molecules, and their interactions to regulate cell activities; a biological neural network consisting of

functionally related neurons that perform a specific physiological function. All of these are relatively small complex networks compared to the majority of complex networks seen in real life

The last ten years has seen significant interest and attention devoted to understanding the infrastructure underlying complex networks, particularly their topologies and the large-scale properties that can be derived. The topology of a complex network is usually represented as a large graph. In this perspective, each unit of a complex network can be represented by a site (physics), node (computer science), actor (sociology), or vertex (graph theory) and the connection/interaction between two units may corresponds to a bond (physics), link (computer science), tie (sociology) or edge (graph theory). The study of the topological structure of complex networks is one the most fundamental steps for gaining a basic understanding of certain aspects of real-world phenomena of many kinds. The structure of a network can determine many, it not all, of the properties of the complex system represented by it [52]. The structure of a network always affects its functions. Structure is defined as the 'arrangement of and relations between the parts or elements of something complex' or 'the way in which the parts of a system or objects are arranged or organised' [52]. The study and understanding of topological networks' structure also plays an important role in evaluating and designing networks regulations and protocols that run on top of them. Understanding complex networks' topologies can also protect networks from failures and attacks, so as to achieve a better design and evolution of networks. Social networks' topologies can help to prevent pandemic influenza from spreading when available to health care.

The study of complex networks' topologies has not been a simple problem over the past decade. This may be explained by the fact that large-scale networks are often a collection of thousands or millions of nodes and there is no single place

from which one can obtain a complete picture of the topology. Aside from that, complex networks can change dramatically and evolve constantly. For example, a web page on the World Wide Web (WWW) can be created or removed on a daily basis, and therefore it is difficult to obtain a snapshot of this network. Furthermore, because the network does not lend itself naturally to direct inspection, the task of discovering topologies has been left to experimentalists who develop more or less sophisticated methods to infer its topology from appropriate network measurements. The elaborate nature of the network means that there are a multitude of possible measurements that can be made, each having its own strengths, weaknesses and limitations and each resulting in a distinct specific view of the network topology. In order to fully understand the structure of complex networks we need some reference model with which we can compare them.

As a consequence of these challenges, the recent use of network models to describe complex systems has emphasised the study of graph theoretic properties as a means to characterise the similarities and differences in the structures and the functions of systems across a variety of domains [3, 26, 94]. Many more studies have been conducted on the empirical analysis of graph theoretic properties of real systems and trying to find unifying properties across many complex networks. Even more attention has focused on developing generic and universal models in an attempt to explain such unifying properties, so as to infer more properties that are not easy to obtain by empirical analysis. An implicit assumption in many of these works is that graph theoretic properties adequately capture key system features in order to serve as a basis for comparison.

The well-known model of a network is the one introduced by Erdős and Rényi in 1960 [47]. This model is also known as the Erdős-Rényi model and is sometimes called a 'classical random' network. The model begins with n isolated nodes and

each pair of nodes is connected with a given probability. A typical characteristic of the classical random network is that the probability of selecting at random a node of degree k follows a Poisson distribution when n is large [47]. However, it has now been realised that there are many complex networks, which cannot be described by the random model.

In 1998, Watts and Strogatz proposed the Small-World network model [123]. A Small-World network is between a regular network and a stochastic network. In a ring network, an arbitrary edge between adjacent nodes constantly reconnects with other nodes according to a certain probability. It can constitute a Small-World network. When $p = 0$, it is a regular network. When $p = 1$, it is a random network. When $0 < p < 1$, it is a new network with a higher cluster character than a regular network and a lower average path length than the random network. A complex network with these two properties is called a Small-World network.

One of the most popular properties that has been discovered across many topologies of real complex networks systems is the high variability in the degree distribution. This high changeability deviates significantly from low variability distributions such as the Poisson and exponential distributions in classic random networks. In particular these highly variable distributions follow a power-law relationship [3, 59] in many real complex networks, such as both the router-level and the AS-level topologies of the internet [59], the World Wide Web [4], the network of citations between scientists' papers [107], metabolic reaction networks [71], and the telephone call graph [1]. Since traditional graph theory on regular graphs or random graphs [47] cannot explain the high changeability of degree sequence, the discovery of the power-law degree distribution has stimulated a great deal of work in the construction of the so-called 'Scale-free' networks, aiming to match the power-law distribution and other scale statistical properties, as well as to provide a

universal theory to understand all complex networks. The well known model that exhibits a power-law characteristic was proposed by Barabási and Albert in 1999. They described a growing process called preferential attachment for a complex network in which a new node is added to the network with probability proportional to the degrees of existing nodes. As the high degree nodes can connect to more and more nodes, these nodes significantly contribute to the high variability in the power-law distribution. Since then, numerous refinements and modifications to the original Barabási and Albert construction have been proposed and have resulted in many types of scale-free network models that can reproduce power-law degree distributions with different variations, for example the ability to tune the parameters of the power-law distribution in order to agree with different complex networks.

Despite these variations, scale-free networks have many common characteristics. The most attractive one is that they have power-law degree distribution which makes them a plausible model for many complex networks. In fact scale-free theory has dominated the current literature of complex networks and has been considered as the universal law for any large-scale networks since none of the previous graph theory can explain the power-law degree distribution. Scale-free networks have highly connected hubs, which hold the network together. The structure of such networks are highly vulnerable (i.e. can fragment) to attacks that target these hubs. At the same time they are resilient to attacks that knock out nodes at random, since a randomly chosen node is unlikely to be a hub, and thus its removal has minimal effect on network connectivity.

The node degrees of stochastic networks and Small-World networks obey a Poisson distribution. This distribution is bell-shaped and the peak value just corresponds with the average value of the degree of all the nodes. In both sides

of the peak value, the distribution probability obeys exponential decline, which indicates that most node degrees are concentrated near the average value of the degree. Therefore, this type of network is called a homogeneous network. There is no peak value in the degree distribution of scale-free networks. There is a descending line showing the scale-free characteristics in bilogarithmic coordinates. Therefore, scale-free networks are called inhomogeneous networks or heterogeneous networks.

0.2 Spreading in Complex Networks

Spreading in networks includes the propagation of any kind of information such as infections, rumours, influences, fashion etc. We will particularly study the case of infections spreading. The main paradigm of the study of dynamic processes in complex networks is that information is transmitted through the paths that connect pairs of nodes [3, 18, 94, 116]. Such paths are formed by sequences of nodes representing the entities of a complex system which are connected by links representing the interactions between these entities. This paradigm is particularly useful for studying the spreading of information in complex networks [18], in particular for studying how “infections” propagate and become epidemics in social, ecological, technological and economical systems [6, 10, 12, 20, 37, 38, 58, 78, 85, 90, 113]. Since the complex network research with small-world networks and scale-free networks appeared, many scholars have adopted complex networks to study the spreading of diseases and a large arsenal of theoretical methods has been developed for modelling the propagation of infections. The earliest of these models assumed a homogeneous distribution of the number of contacts per node in a network [6, 85, 113]. However, since the discovery that many real-world networks deviate from this ho-

mogeneity [24] several models have been proposed to study epidemic spreading in scale-free networks [24, 90, 101]. For instance Watts and Strogatz simulated the spread of disease model and found that disease spreading in small world networks is faster and easier than in regular networks [123]. Newman and Watts thoroughly discussed disease spreading problems in social networks and proposed an improved Small-World model namely the NW model [96]. Pastor-Satorras and Vespignani studied the infinite scale-free network SIS model, and they were surprised to find that the propagation threshold does not exist [101]. Yang and others studied the spreading mechanism of bird flu based on the complex network approach [124]. In 2008, Chakrabarti et al. [32] developed a nonlinear dynamical system (NLDS), which models the propagation of an infection in a network of arbitrary topology. This model is based on the susceptible-infected-susceptible paradigm of epidemic contagion [18] and is applicable to a network with any degree distribution. More recently, by using the same assumptions as in [32], S. Gomèz, A. Arenas, J. Borge-Holthoefer, S. Meloni, and Y. Moreno [63, 64] developed a probabilistic framework for epidemic spreading in complex networks, which is a Discrete-time Markov chain approach to contact-based disease spreading in complex networks.

One of the most important challenges of modelling the spread of epidemics is the determination of the network of social contacts that allow the transmission of the infection. While in some situations, like in the spreading of sexually-transmitted diseases or computer viruses, knowing the network of contacts is not so difficult, in those cases involving the transmission of airborne or close contact infections the contact network is quite hard to define [45]. This is, for instance, the case of the Severe Acute Respiratory Syndrome (SARS), which was propagated when a medical doctor from Guangzhou, China, eventually met at a hotel in Kowloon, people from Singapore, Viet Nam, Canada and Hong Kong, who were

not among his “close” social contacts [115]. This also includes the case of diseases such as Chickenpox, Acute coryza (or the cold), Influenza (or Flu), Tuberculosis and Mumps which are caused by pathogenic microbial agents and transmitted through the air. These pathogens ride on either dust particles or small respiratory droplets and can stay suspended in the air and are capable of travelling distances on air currents. These kind of encounters between individuals who can facilitate the transmission of an infection are referred to as “casual” contacts in order to distinguish them from the more frequent “close” contacts among individuals [13, 14, 44, 79]. These “casual” contacts can play a major role in a variety of phenomena, which include, for instance, imitative obesity as “it may be easier to be fat in a society that is fat” [23], or the fact that “the spread of obesity is related to the environment in which individuals live” [36] in addition to their social ties [33]. Other examples can include epidemic hysteria [29] as well as the recent growth of “binge” drinking in the UK as a “fashion-related phenomenon” [99].

Due to the importance of the social contacts, both “close” and “casual”, among individuals in our society for understanding disease and attitude spreading, there have been serious attempts to account for them in an experimental basis. The first attempt traced the route of the circulation of bank notes in the United States [30]. The second one studied the trajectory of 100,000 mobile phone users by detecting their positions during a period of half a year [65]. The results of these studies are both theoretically and practically interesting. However, we never make commercial transactions in our elevators, buses, trains or airplanes, and do not necessarily use our mobile phones all at the same time and place. Then, the problem of determining the social contacts of individuals in a society is a very difficult and challenging problem of tremendous importance. More recently, however, some attempts at quantifying all “close” and “casual” contacts among individu-

als have been conducted in a series of European cities [91]. This study and its implications will be analysed later in this thesis. The division of social contacts between “close” and “casual” is somehow artificial but it allows some important theoretical approaches. For instance, by knowing the network of “close” contacts among individuals it is possible to include some effects produced by the “casual” encounters among individuals. This has been generally done by considering that these “casual” contacts occur at random. We will analyse the implications of this assumption in this thesis.

0.3 Thesis Contributions

This thesis proposes a model that accounts for both the “close” and “casual” contacts among individuals by considering the transmission of an infection through paths and by long-range Interactions (LRI) in a complex network. Both processes are assumed to be independent. The main paradigm used by this model is that if we know the structure of the network of “close” contacts we can infer the “casual” contacts by means of the long-range interactions between two individuals, which here are assumed to depend on the social distance between them. We also assume that the long-range ‘infectability’ of a node depends on the shortest path distance from it to an infected node as well as on the ‘conductance’ of the medium to the transmission of the infection. These concepts will be explained in this thesis when we will introduce a generalisation of the NLDS as a way for modelling epidemic spreading in networks with LR interactions. Further, we analyse this model in random networks having different kinds of degree distributions as well as in some real-world scenarios. Using this model we study how an infected node can propagate an infection in random and real-world networks. We also generalise concepts

of degree, subgraph centrality or self-communicability, communicability, communicability betweenness, closeness etc. and connect some of them to spreading in networks using the long-range interactions.

0.4 Thesis structure

The thesis consists of eight chapters organised into two main parts which follow the introduction giving an overview on complex networks and the essentials of graph theory. The first part (theory) gives background on complex networks, dynamics on networks, spreading in networks and introduces and motivates the idea of long-range interactions. The second part (results and discussions) describes the mechanism of long-range interactions in general and its application to the case of spreading in networks.

Part I: Theory

In Chapter 1 we present network structures and their models that will be relevant for this thesis. In Chapter 2 we review some concepts of dynamical systems (linear and non-linear) that will be useful in this thesis. Chapter 3 is devoted to epidemic spreading in networks. We present and discuss some of the models for epidemic spreading in populations and networks. In Chapter 4 we introduce the concept of long-range interactions (LRI) in complex networks. Several examples are given to illustrate where long-range interactions in networks occur and how they are used. In Chapter 5, the last chapter of Part I, the topic of social contacts, close and casual, and provide empirical evidences for the implications of casual contacts in the transmission of infections in networks.

Part II: Results and Discussions

In Chapter 6, we provide a network model for accounting for close and casual contacts in complex networks. Based on the new model developed in this chapter, we generalise the concepts of degree and centrality measures and others. In Chapter 7 we review a discrete Non-Linear Dynamical System (NDLS) model for the spread of epidemics that can be applied to any kind of network. In Chapter 8 we generalise the NDLS model to a Generalised Non-Linear Dynamical System (GNLDS) and apply it to model the spreading of epidemics in networks when casual contacts are allowed by the means of long-range interactions (LRI).

0.5 Essentials of Graph Theory

In this chapter we are going to cover essential material on graph theory that will be useful through this thesis. More about graph theory may be found in the literature [27].

0.5.1 Graph

Let V be a *finite* set, and denote by

$$E(V) = \{\{u, v\} | u, v \in V, u \neq v\},$$

the subsets of two distinct elements.

Definition 0.5.1 *A pair $G = (V, E)$ with $E \subseteq E(V)$ is called a graph on V . The elements of V are the vertices of G , and those of E the edges of G . The vertex set of the graph G will be denoted by $V(G)$ and its edge set by $E(G)$. Therefore $G = (V_G, E_G)$.*

Most often, graphs are also called *simple graphs*; vertices are called *nodes* or *points*; and edges are called *lines* or *links*. A pair $\{u, v\}$ is usually written as uv (sometimes (u, v)). Notice that then $uv = vu$. In order to simplify notations, we also write $v \in G$ and $e \in E$ instead of $v \in V(G)$ and $e \in E(G)$.

Definition 0.5.2 For a graph G , we denote

$$n = |V(G)| \quad m = |E(G)|.$$

The number of vertices n is called the *order* of G , and m is the size of G . For an edge $e = uv \in G$, the vertices u and v are *adjacent* or *neighbours*, if $uv \in G$. Two edges $e_1 = uv$ and $e_2 = uw$ having a common end, are said to be *adjacent* with each other.

A graph G can be represented as a plane figure by drawing a line (or a curve) between the points u and v (representing vertices) if $e = uv$ is an edge of G . For example, the Figure 1 (right) is the geometric representation of the graph G with $V(G) = \{a, b, c, d, e, f\}$ and $E(G) = \{ab, ac, ce, be, ef, cd, ed\}$. Graphs can be

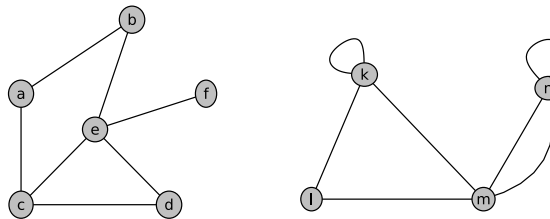


Figure 1: Illustration of graph representations

generalised by allowing *loops* vv and *parallel* (or *multiple*) *edges* between vertices to obtain a *multigraph* $G = (V, E, \phi)$, where $E = \{e_1, e_2, \dots, e_m\}$ is a set (of symbols) and $\phi : E \rightarrow E(V) \cup \{vv | v \in V\}$ is a function that attaches an unordered pair of vertices to each $e \in E : \phi(e) = uv$.

Note that we can have $\phi(e_1) = \phi(e_2)$. This is drawn in the figure of G by placing two (parallel) edges that connect common ends. In Figure 1 (left) is (a drawing of) a multiple G with vertices $V = \{k, l, m, n\}$ and edges $\phi(e_1) = kl$, $\phi(e_2) = km$, $\phi(e_3) = lm$, $\phi(e_4) = kk$, $\phi(e_5) = nm$, $\phi(e_6) = mn$, $\phi(e_7) = nn$. We will only concentrate on simple graphs.

Definition 0.5.3 *A directed graph or a digraph $D = (V, E)$ is a graph where the edges have a direction, that is, the edges are ordered: $E \subseteq V \times V$. In this case $uv \neq vu$.*

The directed graphs have representations, where the edges are drawn as arrows. A digraph can contain edges uv and vu of opposite directions.

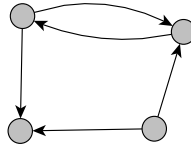


Figure 2: A digraph with 4 vertices and 5 edges

Definition 0.5.4 *A weighted graph is a graph in which each edge e is associated with a real number $w(e)$, called its weight. A weighted graph is often written as $G = (V(G), E(G), W(G))$ where $W(G)$ is the set of edge weights.*

In applications of graph theory weights may have several interpretations. It can mean for example intensity of friendship in a friendship graph, or the costs in a communication graph, etc..

Definition 0.5.5 *Two graphs G and H are identical (written $G = H$) if $V(G) = V(H)$, $E(G) = E(H)$, and $\phi_G = \phi_H$.*

Identical graphs can be represented by identical diagrams. However, it is also possible for graphs that are not identical to have the same diagrams.

Isomorphism of Graphs

Definition 0.5.6 Two graphs G and H are isomorphic, denoted by $G \cong H$, if there exists a bijection $\alpha : V(G) \rightarrow V(H)$ and $\gamma : E(G) \rightarrow E(H)$ such that

$$\phi_G(e) = uv \iff \phi_H(\gamma(e)) = \alpha(u)\alpha(v)$$

for all $u, v \in G$.

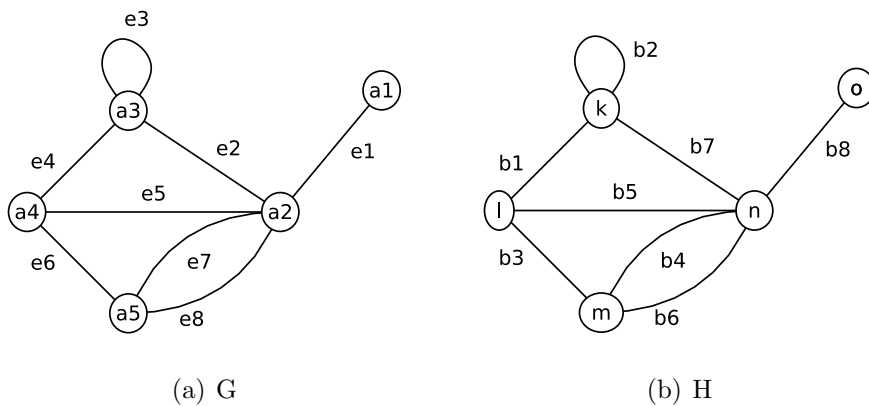


Figure 3: Two isomorphic graphs

The pair (α, γ) is called an isomorphism between G and H .

Example 0.5.7 The graph in the Figure 3 where

$$G = (V(G), E(G), \phi_G),$$

where

$$V(G) = \{a_1, a_2, a_3, a_4, a_5\},$$

$$E(G) = \{e_1, e_2, e_3, e_4, e_5, e_6, e_7, e_8\},$$

and ϕ_G is defined by

$$\phi_G(e_1) = a_1a_2, \phi_G(e_2) = a_2a_3, \phi_G(e_3) = a_3a_3, \phi_G(e_4) = a_3a_4,$$

$$\phi_G(e_5) = a_2a_4, \phi_G(e_6) = a_4a_5, \phi_G(e_7) = a_2a_5, \phi_G(e_8) = a_2a_5,$$

is isomorphic to the graph

$$G = (V(H), E(H), \phi_H),$$

where

$$V(H) = \{k, l, m, n, o\},$$

$$E(H) = \{b_1, b_2, b_3, b_4, b_5, b_6, b_7, b_8\},$$

and ϕ_H is defined by

$$\phi_G(b_1) = kl, \phi_G(b_2) = kk, \phi_G(b_3) = lm, \phi_G(b_4) = mn,$$

$$\phi_G(b_5) = ln, \phi_G(b_6) = mn, \phi_G(b_7) = kn, \phi_G(b_8) = no.$$

Indeed the pair of mappings (α, γ) defined by

$$\alpha(a_1) = o, \alpha(a_2) = n, \alpha(a_3) = k, \alpha(a_4) = l, \alpha(a_5) = m,$$

and

$$\gamma(e_1) = b_8, \gamma(e_2) = b_7, \gamma(e_3) = b_2, \gamma(e_4) = b_1,$$

$$\gamma(e_5) = b_5, \gamma(e_6) = b_3, \gamma(e_7) = b_4, \gamma(e_8) = b_6,$$

is an isomorphism between the graphs G and H . The graphs G and H have the same structure and differ only in the names of their vertices and their edges. As we are only interested in the structural properties of a graph, labels are often omitted when drawing graphs. An unlabelled graph can be thought of as a representative of an equivalence class of isomorphic graphs. We assign labels to vertices and edges in a graph mainly for the purpose of referring to them. For example in a simple graph, it is often convenient to refer to the edge with ends u and v as the ‘edge uv ’. This convention results in non ambiguity since, in a simple graph, at most one edge joins any pair of vertices.

0.5.2 Adjacency Matrix

An adjacency matrix \mathbf{A} is a means of representing which vertices of a graph are adjacent to which other vertices. Specifically, the adjacency matrix of a finite graph G on n vertices is the $n \times n$ matrix where the non diagonal entry a_{ij} is the number of edges from vertex i to vertex j , and the diagonal entry a_{ii} , depending on the convention, is either 1 or twice the number of edges (loops) from vertex i to itself. Undirected graphs often use the former convention of counting loops twice, whereas directed graphs typically use the latter convention. The adjacency matrix is defined to be

$$a_{i,j} = \begin{cases} 1 & \text{if } (i,j) \in E \\ 0 & \text{otherwise.} \end{cases} \quad (1)$$

There exists a unique adjacency matrix for each graph (up to permuting rows and columns) which is not the adjacency matrix of any other graph. In the special case of a finite simple graph, the adjacency matrix is a $(0, 1)$ -matrix with zeros on

its diagonal. If the graph is undirected, the adjacency matrix is symmetric. For a directed graph the adjacency matrix is defined to be:

$$a_{i,j} = \begin{cases} 1 & \text{if there is an edge from } j \text{ to } i \\ 0 & \text{otherwise.} \end{cases} \quad (2)$$

This matrix is not symmetric. Another matrix representation for a graph is the incidence matrix. If we denote the vertices of G by v_1, v_2, \dots, v_n and the edges by e_1, e_2, \dots, e_m , then the incidence matrix of G is the matrix $\mathbf{B}(G) = (b_{ij})$, where b_{ij} is the number of times (0, 1 or 2) that v_i and e_j are incident. The adjacency matrix of a weighted graph $G = (V, E, W)$ reads

$$b_{i,j} = \begin{cases} w_{i,j} & \text{if } (i,j) \in E \\ 0 & \text{otherwise} \end{cases} \quad \text{for } i, j = 1, \dots, n. \quad (3)$$

For unweighted networks, $w_{i,j}$ are replaced by 1. The adjacency matrix of a graph is generally considerably smaller than its incidence matrix, and it is in this form that graphs are commonly stored in computers.

0.5.3 Subgraphs

Definition 0.5.8 *A graph H is a subgraph of G (written $H \subseteq G$) if $V(H) \subseteq V(G)$, $E(H) \subseteq E(G)$, and ϕ_H is a restriction of ϕ_G to $E(H)$. H is a proper subgraph of G when $H \subseteq G$ but $H \neq G$ and we write $H \subset G$. If H is subgraph of G , then G is a supergraph of A .*

A *spanning subgraph* (or a *spanning supergraph*) of G is a subgraph (or supergraph) H with $V(H) = V(G)$. The *underlying graph* of G is the graph obtained by deleting all loops and, for every adjacent vertex, all but one link joining them. The

induced subgraph of G induced by $V' \subset V$, $V' \neq \emptyset$ (written $G[V']$) is the subgraph of G whose vertex set is V' and whose edge set is the set of those edges of G that have ends in V' , i.e.

$$E(G[V']) = E(G) \cap E(V').$$

The induced subgraph $G[V \setminus V']$ is denoted by $G - V'$. It is the subgraph obtained from G by deleting the vertices in V' together with their incident edges. If $V' = \{v\}$, we write $G - v$ for $G - \{v\}$. To a non-empty subset $A \subseteq V(G)$, there corresponds a unique induced subgraph

$$G[A] = (A, E_G \cap E(A)).$$

To each subset $F \subseteq E(G)$ of edges there corresponds a unique spanning subgraph of G ,

$$G[F] = (V(G), F).$$

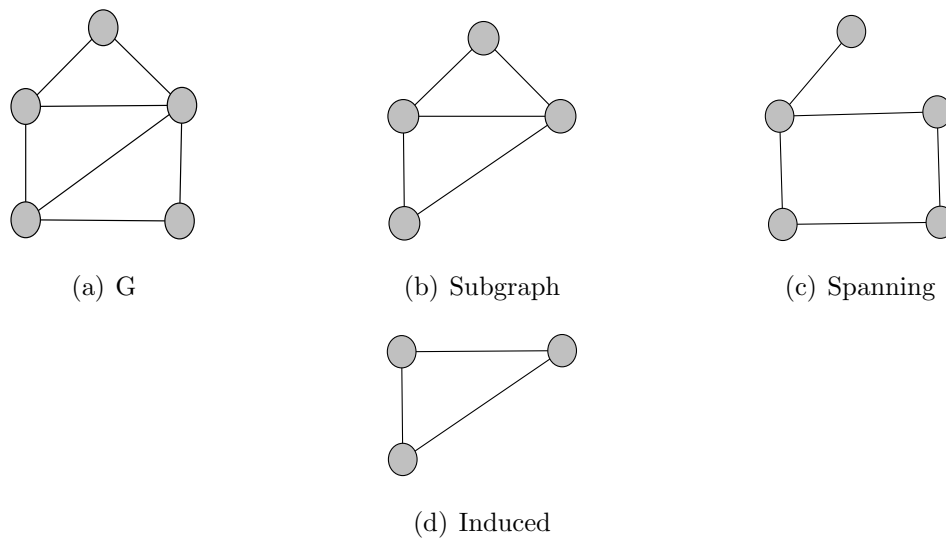


Figure 4: Graph (a) and its subgraph (b), spanning graph (c) and induced graph (d).

Let $E' \subseteq E$ be a non-empty subset. The subgraph of G whose vertex set is the ends of the edges in E' and whose edge set is in E' is called the subgraph induced by E' written $G[E']$. The subgraph $G[E']$ is also called an *edge induced subgraph* of G .

The spanning subgraph of G with edge set $E \setminus E'$ is simply written as $G - E'$. It is the subgraph obtained from G by deleting the edges in E' . Similarly, the graph obtained from G by adding a set of edges E' is denoted by $G + E'$. If $E' = \{e\}$ we write $G - e$ and $G + e$ instead of $G - \{e\}$ and $G + \{e\}$.

Let G_1 and G_2 be subgraphs of G . We say that G_1 and G_2 are *disjoint* if they have no vertices in common, and *edge-disjoint* if they have no edges in common. The *union* $G_1 \cup G_2$ of G_1 and G_2 is the subgraph with vertex set $V(G_1) \cup V(G_2)$ and edge set $E(G_1) \cup E(G_2)$.

0.5.4 Degree of Vertices

Definition 0.5.9 *Let $v \in G$ be a vertex of a graph G . The neighbourhood of v is the set*

$$N_G(v) = \{u \in G \mid vu \in E\}. \quad (4)$$

The degree of the node v is defined to be

$$k_v = |N_G(v)|. \quad (5)$$

The degree k_v is also the number of entries in the v th row or column of the adjacency matrix \mathbf{A} of the graph G . It represents the number of nearest neighbours of v . The node degree of a vertex v is also considered as the number of edges of G incident with v where each loop is counted as two edges. If $k_v = 0$, then v is said to be *isolated* in G , and if $k_v = 1$, then v is a *leaf* of the graph. The *minimum*

degree and the *maximum degree* of G are defined as

$$k_{\min}(G) = \min\{k_v | v \in G\} \quad \text{and} \quad k_{\max}(G) = \max\{k_v | v \in G\}. \quad (6)$$

The column vector of node degrees for a graph G is given by

$$\mathbf{k} = (\mathbf{1}^T \mathbf{A})^T = \mathbf{A} \mathbf{1} \quad (7)$$

where $\mathbf{1}$ is a $|V| \times 1$ column vector and $\mathbf{1}^T$ its transpose and \mathbf{A} its adjacency matrix. For an directed graph we define two types of degree; the *in-degree* which is the number of links pointing towards a given vertex defined by

$$\mathbf{k}^{in} = (\mathbf{1}^T \mathbf{A})^T, \quad (8)$$

or, for each component,

$$k_i^{in} = \sum_j a_{ji}, \quad (9)$$

and the *out-degree* which is the number of links departing from the corresponding node and defined by

$$\mathbf{k}^{out} = \mathbf{A} \mathbf{1} \quad (10)$$

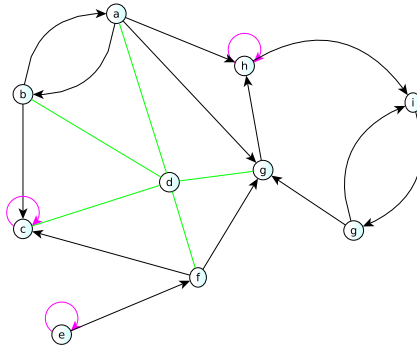
or, for each component,

$$k_i^{out} = \sum_j a_{ij}. \quad (11)$$

The total degree of a node in this case is then given by

$$\mathbf{k} = \mathbf{k}^{in} + \mathbf{k}^{out}. \quad (12)$$

For example the in-degree, out-degree and the degree of the node g in the below



graph are

$$k_g^{in} = 4, \quad k_g^{out} = 1, \quad \text{and } k_g = k_g^{in} + k_g^{out} = 5,$$

respectively. The *average node degree* in a graph is defined by

$$\bar{k} = \frac{1}{n} \mathbf{1}^T \mathbf{k} = \frac{1}{n} \sum_{i=1}^n k_i. \quad (13)$$

The list of node degrees of a graph is called the *degree sequence*. The degree matrix \mathbf{K} is the matrix which has the node degrees as its main diagonal and is given by

$$\mathbf{K} = \text{diag}(\mathbf{k}). \quad (14)$$

The adjacency matrix \mathbf{A} , the incidence matrix \mathbf{B} and the degree matrix \mathbf{K} are related by the relation

$$\mathbf{A} = \mathbf{B}\mathbf{B}^T - \mathbf{K}. \quad (15)$$

Let us mention a useful lemma that was proved by Euler in 1736 and is known in graph theory as the *handshaking lemma*.

Lemma 0.5.10 *In a graph G , the sum of all node degrees is equal to twice the*

number of links. That is,

$$\sum_{i=1}^n k_i = 2|E(G)| = 2m.$$

Moreover, the number of vertices of odd degree is even.

proof 0.5.11 Every edge $e \in E(G)$ has two ends. The second claim follows immediately from the first one.

Lemma 0.5.10 holds equally well for multigraphs, where k_v is defined to be the number of edges that have v as an end and where each loop vv is counted twice. Note that the degrees of a graph G do not determine G . Indeed, there are graphs $G = (V, E(G))$ and $H = (V, E(H))$ on the same set of vertices that are not isomorphic, but for which $\mathbf{k}_G(v) = \mathbf{k}_H(v)$ for all $v \in V$. The sum of all node degrees is given by

$$\mathbf{1}^T \mathbf{A} \mathbf{1} = \mathbf{K}^T = \sum_{i=1}^n k_i = 2|E(G)|. \quad (16)$$

Therefore, the average degree is given by

$$\bar{k} = \frac{2|E|}{n} = \frac{2m}{n}. \quad (17)$$

0.5.5 Special Graphs

Definitions.

- A graph $G = (V, E)$ is *trivial*, if it has only one vertex, i.e., $|V(G)|=1$; otherwise G is *nontrivial*.
- The graph $G = K_{V(G)}$ is the *complete graph* on $V(G)$, if every two vertices are adjacent: $E = E(G)$. All complete graphs of order n are isomorphic to each other, and they will be denoted by K_n .

- The complement of a graph G is the graph \overline{G} on V_G , where $E_{\overline{G}} = \{e \in E(V) | e \notin E_G\}$. The complement of a complete graph is a discrete graph. In a discrete graph $E(G) = \emptyset$. All discrete graphs of order n are isomorphic to each other.
- A regular graph is a graph G in which every vertex has the same degree. If this degree is equal to k , then G is a k -regular of degree k .
- A discrete graph is 0-regular, and a complete graph K_n is $(n - 1)$ -regular. In particular $|V(K_n)| = n(n - 1)/2$, and therefore $|V(G)| \leq n(n - 1)/2$ for all graphs that have order n .
- A star graph S_n is a graph having $n - 1$ leaves (nodes of degree 1) and one central node having degree $n - 1$. A star graph can also be seen as a complete bipartite graph $K_{1,n}$.

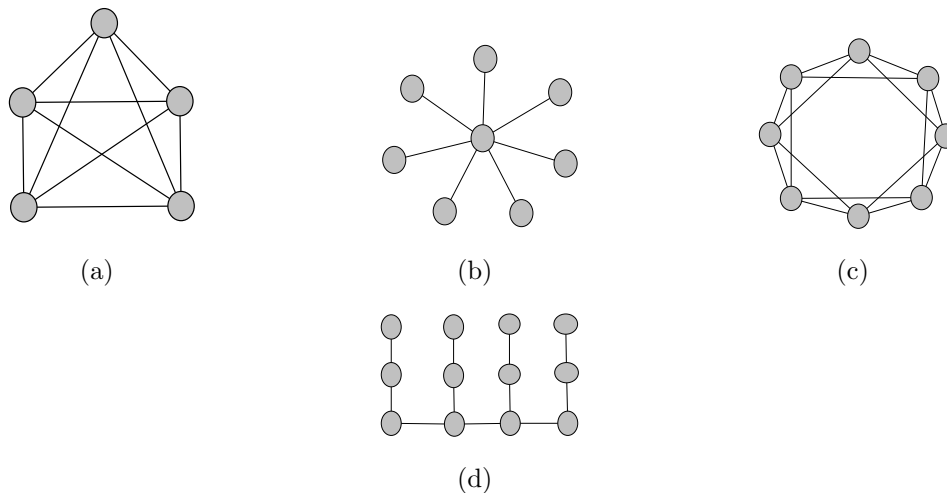


Figure 5: Complete graph K_5 on 5 nodes (a), a star graph S_7 having 6 leaves (b), and a 4-regular graph on 8 nodes (c) and a comb graph (d).

0.5.6 Paths and cycles

0.5.7 Walks

Definition 0.5.12 Let $e_i = u_i u_{i+1} \in G$ be edges of G for $i \in [1, k]$. The sequence $W = e_1 e_2 \cdots e_k$ is a walk of length k from u_1 to u_{k+1} .

Here e_i and e_{i+1} are compatible in the sense that e_i is adjacent to e_{i+1} for all $i \in [1, k - 1]$. We write, more informally,

$$W : u_1 \rightarrow u_2 \cdots \rightarrow u_k \rightarrow u_{k+1} \quad (18)$$

or

$$W : u_1 \xrightarrow{k} u_{k+1}, \quad (19)$$

meaning that W is a walk of length k starting at node u_1 and ending at node u_{k+1} .

We write

$$W : u \xrightarrow{*} v$$

to say that there is a walk of some length from u to v . We understand that $W : u \xrightarrow{*} v$ is always a specific walk, $W = e_1 e_2 \cdots e_k$, although we sometimes do not mention the edges e_i on it. The length of a walk W is denoted by $|W|$.

Definitions Let $W = e_1 e_2 \cdots e_k$ ($e_i = u_i u_{i+1}$) be a walk.

- W is *closed*, if $u_1 = u_{k+1}$.
- W is a *path*, if $u_i \neq u_j$ for all $i \neq j$.
- W is a *cycle*, if it is closed, and $u_i \neq u_j$ for $i \neq j$ with the exception that $u_1 = u_{k+1}$.
- W is a *trivial path*, if its length is 0.

- A trivial path has no edges.
- The inverse W^{-1} of a walk $W : u = u_1 \rightarrow \cdots \rightarrow u_{k+1} = v$, is a walk which is such that $W^{-1} : v = u_{k+1} \rightarrow \cdots \rightarrow u_1 = u$.

A vertex u is an *end* of a path P , if P starts or ends at u . The *join* of two walks $W_1 : u \xrightarrow{*} v$ and $W_2 : v \xrightarrow{*} w$ is the walk $W_1W_2 : v \xrightarrow{*} w$. The end v must be common to the walks. Paths P and Q are *disjoint*, if they have no vertices in common, and they are *independent*, if they share only their ends.

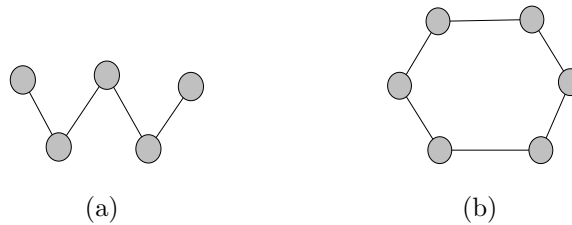


Figure 6: Path P_4 (a) and cycle C_6 (b).

A (sub)-graph, which is a path (cycle) of length $k - 1$ (k , respectively) having k vertices is denoted by P_k (C_k , respectively). If k is even (odd), we say that the path or cycle is even (odd). All paths of length k are isomorphic. The same holds for cycles of fixed length.

Definition 0.5.13 *If there exists a walk (and hence) a path from u to v in G , let*

$$d_{uv} = d_G(u, v) = \min\{k \mid u \xrightarrow{k} v\}$$

be the distance between u and v . If there are no walks $u \xrightarrow{} v$, let $d_G(u, v) = \infty$ by convention.*

Definition 0.5.14 *A graph is connected, if $d_G(u, v) < \infty$ for all $u, v \in G$; otherwise it is disconnected.*

Connection is an equivalence relation on the vertex set V . Indeed there is a partition of V into non-empty subsets $V_1, V_2, \dots, V_\omega$ such that two vertices u and v are connected if and only if both u and v belong to the same V_i . The maximal subgraphs $G[V_1], G[V_2], \dots, G[V_\omega]$ are called *connected components* of G . The number of connected component of G is denoted $c(G)$. If $c(G) = 1$, then G is, of course, connected.

Definition 0.5.15 *A bipartite graph is one whose vertex set can be partitioned into two subsets X and Y , such that each edge has one end in X and one in Y ; such a partition (X, Y) is called a bipartite graph with bipartition (X, Y) in which each vertex of X is joined to each vertex of Y ; if $|X| = m$ and $|Y| = n$, such a graph is denoted by $K_{m,n}$.*

The adjacency matrix of a bipartite graph having two sets of disjoint nodes V_1 and V_2 , such as $|V_1| = n_1$ and $|V_2| = n_2$ can be written as

$$\mathbf{A} = \begin{pmatrix} \mathbf{0} & \mathbf{R}^T \\ \mathbf{R} & \mathbf{0} \end{pmatrix},$$

where \mathbf{R} is a $n_1 \times n_2$ matrix and $\mathbf{0}$ is an all-zeros matrix. A subset $X \subseteq V_G$ is *stable*, if $G[X]$ is a discrete graph.

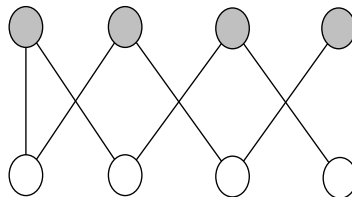


Figure 7: A $K_{4,4}$ bipartite graph

0.5.8 Shortest Paths

Definition 0.5.16 Let G^δ be an edge weighted graph, that is G^δ is a graph together with a weight function $\delta : E(G) \rightarrow \mathbb{R}$ on its edges. For $H \subseteq G$, let

$$\delta(H) = \sum_{e \in H} \delta(e) \quad (20)$$

be the total weight of H . In particular, if $P = e_1 e_2 \cdots e_k$ is a path, then its weight is $\delta(P) = \sum_{i=1}^k \delta(e_i)$. The minimum weighted distance between two vertices is

$$d_G^\alpha(u, v) = \min\{\alpha(P) \mid P : u \xrightarrow{*} v\}.$$

In extremal problems we seek an optimal subgraph $H \subseteq G$ satisfying specific conditions. In practice we encounter situations where G might represent

- a distribution or transportation network where the weights on edges are *distances*, *travel expenses*, or *rates of flow* in the network;
- a system of channels in (tele)-communication or computer architecture, where weights represent *unreliability* or *frequency of action* of the connections;
- a model of chemical bonds, where the weights measure molecular *attraction*.

In these examples we look for a subgraph with the smallest weight and which connects two given vertices, or all vertices (if we want to travel around). On the other hand, if the graph represents a network of pipelines, the weights are volumes or capacities, and then one wants to find a subgraph with the maximum weight.

The shortest Path Problem

Given a connected graph G with a weight function $\alpha : E(G) \rightarrow \mathbb{N}$, find $d_G^\alpha(u, v)$ for all $u, v \in G$.

Assume that G is a connected graph. Dijkstra's algorithm solves the problem for every pair u, v , where u is a fixed starting point and $v \in G$. Let us use the convention that $\alpha(u, v) = \infty$, if $uv \notin G$.

Dijkstra's algorithm

1. Set $u_0 = u$, $t(u_0) = 0$ and $t(v) = \infty$ for all $v \neq u_0$.
2. For $i \in [0, \nu_G - 1]$: for each $v \notin \{u_1, \dots, u_i\}$,
replace $t(v)$ by $\min\{t(v), t(u_i) + \alpha(u_i v)\}$.
Let $u_{i+1} \notin \{u_1, \dots, u_i\}$ be any vertex with the least value of $t(u_{i+1})$.
3. Conclusion: $d_G^\alpha(u, v) = t(v)$.

Example 0.5.17 Consider the weighted graph G in Figure 8. Apply Dijkstra's algorithm to the vertex v_0 .

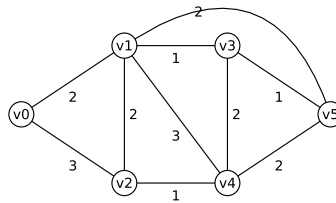


Figure 8: Weighted graph

- $u_0 = v_0$, $t(u_0) = 0$, and all others are ∞
- $t(v_1) = \min\{\infty, 2\} = 2$, $t(v_2) = \min\{\infty, 3\} = 3$,
and all others are ∞ . Thus $u_1 = v_1$.
- $t(v_2) = \min\{3, t(u_1) + \alpha(u_1 v_2)\} = \min\{3, 4\} = 3$,
 $t(v_3) = 2 + 1 = 3$, $t(v_4) = 2 + 3 = 5$, $t(v_5) = 2 + 2 = 4$.
Thus choose $u_2 = u_3$.

- $t(v_2) = \min\{3, \infty\} = 3$, $t(v_4) = \min\{5, 3 - 2\} = 5$,
 $t(v_5) = \min\{4, 3 + 1\} = 4$. Thus set $u_3 = v_2$.
- $t(v_4) = \min\{5, 3 + 1\} = 4$, $t(v_5) = \min\{4, \infty\} = 4$. Thus choose $u_4 = v_4$.
- $t(v_5) = \min\{4, 4 + 1\} = 4$. The algorithm stops.

We have obtained:

$$t(v_1) = 2, t(v_2) = 3, t(v_3) = 3, t(v_4), t(v_5) = 4.$$

These are the minimal weights from v_0 to each v_i . The steps of the algorithm can also be rewritten as a tale:

v_1	2	-	-	-	-
v_2	3	3	3	-	-
v_3	∞	3	-	-	-
v_4	∞	5	5	4	-
v_5	∞	4	4	4	4

0.5.9 Tree

A graph is called *acyclic*, if it has no cycle. An acyclic graph is also called a *forest*.

A *tree* is a connected acyclic graph.

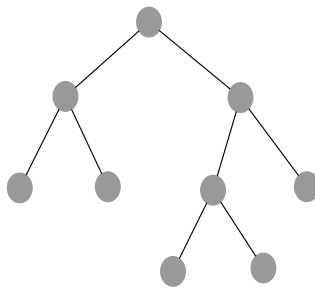


Figure 9: A tree having 9 nodes.

Part I

Theory

Chapter 1

Networks Structure and Models

In this chapter we are going to introduce some network structures and models which are of relevant importance for this thesis. We will only scratch the surface as there is a huge amount of literature on network structures and dynamics and other advanced topics [52, 93].

Definition 1.0.18 *A network $G = (V, E, \gamma, \theta)$ consists of:*

- *A graph $G = (V, E)$, where V is the set of vertices, E_1 is the set of arcs, E_2 is the set of edges, and $E = E_1 \cup E_2$ is the set of lines, $n = \text{card}(V)$, $m = \text{card}(E)$.*
- *γ vertex value functions/properties: $\gamma : V \rightarrow A$.*
- *θ line value functions/weights: $\theta : E \rightarrow B$.*

We will designate a network by its underlying graph, i.e. $G = (V, E)$. For instance if we consider the simple network shown in Figure 1.1 for which the set of vertices is $V = \{a, b, c, d\}$, the set of arcs $E_1 = \{a_1, a_2, a_3, a_4\}$, where $a_1 = (a, b)$, $a_2 = (b, a)$, $a_3 = (d, a)$, $a_4 = (d, d)$, the set of edges $E_2 = \{e_1, e_2\}$, with $e_1 = (b, c)$, $e_2 = (c, d)$ and vertex value properties (these can be node ages for example) $\gamma(a) = 10$,

$\gamma(b) = 12$, $\gamma(c) = 20$, $\gamma(d) = 18$ and line value functions (these can be the cost of maintaining the links for example) $\theta(a_1) = 1.0$, $\theta(a_2) = 2.1$, $\theta(a_3) = 1.7$, $\theta(a_4) = 0.5$, $\theta(e_1) = 1.2$, $\theta(e_2) = 2.1$.

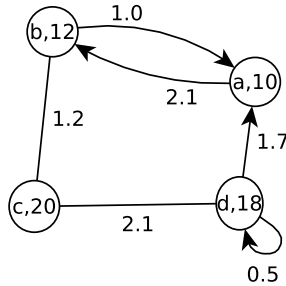


Figure 1.1: Very simple networks, with node values and lines values.

1.1 Some Example of Networks

- Computer Networks: The Internet topology (at both the Router and the Autonomous System (AS) levels) is a graph, with edges connecting pairs of routers/AS. This is a self-graph, which can be both weighted or unweighted.
- Ecology: Food webs are self-graphs with each node representing a species, and the species at one endpoint of an edge eats the species at the other endpoint.
- Biology: Protein interaction networks link two proteins if both are necessary for some biological process to occur.
- Sociology: Individuals are the nodes in a social network representing ties (with labels such as friendship, business relationship, trust, etc.) between people.

- User Psychology: Clickstream graphs are bipartite graphs connecting internet users to the websites they visit, thus encoding some information about the psyche of the web user.

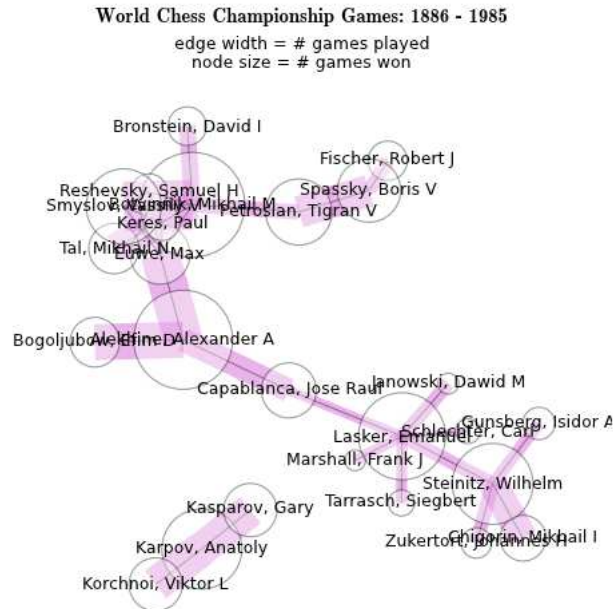


Figure 1.2: Chess masters network containing all 685 World Chess Championship matches from 1886-1985. Each node is the last name of a chess master. Each edge is directed from white to black and contains selected game info. The network consisted of 25 players (nodes) and 685 edges (number of games). This network was produced using NetworkX [9] in Python.

1.2 Properties of Networks

Degree Distributions

From the information provided by the node degrees of a network we can find some important insights about the structure of all the network. This analysis is based on the distribution of node degrees in the network. For example, in Figure 1.4 we are illustrating the plot of the adjacency matrices of the network of jazz musicians

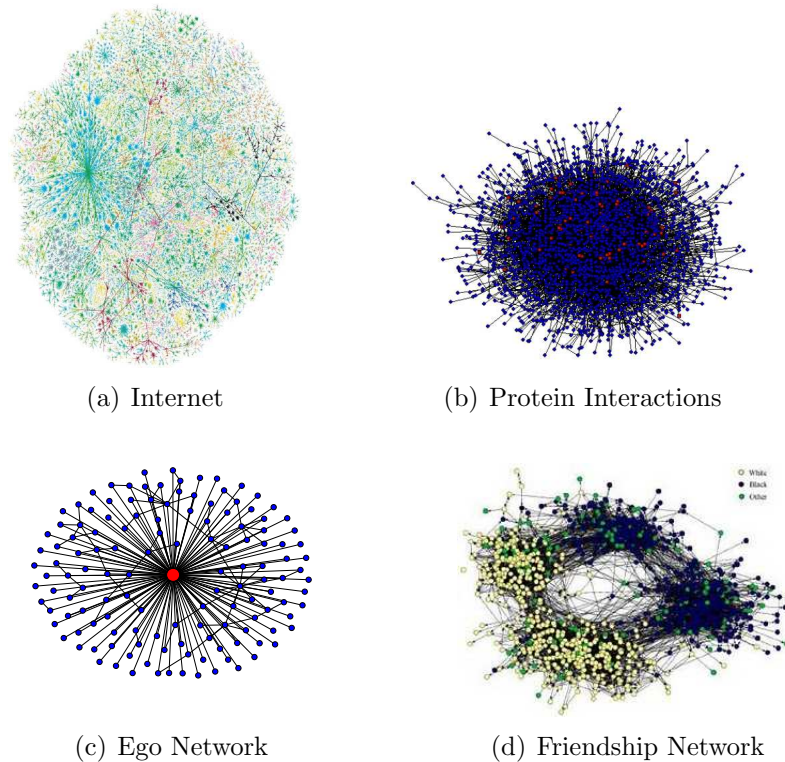


Figure 1.3: Examples of networks (a) the Internet network, (b) The network of Protein Interaction, (c) Ego network of the largest hub in a Barabási-Albert network. An Ego network consist of a focal node (‘ego’) and the nodes to whom ego is directly connected to (these are called ‘alters’) plus the ties, if any, among the alters, and (d) the Friendship network.

[62] and the network of corporate directors of the top 500 corporations in the United States of America (USA) [41]. The jazz network consists of 1258 nodes and 38562 edges and the one for corporate directors in the USA consists of 1586 nodes. It can be seen from these plots that the two networks show very different characteristics. The node degree looks more uniformly distributed in the second plot (b) than in the right plot (a) of Figure 1.4. The degree distribution is the most fundamental topological characterisation of a network. It may be obtained in terms of the probability $p(k)$, which is defined as the probability that a node chosen uniformly at random has degree k or equivalently as the fraction of nodes in the graph having degree k . The probability $p(k)$ is given by

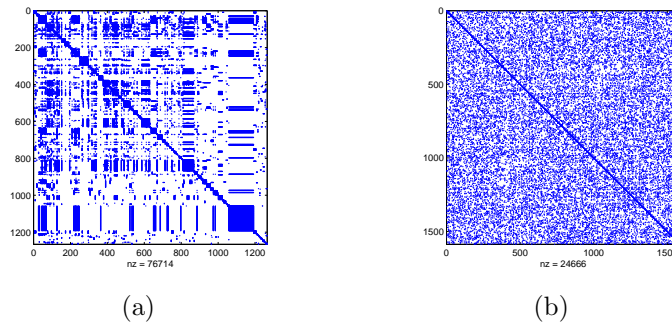


Figure 1.4: Plots of the adjacency matrices of the Jazz musician network (a) and the network of the top 500 corporations in the USA (b).

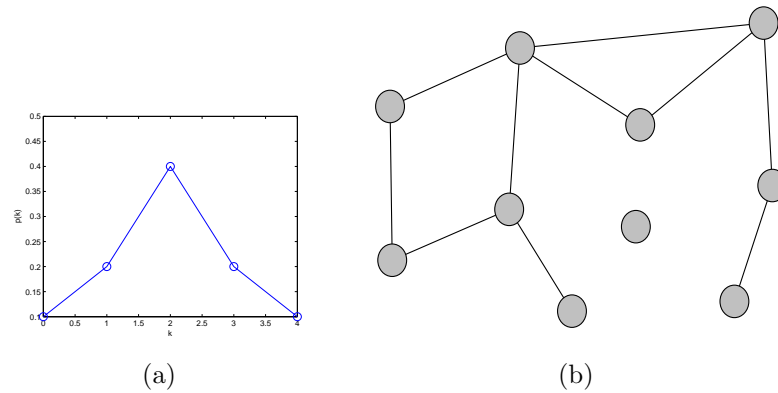


Figure 1.5: Illustration of the degree distribution (b) for a simple network in (a).

$$p(k) = \frac{n(k)}{n}, \tag{1.1}$$

where $n(k)$ is the number of nodes having degree k in a network of size n . For example the network in Figure 1.5 (a) has $n = 10$ vertices, for which 1 has degree 4, 2 have degree 3, 4 have degree 2, 2 have degree 1 and 1 has degree 0. Hence the values of $p(k)$ for $k = 0, \dots, 4$ are: $\frac{1}{10}, \frac{2}{10}, \frac{4}{10}, \frac{2}{10}, \frac{1}{10}$. The degree distribution

k	0	1	2	3	4
$p(k)$	$\frac{1}{10}$	$\frac{2}{10}$	$\frac{4}{10}$	$\frac{2}{10}$	$\frac{1}{10}$

Table 1.1: Degree distribution of the simple network in Figure 1.5 (b).

given in Table 1.1 completely determines the structure of the network in Figure

1.5 (a). However, in many cases this is not the case. We can have another network which is different from the one in Figure 1.5 (a) but has exactly the same degree distribution. The degree distribution gives us some important information about the network but it does not give us all the information. In the case of directed networks one needs to consider two distributions, the in-degree distribution of node $p(k^{in})$ with $k_i^{in} = \sum_j a_{ji}$ and the out-degree distribution of $p(k^{out})$ with $k_i^{out} = \sum_j a_{ij}$. Information on how the degree is distributed among the nodes of an undirected network can be obtained either by a plot of $p(k)$ versus the degree k , often in log-log scale which gives a qualitative idea about the kind of statistical distribution followed by the node degrees or by the calculation of the moments of the distribution. The n -moment of $p(k)$ is defined as follows:

$$\langle k^n \rangle = \sum_k k^n p(k). \quad (1.2)$$

The first moment $\langle k \rangle$ (sometimes written \bar{k}) is the mean degree of the network. The second moment $\langle k^2 \rangle$ called the divergence measures the fluctuations of the connectivity distribution. In the limit of infinite graph size, $\langle k^2 \rangle$ radically changes the behaviour of the dynamical processes that take place over the network. In Figure 1.6 we are illustrating histogram plots of the degree distributions of the jazz musician network and the network of corporate directors in the USA. In Figure 1.7 we are illustrating plots of some degree distributions in networks, the Poisson distribution, the Gaussian distribution, the power-law distribution and the exponential distribution.

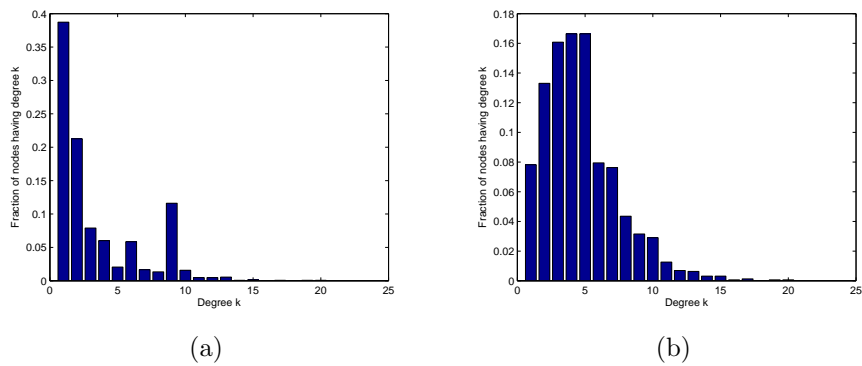


Figure 1.6: A histogram of the degree distribution of the network of Jazz musicians (a) and the network of corporate directors in the USA (b).

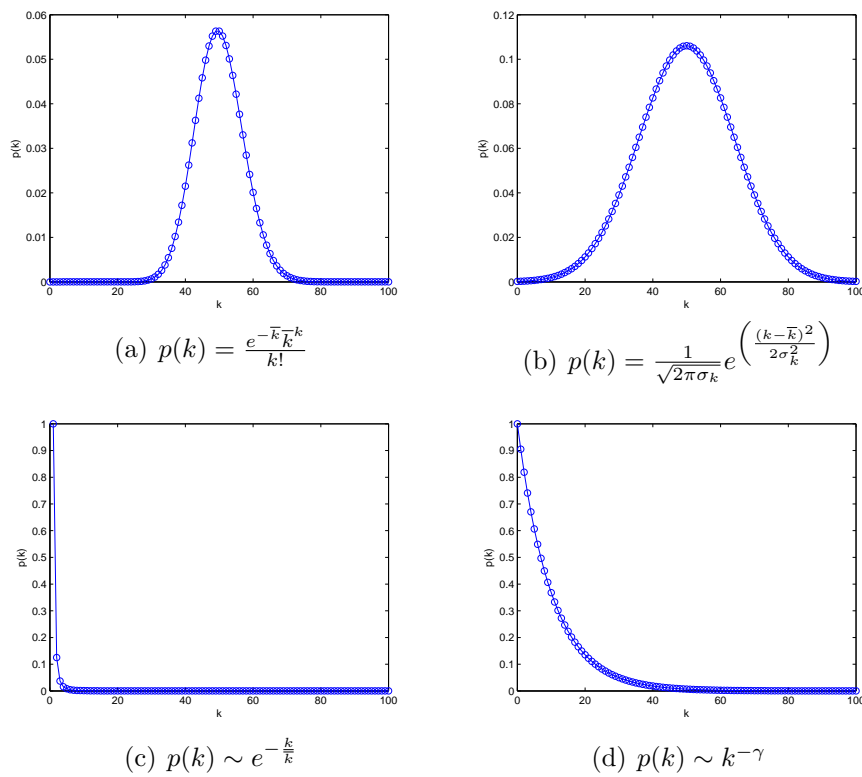


Figure 1.7: Degree distributions in networks (a) Poisson distribution, (b) Gaussian distribution, (c) Power-law distribution, (d) Exponential distribution.

1.3 Binomial Distribution

Sequences of Bernoulli Trials

Sequences of Bernoulli trials are sequences of independent identical trials, each of which is a success with probability p , for some fixed $p \in (0, 1)$, and a failure with

probability $1 - p$. Such sequences of trials form one of the fundamental models of probability theory, with many applications [66, 100]. We may conveniently speak of successes and failures no matter what is being modelled: thus, in the case of repeatedly tossing a coin which lands heads with probability p we may regard a head as a success and a tail as a failure. Let us define a sequence of independent identically distributed random variables X_1, X_2, \dots by setting

$$X_i = \begin{cases} 1 & \text{if the } i\text{th trial is a } \textit{success}, \\ 0 & \text{if the } i\text{th trial is a } \textit{failure}. \end{cases} \quad (1.3)$$

Thus, for each i ,

$$P(X_i = 0) = 1 - p, \quad P(X_i = 1) = p. \quad (1.4)$$

Let us consider a sequence of independent identical random variables X_1, X_2, \dots, X_n with

$$P(X_i = 1) = p \quad \text{and} \quad P(X_i = 0) = 1 - p. \quad (1.5)$$

We also define

$$S_0 = 0, \quad S_n = \sum_{i=1}^n X_i.$$

Consider the distribution, for fixed n , of the random variable S_n . Since this is the total number of successes in a sequence of n independent identically distributed trials, it is known that S_n has a *binomial distribution* with parameters n and p , i.e. that

$$P(S_n = k) = \binom{n}{k} p^k (1 - p)^{n-k}, \quad k = 0, 1, \dots, n, \quad (1.6)$$

and we write $S_n \sim B(n, k)$. It can be shown that the mean of E and the variance Var of S_n are given by [66]:

$$E(S_n) = np, \quad Var(S_n) = nVar(X_1) = np(1 - p).$$

1.4 Poisson Distribution

By letting p vary with n and taking limits we obtain a different fundamental law, the *Poisson law*. Specifically,

Lemma 1.4.1 *if $p_n = \frac{\lambda}{n} + o(1/n)$ as $n \rightarrow \infty$ then*

$$P(S_n = k) \rightarrow \frac{\lambda^k}{k!} e^{-\lambda} \quad (1.7)$$

proof 1.4.2 *We have that*

$$\begin{aligned} P(S_n = k) &= \frac{n!}{k!(n-k)!} p_n^k (1-p_n)^{n-k} \\ &= \frac{1}{k!} \frac{n(n-1) \cdots (n-k+1)}{n^k} (np_n)^k (1-p_n)^n (1-p_n)^{-k} \\ &\rightarrow \frac{1}{k!} \cdot 1 \cdot \lambda^k \cdot e^{-\lambda} \cdot 1 \\ &= \frac{\lambda^k}{k!} e^{-\lambda}. \end{aligned} \quad (1.8)$$

This is the Poisson distribution (law) with parameter λ . The Poisson law is fundamental when, roughly speaking, we deal with independent rare events. If X is random variable that follows a Poisson law, its mean and variance are given by

$$EX = \lambda \text{ and } Var(X) = \lambda$$

respectively.

1.5 Power-Law Degree Distribution

Among all the possible degree distributions, the power-law degree distribution is the one that has attracted most of the attention in scientific and even popular literature.

Definition 1.5.1 (*Non-stochastic*) *Let us consider a finite sequence $k = (k_1, \dots, k_n)$ of real numbers, such that $k_1 \leq k_2 \leq \dots \leq k_n$. The sequence k is said to follow a power-law or scaling relationship if*

$$r = ck_r^{-\gamma}, \quad (1.9)$$

where r (by definition) is the rank of k_r , c is a fixed constant, and γ is called the scaling index. The definition is said to be non-stochastic in the sense that there is no underlying probability model for the given sequence. The relationship for the rank r versus k appears as a line of slope $-\gamma$ when plotted on a log-log scale. Indeed we have

$$\log(r) = \log(c) - \gamma \log(k_r). \quad (1.10)$$

The relationship (1.9) is referred to as the size-rank (or cumulative) form of scaling. While the definition of scaling in (1.9) is fundamental, a more common usage of power-laws and scaling occurs in the context of random variables and their distributions.

Definition 1.5.2 (*Stochastic*) *Let us assume an underlying probability model P for a non-negative random variable X , let $F(x) = P[X \leq x]$ for $x \geq 0$ denote the (cumulative) distribution function (CDF) of X , and let $\bar{F}(x) = 1 - F(x)$ denote the complementary CDF (CCDF) or the tail function [66, 100]. In this context, a random variable X or its corresponding distribution function F is said to follow a*

power-law or is scaling with index $\lambda > 0$ if as $x \rightarrow \infty$,

$$P[X > x] = 1 - F(x) \sim cx^{-\lambda}, \quad (1.11)$$

for some $0 < c < \infty$ and a tail index $\lambda > 0$.

Here, we write $f(x) \sim g(x)$ as $x \rightarrow \infty$ if $f(x)/g(x) \rightarrow 1$ as $x \rightarrow \infty$. Requiring the existence of the cumulative distribution function $F(x)$, the probability density function (pdf) of the random variable X is defined to be [66, 100]:

$$f(x) = dF(x)/dx, \quad (1.12)$$

so for the random variable X , its stochastic cumulative form of scaling or size-rank relationship (1.11) has an equivalent non-cumulative or size-frequency counterpart given by

$$f(x) \sim cx^{-(1+\gamma)} \quad (1.13)$$

which appears similarly as a line of slope $-(1 + \gamma)$ on a log-log scale. If X is a continuous random variable, its first moment, i.e. its mean, is given by

$$E(X) = \int_{-\infty}^{\infty} xf(x)dx = c\lambda \int_{x_{min}}^{\infty} \frac{1}{x^\lambda} = \frac{c\lambda}{1-\lambda} \frac{1}{x^{\lambda-1}} \Big|_{x_{min}}^{\infty} dx. \quad (1.14)$$

For $1 < \lambda < 2$, the first moment is finite but the second moment/variance is infinite and for $0 < \lambda \leq 1$, both the second moment/variance and the first moment/mean are infinite. For this reason power-law distributions are sometimes called heavy tail distributions. In general, all moments of F of order $\beta \geq \gamma$ are infinite. Since relationship (1.11) implies $\log(P[X > x]) \approx \log(c) - \lambda \log(x)$, doubly logarithmic plots of x versus $1 - F(x)$ yield straight lines of slope $-\lambda$, at least for large x . If

$x > u$, then the conditional distribution of X given that $X > u$ is given by

$$P\{[X > x|X > u]\} = \frac{P\{[X > x] \cap [X > u]\}}{P[X > u]} = \frac{P[X > x]}{P[X > u]} \sim c_1 x^{-\gamma}, \quad (1.15)$$

where the constant c_1 is given by $1/u^{-\gamma}$ and does not depend on x . Hence, when x is large, the conditional probability $P[X > x|X > u]$ is identical to the (unconditional) distribution $P[X > x]$, except for a change in scale. Owing to this fact, power-law distributions are often called *scaling distributions* or *scale-free distributions*. The usual way of referring to power-law networks is scale-free networks meaning that there exists a power-law relationship between the probability density function (or probability mass function for discrete random variables) and the node degree often translates as

$$p(k) = Bk^{-\gamma}. \quad (1.16)$$

If we scale the degree by a constant factor, say c , then this produces only a proportionate scaling of the function, i.e.

$$p(k, c) = B(ck)^{-\gamma} = Bc^{-\gamma}.p(k) \quad (1.17)$$

which is identical to $p(k)$ except for a change of scale. In a log – log scale equation (1.16) results in a straight line of slope $-\gamma$. Most of the time degree distributions do not follow equation (1.16). In fact, the degree distribution is not monotonic for small values of k . A true power-law distribution is decreasing monotonically over the entire range of values of k . Hence in this case, the degree distribution characterised by the equation (1.16) deviates from the power-law for small values of k . In many scenarios the power-law relationship (1.16) is satisfied only in the *tail* of the distribution, when the value of k tends to infinity but

not for small values of k . Therefore, we usually write

$$p(k) \sim k^{-\gamma}. \quad (1.18)$$

When we say that a network has a power-law degree distribution we mean that the power-law behaviour is only followed in the tail of the distribution. In Figure 1.8

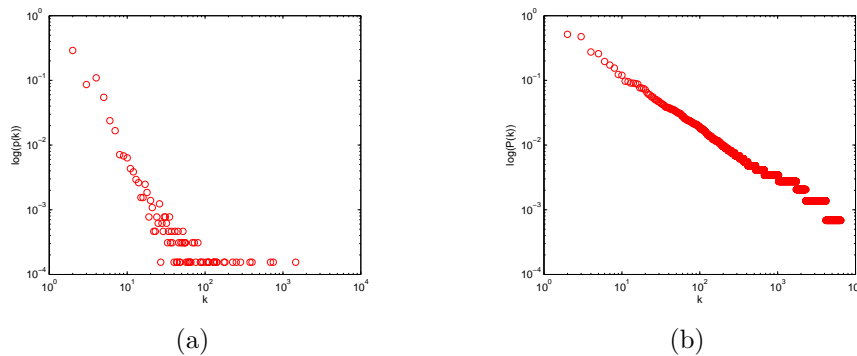


Figure 1.8: Probability (a) and cumulative distribution functions (b) for the version of the internet at autonomous system (AS) level displaying a power-law degree distribution.

(a) we are plotting in a log-log scale the probability $p(k)$ versus k for the version of the internet at autonomous system (AS) level. We can see that the tail of the distribution is very noisy and one way to solve this problem is to consider the cumulative distribution function (CDF) given by

$$P(k) = \sum_{k'=k}^{\infty} p(k') \quad (1.19)$$

which represents the fraction of nodes having degree k or greater or a probability of choosing a node with degree greater than or equal to k . For this case we can show that $P(k)$ also shows a power-law decay with the degree. In fact

$$P(k) = \sum_{k'=k}^{\infty} p(k') = C \sum_{k'=k}^{\infty} k'^{-\gamma} \simeq \int_k^{\infty} k'^{-\gamma} dk' = \frac{C}{\gamma-1} k^{\gamma-1}, \quad (1.20)$$

where $p(k'^{-\gamma}) = Ck'^{-\gamma}$ and $k \geq k_{kmin}$. In the Figure 1.8 (b) we illustrate a plot for the case of the (AS) version of the internet. As we can see the CDF plot significantly reduced the noise compared to the plot in (a) of the same figure.

Another approach to reduce the noise in the tail of the distribution is to use the logarithmic binning of the form $a^{n-1} \leq k < a^n$ where $a = 2$ and n runs in the range of nodes. For example the first bin for $n = 1$ is $1 \leq k < 2$ and all nodes of degree 1 fall in that bin. The second bin is $2 \leq k < 4$ and contains nodes of degree 2 and 3 and so on. Doing so, we are using wider bins in the tail of the distribution than for nodes having lower degree. We have to divide each bin by its width $a^n - a^{n-1} = (a - 1)a^{n-1}$ if we want to compare the count in those different bins.

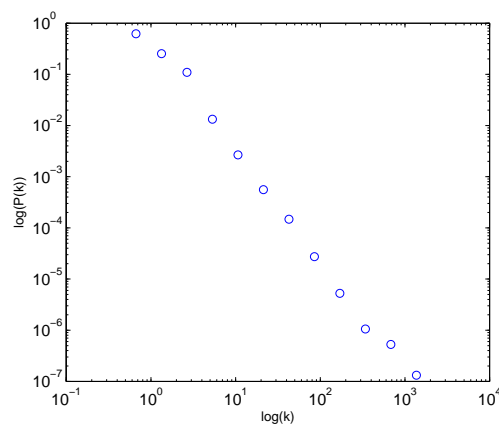


Figure 1.9: Cumulative distribution functions for the version of the internet using logarithmic bins displaying a power-law degree distribution.

All power laws with a particular scaling exponent are equivalent up to constant factors, since each is simply a scaled version of the others. This behaviour is what produces the linear relationship when logarithms are taken of both $p(x)$ or $P(x)$ and x (see Figures 1.8 (b) or 1.9) and the straight-line on the log-log plot is often called the signature of a power law. However, with real data, such straightness is a necessary, but not sufficient, condition for the data following a power-law

relation. Often the probability density function $p(x)$ or the probability distribution is estimated by constructing a histogram and the resulting function can be fitted to the linear form by least square linear regression. The slope of the fit is interpreted as the estimate $\hat{\alpha}$ of the scaling parameter and the variance r^2 is taken as an indicator of the quality of the fit. There are many ways to generate finite amounts of data that mimic this signature behaviour, but, in their asymptotic limit, are not true power laws. Thus, accurately fitting and validating power-law models is an active area of research in statistics. Let us consider for instance the following distributions:

1. Power-law distribution with density function $p(x) = x^{-\alpha}$, with $\alpha = 2.5$,
2. Log-normal distribution with density function $p(x) = \frac{1}{x} \exp[-\frac{(\ln x - \mu)^2}{2\sigma^2}]$, with $\mu = 0.25$, $\sigma = 0.18$,
3. Exponential distribution with density function $p(x) = \exp(-\lambda x)$, with $\lambda = 0.125$.

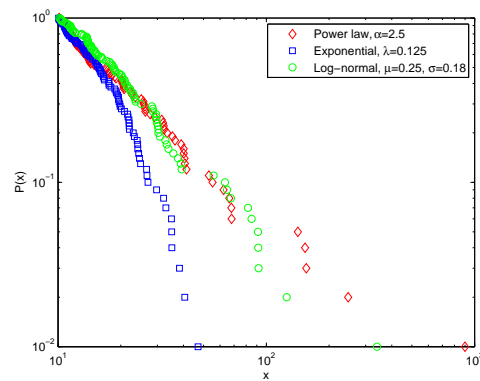


Figure 1.10: The CDFs of three small samples drawn from continuous distributions: a power law with $\alpha = 2.5$, a log normal with $\mu = 0.25$, $\sigma = 0.18$ and exponential with $\lambda = 0.125$. Visually these three CDF appear roughly straight on the logarithmic scales used, but only one is a true power-law.

As can be seen from the Figure 1.10 the log-log plots are close to a straight line for the distributions we have considered. In reality one of them is a power law distribution and it will be a mistake to infer that the others distributions are also power-law just because they are close to a straight line.

In practice we can not be certain that an observed quantity is drawn from a power-law distribution or not. The question of how to recognise a power law is one the most difficult one. Clauset et al. [34] described in some details a set of statistical analysis that allow one to decide whether an observed quantity follow a power law as well as the methods of calculating the parameters of the power law. The first step in this direction is the fitting power laws to empirical data. For this one need to estimate the lower bound x_{\min} on power law behaviour and the scaling parameter α from the data.

Estimating the Lower Bound on Power-Law behaviour

Empirical data do not follow a power law for all values of x , but they do so above a certain value x_{\min} . Therefore before estimating the scaling parameter, one needs to estimate the point x_{\min} and eliminate those values for which the power law properties does not follow. Often, the estimate \hat{x}_{\min} is chosen by visualising the point beyond which the probability density $p(x)$ or the probability distribution $P(x)$ becomes roughly straight on a log-log plot, or to plot the estimate $\hat{\alpha}$ as a function of \hat{x}_{\min} and identify a point beyond which the value appears relatively stable. This approach is not rigorous and can be sensitive to noise or fluctuations in the tail of the distribution. One candidate approach which is objective to determine \hat{x}_{\min} is the the Bayesian information criterion or BIC [34] which consists in maximizing the marginal likelihood or the likelihood of the data given the number of model parameters, integrated over the parameters' possible value.

Another approach for estimating \hat{x}_{\min} , is proposed by Clauset et al. [34] and can be applied to both discrete and continuous data. The approach chooses a value \hat{x}_{\min} that makes the probability distribution of the measured data and the best-fit power law model as similar as possible above \hat{x}_{\min} . For quantifying the distance between two probabilities, the Kolmogorov-Smirnov or KS statistic, was used. This statistic is the maximum distance between the CDFs of the data and the fitted model, that is :

$$D = \max_{x \geq x_{\min}} |S(x) - P(x)|, \quad (1.21)$$

where $S(x)$ is the CDF of the data for the observations which value at least x_{\min} , and $P(x)$ is the CDF for the power law model that best fits the data in the region $x \geq x_{\min}$. The estimate \hat{x}_{\min} is then the value of x_{\min} that maximises D . It has been shown that the KS model produces better results than the BIC approach. (See details in [34] paragraph 3.4).

Maximum Likelihood Estimators for the Power Law

If we assume that the lower bound x_{\min} of power-law is known, then the scaling parameter can be found by using the method of maximum likelihood, which gives accurate parameter estimates in the limit of large sample size [34].

1. Continuous data

The probability density $p(x)$ ($x > x_{\min}$) in the case of continuous data is such:

$$p(x)dx = Pr(x \leq X \leq x + dx) = Cx^{-\alpha}dx, \quad (1.22)$$

where X is the observed value and C is the normalisation constant and is

such that

$$\begin{aligned} \int_{x_{\min}}^{\infty} p(x)dx &= \int_{x_{\min}}^{\infty} Cx^{-\alpha}dx \\ &= C \left[\frac{x^{-\alpha+1}}{-\alpha+1} \right]_{x_{\min}}^{\infty} \\ &= 1. \end{aligned}$$

Provided $\alpha > 1$, we have

$$C = \frac{\alpha - 1}{x_{\min}^{-\alpha+1}}, \tag{1.23}$$

and substituting C in (1.22) we have

$$p(x) = \frac{\alpha - 1}{x_{\min}} \left(\frac{x}{x_{\min}} \right)^{-\alpha}. \tag{1.24}$$

The probability that the data were drawn from the model is given by the likelihood [100] of the data

$$p(x|\alpha) = \prod_{i=1}^n \frac{\alpha - 1}{x_{\min}} \left(\frac{x}{x_{\min}} \right)^{-\alpha}. \tag{1.25}$$

The data are most likely to have been generated by the model with the scaling parameter α that maximises the function (1.25) [100]. For simplicity, the logarithm L of the likelihood is considered and has its maximum at the same point,

$$L = \ln p(x|\alpha) = \ln \prod_{i=1}^n \frac{\alpha - 1}{x_{\min}} \left(\frac{x}{x_{\min}} \right)^{-\alpha} \tag{1.26}$$

$$= \sum_{i=1}^n \left[\ln(\alpha - 1) - \ln x_{\min} - \alpha \ln \frac{x_i}{x_{\min}} \right], \tag{1.27}$$

and

$$\frac{\partial L}{\partial \alpha} = \sum_{i=1}^n \left[\frac{1}{\alpha - 1} - \ln \frac{x_i}{x_{\min}} \right]. \quad (1.28)$$

Setting $\frac{\partial L}{\partial \alpha} = 0$ and solving for α , we obtain the maximum likelihood estimate (MLE) for the scaling parameter:

$$\hat{\alpha} = 1 + n \left[\sum_{i=1}^n \ln \frac{x_i}{x_{\min}} \right]^{-1}. \quad (1.29)$$

The standard error on $\hat{\alpha}$, which is derived from the width of the likelihood maximum [34, 100] is,

$$\sigma = \frac{\hat{\alpha} - 1}{\sqrt{n}} + O(1/n). \quad (1.30)$$

There are a number of reasons that motivate the use of the maximum likelihood. We state here some of them without proof [100].

Proposition 1.5.3 (*consistency*) *Under mild regularity conditions, if the data are independent, identically distributed drawn from a distribution with parameter α , then as the sample size $n \rightarrow \infty$, $\hat{\alpha} \rightarrow \alpha$ almost surely.*

Proposition 1.5.4 *The maximum likelihood estimator $\hat{\alpha}$ of the continuous power-law converges almost surely on the true value α .*

Proposition 1.5.5 (*asymptotic consistency*) *The MLE of the continuous power law is asymptotically Gaussian with variance $(\alpha - 1)^2/n$.*

2. Discrete data

When the random variable X can takes only discrete values x ($x > x_{\min}$), the probability distribution is given by:

$$p(x) = Pr(X = x) = Cx^{-\alpha}, \quad (1.31)$$

where the constant C is the normalisation constant and is such that

$$\begin{aligned} \sum_{x=x_{\min}}^{\infty} p(x) &= \sum_{x=x_{\min}}^{\infty} Cx^{-\alpha}, \\ &= 1. \end{aligned} \tag{1.32}$$

So that

$$C = \frac{1}{\sum_{x=x_{\min}}^{\infty} x^{-\alpha}} = \frac{1}{\zeta(\alpha, x_{\min})}, \tag{1.33}$$

where

$$\zeta(\alpha, x_{\min}) = \sum_{n=0}^{\infty} (n + x_{\min})^{-\alpha}. \tag{1.34}$$

The normalised probability distribution is:

$$p(x) = \frac{x^{-\alpha}}{\zeta(\alpha, x_{\min})}. \tag{1.35}$$

In this case the log-likelihood function is given by:

$$L = \ln \prod_{i=1}^n \frac{x_i^{-\alpha}}{\zeta(\alpha, x_{\min})} = -\alpha \sum_{i=1}^n \ln x_i - n \ln \zeta(\alpha, x_{\min}), \tag{1.36}$$

and

$$\frac{\partial L}{\partial \alpha} = \frac{-n}{\zeta(\alpha, x_{\min})} \frac{\partial}{\partial \alpha} \zeta(\alpha, x_{\min}) - \sum_{i=1}^n \ln x_i. \tag{1.37}$$

Setting $\frac{\partial L}{\partial \alpha} = 0$, we find that the maximum likelihood estimator $\hat{\alpha}$ for the scaling parameter is the solution to the equation

$$\frac{\zeta'(\hat{\alpha}, x_{\min})}{\zeta(\hat{\alpha}, x_{\min})} + \frac{1}{n} \sum_{i=1}^n \ln x_i = 0, \tag{1.38}$$

and this equation can be solved numerically for $\hat{\alpha}$. When x_{\min} is large, an approximate solution of $\hat{\alpha}$ can be found by the following way: Let $f(x)$ be a

differentiable function then we have:

$$\int_{x-\frac{1}{2}}^{x+\frac{1}{2}} f(\theta)d\theta = F(x + \frac{1}{2}) - F(x - \frac{1}{2}), \quad (1.39)$$

where $F(x)$ is such that $F'(x) = f(x)$. We can expand the right hand side of (1.39) by using the following Taylor expansion

$$h(x_0 + \Delta x) = h(x_0) + h'(x_0)\Delta x + \frac{1}{2!}h''(x_0)(\Delta x)^2 + \frac{1}{3!}h'''(x_0)(\Delta x)^3 + \dots, \quad (1.40)$$

in which $x \equiv x_0$ and $\Delta x \equiv \frac{1}{2}$ to get

$$\int_{x-\frac{1}{2}}^{x+\frac{1}{2}} f(x) = f(x) + \frac{1}{24}f''(x) + \dots \quad (1.41)$$

Now if we take the sum of these terms from x_{\min} to ∞ we have:

$$\int_{x_{\min}-\frac{1}{2}}^{\infty} f(\theta)d\theta = \sum_{x=x_{\min}}^{\infty} f(x) + \frac{1}{24} \sum_{x=x_{\min}}^{\infty} f''(x) + \dots \quad (1.42)$$

If $f(x) = x^{-\alpha}$ ($\alpha > 1$), then we have $f''(x) = \alpha(\alpha - 1)x^{-\alpha-2}$ and

$$\begin{aligned} \int_{x_{\min}-\frac{1}{2}}^{\infty} \theta^{-\alpha}d\theta &= \frac{(x_{\min} - \frac{1}{2})^{-\alpha+1}}{\alpha - 1} \\ &= \sum_{x=x_{\min}}^{\infty} x^{-\alpha} + \frac{\alpha(\alpha - 1)}{24} \sum_{x=x_{\min}}^{\infty} x^{-\alpha-2} + \dots \\ &= \sum_{x=x_{\min}}^{\infty} x^{-\alpha} \left[1 + \frac{\alpha(\alpha - 1)}{24} \sum_{x=x_{\min}}^{\infty} x^{-2} + \dots \right] \\ &= \zeta(\alpha, x_{\min}) [1 + O(x_{\min}^{-2})], \end{aligned} \quad (1.43)$$

where in the last equality we have made use of the fact that $x^{-2} \leq x_{\min}^{-2}$.

Therefore

$$\zeta(\alpha, x_{\min}) = \frac{(x_{\min} - \frac{1}{2})^{-\alpha+1}}{\alpha - 1} [1 + O(x_{\min}^{-2})], \quad (1.44)$$

and

$$\zeta'(\alpha, x_{\min}) = -\frac{(x_{\min} - \frac{1}{2})^{-\alpha+1}}{\alpha - 1} \left[\frac{1}{\alpha - 1} + \ln(x_{\min} - \frac{1}{2}) \right] [1 + O(x_{\min}^{-2})] \quad (1.45)$$

Substituting expressions (1.44) and (1.45) into Equation (1.38) we have

$$-\left[\frac{1}{\alpha - 1} + \ln(x_{\min} - \frac{1}{2}) \right] [1 + O(x_{\min}^{-2})] + \frac{1}{n} \sum_{i=1}^n \ln x_i = 0, \quad (1.46)$$

An approximate of the estimator $\hat{\alpha}$ can be found by solving Equation (1.46).

For large x_{\min} we can neglect high order terms in x_{\min} and solve for $\hat{\alpha}$ to get,

$$\hat{\alpha} \simeq 1 + n \left[\sum_{i=1}^n \ln \frac{x_i}{x_{\min} - \frac{1}{2}} \right]^{-1}. \quad (1.47)$$

In this case the standard error on $\hat{\alpha}$ is given by [34]:

$$\sigma = \frac{1}{\sqrt{n \left[\frac{\zeta''(\hat{\alpha}, x_{\min})}{\zeta(\hat{\alpha}, x_{\min})} - \left(\frac{\zeta'(\hat{\alpha}, x_{\min})}{\zeta(\hat{\alpha}, x_{\min})} \right)^2 \right]}}. \quad (1.48)$$

Goodness-of-fit tests

Given an observed data set and a hypothesised power-law distribution from which the data are drawn, we would like to know whether the power-law hypothesis is a plausible one, given the data. A goodness-of-fit tests answers to this question by generating a p -value that quantified the plausibility of the power law hypothesis. This method can be summarised in the following points [34]:

- (i.) fit the empirical data to the power law model using the method described previously and calculate the KS statistic;
- (ii.) generate a large number of power-law distributed synthetic data sets with scaling parameter α and lower x_{\min} equal to those of the distribution that best fits the observed data;
- (iii.) fit each synthetic data set individually to its own power law model and calculate the KS statistic for each one relative to its own model;
- (iv.) count the fraction of the time the resulting statistic is larger than the value for the empirical data. This fraction is the p -value;
- (v.) if $p < 0.1$ then the power law is ruled out. Some authors use the rule $p < 0.05$, reducing then the chance of really following a power-law.

A large value of p does not necessarily mean that the power-law is correct. In fact there may be another distribution that matches the data well over the range of x observed and it is possible that for small values of n the empirical distribution follows a power-law closely and has a large p -value, even when the power-law is the wrong model for the data (See Figure 1.10). The performance of the goodness-of-fit test has been verified in [34] by detecting the true power-law in plots such as the one shown in Figure 1.10. Alternative methods are described in [34] when there are competitive distributions that also fit the data well. One cannot compare the power-law distribution to all existing distributions. A reasonable hypothesis on the data will guide one in deciding which distribution fits the data well.

1.6 Small World Effect

Average Shortest Path Length

A measure of the typical separation between two nodes in the graph is given by the average shortest path length, also known as characteristic path length, defined as the mean of geodesic lengths over all pairs of nodes [102, 121]:

$$L = \frac{1}{n(n-1)} \sum_{i,j \in V, i \neq j} d_{ij}, \quad (1.49)$$

where d_{ij} is the shortest distance between nodes i and j . Shortest paths play an important role in networks. For example in the internet, if we need to send a data packet from one computer to another, then the geodesic path provides an optimal path way, since one would achieve a fast transfer and save system resources [122]. In a real network like the World Wide Web, a short average path length facilitates the quick transfer of information and reduces costs. The efficiency of mass transfer in a metabolic network can be judged by studying its average path length. A power grid network will have less losses if its average path length is minimised. For such a reason, shortest paths have also played an important role in the characterisation of the internal structure of a graph [123]. All shortest path lengths of a given network are represented by a matrix $\mathbf{D}(G)$ in which the entry d_{ij} is the length of the geodesic from node i to node j .

Diameter

The maximum value of d_{ij} is called the diameter of the network denoted and given by

$$\text{Diam}(G) = \max\{d_{ij}\}. \quad (1.50)$$

In the case of a disconnected network we cannot use relation (1.49) otherwise the average shortest path length is not defined. To overcome this problem we use instead the harmonic mean [82] of geodesic lengths, and define the so-called efficiency of the network as [82, 83]:

$$\bar{e} = \frac{1}{n(n-1)} \sum_{i,j \in V, i \neq j} \frac{1}{d_{ij}}. \quad (1.51)$$

According to (1.51) any two pairs of nodes belonging to different connected components yield a zero contribution. Most real networks have a very short average path length leading to the concept of a small world where everyone is connected to everyone else through a very short path. The results of Milgram's experiment [117] are the first demonstrations of the small world effect.

Milgram's Experiment

The experiment consisted in selecting at random several people in the U.S. cities of Omaha (Nebraska) and Wichita (Kansas), which are located at the centre of the continental U.S., and asking those people to send a letter to a target person who lives in Boston (Massachusetts) in the west coast. The individuals at the starting points were asked to send the letters to somebody they know on a first-name basis. In those cases in which the letter arrived at its target, the researcher had the opportunity of following the trajectory that the letter followed in the U.S. If you were selected as one of the starting points you must first think if you know personally the target, in which case you simply direct the letter to him/her. If not then you must think about somebody you know personally that you think has a large probability of knowing the target personally. If we consider that the starting points and the target are separated by more than 2000 km, it is strange to think

that the number of steps that a letter needs to take is very large. The results then came with the following conclusions:

1. The average number of steps used for the letters that arrived at their targets was around 5.5 or 6.
2. There was large group interconnection, resulting in an acquaintance of one individual feeding back into his/her own circle, normally eliminating new contact.

As a result, most models of real networks are created with this condition in mind. One of the first models which tried to explain real networks was the random network model. It was later followed by the Watts and Strogatz model, and even later there were the scale-free networks starting with the Barabási-Albert (BA) model. All these models have one thing in common: they all predict very short average path length. The average path length depends on the system size but does not change drastically with it. Small world network theory predicts that the average path length changes proportionally to $\log n$, where n is the number of nodes in the network.

1.7 Clustering Coefficient

Clustering, also known as transitivity, is a typical property of acquaintance networks, where two individuals with a common friend are likely to know each other. In terms of network topology, transitivity means the presence of a high number of triangles. A triangle being a set of three vertices each of which is connected to each other [121]. Two versions of this measure exist: the global and the local clustering coefficient. The global version was designed to give an overall indica-

tion of the clustering in the network, whereas the local gives an indication of the embeddedness of single nodes.

Global Clustering Coefficient

The global clustering coefficient can be quantified by defining the clustering C of the network as the relative number of transitive triples (expression borrowed from the sociology literature), i.e. the fraction of connected triples of nodes (triads) which also form triangles [92, 94, 104]:

$$C = \frac{3 \times \text{number of triangles in the network}}{\text{number of connected triplets in the network}} \quad (1.52)$$

or

$$C = \frac{\text{number of closed triplets}}{\text{number of connected triplets of vertices}}. \quad (1.53)$$

A triplet is three nodes that are connected by either two (open triplet) or three (closed triplet) undirected ties. A triangle consists of three closed triplets, one centred on each of the nodes. The global clustering coefficient is the number of closed triplets (or $3 \times$ triangles) over the total number of triplets (both open and closed). The factor 3 in the numerator compensates for the fact that each complete triangle of three nodes contributes three connected triplets, one centred on each of the three nodes, and ensures that $0 \leq C \leq 1$, with $C = 1$ for the complete graph K_N . The global clustering coefficient can also be written in the form

$$C = \frac{6 \times \text{number of triangles in the network}}{\text{number of path of length two}}. \quad (1.54)$$

Local Clustering Coefficient

Watts and Strogatz introduced an alternative definition for the clustering coefficient of a network [123] which is widely used. This measure is defined as follows. A quantity c_i , the local clustering coefficient of node i is first introduced, expressing how likely $a_{kj} = 1$ for two neighbours k and j of node i . It is also the probability that nearest neighbours of a node are themselves nearest neighbours. Concretely if node i has k_i nearest neighbours with e_i connections i.e. the value obtained by counting the actual number of edges in G_i (the subgraph of neighbours of i). In some cases, G_i can be, unconnected. Hence, the local clustering coefficient is defined as the ratio between e_i and $k_i(k_i - 1)/2$, the maximum possible number of edges in G_i [122, 123]:

$$c_i = \frac{e_i}{k_i(k_i - 1)/2}. \quad (1.55)$$

For this alternative, the clustering coefficient of a network is defined to be the average of c_i over all the nodes in the network:

$$\bar{C} = \frac{1}{n} \sum_{i=1}^n c_i. \quad (1.56)$$

We are going to show by an illustrative example that relation (1.56) is not equivalent to relation (1.52), relation (1.53) or relation (1.54), i.e. the two versions of clustering coefficient are not equivalent (See Figure 1.11).

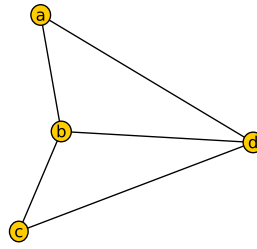


Figure 1.11: Illustration of the definitions of the clustering coefficient C , using equation (1.52), this network has two triangles and six connected triples (three for each triangle), $C = 3 \times 2/6 = 1$ or if we use equation (1.53), the network has six closed triples and six connected triples, $C = 6/6 = 1$ and using equation (1.54), the network has two triangles and twelve closed path of length two, $C = 6 \times 2/12 = 1$. The individual vertices have local clustering coefficients $c_a = c_c = 1$ and $c_b = c_d = 2/3$ using equation (1.55) and for the mean value $\bar{C} = 5/6$ when using equation (1.56).

1.8 Degree-degree Correlations and Assortativity

Another interesting characteristic of complex networks is the existence of different types of degree-degree correlation. The degree-degree correlation accounts for the ways in which nodes with given degree are connected in networks. For instance, a network in which high-degree nodes tend to connect to each other displays positive degree-degree correlation and they are called assortative networks. On the other hand, networks in which high-degree nodes tend to be linked to low-degree nodes display negative degree-degree correlation and are called 'disassortative' networks. The assortativity of a network is quantified by measuring the correlation coefficient of its degree correlation, that is by computing the correlation coefficients for the degree of nodes existing at both sides of all links in a network [94]. Let $e(k_i k_j)$ be the fraction of links that connect a node of degree k_i to a node of degree k_j . As in [93] we considered for mathematical convenience the degree minus one instead

of the degree of the corresponding nodes, and named them ‘excess degree’. Let $p(k_j)$ be the probability that a node selected at random in the network has degree k_j . Then, the distribution of the excess degree of a node at the end of a randomly chosen link is:

$$q(k_j) = \frac{(k_j + 1)p(k_j + 1)}{\sum_i k_i p(k_i)}. \quad (1.57)$$

The assortativity coefficient is defined as

$$r = \frac{\sum_{k_i k_j} k_i k_j [e(k_i k_j) - q(k_i)q(k_j)]}{\sigma_q^2}, \quad (1.58)$$

where σ_q^2 is the standard deviation of the distribution $q(k_j)$. For regular networks the assortativity coefficient in (1.58) is not defined. In the case of directed networks the assortativity coefficient is calculated by considering the distribution of the two types of ends and their respective standard deviation [93]. This coefficient, which is the Pearson correlation coefficient of the degree of nodes at both ends of links, is given by

$$r = \frac{m^{-1} \sum_e k_i(e)k_j(e) - [m^{-1} \sum_e \frac{1}{2}(k_i(e) + k_j(e))]^2}{m^{-1} \sum_e \frac{1}{2}(k_i(e) + k_j(e)) - [m^{-1} \sum_e \frac{1}{2}(k_i(e) + k_j(e))]^2}, \quad (1.59)$$

where $k_i(e)$ and $k_j(e)$ are the degrees at both ends of the link e , and $m = |E|$. The expression (1.59) can be written in matrix form as follows [52]:

$$r = \frac{\langle \nu | \mathbf{A} | \nu \rangle - \frac{1}{2m} (\langle \mathbf{1} | \mathbf{E}' | \mathbf{1} \rangle)^2}{\langle \mathbf{1} | \mathbf{E}'^2 | \mathbf{1} \rangle - \langle \nu | \mathbf{A} | \nu \rangle - \frac{1}{2m} (\langle \mathbf{1} | \mathbf{E}' | \mathbf{1} \rangle)^2}, \quad (1.60)$$

where \mathbf{E}' denotes the modified link adjacency matrix, that is $\mathbf{E}' = \mathbf{B}^T \mathbf{B} = \mathbf{E} + 2\mathbf{I}$. We distinguish the following types of assortativity depending of the sign of coefficient r :

1. If $r < 0$ we say that the network displays disassortative mixing of degrees

and the network is disassortative. Disassortative mixing of degrees implies that high-degree nodes are preferentially attached to low-degree nodes.

2. If $r > 0$ we say that the network displays assortative mixing of degrees and the network is assortative. Assortative mixing of degrees means that low-degree nodes prefer to join to other low-degree nodes, while high-degree nodes are preferentially bonded to other high-degree nodes.
3. If $r = 0$ we say that the network displays neutral mixing of degrees.

E. Estrada [52] gives an illustration of the different types of degree assortativity. It is reported in [52] that almost all networks seem to be disassortative, except for the social networks which are normally assortative. The presence of high clustering and community structure is among the possible causes for this characteristic mixing pattern of social networks. A clear structural explanation is given in [52] explaining why some networks display assortative mixing of node degrees while other show a disassortative pattern. To learn more about the structure of complex networks for the assortativity coefficient or to know what kind of structural characteristic makes some networks assortative or disassortative we write the assortative coefficient in the form:

$$r = \frac{2M_2 - \frac{|P_2|^2}{m} - 2m - 4|P_2|}{M_1^e + 4|P_2| + 2m - 2M_2 - \frac{|P_2|^2}{m}}, \quad (1.61)$$

where $|P_2|$ stands for the number of paths of length 2, m is the number of links, and M_2 and M_1^e are known as the second Zagreb index of the graph and the first Zagreb index of the line graph, respectively, and can be expressed as

$$M_1^e = 2|P_2| + 2|P_3| + 6|S_{1,3}| + 6|C_3| \quad (1.62)$$

and

$$M_2 = m + 2|P_2| + |P_3| + 3|C_3|. \quad (1.63)$$

Therefore the assortativity coefficient in structural terms reads:

$$r = \frac{|P_2|(|P_{3/2}| + C - |P_{2/1}|)}{3|S_{1,3}| + |P_2|(1 - |P_{2/1}|)}, \quad (1.64)$$

where C is the ratio of three times the number of triangles to the number of 2-paths, i.e. the clustering coefficient and $|P_{r/s}| = |P_r|/|P_s|$. The denominator of (1.64) can be written as:

$$\left[\frac{1}{4} \sum_{i<j} k_i k_j (k_i^2 + k_j^2) - \frac{1}{2} \sum_{i<j} (k_i k_j)^2 \right] / |P_1|. \quad (1.65)$$

As

$$\frac{1}{4} \sum_{i<j} k_i k_j (k_i^2 + k_j^2) \geq \frac{1}{2} \sum_{i<j} (k_i k_j)^2, \quad (1.66)$$

the denominator of (1.64) is always larger than, or equal to zero. Equality occurs for the regular graph for which the assortativity is not defined. Depending on the sign of the numerator we have the following cases:

1. assortative ($r > 0$) if, and only if, $|P_{2/1}| < |P_{3/2}| + C$,
2. disassortative ($r < 0$) if, and only if, $|P_{2/1}| > |P_{3/2}| + C$.

1.9 Laplacian of a Network

Definition 1.9.1 *The matrix \mathbf{L} whose entries are defined as follows:*

$$\mathbf{L}(i, j) = \begin{cases} d_i & \text{if } i = j \\ -1 & \text{if } i \text{ and } j \text{ are adjacent,} \\ 0 & \text{otherwise.} \end{cases} \quad (1.67)$$

is called the Laplacian matrix of the network.

If \mathbf{D} is the diagonal matrix whose entries are the degrees of the vertices of the network, i.e.

$$\mathbf{D}(i, j) = \begin{cases} d_i & \text{if } i = j \\ 0 & \text{otherwise,} \end{cases} \quad (1.68)$$

then, the Laplacian of the network is also defined to be

$$\mathbf{L} = \mathbf{D} - \mathbf{A}. \quad (1.69)$$

The Normalised Laplacian

The normalised Laplacian may have a different form depending on the normalisation factor chosen. Here are examples of two different normalised Laplacian matrices.

- The normalised Laplacian denoted by \mathcal{L} whose entries are given by:

$$\mathcal{L}(i, j) = \begin{cases} 1 & \text{if } i = j \text{ and } d_i \neq 0 \\ -\frac{1}{\sqrt{d_i d_j}} & \text{if } i \text{ and } j \text{ are adjacent,} \\ 0 & \text{otherwise.} \end{cases} \quad (1.70)$$

- The normalised Laplacian denoted Δ whose entries are given by:

$$\Delta(i, j) = \begin{cases} 1 & \text{if } i = j \text{ and } d_i \neq 0 \\ -\frac{1}{d_j} & \text{if } i \text{ and } j \text{ are adjacent,} \\ 0 & \text{otherwise.} \end{cases} \quad (1.71)$$

The relationship between the normalised Laplacian \mathcal{L} , the degree matrix \mathbf{D} and the Laplacian \mathbf{L} is given by:

$$\mathcal{L} = \mathbf{D}^{-1/2} \mathbf{L} \mathbf{D}^{-1/2} \quad (1.72)$$

$$= \mathbf{I} - \mathbf{D}^{-1/2} \mathbf{A} \mathbf{D}^{-1/2}, \quad (1.73)$$

where \mathbf{I} is the identity matrix and the matrix $\mathbf{D}^{-1/2}$ is such that $\mathbf{D}^{-1/2} = \frac{1}{\sqrt{d_i}}$. We also have a similar relationship involving the normalised Laplacian Δ

$$\Delta = \mathbf{D}^{1/2} \mathcal{L} \mathbf{D}^{-1/2}. \quad (1.74)$$

The matrices Δ and \mathcal{L} are then similar and have the same spectrum. The Lapla-

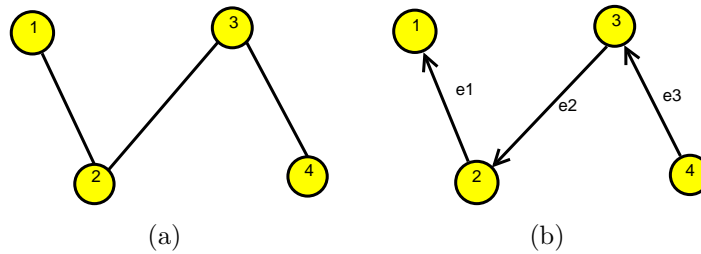


Figure 1.12: The orientation of arbitrary edges in (b) of the corresponding undirected graph in (a)

ian \mathbf{L} for the network in Figure 1.12 is given by

$$\mathbf{L} = \begin{pmatrix} 1 & -1 & 0 & 0 \\ -1 & 2 & -1 & 0 \\ 0 & -1 & 2 & -1 \\ 0 & 0 & -1 & 1 \end{pmatrix}, \quad \mathbf{Q} = \begin{pmatrix} -1 & 0 & 0 \\ 1 & -1 & 0 \\ 0 & 1 & -1 \\ 0 & 0 & 1 \end{pmatrix}.$$

Given any orientation of the edges, let us label the edges as in Figure 1.12 (a) and define the vertex edge matrix \mathbf{Q} by

$$\mathbf{Q}(i, j) = \begin{cases} 1 & \text{if } e_j \text{ starts from } i \\ -1 & \text{if } e_j \text{ ends at } i \\ 0 & \text{otherwise.} \end{cases} \quad (1.75)$$

The matrix \mathbf{Q} for the network in Figure 1.12(b) is given above. We have the following properties for:

- $\mathbf{L} = \mathbf{Q}\mathbf{Q}^T$. Does not depend on the orientation. So \mathbf{L} is semi-positive definite.
- $\mathbf{x}^T \mathbf{L} \mathbf{x} = \sum_{i \sim j} (x_i - x_j)^2$

Many other interesting properties of the Laplacian matrix of a network can be found in [52].

1.10 Network Spectrum

The spectrum of a network is the set of the eigenvalues of its adjacency matrix \mathbf{A} and their multiplicities. Let

$$\lambda_1(\mathbf{A}) \geq \lambda_2(\mathbf{A}) \geq \cdots \geq \lambda_n(\mathbf{A})$$

be the distinct eigenvalues of \mathbf{A} and let

$$m(\lambda_1(\mathbf{A})), m(\lambda_2(\mathbf{A})), \cdots, m(\lambda_n(\mathbf{A}))$$

be their multiplicities, i.e., the number of times each of them appears as an eigenvalue of \mathbf{A} . Then, the spectrum of \mathbf{A} is written as

$$Sp\mathbf{A} = \begin{pmatrix} \lambda_1(\mathbf{A}) & \lambda_2(\mathbf{A}) & \cdots & \lambda_n(\mathbf{A}) \\ m(\lambda_1(\mathbf{A})) & m(\lambda_2(\mathbf{A})) & \cdots & m(\lambda_n(\mathbf{A})) \end{pmatrix}. \quad (1.76)$$

The eigenvalues of the adjacency matrix \mathbf{A} are the zeros of the characteristic polynomial of the network, $\det(\lambda\mathbf{I} - \mathbf{A})$ and the numbers λ satisfy the equation

$$\mathbf{A}\mathbf{u} = \lambda(\mathbf{A})\mathbf{u}, \quad (1.77)$$

where each non-zero vector \mathbf{u} is called an eigenvector of \mathbf{A} . For simple undirected networks the adjacency matrix \mathbf{A} is real and symmetric, therefore its eigenvalues $\lambda_1(\mathbf{A}) \geq \lambda_2 \geq \mathbf{A} \cdots \geq \lambda_n(\mathbf{A})$ are real and the associate eigenvectors are orthogonal. When the network is directed, the eigenvalues may have imaginary parts. The largest eigenvalue of the adjacency matrix \mathbf{A} is called the index of the network or its spectral radius denoted by $\rho(\mathbf{A})$. Here are some spectra of some particular

networks [52]:

1. Path, $P_n : \lambda_j(\mathbf{A}) = 2 \cos\left(\frac{\pi j}{n+1}\right), j = 1, \dots, n,$
2. Cycle, $C_n : \lambda_j(\mathbf{A}) = 2 \cos\left(\frac{\pi j}{n}\right), j = 1, \dots, n,$
3. Star, $S_n : Sp(\mathbf{A}) = \{\sqrt{n} \ 0^{n-2} \ -\sqrt{n}\},$
4. Complete, $K_n : Sp(\mathbf{A}) = \{1 \ -1^{n-1}\},$
5. Complete bipartite, $K_{n_1, n_2} : Sp(\mathbf{A}) = \{\sqrt{n_1 n_2} \ 0^{n-2} \ -\sqrt{n_1 n_2}\}.$

By the Perron-Frobenius Theorem [97], if $\lambda_1(\mathbf{A})$ is the index of a connected undirected network, then it has multiplicity equal to one and its associate eigenvector, called the principal eigenvector is positive. Furthermore, this index is such that $|\lambda_i(\mathbf{A})| < \lambda_1(\mathbf{A})$ for all eigenvalues different from $\lambda_1(\mathbf{A})$. The same theorem also states that for a connected undirected network we have $k_{\min} < \bar{k} < \lambda_1(\mathbf{A}) < k_{\max}$ or $k_{\min} = \bar{k} = \lambda_1(\mathbf{A}) = k_{\max}$. The later holds only if the network is regular. The values k_{\min} and k_{\max} are the minimum and the maximum, respectively, degree of the network. The index of any network satisfies the following inequality:

$$2 \cos \frac{\pi}{n+1} \leq \lambda_1(\mathbf{A}) \leq n-1, \tag{1.78}$$

where the lower bound is obtained for the path P_n and the upper one is obtained for the complete network K_n . In a similar way as for the network spectrum based on the adjacency matrix, the spectrum of the Laplacian matrix is given by:

$$Sp\mathbf{L} = \begin{pmatrix} \lambda_1(\mathbf{L}) & \lambda_2(\mathbf{L}) & \dots & \lambda_n(\mathbf{L}) \\ m(\lambda_1(\mathbf{L})) & m(\lambda_2(\mathbf{L})) & \dots & m(\lambda_n(\mathbf{L})) \end{pmatrix}, \tag{1.79}$$

where the eigenvalues of \mathbf{L} are such that: $\lambda_1(\mathbf{L}) \leq \lambda_2(\mathbf{L}) \leq \dots \leq \lambda_n(\mathbf{L})$. The eigenvalues of the Laplacian matrix \mathbf{L} are bounded as

$$0 \leq \lambda_j(\mathbf{L}) \leq 2k_{\max} \quad (1.80)$$

and

$$\lambda_n \geq k_{\max}. \quad (1.81)$$

The multiplicity of the eigenvalue of \mathbf{L} , $\lambda_1(\mathbf{L}) = 0$ (associate to the eigenvector $\mathbf{1} = (1, \dots, 1)^T$) is equal to the number of connected components in the network. The second eigenvalue is such that $\lambda_2(\mathbf{L}) > 0$ if and only if the network is connected [52] and this eigenvalue is usually called the algebraic connectivity of the network. On the other hand, the normalised Laplacian matrix \mathcal{L} is also positive semi-definite having eigenvalues $0 = \lambda_1(\mathcal{L}) \leq \lambda_2(\mathcal{L}) \leq \dots \leq \lambda_n(\mathcal{L})$ which are bounded as

$$0 \leq \lambda_j(\mathcal{L}) \leq 2 \quad (1.82)$$

and

$$\lambda_n \geq \frac{n}{n-1}. \quad (1.83)$$

More on the spectrum of the normalised Laplacian \mathcal{L} can be found in [52]. The spectra of matrices \mathbf{A} , \mathbf{L} and \mathcal{L} are related by the following inequalities:

$$k_{\max} - \lambda_n(\mathbf{A}) \leq \lambda_n(\mathbf{L}) \leq k_{\max} - \lambda_1(\mathbf{A}) \quad (1.84)$$

and

$$\lambda_j(\mathcal{L}) \leq \lambda_j(\mathbf{L}) \leq \lambda_j(\mathcal{L})k_{\max}. \quad (1.85)$$

1.11 Random Models of Networks

It is only in the last 10 years that complex networks have attracted a lot of attention. Before then, an important source of ideas was the study of random graphs introduced in the 1960s by Paul Erdős and Alfréd Rényi [46–48] after they found that probabilistic methods were often useful in solving problems in graph theory. Random graphs are graphs in which the edges are distributed at random. Networks with a complex topology and unknown organising principles often appear random; thus random-graph theory is regularly used in the study of complex networks. A detailed review of the field of random graphs can be found in the classic book of Bollobás [15]. Here we briefly describe the most important results of random graph theory, focusing on the aspects that are of direct relevance to complex networks and used in the present thesis.

1.11.1 Erdős-Rényi (ER) Model

A random network is a model in which some parameters are fixed. Today the best known model of random networks is the one that was introduced by Erdős and Rényi in 1960. This model is called the Erdős-Rényi (ER) model and is sometimes called a ‘classical’ random network because of the emergence of “quantum” random graph models [52]. In this model we fix the number of vertices n and the number of edges m . This means we take n vertices and place m edges at random from $n(n-1)/2$ possible edges [93]. This model is often denoted by $G(n, m)$. An equivalent definition of the model is to say that the network is created by choosing a network uniformly at random from the set of all possible graphs with exactly n vertices and m edges. Therefore the random network model is defined as an ensemble of networks (and one element of the ensemble is called a realisation), i.e.

a probability distribution over possible networks. Thus the model $G(n, m)$ is seen as a probability distribution $P(G)$ over all graphs such that $P(G) = 1/\Omega$, where Ω is the total number of such graphs. Many properties of the $G(n, m)$ random graph are calculated by using an equivalent model. This model is called $G(n, p)$ or the Gilbert model [42, 93]. This model is defined by taking a fixed number n of vertices labelled $i = 1, \dots, n$ and interlinking them with a fixed probability p . Every element $G \in G(n, p)$ appears with the probability

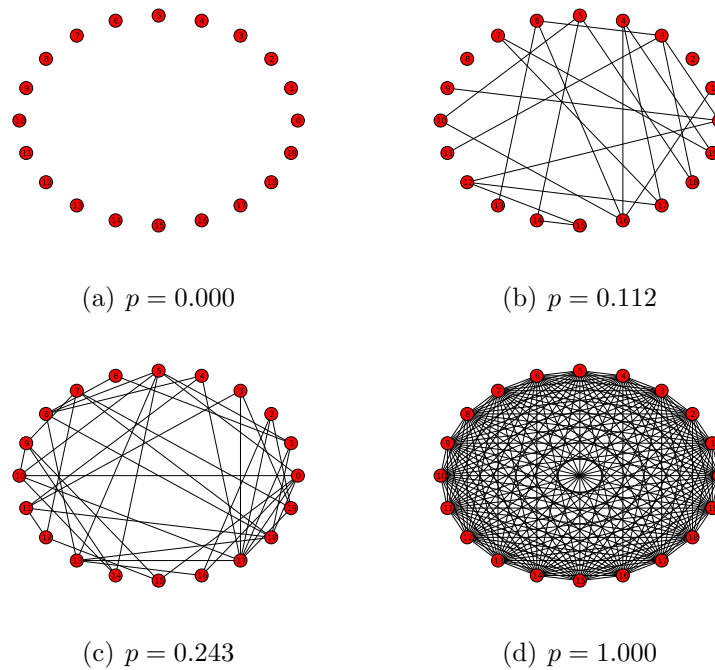


Figure 1.13: Illustrations of some realisations/configurations of Erdős-Rényi random networks with 20 nodes and different interlink probabilities (for each probability only one member of the ensemble $G(n, p)$ is shown).

$$P(G) = p^m(1 - p)^{\binom{n}{2} - m}, \quad (1.86)$$

where m is the number of edges in G . The probability of drawing a graph with m edges from the ensemble $G(n, p)$ is given by

$$P(m) = \binom{\binom{n}{2}}{m} (1-p)^{\binom{n}{2}-m}, \quad (1.87)$$

therefore the mean number of links or edges is given by

$$\bar{m} = \sum_{m=0}^{\binom{n}{2}} m P(m) = \frac{n(n-1)}{2} p. \quad (1.88)$$

The mean degree in $G(n, m)$ is $\bar{k} = \frac{2m}{n}$ and hence the mean degree in $G(n, p)$ is given by

$$\bar{k} = \sum_{m=0}^{\binom{n}{2}} \frac{2m}{n} P(m) = (n-1)p. \quad (1.89)$$

The degree k_i of a node i follows a binomial distribution with parameters $n-1$ and p , i.e.

$$p(k_i = k) = \binom{n-1}{k} p^k (1-p)^{n-1-k}. \quad (1.90)$$

This probability represents the number of ways in which k edges can be drawn from a certain node. To find the degree distribution of the graph, we need to study the number of nodes $n(k)$ with degree k . We need to find the probability that $n(k)$ takes a certain value, $p(n(k) = r)$. Using equation (1.90) we can find the expected number of nodes with degree k as follows:

$$E(n(k)) = n(k)p(k) = \lambda_k, \quad (1.91)$$

where

$$\lambda_k = \binom{n-1}{k} p^k (1-p)^{n-1-k}. \quad (1.92)$$

The distribution of $n(k)$ approaches the Poisson distribution for large n ($n \rightarrow \infty$):

$$p(n(k) = r) = \frac{\lambda_k^r}{r!} e^{-\lambda_k}. \quad (1.93)$$

The probability that any two vertices are neighbours of each other in a random graph is exactly the same and can be found from equation (1.89)

$$p = \frac{\bar{k}}{n-1}. \quad (1.94)$$

Therefore, the Watts-Strogatz clustering coefficient of an undirected Erdős-Rényi random network $G(n, p)$ is given by [17]:

$$\bar{C} = p = \frac{\bar{k}}{n-1}. \quad (1.95)$$

As we can see, this clustering coefficient tends to zero as n become very large. The clustering coefficient defined in equation (1.95) is also called the density of the network.

There is no known exact result for the average path length of this undirected network. A widely known scaling relationship [17, 116] can be used to provide qualitative guidance on how L changes with the network size and mean degree \bar{k} :

$$L \sim \frac{\log n}{\log \bar{k}}. \quad (1.96)$$

This scaling relationship says that for fixed mean degree, the average path length is expected to increase logarithmically with the network size. Less well known is an approximation to the average path length due to Fronczak et al. [60], which

states that for n sufficiently large and $k \ll n$,

$$L \simeq \frac{\log n - 0.557}{\log \bar{k}} + 0.5. \quad (1.97)$$

Although the theory of random graphs is elegant and simple, Erdős and many other authors in the social sciences [108–111] believed it corresponded to the fundamental truth. However, the real world interpreted as a network by current science are not aleatory. The established links between the nodes of various domains of reality follow fundamental natural laws. Despite the fact that some edges might be set up at random, and that they might play a non-negligible role, randomness is not the main feature in real networks. Therefore, the development of new models to capture real-life system's features other than randomness has motivated novel developments. Two of these new models occupy a prominent place in contemporary thinking about complex networks. Here we define and briefly discuss one of them.

1.11.2 Scale Free Networks

There are some real-world phenomena that small-world phenomena cannot capture, the most relevant one being evolution. (Small world models will be studied later on). In 1999, Barabási and Albert presented some data and formal work that has led to the construction of various scale-free models that, by focusing on the network dynamics, aim to offer a universal theory of network evolution [16]. Several empirical results demonstrate that many large networks are scale free, that is, their degree distribution follows a power law for large k . The important question is then: what is the mechanism responsible for the emergence of scale free networks? Answering this question requires a shift from modelling network topology to modelling the network assembly and evolution. While the goal of the former

models is to construct a graph with correct topological features, the modelling of scale-free networks will put the emphasis on capturing the network dynamics.

In the first place, the network models discussed up to now (random network) assume that graphs start with a fixed number n of vertices that are then randomly connected or rewired, without modifying n . In contrast, most real-world networks describe open systems that grow by the continuous addition of new nodes. Starting from a small nucleus of nodes, the number of nodes increases throughout the lifetime of the network by the subsequent addition of new nodes. For example, the World Wide Web grows exponentially in time by the addition of new web pages. Secondly, network models discussed so far assume that the probability that two nodes are connected is independent of the node's degrees, i.e. new edges are placed randomly. However, most real networks exhibit preferential attachment, such that the likelihood of connecting to a node depends on the node's degree. For example, a web page will be more likely to include hyperlinks to popular documents with already high degrees, because such highly connected documents are easy to find and are thus well known.

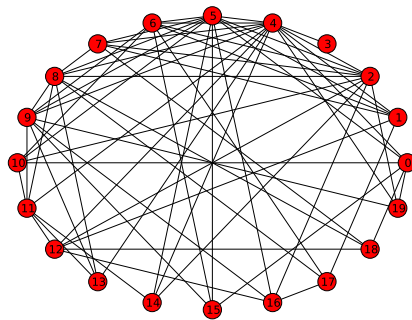


Figure 1.14: Example of a random network obtained with the preferential attachment method of Barabási and Albert with $n = 20$ and $d = 4$.

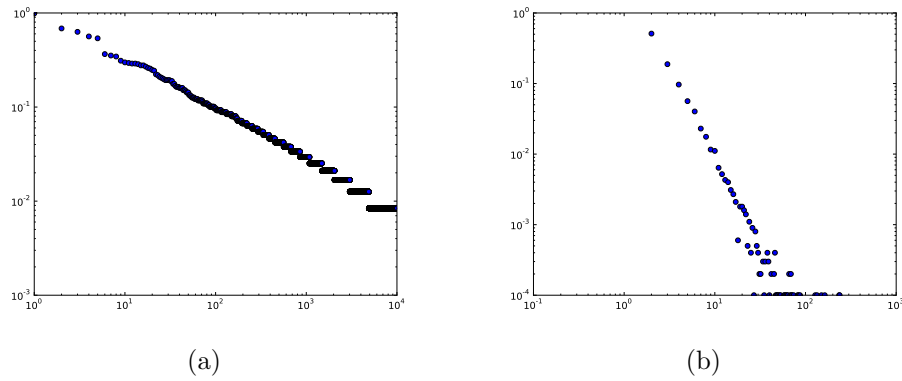


Figure 1.15: Cumulative degree distribution (a) and probability distribution (b) for a SF with $n = 10000$, constructed according to the BA model. For each node entering the network, 2 new edges are placed.

1.11.2.1 The Barabási-Albert (BA) Model

These two ingredients, growth and preferential attachment, inspired the introduction of the Barabási-Albert model (BA), which led for the first time to a network with a power-law degree distribution. The algorithm of the BA model is the following:

1. Growth: Starting with a small number (m_0) of nodes, at every time step, we add a new node with $m(\leq m_0)$ edges that links the new node to m different nodes already present in the system.
2. Preferential attachment: When choosing the nodes to which the new node connects, we assume that the probability \prod_i that a new node will be connected to node i depends on the degree k_i , such that

$$\prod_i = \frac{k_i}{\sum_j k_j}. \quad (1.98)$$

The Barabási and Albert (1999) network produces a network with the following approximate probability distribution for the degrees within the network:

$$p(k) = \frac{2m^2}{k^3}, \quad k = m, m + 1, \dots, n. \quad (1.99)$$

This power-law relationship conforms with the definition of scale-free introduced earlier, with $\gamma = 3$. However, this is only an approximation to the degree distribution which should be clear if one attempts to sum up $P(n)$ for all n , since the result will not be unity. An exact result for the degree distribution due to Dorogovtsev et al. [43] is that

$$p(k) = \frac{2m(m+1)}{k(k+1)(k+2)}, \quad k = m, m + 1, \dots, n. \quad (1.100)$$

For large k , i.e. when $k \rightarrow \infty$, we have that

$$p(k) \sim k^{-3} \quad (1.101)$$

which immediately implies that the cumulative degree distribution is given by

$$P(k) \sim k^{-2}. \quad (1.102)$$

Since the algorithm always adds m links at each of the $n - m_0$ steps, the total number of (undirected) links in the final network is always $m_0(m_0 - 1)/2 + m(n - m_0)$, and therefore the mean degree is [106]

$$\bar{k} = 2 \frac{0.5m_0(m_0 - 1) + m(n - m_0)}{n} = \frac{m_0(m_0 - 1) + 2m(n - m_0)}{n}, \quad (1.103)$$

and when $n \rightarrow \infty$, with m_0 small we get

$$\bar{k} \simeq 2m. \quad (1.104)$$

No exact expression for the average path length is known, however, the approximate scaling $L \sim (\log(n)/\log(\log(n)))$ is derived in [25] and the expression for the approximate pathlength

$$L \simeq \frac{\log(n) - \log(m/2) - 1 - 0.577}{\log(\log(n)) + \log(m/2)} + 1.5 \quad (1.105)$$

is derived in [60]. The clustering coefficient is not known exactly. It was shown in [3] that the clustering coefficient decreases with n , but less slowly than it decreases for an Erdős-Rényi network. Recently, the approximate expression for the clustering coefficient

$$\bar{C} \sim \frac{m \log(n)^2}{8n} \quad (1.106)$$

has been derived [75]. However, since the clustering coefficient decreases with n we can expect that the clustering coefficient will become close to zero as n increases.

Chapter 2

An Overview of Dynamical Systems

We find it necessary to review some notions on dynamical systems, as later in this thesis we will be dealing with dynamic processes on complex networks. We are not going to cover everything in this field, but we present some simple concepts that are relevant in some way to this thesis. Literature on the topic of dynamical systems is huge and here we just scratch its surface.

2.1 Dynamical Systems

A dynamical system is any system whose state, as represented by some set of quantitative variables, changes over time according to some given rules or equations. More precisely, a dynamical system is specified by a state vector $\mathbf{x} \in \mathbb{R}^n$ (a list of numbers which may change as time progress) and a function $f : \mathbb{R}^n \rightarrow \mathbb{R}^n$ which describes how the system evolves over time. There are two types of dynamical systems, continuous and discrete-time ones and they can be either deterministic

or stochastic. Discrete dynamical systems are specified by the equations:

$$\mathbf{y}_{t+1} = f(\mathbf{y}_t); \quad \mathbf{y}(0) = \mathbf{y}_0. \quad (2.1)$$

Dynamic system (2.1) is often called the difference equation. It thus follows that $\mathbf{y}_t = f^n(\mathbf{y}_0)$, where $f^n = f \circ f \circ \dots \circ f$ is the n -fold application of f to \mathbf{y}_0 . Continuous dynamical systems are specified by the equations:

$$\mathbf{y}'(t) = f(\mathbf{y}_t); \quad \mathbf{y}(0) = \mathbf{y}_0. \quad (2.2)$$

A deterministic dynamical system is that in which the equations that describe the time evolution are continuous functions. This includes for instance the epidemic models on populations that will be described in a separate chapter. On the other hand, the simulation of an epidemic, lets say SIS, on a network is stochastic because of the probabilistic aspect that a susceptible node can be infected by an infected node. Time may be represented in discrete time-steps or continuous time steps depending on the choice of the researchers. We will be focusing later on discrete dynamical systems on networks. In this chapter we simply review concepts of one-dimensional and multi-dimensional first order discrete dynamical systems that will be useful later in this thesis.

2.1.1 One-Dimensional First-Order Discrete Dynamical Systems

Linear Systems

In this section we study dynamical systems in which the function f is particularly nice: we assume f is linear and to gain intuition we begin with the case where f

is a function of only one variable. Let consider the one-dimensional, autonomous, first-order, linear difference equation

$$y_{t+1} = ay_t + b; \quad t = 0, 1, 2, \dots, \infty, \quad (2.3)$$

where the *state variable* at time t , y_t , is one-dimensional, $y_t \in \mathbb{R}$, the parameters a and b are constant across time (i.e., the dynamical system is autonomous), $a, b \in \mathbb{R}$, and the initial value of the state variable at time $t = 0$, y_0 , is given.

The Solution

A solution to the difference equation $y_{t+1} = ay_t + b$ is a *trajectory* (or *orbit* or a *curve*), $\{y_t\}_{t=0}^{\infty}$, that satisfies this equation at any point in time. It relates the value of the state variable at time t , y_t , to the initial condition y_0 and to the parameters a and b . The derivation of a solution may follow several methods. In particular the intuitive method of iterations generates a pattern that can be easily generalised to a solution rule. Given the value of the state variable at $t = 0$

$$\begin{aligned} y_1 &= ay_0 + b; \\ y_2 &= ay_1 + b = a(ay_0 + b) + b = a^2y_0 + ab + b; \\ y_3 &= ay_2 + b = a(a^2y_0 + ab + b) + b = a^3y_0 + a^2b + ab + b; \\ &\vdots \\ y_t &= a^t y_0 + a^{t-1}b + a^{t-2}b + \dots + ab + b \\ &= a^t y_0 + b \sum_{j=0}^{t-1} a^j. \end{aligned} \quad (2.4)$$

Since $\sum_{j=0}^{t-1} a^j$ is the sum of a geometric series, it follows that

$$y_t = \begin{cases} a^t y_0 + b \frac{1-a^t}{1-a} & \text{if } a \neq 1 \\ y_0 + bt & \text{if } a = 1, \end{cases} \quad (2.5)$$

or

$$y_t = \begin{cases} \left(y_0 + \frac{b}{1-a}\right) a^t + \frac{b}{1-a} & \text{if } a \neq 1 \\ y_0 + bt & \text{if } a = 1. \end{cases} \quad (2.6)$$

Therefore, if the initial condition of the state variable is given, the trajectory of the dynamical system is uniquely determined. The trajectory given by (2.6) reveals the qualitative role that the parameters a and b play in the evolution of the state variable over time. These parameters determine whether the dynamical system evolves monotonically or in oscillations, and whether the state variable diverges, or converges in the long-run to either a stationary state or a periodic orbit.

Existence of Stationary Equilibria

Steady-state equilibria provide an essential reference point for a qualitative analysis of the behaviour of dynamical systems. A *steady-state equilibrium* (or alternatively, a *stationary equilibrium*, a *rest point*, an *equilibrium point*, or a *fixed point*) is a value of the state variable y_t that is invariant under further iterations of the dynamical system. More precisely,

Definition 2.1.1 A *Steady-state equilibrium* of the difference equation $y_{t+1} = ay_t + b$ is a value $\bar{y} \in \mathbb{R}$, such that

$$\bar{y} = a\bar{y} + b. \quad (2.7)$$

Then,

$$\bar{y} = \begin{cases} \frac{b}{1-a} & \text{if } a \neq 1 \\ y_0 & \text{if } a = 1 \text{ and } b=0. \end{cases} \quad (2.8)$$

When $a = 1$ and $b \neq 0$ a steady-state equilibrium does not exist. Hence, the necessary and sufficient conditions for the existence of a steady-state equilibrium are as follows:

Proposition 2.1.2 *A Steady-state equilibrium of the difference equation $y_{t+1} = ay_t + b$ exists if and only if*

$$\{a \neq 1\} \text{ or } \{a = 1 \text{ and } b = 0\} \quad (2.9)$$

Using expression (2.8), the solution to the difference equation derived in (2.4) can be written in terms of the deviation of the initial value of the state variable from its steady-state value:

$$y_t = \begin{cases} (y_0 - \bar{y})a^t + \bar{y} & \text{if } a \neq 1 \\ y_0 + bt & \text{if } a = 1. \end{cases} \quad (2.10)$$

Uniqueness of Steady-State Equilibrium

A steady state of a linear dynamical system is not necessarily unique. As can be seen in Figure 2.1 (a),(b),(c) and (d) for $a \neq 1$, the steady-state equilibrium is unique, whereas as shown in Figure 2.1 (e), for $a = 1$ and $b = 0$, a continuum for steady-state equilibria exists and the system remains where it starts.

Proposition 2.1.3 *A steady-state equilibrium of the difference equation $y_{t+1} = ay_t + b$ is unique if and only if [118]*

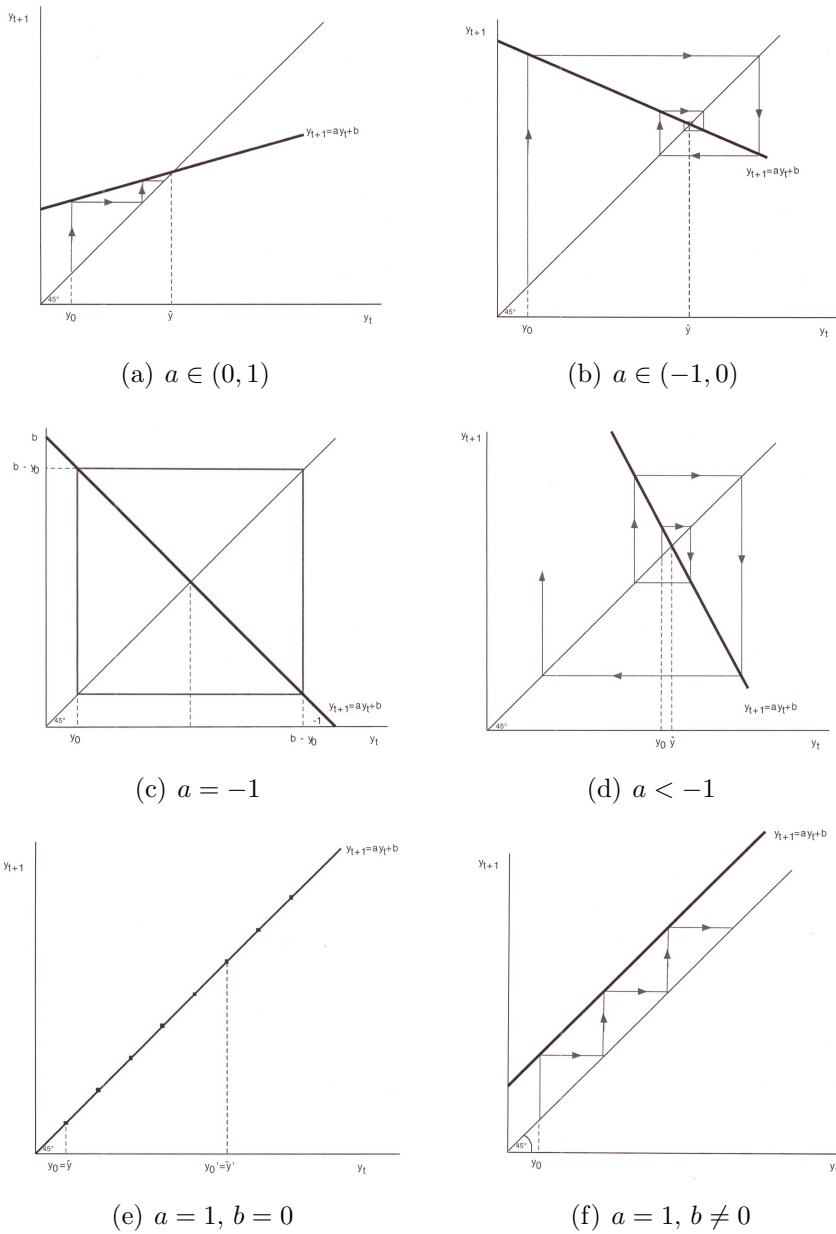


Figure 2.1: Unique, globally stable, steady-state, equilibrium (monotonic convergence) (a), Unique, globally stable, steady-state equilibrium (oscillatory convergence) (b), two periodic cycles (c), Unique and unstable steady-state equilibrium (oscillatory divergence) (d), Continuum of unstable steady-state equilibrium (e), Continuum of unstable steady-state equilibrium (f).

$$a \neq 1.$$

Stability of the Steady-State Equilibrium

The stability analysis of steady-state equilibria determines the nature of a steady-state equilibrium (e.g., attractive, repulsive, etc.). It facilitates the study of the local, and often the global, behaviour of a dynamical system, and it permits the analysis of the implications of small, and often large, perturbations that occur once the system is in the vicinity of a steady-state equilibrium. If for a sufficiently small perturbation the dynamical system converges asymptotically to the original equilibrium, the system is locally stable, whereas if regardless of the magnitude of the perturbation the system converges asymptotically to the original equilibrium, the system is globally stable. Formally the definition of local and global stability are as follows

Definition 2.1.4 *A steady-state equilibrium, \bar{y} of the difference equation $y_{t+1} = ay_t + b$ is*

1. *globally (asymptotically) stable, if*

$$\lim_{t \rightarrow \infty} y_t = \bar{y} \quad \forall y_0 \in \mathbb{R}$$

2. *locally (asymptotically) stable if*

$$\exists \epsilon > 0 \quad \text{such that} \quad \lim_{t \rightarrow \infty} y_t = \bar{y} \quad \forall y_0 \in B_\epsilon(\bar{y}).$$

Thus, a steady-state equilibrium is *globally* (asymptotically) stable if the system converges to the steady-state equilibrium regardless of the level of the initial condition, whereas a steady-state equilibrium is *locally* (asymptotically) stable if there

exists an ϵ -neighbourhood of the steady-state equilibrium such that for every initial condition within this neighbourhood the system converges to this steady-state equilibrium. Clearly, the existence of a globally unique steady-state equilibrium necessitates the absence of any additional steady-state equilibrium (i.e., the absence of any point in the space from which there is no escape.)

Corollary 2.1.5 *A steady-state equilibrium, \bar{y} , of the difference equation $y_{t+1} = ay_t + b$ is globally (asymptotically) stable only if the steady-state equilibrium is unique [118].*

Following equation (2.10)

$$\lim_{t \rightarrow \infty} y_t = \begin{cases} (y_0 - \bar{y}) \lim_{t \rightarrow \infty} a^t + \bar{y} & \text{if } a \neq 1; \\ y_0 + b \lim_{t \rightarrow \infty} t & a = 1, \end{cases} \quad (2.11)$$

and therefore

$$\lim_{t \rightarrow \infty} |y_t| = \begin{cases} \bar{y} & \text{if } |a| < 1; \\ y_0 & \text{if } a = 1; b = 0; \\ \begin{cases} y_0 & (t = 0, 2, 4, \dots) \\ (b - y_0) & (t = 1, 3, 5 \dots) \end{cases} & \text{if } a = -1; \\ \bar{y} & \text{if } |a| > 1 \text{ and } y_0 = \bar{y}; \\ \infty & \text{otherwise.} \end{cases} \quad (2.12)$$

Discussions

1. if $|a| < 1$, then the system is globally (asymptotically) stable, converging to the steady-state equilibrium $\bar{y} = b/(1 - a)$ regardless of the initial condition y_0 . In particular, if $a \in (0, 1)$ then the system, as show in Figure 2.1 (a),

is characterised by monotonic convergence, whereas if $a \in (-1, 0)$, then as shown in Figure 2.1(b), the convergence is oscillatory. Further, we call \bar{y} an *attractive* or stable fixed point because the system is attracted to this point.

2. if $a = 1$ and $b = 0$, the system, as shown in Figure 2.1 (e), is neither globally stable nor locally (asymptotically) stable. The system is characterised by a continuum of steady equilibria. Each equilibria can be reached if and only if the system starts at this equilibrium. Thus, the equilibria are unstable.
3. if $a = 1$ and $b \neq 0$, the system has no steady-state equilibrium, as shown in Figure 2.1 (f) $\lim_{t \rightarrow \infty} y_t = +\infty$ if $b > 0$ and $\lim_{t \rightarrow \infty} y_t = -\infty$ if $b < 0$.
4. if $a = -1$, then the system, as seen in Figure 2.1 (c) is characterised by (an asymptotically unstable) two-period cycle, and the unique steady-state equilibrium, $\bar{y} = b/2$, is (asymptotically) unstable.
5. if $|a| > 1$ then the system, as shown in Figure 2.1 (d) and (f), is unstable. For $y_0 \neq b/(1 - a)$, $\lim_{t \rightarrow \infty} y_t = +\infty$, whereas for $y_0 = b/(1 - a)$ the system starts at the steady-state equilibrium where it remains thereafter. Every minor perturbation, however, causes the system to step on a diverging path. If $a > 1$ the divergence is monotonic whereas if $a < -1$ the divergence is oscillatory.

Proposition 2.1.6 *A steady-state equilibrium of the difference equation $y_{t+1} = ay_t + b$ is globally stable if and only if*

$$|a| < 1.$$

2.2 Non-linear System

Let us consider the one-dimensional first-order non-linear equation

$$y_{t+1} = f(y_t); \quad t = 0, 1, 2, \dots, \infty, \quad (2.13)$$

where $f : \mathbb{R} \rightarrow \mathbb{R}$ is a differential single-variable function and the initial value of the state variable, y_0 , is given.

The Solution

Using the method of iterations, the trajectory of the non-linear system, $\{y_t\}_{t=0}^{\infty}$ can be written as follows:

$$\begin{aligned} y_1 &= f(y_0); \\ y_2 &= f(y_1) = f(f(y_0)) \equiv f^2(y_0); \\ &\vdots \\ y_t &= f^t(y_0) \end{aligned} \quad (2.14)$$

Unlike the solution to the linear system (2.3), the solution for the non-linear system (2.14) is not very informative. Hence, additional methods of analysis are required in order to gain an insight about the qualitative behaviour of this non-linear system. In particular, a local approximation of the non-linear system by a linear one is instrumental in the study of the qualitative behaviour of non-linear dynamical systems [118].

Existence, Uniqueness and Multiplicity of Stationary Equilibria

Definition 2.2.1 A steady-state equilibrium of the difference equation $y_{t+1} = f(y_t)$ is a level $\bar{y} \in \mathbb{R}$ such that

$$\bar{y} = f(\bar{y}). \quad (2.15)$$

Generically, a non-linear system can be characterised by either the existence of a unique steady-state equilibrium, the non-existence of a steady-state equilibrium, or the existence of a multiplicity of (distinct) steady-state equilibria. Figure 2.2 (a) shows a system with a globally stable unique steady-state equilibrium, whereas Figure 2.2 (b) depicts a system with multiple distinct steady-state equilibria.

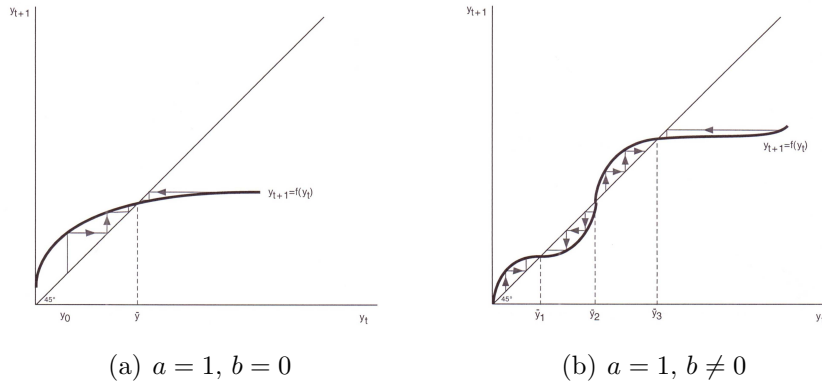


Figure 2.2: Unique and globally stable steady-state equilibrium (a), Multiple locally stable steady-state equilibria (b).

Linearisation and Local Stability of Steady-State Equilibria

The behaviour of a non-linear system around a steady-state equilibrium, \bar{y} , can be approximated by a linear system. Consider the Taylor expansion of $y_{t+1} = f(y_t)$ around \bar{y} . Namely,

$$y_{t+1} = f(y_t) = f(\bar{y}) + f'(\bar{y})(y_t - \bar{y}) + \frac{f''(\bar{y})(y_t - \bar{y})^2}{2!} + \dots + R_n. \quad (2.16)$$

The linearised system around the steady-state equilibrium \bar{y} is therefore

$$\begin{aligned} y_{t+1} &= f(\bar{y}) + f'(\bar{y})(y_t - \bar{y}) \\ &= f'(\bar{y})y_t + f(\bar{y}) - f'(\bar{y})\bar{y} \\ &= ay_t + b, \end{aligned} \tag{2.17}$$

where, $a = f'(\bar{y})$ and $b = f(\bar{y}) - f'(\bar{y})\bar{y}$ are given constants. Applying the stability results established for the linear system, the linearised system is globally stable if $|a| \equiv |f'(\bar{y})| < 1$. However, since the linear system approximates the behaviour of the non-linear system only in a neighbourhood of a steady-state equilibrium, the global stability of the linearised system implies only the local stability of the non-linear difference equation. Thus, the following proposition is established:

Proposition 2.2.2 *The dynamical system $y_{t+1} = f(y_t)$ is locally stable around the steady-state equilibrium \bar{y} , if and only if*

$$\left| \frac{dy_{t+1}}{dy_t} \right| < 1.$$

Consider Figure 2.2 (b) where the dynamical system is characterised by four steady-state equilibria. Since $f_0(y_1) < 1$ and $f_0(y_3) < 1$, then y_1 and y_3 are locally stable steady-state equilibria.

2.2.1 Multi-Dimensional First-Order Systems

Linear-System

Consider a system of autonomous, first-order, linear difference equations

$$z_{t+1} = Nz_t + M, \quad t = 0, 1, 2, \infty, \tag{2.18}$$

where the state variable z_t is an n -dimensional vector; $z_t \in \mathbb{R}^n$, N is a $n \times n$ matrix of parameters which are constant across time; $N = (n_{ij})$, $n_{ij} \in \mathbb{R}$, $\forall i, j = 1, 2, \dots, n$, and M is a n -dimensional column vector of constant parameters. The initial value of the state variable z_0 is given.

The Solution

A solution to the multi-dimensional linear system $z_{t+1} = Nz_t + M$ is a trajectory $\{z_t\}_{t=0}^{\infty}$ of the vector $\{z_t\}$ that satisfies this equation at any point in time and relates the value of the state variable at time t , z_t to the initial condition z_0 and the set of parameters embodied in the vector M and the matrix N . Given the value of the state variable at time 0, z_0 , the method of iterations generates a pattern that constitutes a general solution:

$$\begin{aligned} z_1 &= Nz_0 + M; \\ z_2 &= Nz_1 + M = N(Nz_0 + M) + M = N^2z_0 + NM + M; \\ z_3 &= Nz_2 + M = N(N^2z_0 + NM + M) + M = N^3z_0 + N^2M + NM + M; \\ &\vdots \\ z_t &= N^t z_0 + N^{t-1}M + N^{t-2}M + \dots + NM + M \\ &= N^t z_0 + \sum_{j=0}^{t-1} N^j M. \end{aligned}$$

Unlike the one-dimensional case, the solution depends on the sum of a geometric series of matrices rather than of scalars.

Lemma 2.2.3 *Let N be a matrix such that $|I - N| \neq 0$. Then*

$$\sum_{j=0}^{t-1} N^j = (I - N^t)(I - N)^{-1}.$$

proof 2.2.4 *We have that*

$$\sum_{j=0}^{t-1} N^j (I - N) = I + N + N^2 + \cdots + N^{t-1} - (N + N^2 + N^3 + \cdots + N^t) = I - N^t.$$

Hence, post multiplication of both sides of the equation by the matrix $(I - N)^{-1}$ establishes the lemma.

By Lemma 2.2.3 it follows that

$$z_t = N^t(z_0 - (I - N)^{-1}M) + (I - N)^{-1}M \quad \text{if } |I - N| \neq 0. \quad (2.19)$$

As will be shown below, the qualitative behaviour of the solution will be determined by the parameters of the matrix N .

Existence and Uniqueness of Stationary Equilibria

Definition 2.2.5 *A steady-state equilibrium of a system of difference equations $z_{t+1} = Nz_t + M$ is a vector \bar{z} such that*

$$\bar{z} = N\bar{z} + M. \quad (2.20)$$

Following the definition, in analogy to the analysis of the one-dimensional system, there exists a unique steady-state equilibrium

$$\bar{z} = (I - N)^{-1}M \quad \text{if } |I - N| \neq 0. \quad (2.21)$$

Analogous to Proposition 2.1.3, the following result concerning the uniqueness of steady-state equilibrium holds:

Proposition 2.2.6 *A steady-state equilibrium of the system $z_{t+1} = Nz_t + M$ is*

unique if and only if

$$|I - N| \neq 0. \quad (2.22)$$

Remark 2.2.7 *The necessary and sufficient condition for uniqueness is the non-singularity of the matrix $I - N$. It is analogous to the requirement that $a \neq 1$ in the one-dimensional case.*

Using (2.21), we can write the solution of the system in the form

$$z_t = N^t(z_0 - \bar{z}) + \bar{z} \quad \text{if } |I - N| \neq 0. \quad (2.23)$$

Results from Linear Algebra

Details of those results can be found in [7, 86].

Lemma 2.2.8 *Let N be an $n \times n$ matrix where $n_{ij} \in \mathbf{R}^n$, $i, j = 1, 2, \dots, n$. Then, there exists a $n \times n$ non-singular matrix Q such that $N = QDQ^{-1}$, where*

-

$$D = \begin{pmatrix} D_1 & 0 & 0 & \cdots & 0 & 0 \\ 0 & D_2 & 0 & \cdots & 0 & 0 \\ 0 & 0 & D_3 & \cdots & 0 & 0 \\ 0 & 0 & 0 & \cdots & 0 & 0 \\ 0 & 0 & 0 & \cdots & 0 & 0 \\ 0 & 0 & 0 & \cdots & 0 & D_m \end{pmatrix}$$

is the Jordan matrix and Q is an $n \times n$ matrix whose columns are the eigenvectors of N .

- *For distinct real eigenvalues:*

$$D_i = \lambda_i,$$

where

$$y_{1t} = \lambda_1^t y_{10}$$

and

$$y_{2t} = \lambda_2^t y_{20}.$$

The phase diagram of this dynamical system depends upon the sign of the eigenvalues, their relative magnitude, and their absolute value relative to unity. We only summarise the results for the case of real eigenvalues. More can be found in [118].

1. Positive Eigenvalues:

- Stable Node: $0 < \lambda_2 < \lambda_1 < 1$. See Figure 2.3 (a).

The steady-state equilibrium is globally stable. Namely, $\lim_{t \rightarrow \infty} y_{1t} = 0$ and $\lim_{t \rightarrow \infty} y_{2t} = 0$, $\forall (y_{10}, y_{20}) \in \mathbb{R}^2$. The convergence to the steady-state equilibrium is monotonic. However, since $\lambda_2 < \lambda_1$ the convergence of y_{2t} is faster.

- Saddle : $0 < \lambda_2 < 1 < \lambda_1$. See Figure 2.3 (b).

The steady-state equilibrium is a saddle point. Namely, $\lim_{t \rightarrow \infty} y_{2t} = 0$ $\forall y_{20} \in \mathbb{R}$, whereas $\lim_{t \rightarrow \infty} y_{1t} = 0$ if and only if $y_{10} = 0$. The convergence along the saddle path (i.e., the stable eigenspace or alternatively, the stable manifold) is monotonic.

- Focus: $0 < \lambda_1 = \lambda_2 < 1$. See Figure 2.3 (c).

The steady-state equilibrium is globally stable. Namely, $\lim_{t \rightarrow \infty} y_{1t} = 0$ and $\lim_{t \rightarrow \infty} y_{2t} = 0$, $\forall (y_{10}, y_{20}) \in \mathbb{R}^2$. Convergence is monotonic and the speed

of convergence is the same for each variable. Consequently every trajectory can be placed along a linear curve.

- Source: $1 < \lambda_1 < \lambda_2$. See Figure 2.3 (d).

The steady-state equilibrium is unstable. Namely, $\lim_{t \rightarrow \infty} y_{1t} = \mp \infty$ and $\lim_{t \rightarrow \infty} y_{2t} = \mp \infty$, $\forall (y_{10}, y_{20}) \in \mathbb{R}^2 - \{0\}$. The divergence is monotonic. However, since $\lambda_2 > \lambda_1$ the divergence of y_{2t} is faster.

2. Negative Eigenvalues:

- Stable Node (oscillating convergence): $-1 < \lambda_2 < \lambda_1 < 0$.

The steady-state equilibrium is globally stable. The convergence of both variables towards the steady-state equilibrium is oscillatory. Since $\lambda_2 < \lambda_1$ the convergence of y_{2t} is faster.

- Saddle (oscillatory convergence/divergence) $\lambda_2 < -1 < \lambda_1 < 0$.

The steady-state equilibrium is a saddle. The convergence along the saddle path is oscillatory. Other than along the stable and the unstable manifolds, one variable converges in an oscillatory manner while the other variable diverges in an oscillatory manner.

- Focus (oscillatory convergence): $-1 < \lambda_1 = \lambda_2 < 0$.

The steady-state equilibrium is globally stable. Convergence is oscillatory.

- Source (oscillatory divergence): $\lambda_2 < \lambda_1 < -1$.

The steady-state equilibrium is unstable. Divergence is oscillatory.

3. Mixed Eigenvalues (one positive and one negative eigenvalue): one variable converges (diverges) monotonically while the other is characterised by oscillatory convergence (divergence). Iterations are therefore reflected around one of the axes.

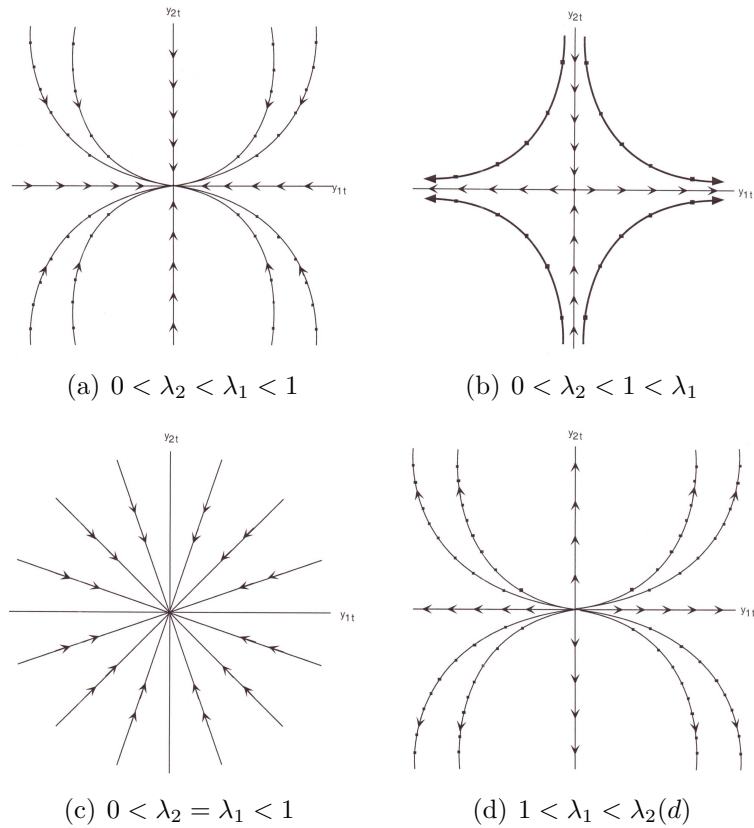


Figure 2.3: Stable node (a), Saddle node (b), Focus (c), Source (d)

Stable and Unstable Eigenspaces

In a linear system the stable eigenspace relative to the steady-state equilibrium \bar{x} , is defined as

$$E^s(\bar{x}) = \text{span}\{\text{eigenvectors whose eigenvalues are of modulus smaller than } 1\}.$$

In an homogeneous two-dimensional autonomous linear system, $x_{t+1} = \mathbf{A}x_t$, the eigenspace is

$$E^s(\bar{x}) = \{(x_{1t}, x_{2t}) \mid \lim_{n \rightarrow \infty} \mathbf{A}^n \mathbf{x}_t = \bar{\mathbf{x}}\}. \quad (2.24)$$

Namely, the stable eigenspace is the geometric locus of all pairs (x_{1t}, x_{2t}) that upon a sufficient number of forward iterations are mapped in the limit towards the steady-state equilibrium, \bar{x} .

The unstable eigenspace relative to the steady-state equilibrium \bar{x} , is defined as

$$E^u(\bar{x}) = \text{span}\{\text{eigenvectors whose eigenvalues are of modulus greater than } 1\}.$$

In an homogeneous two-dimensional autonomous linear system, $x_{t+1} = \mathbf{A}x_t$,

$$E^u(\bar{x}) = \{(x_{1t}, x_{2t}) \mid \lim_{n \rightarrow \infty} \mathbf{A}^{-n} \mathbf{x}_t = \bar{\mathbf{x}}\}. \quad (2.25)$$

That is, the unstable eigenspace is the geometric locus of all pairs (x_{1t}, x_{2t}) that upon a sufficient number of backward iterations are mapped in the limit to the steady-state equilibrium .

The Solution in Terms of the Jordan Matrix

It is desirable to express the solution to the multi-dimensional, first-order, linear system, $z_{t+1} = Nz_t + M$, in terms of the Jordan Matrix. This reformulation of the solution facilitates the analysis of the qualitative nature of the multi-dimensional system.

Proposition 2.2.9 *A non-homogeneous system of first-order linear difference equa-*

tions of the form

$$z_{t+1} = Nz_t + M \quad (2.26)$$

can be transformed into an homogeneous system of first-order linear difference equations $u_{t+1} = Nu_t$, where $u_t = z_t - \bar{z}$ and $\bar{z} = (I - N)^{-1}M$ with $I - N \neq 0$

proof 2.2.10 Given that $z_{t+1} = Nz_t + M$ and $u_t = z_t - \bar{z}$, it follows that

$$u_{t+1} = N(z_t + \bar{z}) + M - \bar{z} = Nz_t - (I - N)\bar{z} + M.$$

Therefore, since $\bar{z} = (I - N)^{-1}M$,

$$u_{t+1} = Nu_t.$$

Thus, the non-homogeneous system is transformed into a homogeneous one by shifting the origin of the non-homogeneous system to the steady-state equilibrium.

Proposition 2.2.11 *The solution of a non-homogeneous first-order linear difference equations*

$$z_{t+1} = Nz_t + N \quad (2.27)$$

is

$$z_t = QD^tQ^{-1}(z_0 - \bar{z}) + \bar{z}, \quad (2.28)$$

where D is the Jordan matrix corresponding to N .

Stability

In order to analyse the qualitative behaviour of the dynamical system a distinction will be made among four possible cases each defined in terms of the corresponding

nature of the eigenvalues: (1) distinct real eigenvalues, (2) repeated real eigenvalues, (3) distinct complex eigenvalues, and (4) repeated complex eigenvalues. We only look at the case where the matrix N has n distinct real eigenvalues.

The matrix N has n distinct real eigenvalues

Consider the system

$$z_{t+1} = Nz_t + M.$$

As established in Lemma 2.2.8 and equation (2.28), if N has n distinct eigenvalues $\{\lambda_1, \lambda_2, \dots, \lambda_n\}$, then there exists a non-singular matrix Q , such that

$$z_t = Qu_t + \bar{z}.$$

Furthermore,

$$u_{t+1} = Du_t,$$

where

$$D = \begin{pmatrix} \lambda_1 & & & 0 \\ & \lambda_2 & & \\ & & \dots & \\ 0 & & & \lambda_n \end{pmatrix}.$$

Following the method of iterations

$$u_t = D^t u_0$$

where

$$D^t = \begin{pmatrix} \lambda_1^t & & 0 \\ & \lambda_2^t & \\ & & \cdots \\ 0 & & & \lambda_n^t \end{pmatrix}$$

and therefore,

$$\begin{aligned} u_{1t} &= \lambda_1^t u_{10} \\ u_{2t} &= \lambda_2^t u_{20} \\ &\vdots \\ u_{nt} &= \lambda_n^t u_{n0}. \end{aligned} \tag{2.29}$$

Since

$$z_t = Qu_t + \bar{z},$$

it follows that

$$\begin{pmatrix} z_{1t} \\ z_{2t} \\ \vdots \\ z_{nt} \end{pmatrix} = \begin{pmatrix} Q_{11} & Q_{12} & \cdots & Q_{1n} \\ Q_{21} & Q_{22} & \cdots & Q_{2n} \\ \vdots & & & \\ Q_{n1} & Q_{n2} & \cdots & Q_{nn} \end{pmatrix} \begin{pmatrix} \lambda_1^t u_{10} \\ \lambda_2^t u_{20} \\ \vdots \\ \lambda_n^t u_{n0} \end{pmatrix} + \begin{pmatrix} \bar{z}_1 \\ \bar{z}_2 \\ \vdots \\ \bar{z}_n \end{pmatrix},$$

and therefore

$$z_{it} = \sum_{j=1}^n K_{ij} \lambda_j^t + \bar{z}_i \quad \forall i = 1, 2, \dots, n, \tag{2.30}$$

where $K_{ij} = Q_{ij} u_{j0}$.

Equation (2.30) provides the general solution for z_{it} in terms of the eigenvalues $\lambda_1, \dots, \lambda_n$, the initial conditions $u_{10}, u_{20}, \dots, u_{n0}$, and the steady-state value z_i .

It sets the stage for the stability result stated in the following main theorem.

Theorem 2.2.12 *Consider the system $z_{t+1} = Nz_t + M$, where $z_t \in \mathbb{R}^n$ and z_0 is given. Suppose that $|I - N| \neq 0$ and N has n distinct real eigenvalues $\{\lambda_1, \dots, \lambda_n\}$. Then,*

- *the steady-state equilibrium $\bar{z} = (I - N)^{-1}M$ is globally stable if and only if*

$$|\lambda_j| < 1, \forall j = 1, 2, \dots, n;$$

- *$\lim_{t \rightarrow \infty} z_t = \bar{z}$ if and only if $\forall j = 1, 2, \dots, n$*

$$\{|\lambda_j| < 1 \text{ or } z_{j0} = 0\},$$

where $u_0 = Q^{-1}(z_0 - \bar{z})$, and Q is a non-singular $n \times n$ matrix whose columns are the eigenvectors of the matrix N .

proof 2.2.13 *The steady-state equilibrium is globally stable if $\forall z_0 \in \mathbb{R}^n \lim_{t \rightarrow \infty} z_{it} = \bar{z}_i$ for $\forall i = 1, 2, \dots, n$, thus it follows from equation (2.30) that global stability is satisfied if and only if $\forall k_{ij} \in \mathbb{R} \lim_{t \rightarrow \infty} \sum_j K_{ij} \lambda_j^t = 0$, namely if and only if $|\lambda_j| < 1 \forall j = 1, 2, \dots, n$. As follows from equation (2.30) $\lim_{t \rightarrow \infty} z_{it} = \bar{z}_i$ if and only if either $|\lambda_j| < 1$, or $\{|\lambda_j| \geq 1 \text{ and } z_{j0} = 0\} \forall j = 1, 2, \dots, n$. Thus the second part follows as well.*

2.2.2 Non-Linear System

Let us consider the system of autonomous nonlinear first-order difference equations

$$z_{t+1} = \theta(z_t); \quad t = 0, 1, 2, \dots, \infty, \quad (2.31)$$

where

$$\theta : \mathbb{R}^n \rightarrow \mathbb{R}^n,$$

and the initial value of the n -dimensional state variable vector, z_0 , is given. Namely,

$$\begin{aligned} z_{1t+1} &= \theta^1(z_{1t}, z_{2t}, \dots, z_{nt}) \\ z_{2t+1} &= \theta^2(z_{1t}, z_{2t}, \dots, z_{nt}) \\ &\vdots \\ z_{nt+1} &= \theta^n(z_{1t}, z_{2t}, \dots, z_{nt}). \end{aligned} \tag{2.32}$$

Local Analysis

Suppose that the dynamical system has a steady-state equilibrium, \bar{z} . Namely $\exists \bar{z} \in \mathbb{R}^n$ such that $\bar{z} = \theta(\bar{z})$. A Taylor expansion of the i^{th} equation, $z_{it+1} = \theta^i(z_t)$, around the steady-state value, z , yields

$$z_{it+1} = \theta^i(z_t) = \theta^i(\bar{z}) + \sum_{j=1}^n \theta_j^i(\bar{z})(z_{jt} - \bar{z}) + \dots + R_n, \tag{2.33}$$

where $\theta_j^i(\bar{z})$ is the partial derivative of $\theta^i(\bar{z})$ with respect to z_{jt} , evaluated at \bar{z} .

Thus, the linearised equation around the steady-state \bar{z} is given by

$$z_{it+1} = \theta_1^i(\bar{z})z_{1t} + \theta_2^i(\bar{z})z_{2t} + \dots + \theta_n^i(\bar{z})z_{nt} + \theta^i(\bar{z}) - \sum_{j=1}^n \theta_j^i(\bar{z})\bar{z}_j. \tag{2.34}$$

The linearised system is therefore:

$$\begin{pmatrix} z_{1t+1} \\ z_{2t+1} \\ \vdots \\ z_{nt+1} \end{pmatrix} = \begin{pmatrix} \theta_1^1(\bar{z}) & \theta_1^2(\bar{z}) & \cdots & \theta_1^n(\bar{z}) \\ \theta_2^1(\bar{z}) & \theta_2^2(\bar{z}) & \cdots & \theta_2^n(\bar{z}) \\ \vdots & \vdots & & \vdots \\ \theta_n^1(\bar{z}) & \theta_n^2(\bar{z}) & \cdots & \theta_n^n(\bar{z}) \end{pmatrix} \begin{pmatrix} z_{1t} \\ z_{2t} \\ \vdots \\ z_{nt} \end{pmatrix} + \begin{pmatrix} \theta^1(\bar{z}) - \sum_j^n \theta_j^1(\bar{z})\bar{z}_j \\ \theta^2(\bar{z}) - \sum_j^n \theta_j^2(\bar{z})\bar{z}_j \\ \vdots \\ \theta^n(\bar{z}) - \sum_j^n \theta_j^n(\bar{z})\bar{z}_j \end{pmatrix}.$$

Thus, the non-linear system has been approximated, locally (around a steady-state equilibrium) by a linear system,

$$z_{t+1} = Nz_t + M, \quad (2.35)$$

where

$$\mathcal{D}\theta(\bar{z}) = \frac{\partial \theta_i}{\partial z_j}(\bar{z}) = \begin{pmatrix} \theta_1^1(\bar{z}) & \theta_1^2(\bar{z}) & \cdots & \theta_1^n(\bar{z}) \\ \theta_2^1(\bar{z}) & \theta_2^2(\bar{z}) & \cdots & \theta_2^n(\bar{z}) \\ \vdots & \vdots & & \vdots \\ \theta_n^1(\bar{z}) & \theta_n^2(\bar{z}) & \cdots & \theta_n^n(\bar{z}) \end{pmatrix} = N$$

is the Jacobian matrix of $\theta(z_t)$ evaluated at \bar{z} , and

$$M = \begin{pmatrix} \theta^1(\bar{z}) - \sum_j^n \theta_j^1(\bar{z})\bar{z}_j \\ \theta^2(\bar{z}) - \sum_j^n \theta_j^2(\bar{z})\bar{z}_j \\ \vdots \\ \theta^n(\bar{z}) - \sum_j^n \theta_j^n(\bar{z})\bar{z}_j \end{pmatrix}.$$

As is established in the previous theorem, the local behaviour of the nonlinear dynamical system can be assessed on the basis of the behaviour of the linear system that approximates the nonlinear one in the vicinity of the steady-state equilibrium. Hence, the eigenvalues of the Jacobian matrix N determine the local behaviour of

the nonlinear system according to the results stated in Theorem 2.2.12 [61, 118]. We end this chapter by giving a general formulation of a continuous dynamic on a complex network along with two examples.

2.3 Simple Dynamical System on a Network

Let us assume that we have independent dynamical variables x_i, y_i, \dots , on each vertex i and that they are coupled together only along the edges of the network. Therefore, equations describing the time evolution of the variables will involve only the variables themselves and other variables on vertex i or more variables on neighbours of vertex i . There is no term involving variables on non nearest neighbours and no term involving more than one adjacent vertex. For instance let us consider the dynamic describing the time evolution of the probability of infection of a vertex in a network of the type (continuous version):

$$\frac{dx_i}{dt} = \beta(1 - x_i) \sum_j A_{ij} x_j. \quad (2.36)$$

The dynamic described by this equation only involve pairs of variables that are connected by edges since these are the only pairs for which A_{ij} is non-zero. In general, for systems with a single variable on each vertex we have the equation [93]:

$$\frac{dx_i}{dt} = f_i(x_i) + \sum_j A_{ij} g_{ij}(x_i, x_j), \quad (2.37)$$

in which the first term only involves variables on vertices and the second term involves variables on adjacent vertices. The function f_i describes how vertex i will evolve on its own without the other vertices and g_{ij} describes only the contribution from the nearest connections themselves. The function g_{ij} also represents the

coupling between variables on different vertices that are directly connected by an edge. Often the dynamic of each vertex is the same and we can simply write,

$$\frac{dx_i}{dt} = f(x_i) + \sum_j A_{ij}g(x_i, x_j). \quad (2.38)$$

We also assume that the network is undirected such that if x_i is affected by x_j then x_j is similarly affected by x_i . The dynamic for which $f(x) = 0$ and $g(x_i, x_j) = \beta(1 - x_i)x_j$ correspond to the SI model of epidemics (this will be presented in the next chapter). The dynamic described by equation (2.38) is non-linear and to study the stability of the fixed point we choose to linearise it in the vicinity of the fixed point.

Linearisation

Let suppose there is a fixed point \bar{x} for equation (2.38) such that

$$f(\bar{x}) + \sum_j A_{ij}g(\bar{x}_i, \bar{x}_j) = 0. \quad (2.39)$$

If we write $x_i = \bar{x}_i + \epsilon_i$, ($\epsilon_i \ll \bar{x}_i$) and use the Taylor expansion around \bar{x} we have

$$f(x_i + \bar{x}) = f(x_i) + \epsilon_i f'(\bar{x}_i) + \epsilon_i^2 f''(\bar{x}_i) + \dots \quad (2.40)$$

and

$$\begin{aligned} g(\bar{x}_i + \epsilon_i, \bar{x}_j + \epsilon_j) &= g(\bar{x}_i, \bar{x}_j) + \epsilon_i \frac{\partial g(x_i, x_j)}{\partial x_i}(\bar{x}_i, \bar{x}_j) + \epsilon_j \frac{\partial g(x_i, x_j)}{\partial x_j}(\bar{x}_i, \bar{x}_j) + \\ &+ 2\epsilon_i \epsilon_j \frac{\partial^2 g(x_i, x_j)}{\partial x_i \partial x_j}(\bar{x}_i, \bar{x}_j) + \epsilon_i^2 \frac{\partial^2 g(x_i, x_j)}{\partial x_i^2}(\bar{x}_i, \bar{x}_j) + \\ &+ \epsilon_j^2 \frac{\partial^2 g(x_i, x_j)}{\partial x_j^2}(\bar{x}_i, \bar{x}_j) + \dots \end{aligned} \quad (2.41)$$

and

$$\frac{dx_i}{dt} = \frac{d\epsilon_i}{dt}. \quad (2.42)$$

Substituting relations (2.40), (2.41) and (2.42) into equation (2.38) and ignoring small terms of second order and higher we get

$$\frac{d\epsilon_i}{dt} = (\alpha_i + \sum_j \beta_{ij} \mathbf{A}_{ij}) \epsilon_i + \sum_j \gamma_{ij} \mathbf{A}_{ij} \epsilon_j, \quad (2.43)$$

or in matrix notation

$$\frac{d\epsilon}{dt} = \mathbf{M}\epsilon, \quad (2.44)$$

where

$$\alpha_i = \frac{\partial f}{\partial \bar{x}_i}(\bar{x}), \quad \beta_{ij} = \frac{\partial g(\bar{x}_i, \bar{x}_j)}{\partial x_i}(\bar{x}_i, \bar{x}_j), \quad \gamma_{ij} = \frac{\partial g(\bar{x}_i, \bar{x}_j)}{\partial x_j}(\bar{x}_i, \bar{x}_j),$$

and

$$\mathbf{M} = \delta_{ij}(\alpha_i + \sum_j \beta_{ij} \mathbf{A}_{ij}) + \gamma_{ij} \mathbf{A}_{ij}.$$

Let us write the solution of (2.44) in the following form

$$\epsilon(t) = \sum_r c_r(t) \mathbf{v}, \quad (2.45)$$

where \mathbf{v} is an eigenvector of the matrix \mathbf{M} . Substituting (2.45) in equation (2.44), we have:

$$\frac{dc_r}{dt} = \mu_r c_r(t) \quad (2.46)$$

and

$$c_r(t) = c_r(0) e^{\mu_r t} \quad (2.47)$$

where μ_r is an eigenvalue of the matrix \mathbf{M} . We summarise the stability of the fixed point as follows: Let $Re(\mu_r)$ be the real part of μ_r , if

- $Re(\mu_r) < 0$ then $c_r(t)$ and ϵ go to zero as $t \rightarrow \infty$ and the fixed point will be stable or attractive.
- If $Re(\mu_r) > 0$ then $c_r(t) \rightarrow \infty$ as $t \rightarrow \infty$ and the fixed point will be unstable or repelling.
- If some real parts of μ_r are positive and others are negative the fixed point will be a saddle point.

2.3.1 Examples: The Diffusion and Synchronisation Processes on Networks

We end this section by two examples illustrating dynamical processes on a network. Apart from the diffusion and synchronisation processes, there are many other processes that can evolve on a network, such as consensus [18], epidemic spreading [18], etc. We simply consider here the case of the diffusion process [93] and synchronisation. The case of epidemics will be analysed in a separate chapter.

The Diffusion Process

Diffusion is known as the process by which gas moves from regions of high density to regions of low density, driven by the radiative pressure or partial pressure of the different regions. We can consider on the other hand diffusion processes on networks and some times those processes serve as simple models of spread across a network, such as the spread of an idea, or the spread of disease or any kind of information. Suppose we have some substance of some kind on the vertices of a

network and let ω_i be the amount of that substance on vertex i . Suppose that the substance moves along the edges, flowing from one vertex j to an adjacent vertex i at a rate $C(\omega_j - \omega_i)$ where C is a constant called the diffusion constant. That is, in a small interval of time the amount of fluid flowing from j to i is $C(\omega_j - \omega_i)dt$. The evolution equation of ω_i on the network is given by:

$$\frac{d\omega_i}{dt} = C \sum_j A_{ij}(\omega_j - \omega_i). \quad (2.48)$$

The adjacency matrix in this expression ensures that the only terms appearing in the sum are those that correspond to vertex pairs that are actually connected by an edge. In the case of an undirected network we can write equation (2.48) as follows:

$$\begin{aligned} \frac{d\omega_i}{dt} &= C \sum_j A_{ij}\omega_j - C\omega_i \sum_j A_{ij} \\ &= C \sum_j A_{ij}\omega_j - C\omega_i k_i \\ &= C \sum_j (A_{ij} - \delta_{ij}k_i)\omega_j \end{aligned} \quad (2.49)$$

where k_i is the degree of vertex i and δ_{ij} is the Kronecker symbol. In matrix notation we have

$$\frac{d\omega}{dt} = C(\mathbf{A} - \mathbf{D})\omega, \quad (2.50)$$

where \mathbf{A} is the adjacency matrix of the network and \mathbf{D} is the matrix with the vertex degrees along its diagonal and ω is a vector whose components are ω_i . By the definition of the Laplacian of the previous chapter, equation (2.50) can be written as

$$\frac{d\omega}{dt} = C\mathbf{L}\omega, \quad (2.51)$$

where $\mathbf{L} = \mathbf{A} - \mathbf{D}$. This equation has the same form as the ordinary diffusion equation for a gas where the the Laplacian operator ∇^2 has been replaced by the Laplacian matrix \mathbf{L} which also occurs in many places such as random walks on networks, resistor networks, graph partitioning and network connectivity.

The Solution

Equation (2.51) can be solved by writing the unknown vector ω as a linear combination of the eigenvector of the Laplacian matrix \mathbf{L} . That is,

$$\omega(t) = \sum_i \alpha_i \mathbf{u}_i. \quad (2.52)$$

Putting together equations (2.51) and (2.52) we have the following:

$$\sum_i \left(\frac{d\alpha_i}{dt} + C\lambda_i \alpha_i \right) \mathbf{u}_i = 0. \quad (2.53)$$

Multiplying both sides of equation (2.52) by \mathbf{u}_j and taking into account that eigenvectors of the Laplacian matrix are orthogonal we get

$$\frac{d\alpha_i}{dt} + C\lambda_i \alpha_i = 0, \quad \forall i, \quad (2.54)$$

which has the solution

$$\alpha_i(t) = \alpha(0)e^{C\lambda_i t}, \quad (2.55)$$

thus the solution to equation (2.50) is

$$\omega(t) = \sum_i \alpha(0)e^{C\lambda_i t} \mathbf{u}_i. \quad (2.56)$$

2.3.2 The Synchronisation Process

Natural systems can be described as a collection of oscillators coupled to each other via an interaction matrix. These systems include, for example, the ecosystem, neurons, cardiac pacemaker cells, or animal and insect behaviour. Coupled systems display synchronised behaviour, that is they are following a common dynamical evolution. Synchronisation properties depend also on the coupling pattern among oscillators which is conveniently represented as an interaction network characterising each system. Networks therefore play a fundamental role in the study of synchronisation phenomena. In this section we are going simply to review the general framework of synchronisation as a process that can take place on a complex network as the diffusion process. More on synchronisation can be found here [8, 18]

General Formulation of Synchronisation in Networks

Let us consider a large number N of oscillators (units) in interaction. Each oscillator/unit i can be described by an internal degree of freedom ϕ_i ($i = 1, \dots, N$) which evolves in time both because of an internal dynamic and because of the coupling with the other units. The time evolution of the system is given in general by the following set of equations

$$\frac{d\phi_i}{dt} = f_i(\phi_1, \dots, \phi_N), \quad i = 1, \dots, N. \quad (2.57)$$

The set of different units can be seen as a network whose nodes represent oscillators and two nodes i and j are connected by a directed edge from j to i if the evolution equation of i depends on the state ϕ_j of j . In the case of symmetric interactions, the evolution of ϕ_j depends on ϕ_i reciprocally and the resulting network is undirected. There are various type of synchronisation that may occur in a complex network of coupled units, these include,

- complete synchronisation [103]: in this case there is an equality of all internal variables evolving in time, i.e.

$$\phi_i = s(t), \quad \forall i,$$

- phase synchronisation [105]: is a weaker form of synchronisation described by a phase and an amplitude consisting in a locking of the phase while the correlation between amplitudes is weak.
- Generalised synchronisation [77]: is an extension of the synchronisation concepts in which two dynamical units interact such that the output of one unit is equal to the output of a function of another unit.

The case of Linearly Coupled Identical Oscillators

In this case the set of governing differential equations are

$$\frac{d\phi_i}{dt} = F(\phi_i), \quad i = 1, \dots, N. \quad (2.58)$$

Since each unit i is interacting with its nearest neighbours j , we consider a simple case corresponding to linear coupling, for which each unit i is coupled to a linear combination of the outputs of its neighbours units which allows us to write the evolution equations in the form

$$\frac{d\phi_i}{dt} = F(\phi_i) + \sigma \sum_{j=1}^N C_{ij} H(\phi_j), \quad i = 1, \dots, N, \quad (2.59)$$

where H is a fixed output function, σ represents the interaction strength, and C_{ij} is the coupling matrix. If the coupling between two units depends only on the

difference between their outputs we have

$$\frac{d\phi_i}{dt} = F(\phi_i) + \sigma \sum_{j \sim i} C_{ij} [H(\phi_j) - H(\phi_i)], \quad i = 1, \dots, N. \quad (2.60)$$

This corresponds to the coupling $\mathbf{C} = \mathbf{L}$ where \mathbf{L} is the Laplacian matrix. If $s(t)$ is the evolution of the uncoupled oscillators, according to equation (2.58), then the fully synchronised behaviour $\phi_i(t) = s(t)$, is a solution of (2.60). The stability of this state can be studied by writing

$$\phi_i = s + \epsilon_i, \quad (2.61)$$

where $\epsilon \ll s$, and we can use the approximation

$$F(\phi_i) \approx F(s) + \epsilon_i F'(s) \quad \text{and} \quad H(\phi_i) \approx H(s) + \epsilon_i H'(s)$$

and

$$\frac{ds}{dt} = F(s(t)).$$

The time evolution equation of $\epsilon_i(t)$ reads

$$\frac{d\epsilon_i}{dt} = F'(s)\epsilon_i + \sigma \sum_j \left(L_{ij} H'(s) \right) \epsilon_j. \quad (2.62)$$

The system can be decoupled by using the set of eigenvectors η_i which are an appropriate set of linear combinations of the perturbations ϵ_i , to obtain

$$\frac{d\eta_i}{dt} = \left(F'(s) + \sigma \lambda_i H'(s) \right) \eta_i \quad (2.63)$$

from which we get the solution

$$\eta_i(t) = \eta_i^0 e^{(F'(s) + \sigma \lambda_i H'(s))t}. \quad (2.64)$$

The perturbation may increase or decrease depending on the sign of $(F'(s) + \sigma \lambda_i H'(s))$.

Chapter 3

Epidemic Spreading in Complex Networks

Epidemic spreading is one of the most studied dynamic processes that take place in complex networks. The study of this subject is becoming a hot and an interesting area of complex networks. Among the most important questions one can ask in this area are, for example, how is an infection spreading in networks? will the infection die out? or will it survive and become an epidemic? how the network topology or structure influence the spreading of an epidemic in a network? A number of approach have been proposed so far for tackling the dynamics of epidemics in networks, some are exact and some are just approximations. Given a specific network, we can always perform computer simulations of epidemics and get numerical answers for the typical disease outbreak. Analytic approaches give more insight and some results are known but they are more confined to a specific class of model network such as a random one. In this chapter we review some interesting and straightforward models of epidemic spreading on population based on the standard approach of compartmental models and the homogeneous assumption.

We will also review the spread of diseases in heterogeneous networks.

3.1 Compartmental Models and the Homogeneous Assumption

In these models it is assumed that the population is divided into classes or compartments related to the stage of the disease [37], such as susceptible (S) those who can contact the infection, infectious (I) those who have contacted the infection and are contagious, and recovered (R) those who have recovered from the disease. Some other compartments may be added. These include for instance the immune or exposed classes, for individuals exposed to the infection but not yet infectious. In this framework, in each compartment individuals are assumed to be *identical* and *homogeneously* mixed, and the larger the number of sick and infectious individuals among one individual's contacts, the higher the probability of transmission of the infection. In these compartmental models there two types of elementary processes ruling the disease dynamics [37]:

Spontaneous Transition (ST)

This case is characterised by the moving of one individual from one class to another. Let $X^{[m]}(t)$ and $X^{[h]}(t)$ be the number of individuals in class $[m]$ and $[h]$, respectively, at time t . A spontaneous transition from class $[m]$ to class $[h]$ can be expressed in the following way:

$$\begin{cases} X^{[m]} \rightarrow X^{[m]} - 1 & \text{move of one individual from class } [m] \\ X^{[h]} \rightarrow X^{[h]} + 1 & \text{move of one individual to class } [m]. \end{cases} \quad (3.1)$$

The number of individuals in the population is given by:

$$N = \sum_m X^{[m]}(t).$$

Spontaneous transition includes for instance the case of spontaneous recovery of infected individuals $I \rightarrow R$ or the passage from a latent condition to an infectious one $L \rightarrow I$. Let v_h^m be the change in number of $X^{[m]}$ due to spontaneous transition from or to the compartment $[h]$ which we define as follow:

$$v_h^m = \begin{cases} 1 & \text{if from class } [h] \\ -1 & \text{if to class } [h] \\ 0 & \text{otherwise.} \end{cases} \quad (3.2)$$

The variation in the number of individuals $X^{[m]}$ due to spontaneous transition is given by:

$$\partial_{t,ST} X^{[m]} = \sum_h v_h^m a_h X^{[h]}, \quad (3.3)$$

where a_h is the rate of transition from class $[h]$.

Binary Interactions

This includes the case of contagion when a susceptible individual enters in interaction with an infectious one,



in this case the change in number of $X^{[m]}$ is given by [37]:

$$\partial_{t,BI} X^{[m]} = \sum_{h,g} v_{h,g}^m a_{h,g} X^{[h]} \frac{X^{[g]}}{N}, \quad (3.5)$$

where $a_{h,g}$ is the transition rate of the process and $v_{h,g} = 1, 0$ or -1 is the change in the number of $X^{[m]}$ due to the interaction. The general deterministic rate equation for the average number of individuals in the class $[m]$ is then given by:

$$\begin{aligned}\partial_t X^{[m]} &= \partial_{t,ST} X^{[m]} + \partial_{t,BI} X^{[m]} \\ &= \sum_h v_h^m a_h X^{[h]} + \sum_{h,g} v_{h,g}^m a_{h,g} X^{[h]} \frac{X^{[g]}}{N}.\end{aligned}\quad (3.6)$$

Equation (3.6) is a general framework that allows us to derive three basic models describing the dynamics of disease spreading. We will review some models in the next sections.

3.2 The Susceptible-Infected (SI) Model

In this model there are only two different classes or states *susceptible* and *infected*. An individual in the susceptible state is someone who does not have the disease yet but could catch it if he comes into contact with someone who is infected. An individual in the infected state is someone who has the disease and can, potentially, pass it on if they come into contact with a susceptible individual.

Model Equation

Let us consider a disease that is spreading in a population of individuals. Let $S(t)$ be the average number of susceptible individuals and $I(t)$ be the average number of infected individuals and let N be the total number of individuals or the size of the population. The number of infected individuals goes up when susceptible individuals contract the disease from infected ones. Individuals that

enter the infected state remain permanently infectious. The epidemic can only grow as the number of infectious individuals increases monotonically and the seed of infectious individuals placed at time $t = 0$. Let us suppose that each individual has, on average, β contacts with randomly chosen others per unit time. There is infection transmission only when an infected individual enters in contact with a susceptible one. The evolution of the SI model is then completely defined by $I(t)$. The probability that an individual picked at random in the population be infected is $S(t)/N$, and therefore, by the homogeneous assumption, an infected individual has contact with an average of $\beta S(t)/N$ susceptible individuals per unit time. The overall average rate of new infected individuals is

$$\beta S(t)I(t)/N. \quad (3.7)$$

The differential equation for the rate of change of $I(t)$ is given by:

$$\frac{dI}{dt} = \beta \frac{SI}{N}. \quad (3.8)$$

At the same time the number of susceptible individuals goes down at the same rate, that is

$$\frac{dS}{dt} = -\beta \frac{SI}{N}, \quad (3.9)$$

where we write $S(t) = S$ and $I(t) = I$ for simplicity. The system of differential equations that describes the evolution SI model reads

$$\begin{cases} \frac{dI(t)}{dt} = \beta \frac{SI}{N}, \\ \frac{dS(t)}{dt} = -\beta \frac{SI}{N}. \end{cases} \quad (3.10)$$

Let s and i be respectively the variables that represent the fractions of susceptible $S(t)$ and infected $I(t)$ individuals, i.e.

$$s = \frac{S}{N}, \quad i = \frac{I}{N}, \quad (3.11)$$

and system (3.10) read,

$$\begin{cases} \frac{ds}{dt} = -\beta si \\ \frac{di}{dt} = \beta si. \end{cases} \quad (3.12)$$

The variables s and i are such that

$$s + i = 1,$$

hence $s = 1 - i$ and using the second equation of (3.12) we get the following differential equation for the number of infected individuals

$$\frac{di}{dt} = \beta i(1 - i). \quad (3.13)$$

If the number of infected individuals is a very small fraction of the total populations, that is $i(t) \ll 1$, then equation (3.13) can be linearly approximated by:

$$\frac{di}{dt} = \beta i, \quad (3.14)$$

which has the following solution

$$i(t) \simeq i_0 e^{t/\tau}, \quad (3.15)$$

where i_0 is the initial fraction of infected individuals and

$$\tau = \frac{1}{\beta}.$$

Equation (3.15) says that the larger the spreading rate β , the faster the outbreak will be. In the SI model the epidemic always propagates in the population until all individuals are infected, but the linear approximation (3.14) breaks down when the fraction of infected individuals becomes large and the shape of $i(t)$ deviates from a simple exponential. If i_0 is the initial value of i at $t = 0$ or the initial number of infected nodes, we can solve the differential equation (3.13) and get the equation that describes the evolution of infectious individuals in time, i.e.

$$i(t) = \frac{i_0 e^{\beta t}}{1 - i_0 + i_0 e^{\beta t}}. \quad (3.16)$$

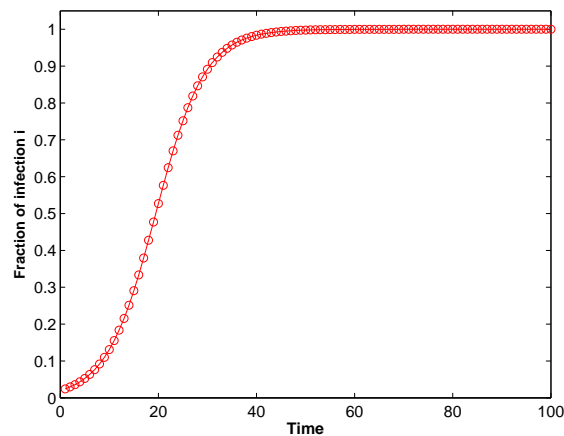


Figure 3.1: Evolution of the number of infected individuals in the SI Model. The rate of infection here is $\beta = 0.2$, the initial number of infected individuals is 20% of the total population $N = 1000$. The curve grows exponentially at the very beginning and the infected individuals infect more and more the susceptible ones. The curve saturates as the number of susceptible get reduced.

3.3 The Susceptible-Infected-Recovered Model (SIR)

In the SI model, if an individual is infected he will stay infected for ever. For many diseases, however, people recover from infection after a certain period of time because their immune system fights off the agent causing the disease. This behaviour is represented in a new model that extends the SI model in some way. A new state is introduced; the state of *recovered* individuals denoted by R and the resulting model is called *susceptible-infected-recovered* (SIR) or SIR model. For certain authors R stands for *removed* in the sense that a recovered individual may die and is removed from the population and the resulting model is called *susceptible-infected-removed*.

Model Equation

There are two stages in the dynamics of the SIR model. In the first stage, susceptible individuals become infected when they have contact with infected individuals. Contacts between individuals are assumed to happen at an average rate of β per person as in the SI model. In the second stage, infected individuals recover (or die) at some constant average rate δ . Without loss of generality, the system of differential equations that describes the evolution of the SIR model in terms of the fractions of susceptible $s(t)$, infected $i(t)$ and removed $r(t)$ is given by [18, 93]:

$$\begin{cases} \frac{ds}{dt} = -\beta si, \\ \frac{di}{dt} = \beta si - \delta i, \\ \frac{dr}{dt} = \delta i, \end{cases} \quad (3.17)$$

and in addition we have:

$$s + i + r = 1. \quad (3.18)$$

As can be seen from system (3.17), all infected individuals will sooner or later enter the recovered state, so it is then obvious that in the infinite time limit the epidemic must fade away. We can solve these equations by eliminating i in the first and third equations of (3.17) to get,

$$(1/s) \frac{ds}{dt} = -\frac{\beta}{\delta} \frac{dr}{dt}. \quad (3.19)$$

If s_0 is the value of s at $t = 0$ integrating both side of equation (3.19) we get

$$s(t) = s_0 e^{-\frac{\beta r(t)}{\delta}}. \quad (3.20)$$

Combining equation (3.20) and equation (3.18) and the third equation of (3.17) we have

$$\frac{dr}{dt} = \delta(1 - r - s_0 e^{-\frac{\beta r}{\delta}}), \quad (3.21)$$

or by integrating both sides of equation (3.21) we get

$$\frac{1}{\delta} \int_0^r \frac{dv}{1 - v - s_0 e^{-\frac{\beta v}{\delta}}} = t. \quad (3.22)$$

The integral on the left hand side of equation (3.22) cannot be evaluated in terms of known functions. We use the Matlab tool ode45 to solve numerically the system (3.17). From Figure 3.2 we draw the following conclusion:

- The number of susceptible individuals is decreasing monotonically during time.
- The number of recovered individuals is increasing monotonically with time and reaches saturation for large values of time. This is because if an individual recovers then he will never get infected again.

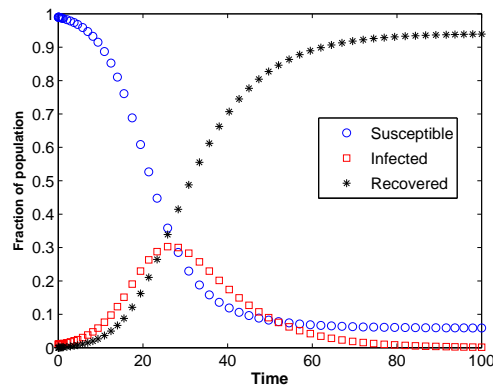


Figure 3.2: Illustration of the time evolution of the SIR model. The curves show the fractions of the population in the susceptible, infected and recovered states as a function of time. The values of the parameters used are $\beta = 0.3$, $\delta = 0.1$, $s_0 = 0.99$, $i_0 = 0.01$, and $r_0 = 0$.

- At the start the number of infected individuals is increasing, then goes down as the individuals recover, and eventually goes to zero as $t \rightarrow \infty$.

The number of susceptible individuals does not go to zero as time increases. This is because, asymptotically when $i \rightarrow 0$ there is no infected individuals to infect the susceptible ones. Some individuals will never get infected until the outbreak has passed. Similarly the fraction of recovered individuals does not quite reach one as $t \rightarrow \infty$. The total number of individuals who ever catch the disease during the entire course of the epidemic is given by the asymptotic value or r , that is when $i \rightarrow 0$:

$$r = 1 - s_0 e^{-\beta r / \delta}, \quad (3.23)$$

and if the initial number of infected individuals is very small, we have $s_0 \simeq 1$ and hence,

$$r = 1 - e^{-\beta r / \delta}. \quad (3.24)$$

Early stage of the epidemic behaviour in the SIR model

It is possible to solve approximately the system of differential equations (3.17) in the early stage of an epidemic. Let us consider the second equation of system (3.17)

$$\frac{di}{dt} = \beta is - \delta i. \quad (3.25)$$

In the early stage of the epidemic we can neglect the fraction of removed i.e. $r = 0$ and substitute $s = 1 - i$ into equation (3.25) to get

$$\begin{aligned} \frac{di}{dt} &= \beta i(1 - i) - \delta i \\ &= \beta i - \beta i^2 - \delta i. \end{aligned} \quad (3.26)$$

We can also ignore the term in i^2 and consider the following linear approximation

$$\frac{di}{dt} \simeq \beta i - \delta i, \quad (3.27)$$

whose solution is

$$i(t) \simeq i_0 e^{t/\tau}, \quad (3.28)$$

where the typical outbreak time is given by

$$\tau^{-1} = \beta - \delta = \delta \left(\frac{\beta}{\delta} - 1 \right). \quad (3.29)$$

The typical outbreak time is the combination of two terms, the spread rate β and the recovery rate δ and can be negative in the case when the recovery rate is large enough. Hence, the infection will not spread across the population but will die out. The key value governing the time evolution of these equations is the so-called

basic reproduction number R_0 which in the case of the SIR model is given by

$$R_0 = \frac{\beta}{\delta}, \quad (3.30)$$

and relation (3.29) can be written as

$$\tau^{-1} = \delta(R_0 - 1), \quad (3.31)$$

where R_0 is considered to be the number of secondary infections caused by a single primary infection. It determines the number of people infected by contact with a single infected person before his death or recovery.

- When $R_0 < 1$ there is no epidemic, i.e. each diseased individual infects fewer than one person before dying or recovering, so the outbreak will die out ($di/dt < 0$).
- When $R_0 > 1$, the infection will be able to propagate in the population, that is each diseased individual infects more than one person, so the epidemic will spread ($di/dt > 0$).
- The point $R_0 = 1$ ($di/dt = 0$) corresponds to the *epidemic threshold* between regimes in which the disease either multiplies or dies out.

In the SI model $R_0 = \infty$ and the infection will propagate for ever and infect more and more susceptible individuals.

3.4 The Susceptible-Infected-Susceptible Model

In this model an individual can only be in two different states, susceptible or infected. In the SI model once an individual gets infected he stays for ever in that

state. However, in the SIS model an infected individual may recover and go back to the susceptible state. In this way the SIS model is also seen as an extension of the SI model. Without loss of generality the system of differential equations for this model is given by [37, 93]:

$$\begin{cases} \frac{ds}{dt} = \delta i - \beta i, \\ \frac{di}{dt} = \beta si - \delta i, \end{cases} \quad (3.32)$$

with

$$s + i = 1. \quad (3.33)$$

3.4.1 The Solution

Substituting $s = 1 - i$ into the second equation of system (3.32) we have

$$\frac{di}{dt} = (\beta - \delta - \beta i)i. \quad (3.34)$$

After separating the variables and integrating we get

$$i(t) = \left(1 - \frac{\delta}{\beta}\right) \frac{C e^{(\beta-\delta)t}}{1 + C e^{(\beta-\delta)t}}. \quad (3.35)$$

Using $i(t = 0) = i_0$, we get the constant

$$C = \frac{\beta i_0}{\beta - \delta - \beta i_0}, \quad (3.36)$$

and substituting C in (3.35), we have the following expression for the evolution of the number of infected individuals over time

$$i(t) = i_0 \frac{(\beta - \delta)e^{(\beta - \delta)t}}{(\beta - \delta) - \beta i_0(1 - e^{(\beta - \delta)t})}. \quad (3.37)$$

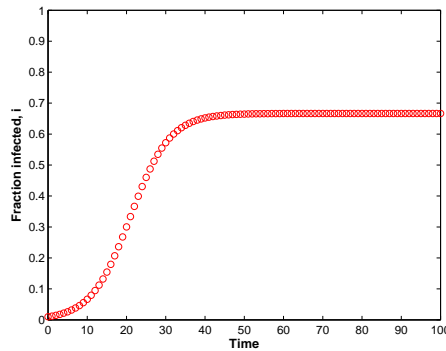


Figure 3.3: Illustration of the time evolution for the SIS model. The fraction of infected in the SIS model grows with time as for the SI model but in this model, the fraction of infected never reaches one, tending instead to a steady state at which the rate of infection and recovery are equal.

- If $\beta > \delta$ we have a curve similar to that of Figure 3.1 but in this case the fraction of infected does not reach one as time evolves. In the long term the fraction of infected reaches an intermediate state at which the rate of infection and recovery are balanced. This fraction of infected is given by

$$i = \frac{\beta - \delta}{\beta} \quad (3.38)$$

and can be obtained from equation (3.34) by setting $di/dt = 0$.

- If $\beta/\delta < 1$ it can be seen from expression (3.37) that the fraction of infected goes to zero and the disease dies out over time. The point $\beta = \delta$ corresponds

to an epidemic transition as for the SIR model marking the transition between a state in which the disease spreads and in which it does not.

- The basic reproduction number R_0 in the SIS model is given by

$$R_0 = \frac{\beta}{\delta}.$$

3.5 The Susceptible-Infected-Recovered-Susceptible (SIRS) model

In this model infected individuals recover, but this recovery is temporary, they go back to the susceptible state again and may catch the disease again. Let η be the average rate at which individuals lose their immunity. Without loss of generality, the system of differential equations for the SIRS model is given by:

$$\begin{cases} \frac{ds}{dt} = \eta r - \beta si, \\ \frac{di}{dt} = \beta si - \delta i, \\ \frac{dr}{dt} = \delta i - \eta r, \end{cases} \quad (3.39)$$

and

$$s + r + i = 1. \quad (3.40)$$

In general the SIRS model cannot be solve analytically. Numerical methods can be used to solve the system (3.39) and treated using linear stability and some others methods of non-linear dynamics. From equation (3.40) we have

$$i = 1 - r - s, \quad (3.41)$$

and the model described by the system (3.39) can be reduced to the following two dimensional system

$$\begin{cases} \frac{ds}{dt} = -\beta si + \eta(1 - s - i) \\ \frac{di}{dt} = \beta si - \delta i. \end{cases} \quad (3.42)$$

Local stability analysis shows that if an endemic equilibrium $e^* = (s^*, i^*)$, $i^* > 0$ exists, then it is locally asymptotically stable. Notice that e^* exists if and only if

$$s^* = \frac{\delta}{\beta} < 1. \quad (3.43)$$

Therefore the total population must be larger than a threshold size of δ/β . Several other models have been proposed to model the spread of a particular disease in a population. Some different extra state may be added, such as the *exposed* state that represents individuals who have caught a disease but whose infection is not yet developed to the point where they can pass it on others.

3.6 Epidemics in Heterogeneous Networks

In the previous models described so far, it was assumed that the network or population that describes the connectivity among individuals is homogeneous, such that, in the first approximation each individual in the system has the same number of connections or contacts. However, many real networks exhibit very heterogeneous topology [51]. Recently, [90] empirical evidence that emphasised the role of heterogeneity by showing that many epidemiological networks are heavy-tailed and therefore the average degree $\langle k \rangle$ (also written \bar{k}) is no longer the relevant variable. We then expect the fluctuations to play a major role in determining the properties and evolution of the epidemics. These include mobility networks as well as the

web of sexual contacts. Computer epidemics can also be studied in the same way as biological epidemics [73]. As a consequence of the topological fluctuations, we need a mathematical model that will take into account the degree variabilities of nodes or vertices. This is achieved by making the following assumption:

- All nodes with the same degree are statistically equivalent resulting in a grouping in the same class or block of nodes with the same degree.

We can then define the fraction of infected i_k and susceptible s_k in the group of nodes having degree k to be

$$i_k = \frac{I_k}{N_k}; \quad s_k = \frac{S_k}{N_k}, \quad (3.44)$$

where N_k is the number of nodes in the group degree k and I_k and S_k the number of infected and susceptible, respectively in the group. The total number of fractions of infected i_k and susceptible s_k is given by:

$$i = \sum_k P(k)i_k; \quad s = \sum_k P(k)s_k \quad (3.45)$$

where $P(k)$ is the degree distribution of the network.

3.6.1 The SI model on Heterogeneous Networks

The differential equation describing the evolution over time of the fraction of infected in this case is given by [18, 24]:

$$\frac{di_k(t)}{dt} = \beta(1 - i_k(t))k\theta_k(t), \quad (3.46)$$

where β stands for the spreading rate across the links/edges of the network, k is the degree, $1 - i_k(t)$ is the probability that a vertex with degree k is not infected

(from neighbours) and the term $\theta_k(t)$ is introduced to account for the density of infected neighbours having degree k . That quantity can also be seen as the average probability that any given neighbour of a vertex of degree k is infected. In general $\theta_k(t)$ is unknown in the heterogeneous model. In the homogeneous model it was equal to the density of infected nodes/individuals. In this case the quantity $\theta_k(t)$ takes into account the different degree classes and the connections between them as well. To get around this difficulty, we simply ignore the degree correlation of nodes and assume that the network is uncorrelated. A network is independent of the degree-correlation if the probability that a link going from a vertex of degree k arrives at a vertex of degree k' does not depend on the initial node and it is shown that [42, 93], any edge can point to a node of degree k' with a probability that is proportional to k' that is:

$$P(k'|k) = k' \frac{P(k')}{\langle k \rangle}, \quad (3.47)$$

where $\langle k \rangle = \sum_{k'} k' P(k')$. We can then write the following expression for $\theta_k(t)$ that does not depend on k :

$$\theta_k(t) = \theta(t) = \frac{\sum_{k'} (k' - 1) P(k') i_{k'}(t)}{\sum_{k'} k' P(k')}. \quad (3.48)$$

The time evolution of $\theta(t)$ is given by:

$$\frac{d\theta(t)}{dt} = \frac{\sum_{k'} (k' - 1) P(k') \frac{di_{k'}(t)}{dt}}{\sum_{k'} k' P(k')}, \quad (3.49)$$

or (using equation(3.46))

$$\begin{aligned}
 \frac{d\theta(t)}{dt} &= \frac{\sum_{k'}(k' - 1)P(k')\beta k'\theta(t)}{\sum_{k'} k' P(k')} \\
 &= \frac{\beta\theta(t) \sum_{k'}(k' - 1)P(k')k'}{\sum_{k'} k' P(k')} \\
 &= \frac{\beta\theta(t) (\sum_{k'} k'^2 P(k') - \sum_{k'} P(k')k')}{\sum_{k'} k' P(k')} \\
 &= \beta \left(\frac{\langle k^2 \rangle}{\langle k \rangle} - 1 \right) \theta(t),
 \end{aligned} \tag{3.50}$$

where,

$$\langle k^2 \rangle = \sum_{k'} k'^2 P(k').$$

Therefore neglecting the term in i^2 , we have

$$\begin{cases} \frac{di_k(t)}{dt} = \beta k \theta(t), \\ \frac{d\theta(t)}{dt} = \beta \left(\frac{\langle k^2 \rangle}{\langle k \rangle} - 1 \right) \theta(t). \end{cases} \tag{3.51}$$

From the second equation of the above system we can solve for $\theta(t)$ and get:

$$\theta(t) = \theta_0 e^{t/\tau}, \tag{3.52}$$

where the initial condition θ_0 can be obtained from expression (3.48)

$$\begin{aligned}
 \theta(t=0) &= i_0 \frac{\sum_{k'} k' P(k') - \sum_{k'} P(k')}{\sum_{k'} k' P(k')} \\
 &= i_0 \frac{\langle k \rangle - 1}{\langle k \rangle},
 \end{aligned} \tag{3.53}$$

and

$$\tau = \frac{\langle k \rangle}{\beta(\langle k^2 \rangle - \langle k \rangle)}. \tag{3.54}$$

Substituting $\theta(t)$ given by expression (3.52) into the first equation of system (3.51) and using the initial condition $i(t = 0) = i_0$ and integrating both sides we have the following expression for $i_k(t)$:

$$i_k(t) = i_0 \left[1 + \frac{k(\langle k \rangle - 1)}{\langle k^2 \rangle - \langle k \rangle} (e^{t/\tau} - 1) \right], \quad (3.55)$$

and

$$\begin{aligned} i(k) &= \sum_k P(k) i_k, \\ &= i_0 \left[\sum_k P(k) + \frac{\sum_k k P(k) \langle k \rangle - \sum_k k P(k)}{\langle k^2 \rangle - \langle k \rangle} (e^{t/\tau} - 1) \right], \\ &= i_0 \left[1 + \frac{\langle k \rangle^2 - \langle k \rangle}{\langle k^2 \rangle - \langle k \rangle} (e^{t/\tau} - 1) \right]. \end{aligned} \quad (3.56)$$

3.6.2 The SIR and the SIS models in Heterogeneous networks

For the SIR and SIS models we have the following equation that describes the time evolution of $i_k(t)$ for uncorrelated networks [18, 24]:

$$\frac{di_k(t)}{dt} = \beta k s_k(t) \theta_k(t) - \delta i_k(t). \quad (3.57)$$

For the SIS model we have

$$s_k(t) = 1 - i_k(t), \quad (3.58)$$

and in the SIR model we have

$$s_k(t) = 1 - i_k(t) - r_k(t), \quad (3.59)$$

and $r_k(t)$ is the density of removed individuals of degree k . Let us analyse the case of the SIR model in the early stage of the epidemic. At this stage we can assume that $r_k(t) \approx 0$ and combining expression (3.59) and equation (3.57) we have

$$\begin{aligned} \frac{di_k(t)}{dt} &= \beta k(1 - i_k(t))\theta_k(t) - \delta i_k(t), \\ &= \beta k\theta_k(t) - \delta i_k(t). \end{aligned} \quad (3.60)$$

The last equation is obtained by neglecting the terms in i^2 in the early stage of the epidemic. Combining equation (3.60) and expression (3.48) we find the time evolution equation of $\theta(t)$ to be

$$\frac{d\theta(t)}{dt} = \frac{\sum_{k'} (k' - 1) P(k') \frac{di_{k'}(t)}{dt}}{\sum_{k'} k' P(k')}. \quad (3.61)$$

Or

$$\begin{aligned} \frac{d\theta(t)}{dt} &= \frac{\sum_{k'} (k' - 1) P(k') \frac{di_{k'}(t)}{dt}}{\sum_{k'} k' P(k')}, \\ &= \frac{\sum_{k'} (k' - 1) P(k') (\beta k' \theta(t) - \mu i_{k'}(t))}{\sum_{k'} k' P(k')}, \\ &= \beta \left(\frac{\langle k^2 \rangle}{\langle k \rangle} - 1 \right) - \delta \theta(t), \\ &= \theta(t) \left[\beta \left(\frac{\langle k^2 \rangle}{\langle k \rangle} - 1 \right) - \delta \right]. \end{aligned} \quad (3.62)$$

Using the initial condition (3.53) we can solve equation (3.62) for $\theta(t)$

$$\theta(t) = \theta_0 e^{t/\tau}, \quad (3.63)$$

where the time scale is given by

$$\tau = \frac{\langle k \rangle}{\beta \langle k^2 \rangle - (\delta - \beta) \langle k \rangle}. \quad (3.64)$$

In order to ensure an epidemic outbreak the basic condition is

$$\tau > 0,$$

or

$$\frac{\beta}{\delta} \geq \frac{\langle k \rangle}{\langle k^2 \rangle - \langle k \rangle}. \quad (3.65)$$

So for heavy-tail networks we have that $\langle k^2 \rangle \rightarrow \infty$ in the limit of networks of infinite size and this results in a null epidemic threshold and relation (3.65) will be always true. In a finite size real-network, a large heterogeneity level leads to a small epidemic threshold. This absence of epidemic threshold for scale-free networks makes them an ideal environment for the spreading of viruses, which even in the case of very weak spreading capabilities are able to pervade the network.

3.6.3 The case of the effect of mixing patterns

In the case of correlated networks, we need to take into consideration the full structure of the conditional correlation function $P(k'|k)$ in order to consider the case of non-trivial correlations. This is not a simple task and we will only look at particular cases.

The Case of the SI Model

For simplicity we are going to restrict ourselves to the case of the SI model. In this case we have the following equations:

$$\frac{di_k(t)}{dt} = \beta(1 - i_k)k\theta_k(t), \quad (3.66)$$

where

$$\theta_k = \sum_{k'} i_{k'} \frac{k' - 1}{k'} P(k' | k). \quad (3.67)$$

This time the density function θ_k depends on k and takes account of the structure of the conditional probability that an infected node having degree k' points to a node having degree k , without any of its $k' - 1$ free edges pointing to the original source of its infection. When there is no correlation we have that $P(k' | k) = k' P(k') / \langle k \rangle$ and we recover the cases of the previous sections. In the presence of correlations in the network measured by $P(k' | k)$ the situation is more complicated. By neglecting the terms in i^2 , the time evolution equation of $i_k(t)$ is given by:

$$\begin{aligned} \frac{di_k(t)}{dt} &= \sum_{k'} \beta k \frac{k' - 1}{k'} P(k' | k) i_{k'}(t), \\ &= \sum_{k'} C_{k,k'} i_{k'}(t), \end{aligned} \quad (3.68)$$

which is a system of linear differential equations whose matrix is given by

$$C_{k,k'} = \beta k \frac{k' - 1}{k'} P(k' | k) \quad (3.69)$$

and whose solution can be written in the form

$$i_k(t) = \sum_j e^{\lambda_j t}, \quad (3.70)$$

where the λ_j are the eigenvalues of the matrix \mathbf{C} . The dominant behaviour of the average prevalence is given by:

$$i_k(t) \sim e^{\lambda_m t}, \quad (3.71)$$

where λ_m is the largest eigenvalue of the matrix \mathbf{C} . So the time scale governing the increase of the prevalence is therefore given by

$$\tau \sim 1/\lambda_m.$$

When the network is uncorrelated, the entries $C_{k,k'}^*$ of the matrix \mathbf{C} are obtained by combining equation (3.47) and equation (3.69), i.e.

$$C_{k,k'}^* = \beta k(k' - 1)P(k')/\langle k \rangle, \quad (3.72)$$

and the matrix \mathbf{C} has a unique eigenvalue that satisfies:

$$\sum_{k'} C_{k,k'} \Phi_{k'} = \lambda_m^* \Phi_k, \quad (3.73)$$

where

$$\lambda_m^* = \beta \frac{\langle k^2 \rangle}{\langle k \rangle} - 1$$

and

$$\Phi_k = k.$$

In the case of correlated networks, Boguñá et al. [24] show by using the Frobenius theorem that the largest eigenvalue is bounded by below as follows:

$$\lambda_m^2 \geq \min_k \sum_{k'} \sum_l (k' - 1)(l - 1)P(l|k)P(k'|l). \quad (3.74)$$

3.7 Large Time Limit of Epidemic Outbreaks

In the previous paragraphs we have solved equations describing the SI, SIS and SIR model only in the early stage of the epidemics. In this section we want to analyse the opposite, that is when $t \rightarrow \infty$. It is evident that for the SI model in the large time limit we have that $i(t) \rightarrow 1$. In the case of the SIS and SIR model the behaviour of the epidemic depends upon the disease parameters of the model and the heterogeneity of the network.

The SIS Model

The full evolution equation of the SIS on a network with arbitrary degree distribution is given by:

$$\frac{di_k(t)}{dt} = -\delta i_k(t) + \beta k(1 - i_k(t))\theta_k(t). \quad (3.75)$$

We consider for simplicity the case of general random networks with no degree correlations. Therefore from the previous section, the average density $\theta_k(t)$ of infected vertices pointed to by any given edge is simply given by:

$$\theta_k = \frac{1}{\langle k \rangle} \sum_{k'} k' P(k') i_{k'}, \quad (3.76)$$

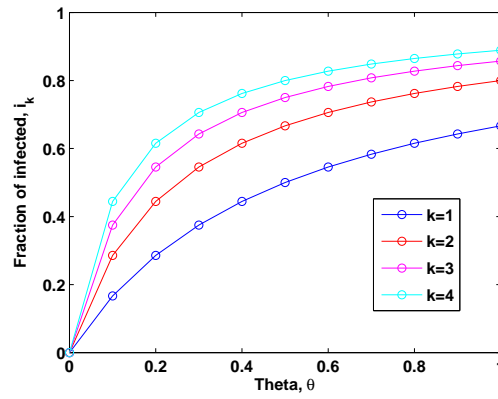


Figure 3.4: Evolution of the fraction of infected as a function of the average density of infected vertices θ and for different degrees.

which does not depend on k and is simply written as $\theta(t)$. To have information on $t \rightarrow \infty$ we simply impose the stationary condition $di_k(t)/dt = 0$. Therefore from equation (3.75) we get the following:

$$i_k = \frac{k\beta\theta}{\delta + k\beta\theta}. \quad (3.77)$$

From the equation (3.77) and Figure (3.4) we can see that the higher the vertex degree, the higher its probability to be in an infected state. Substituting equations (3.77) into equation (3.76) we get an equation of following form for θ

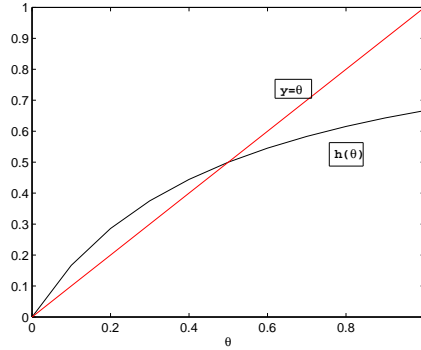
$$\theta = h(\theta) \quad (3.78)$$

where

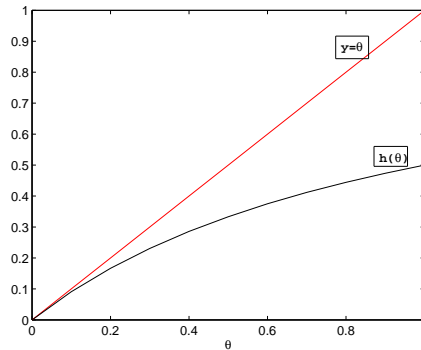
$$h(\theta) = \frac{1}{\langle k \rangle} \sum_k k P(k) \frac{\beta k \theta}{\delta + \beta k \theta}. \quad (3.79)$$

The solution of equation (3.78) depends on the values of the parameters β and δ . The admissible values of these parameters corresponding to a solution $\theta^* > 0$ of that equation will allow us to find the epidemic threshold from equation (3.78).

The function $h(\theta)$ is monotonically increasing between $h(0) = 0$ and $h(1) < 1$. A non trivial solution $\theta^* \neq 0$ exists if the slope of the function $h(\theta)$ at the point $\theta = 0$ is larger than or equal to 1. The situation is illustrated graphically in Figure 3.5 (a) and (b). Mathematically this condition can be translated as:



(a)



(b)

Figure 3.5: Graphic solution of equation (3.78). If the slope of the function $h(\theta)$ is greater than or equal to 1 there is a non trivial solution (a) but if the slope of the function $h(\theta)$ is less than one we only have one trivial solution (b). The solution occurs at the intersection of the curves $h(\theta)$ and $y = \theta$ (see plot (a)).

$$\begin{aligned} \left. \frac{dh(\theta)}{d\theta} \right|_{\theta=0} &= \frac{1}{\langle k \rangle} \sum_k k^2 P(k) \frac{\beta}{\delta} \\ &= \frac{\beta}{\delta} \frac{\langle k^2 \rangle}{\langle k \rangle} \geq 1. \end{aligned} \quad (3.80)$$

The epidemic threshold corresponds to the values of the disease parameters yielding the equality in relation (3.80), that is

$$\tau = \frac{\beta}{\delta} = \frac{\langle k \rangle}{\langle k^2 \rangle}. \quad (3.81)$$

We recover the results obtained from the linear approximation for a short time and confirm that topological fluctuations lower the epidemic threshold.

The SIR Model

In this case the number of infected individuals goes to zero as all the susceptible individuals move to the recovered state after infection. The main information on the course of the epidemic is then provided by the total number of individuals affected by the infection which corresponds to the number of recovered individuals if the starting population was composed only of susceptible individuals. Taking into account of the degree heterogeneity, this number can be expressed as

$$r_\infty = \lim_{t \rightarrow \infty} r(t), \quad (3.82)$$

where

$$r(t) = \sum_k P(k)r_k(t). \quad (3.83)$$

For this we use the SIR equations for the degree classes:

$$\begin{cases} \frac{di_k(t)}{dt} = -\delta i_k(t) + \beta k s_k(t) \theta_k(t), \\ \frac{ds_k(t)}{dt} = -\beta k s_k(t) \theta_k(t), \\ \frac{dr_k(t)}{dt} = \delta i_k(t), \end{cases} \quad (3.84)$$

where $\theta_k(t)$ for an uncorrelated network is given by:

$$\theta_k(t) = \frac{\sum_{k'} (k' - 1) P(k') i_{k'}(t)}{\langle k \rangle}. \quad (3.85)$$

Initial conditions are given by:

$$r_k(0) = 0, \quad i_k(0), \quad \text{and} \quad s_k(0) = 1 - i_k(0). \quad (3.86)$$

We consider the case of a homogeneous initial distribution of infected individuals at time $t = 0$, i.e. $i_k(t) = i_0 \quad \forall k$ and we assume that $i_0 \rightarrow 0$ and $s_k(0) \simeq 1$. The second equation of the system (3.84) gives

$$s_k(t) = e^{-\beta k \rho(t)}, \quad (3.87)$$

and the third equation of the same system gives,

$$r_k(t) = \delta \int_0^t i_k(\eta) d\eta, \quad (3.88)$$

where (using (3.85))

$$\begin{aligned} \rho(t) = \int_0^t \rho(\eta) d\eta &= \int_0^t \frac{\sum_k (k-1) P(k) i_k(\eta)}{\langle k \rangle} d\eta \\ &= \frac{\sum_k (k-1) P(k)}{\langle k \rangle} \int_0^t i_k(\eta) d\eta \\ &= \frac{1}{\delta \langle k \rangle} \sum_k (k-1) P(k) r_k(t), \end{aligned} \quad (3.89)$$

where in the last relation we have used Equation 3.88. The time evolution of $\rho(t)$ is given by

$$\begin{aligned}
 \frac{d\rho(t)}{dt} &= \frac{1}{\delta\langle k \rangle} \sum_k (k-1)P(k) \frac{dr_k(t)}{dt} \\
 &= \frac{1}{\langle k \rangle} \sum_k (k-1)P(k)i_k(t) \\
 &= \frac{1}{\langle k \rangle} \sum_k (k-1)P(k)(1-r_k(t)-s_k(t)) \\
 &= \frac{1}{\langle k \rangle} \sum_k kP(k) - \frac{1}{\langle k \rangle} \sum_k P(k) + \dots \\
 &\quad - \sum_k \frac{1}{\langle k \rangle} (k-1)P(k)r_k(t) + \sum_k \frac{1}{\langle k \rangle} (k-1)P(k)s_k(t) \\
 &= 1 - \frac{1}{\langle k \rangle} - \delta\rho(t) - \sum_k \frac{1}{\langle k \rangle} (k-1)P(k)e^{-\beta k \rho(t)}, \tag{3.90}
 \end{aligned}$$

where we have used equation (3.87) and equation (3.89). Equation (3.90) cannot be solved explicitly for $\rho(t)$, but we can get useful information in the infinite time limit; when there is no epidemic. That is,

$$r_\infty = \sum_k P(k)(1 - e^{-\beta k \rho_\infty}), \tag{3.91}$$

where

$$r_\infty = \sum_k P(k)r_k(\infty), \quad \rho_\infty = \lim_{t \rightarrow \infty} \rho(t), \tag{3.92}$$

using the fact that $r_k(\infty) = 1 - s_k(\infty)$ and equation (3.87) equation (3.88). Since $i_k(\infty) = 0$ we have

$$\lim_{t \rightarrow \infty} \frac{d\rho(t)}{dt} = 0.$$

Then from Equation (3.90) we have the following equation for ρ_∞ :

$$\delta\rho_\infty = 1 - \frac{1}{\langle k \rangle} - \sum_k \frac{1}{\langle k \rangle} (k-1)P(k)e^{-\beta k\rho(\infty)}. \quad (3.93)$$

We can check that $\rho_\infty = 0$ is a solution of equation (3.93) and this equation can also be solved by the same considerations as in the previous section:

$$\delta\rho_\infty = g(\rho_\infty), \quad (3.94)$$

where

$$g(\rho_\infty) = 1 - \frac{1}{\langle k \rangle} - \sum_k \frac{1}{\langle k \rangle} (k-1)P(k)e^{-\beta k\rho(\infty)}.$$

Equation (3.94) has a non zero positive solution if the slope of the function $g(\rho_\infty)$ at zero is greater than the slope of the line $y = \delta\rho_\infty$, that is

$$\left. \frac{d}{d\rho_\infty} \left(1 - \frac{1}{\langle k \rangle} - \sum_k \frac{1}{\langle k \rangle} (k-1)P(k)e^{-\beta k\rho(\infty)} \right) \right|_{\rho_\infty=0} \geq \delta \quad (3.95)$$

or equivalently

$$\frac{\beta}{\langle k \rangle} \sum_k k(k-1)P(k) \geq \delta. \quad (3.96)$$

Therefore the epidemic threshold condition is given by

$$\frac{\beta}{\delta} = \frac{\langle k \rangle}{\langle k^2 \rangle - \langle k \rangle}, \quad (3.97)$$

such that

- If $\frac{\beta}{\mu} < \frac{\langle k \rangle}{\langle k^2 \rangle - \langle k \rangle}$ the epidemic prevalence is $r_\infty = 0$ and,
- If $\frac{\beta}{\mu} > \frac{\langle k \rangle}{\langle k^2 \rangle - \langle k \rangle}$ the epidemic prevalence is such that $r_\infty > 0$.

Remark 3.7.1 *In the stochastic epidemic models presented in this chapter, (described by the mean field equation (3.75) and equation (3.76)) the disease can be eventually eliminated from the population or from the network regardless of the value of the basic reproduction number R_0 and of the initial distribution [88]. This is due to the fact that those stochastic models have an absorbing state, where all infectives equal zero (no nodes are infected), so that the probability of disease extinction approaches one in the infinite time limit. Mathematically, this means that all paths will eventually reach this state and remain there for ever, but in practice as shown in this chapter, the mean field approximations are useful for describing the behaviour over realistic time-scales. The threshold for stochastic models of epidemics is discussed in [88].*

Chapter 4

Long-Range Interactions in Networks

In the previous chapters interactions between network units or components are along the edge of the network. For instance in the diffusion process if a node i possesses some kind of information, this information can be transmitted or spread to the nearest neighbours of that node that are directly connected to it. Another example is the spread of an epidemic where an infected node can only infect nodes that are its nearest neighbours which are separated by distance one. This chapter will analyse and describe the non direct interactions between units of a complex network, here called long-range interactions (LRI).

4.1 Random Long-Range Interactions

4.1.1 Watts-Strogatz Model(WSM)

4.1.1.1 Small world model

In simple terms, the small-world concept describes the fact that despite their often large size, in most networks there is a relatively short path between any two nodes. The distance between two nodes is defined as the number of edges along the shortest path connecting them. The most popular manifestation of small worlds is the “six degrees of separation” concept, uncovered by the social psychologist Stanley Milgram [87, 117], who concluded that there was a path of acquaintances with a typical length of about six between most pairs of people in the United States. This feature (short path lengths) is also present in random graphs. However, in a random graph, since the edges are distributed randomly, the clustering coefficient is considerably smaller. Instead, in most, if not all, real networks the clustering coefficient is typically much larger than it is in a comparable random network (i.e., the same number of nodes and edges as the real network). Beyond Milgram’s experiment, it was not until 1998 that Watts and Strogatz work [123] stimulated the study of such phenomena. Their main discovery was the distinctive combination of high clustering with short characteristic path length, which is typical in real-world networks (either social, biological or technological) that cannot be captured by traditional approximations such as those based on regular lattices or random graphs. From a computational point of view, Watts and Strogatz proposed a one-parameter model that interpolates between an ordered finite dimensional lattice and a random graph. The algorithm behind the model is the following [123]:

1. *Start with order:* Start with a ring lattice with n nodes in which every node is connected to its first k neighbours ($k/2$ on either side). In order to have a

sparse but connected network at all times, consider $n \gg k \gg \ln(n) \gg 1$.

2. *Randomise*: Randomly rewire each edge of the lattice with probability p such that self connections and duplicate edges are excluded. This process introduces $pnk/2$ long-range edges which connect nodes that otherwise would be part of different neighbourhoods. By varying p one can closely monitor the transition between order ($p = 0$) and randomness ($p = 1$).

The rewiring can be considered as the process through which, with probability p we replace each link i, j with a link i, k , where k is a randomly chosen node different from i and j . In the case that i, k is already contained in the modified network no action is considered. This process is illustrated in Figure 4.1. Obviously, as $p \rightarrow 1$ the network tends to a completely random graph (see Figure 4.3). The Watts-Strogatz network is often written as a three-parameters graph: $WS(n, k, p)$. These networks have a high clustering coefficient in comparison with Erdős-Rényi random networks, i.e., if each node has a degree k , where k is even, then [19]

$$\bar{C} = \frac{3(k-2)}{4(k-1)}, \quad (4.1)$$

which means that the clustering coefficient of these networks is independent of the network size and it tends to the value $\bar{C} = 0.75$ for large value of k . The simple but interesting result when applying the algorithm was the following. Even for a small probability of rewiring, when the local properties of the network are still nearly the same as for the original regular lattice and the average clustering coefficient does not differ essentially from its initial value, the average shortest path length is already the same order as that for classical random graphs.

As discussed in [122], the origin of the rapid drop in the average path length L is the appearance of shortcuts between nodes. Every shortcut, created at random,

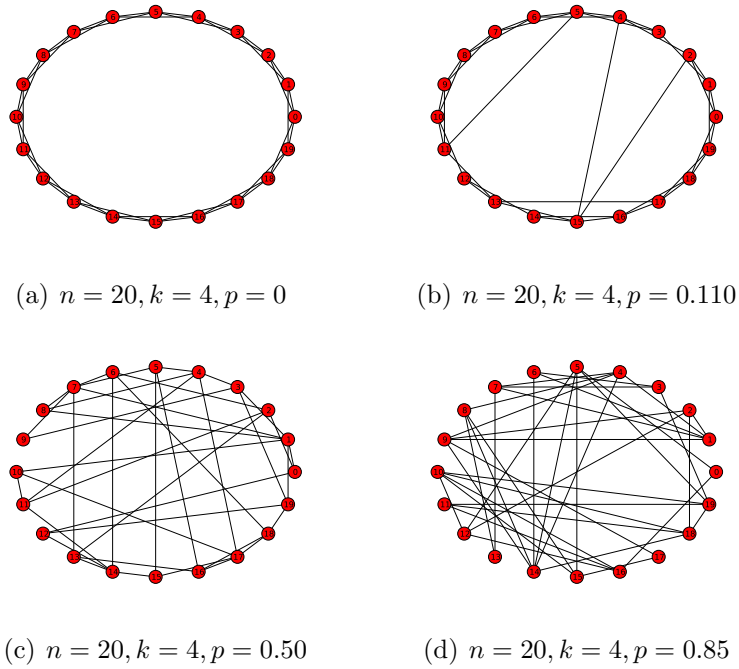


Figure 4.1: Illustrations of the rewiring process, which is the basis of the Watts-Strogatz model for small networks. Starting from a regular lattice network with $n = 20$, $k = 4$ some links are rewiring with probability p .

is likely to connect widely separated parts of the graph, and thus has a significant impact on the characteristic path length of the entire graph. Even a relatively low fraction of shortcuts is sufficient to drastically decrease the average path length, yet locally the network remains highly ordered. In addition to a short average path length, small-world networks have a relatively high clustering coefficient. The Watts-Strogatz model (*SW*) displays this duality for a wide range of the rewiring probabilities p . In a regular lattice the clustering coefficient does not depend on the size of the lattice but only on its topology. As the edges of the network are randomised, the clustering coefficient remains close to $C(0)$ for relatively large values of p .

Although the mean degree is exactly $\bar{k} = k$ [19], no exact expression for the degree distribution for a Watts-Strogatz small-world network is known, except

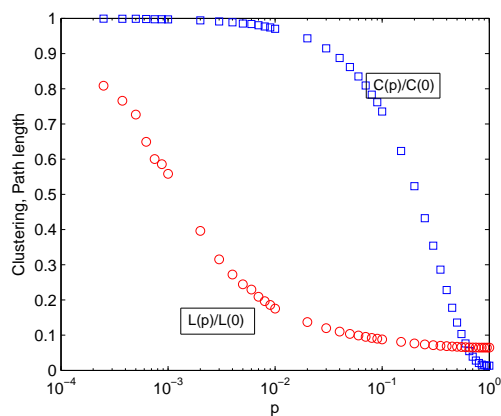


Figure 4.2: Structural evolution of the Watts-Strogatz model. Illustrations of the variation of the average path length and the clustering coefficient with the change of the rewiring probability for a network having $n = 1000$ nodes and $k = 10$. Each point is the average of 50 realisations. The values for the average path length and clustering coefficient are normalised by dividing them by the respective values obtained for $WS(1000, 10, 0)$.

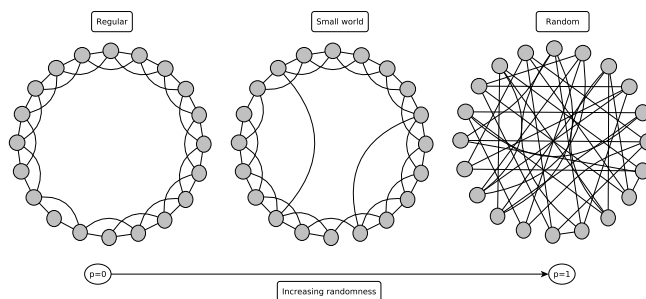


Figure 4.3: Three basic network types in the model of Watts and Strogatz. The leftmost network is a ring of 20 nodes ($n = 20$), where each vertex is connected to its four neighbours ($k = 4$). This is an ordered network which has a high clustering coefficient C and a long pathlength L . By choosing an edge at random, and reconnecting it to a randomly chosen vertex, networks with increasingly random structure can be generated for increasing rewiring probability p . In the case of $p = 1$, the network becomes completely random, and has a low clustering coefficient and a short pathlength. For small values of p so-called small-world networks arise, which combine the high clustering coefficient of ordered networks with the short pathlength of random networks.

when $p = 0$, in which case every node has degree k . An approximation for the case of $0 < p < 1$ has been calculated by Barrat and Weigt [19]. There is also

no known exact expression for the average path length of this network. A scaling approximation is given by [93]:

$$L \sim \frac{n}{K} \frac{1}{\sqrt{u^2 + 4u}} \tanh^{-1} \left(\frac{u}{\sqrt{u^2 + 4u}} \right), \quad (4.2)$$

where $u = pkn$. For the case of fixed p and k , if $k \ll n$ and n is sufficiently large, then the average path length is expected to increase with network size, because the terms involving u converge to a constant for large n [94]. Although the clustering coefficient does also not have a known exact expression, it is well approximated [19] for large n as

$$\bar{C} \sim 0.75 \left(\frac{k-2}{k-1} (1-p)^3 + O\left(\frac{1}{n}\right) \right). \quad (4.3)$$

Since n is assumed to be large, for $p < 1$ the term expressed as $O(1/n)$ can be ignored.

4.2 Kleinberg Model (KM)

There are many generalisations of models of random networks. The Kleinberg model [74] is one model that represents a variation of the WS-model and was introduced by Kleinberg. In designing his network model, Kleinberg sought a simple framework that encapsulates the paradigm of Watts and Strogatz, that is rich in local connections, with a few long-range connections. Rather than using a ring as the basic structure however, the Kleinberg model begins from a two dimensional grid and allows for edges to be directed.

1. Start with a set of nodes (representing individuals in the social network) that are identified with the set of lattice points in an $n \times n$ square, $\{(i, j) : i \in \{1, 2, \dots, n\}, j \in \{1, 2, \dots, n\}\}$, and define the lattice distance or the

Manhattan distance between two nodes (i, j) and (k, l) to be the number of “lattice steps” separating them: $d((i, j), (k, l)) = |k - i| + |l - j|$,

2. for a universal constant $d \geq 1$, the node u has a directed edge to every other node within lattice distance d ; these are its local contacts,
3. for universal constants $q \geq 0$ and $\alpha \geq 0$, construct directed edges from u to q other nodes (the long-range contacts) using independent random trials; the i th directed edge from u has endpoint v with probability proportional to $(d(u, v))^{-\alpha}$. (To obtain a probability distribution, we divide this quantity by the appropriate normalising constant $\sum_v (d(u, v))^{-\alpha}$; we will call this the inverse α th-power distribution.)

Geographically the algorithms means that individuals live on a grid and know their neighbours for some number of steps in all directions (local contacts); they also have some number of acquaintances distributed more broadly across the grid (long-range contacts). For fixed constants d and q we obtain a one-parameter family of network models by tuning the value of the exponent α . The Kleinberg model graph can then be defined by the following set of parameters $G_k(n, d, q, \alpha)$. When $\alpha = 0$, we have the uniform distribution over long-range contacts, the distribution used in the basic network model of Watts and Strogatz in which the long-range contacts are chosen independently of their position on the grid. As α increases, the long-range contacts of a node become more and more clustered in its vicinity on the grid. Thus, α serves as a basic structural parameter measuring how widely ‘networked’ the underlying society of nodes is.

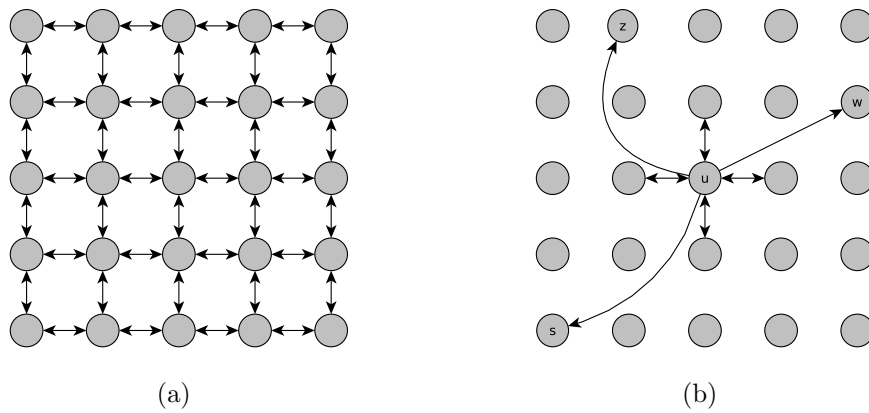


Figure 4.4: A two-dimensional grid network with $n = 6$, $p = 1$, and $q = 1$ (a), and (b) the contacts of a node u with $p = 1$ and $q = 3$. The three long range contacts are v , z and t .

Expected Delivery Time

The concept of local routing of a message in a network refers to sending a message from a source to a target with local information only, as in the case of the Milgram experiment described in the small-world section. One way of studying the transmission of such a message is by using a decentralised algorithm. We start with two arbitrary nodes in the network, denoted s and t ; the goal is to transmit a message from s to t in as few steps as possible. Decentralised algorithms, are mechanisms whereby the message is passed sequentially from a current message holder to one of its (local or long-range) contacts, using only local information. In particular, the message holder u in a given step has knowledge of

1. the set of local contacts among all nodes (i.e. the underlying grid structure);
2. the location, on the lattice, of the target t ; and
3. the locations and long-range contacts of all nodes that have come in contact with the message.

Crucially, u does not have knowledge of the long-range contacts of nodes that have not touched the message. Given this, u must choose one of its contacts v , and forward the message to this contact. The efficiency of such decentralised algorithms is measured by the expected delivery time. That is the expected number of steps taken by the algorithm to deliver the message over a network generated according to an inverse α th-power distribution, from a source to a target chosen uniformly at random from the set of nodes. Of course, constraining the algorithm to use only local information is crucial to the model; if one had full global knowledge of the local and long-range contacts of all nodes in the network, the shortest chain between two nodes could be computed simply by a breadth-first search.

Kleinberg found that the expected delivery time t , which measures the efficiency of the algorithm and corresponds to the expected number of steps needed to forward a message from a random source is bounded by below as follows [52]:

$$t \geq cn^\xi \tag{4.4}$$

where

$$\xi = \begin{cases} (2 - \alpha)/3 & \text{for } 0 \leq \alpha \leq 2, \\ (\alpha - 2)/(\alpha - 1) & \text{for } \alpha > 2 \end{cases} \tag{4.5}$$

As the parameter α increases, a decentralised algorithm can take more advantage of the “geographic structure” implicit in the long-range contacts; at the same time, long-range contacts become less useful in moving the message a large distance. The value $\alpha = 2$ is critical for the delivery time. This means that efficient navigability is a fundamental property of only some small-world structures. In particular, when long-range connections follow an inverse-square distribution, ($\xi = 2$) the delivery time of a message carried out by a decentralised algorithm is

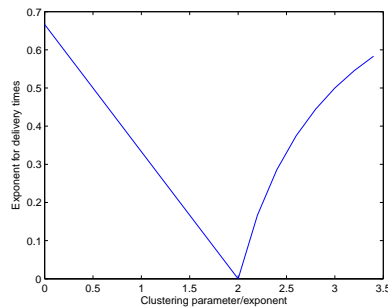


Figure 4.5: The lower bound of the expected delivery time in a decentralised algorithm. The x -axis is the value of α ; the y -axis is the resulting exponent of n .

very fast.

4.3 Range Dependent Model (RDM)

Some models of random networks have been inspired by the structure of biological networks. In this section we will review what Grindrod [67] did. He defined a new class of range dependent random graphs inspired by protein-protein interaction networks that, in some sense, generalise the work of Watts and Strogatz for the small world model. In this model the nodes are ordered in a natural linear way: $i = 1, 2, \dots, n$. Then a link between nodes i and j is created independently of the order of the links, with probability $\alpha\eta^{|j-i|-1}$, where $\alpha > 0$ and $\eta \in (0, 1)$ are fixed parameters. When $\alpha = 1$, all nearest neighbours are connected, and the network contains a Hamiltonian path connecting all nodes independently of η . In general, for a given undirected network the probability that any pair of nodes i, j are connected is given by a function of the form

$$p_{ij} = f(|j - i|) \in [0, 1], \quad (4.6)$$

and the range of an edge $R(i, j)$ is equal to $|i - j|$ and is the length of the shortest path between i and j in the absence of that edge. Grindrod has determined that these networks have the following properties:

$$\bar{k} = \frac{2\alpha}{1 - \eta} \quad (4.7)$$

and

$$\bar{C} = \frac{3\alpha\eta}{(1 + \eta)(1 + 3\eta)}, \quad (4.8)$$

which means that for $\alpha = 1$, $\bar{C} = 3/8$ as $\eta \rightarrow 1$. The clustering coefficient in these networks displays a maximum which is located at $\eta = 3^{-0.5}$. If we consider that $\alpha = \bar{k}(1 - \eta)/2$, we can write the clustering coefficient as

$$\bar{C} = \frac{3\bar{k}(1 - \eta)\eta}{2(1 + \eta)(1 + 3\eta)}, \quad (4.9)$$

which has a maximum at $\eta = (\sqrt{8} - 1)/7 \approx 0.261$, independent of the average degree.

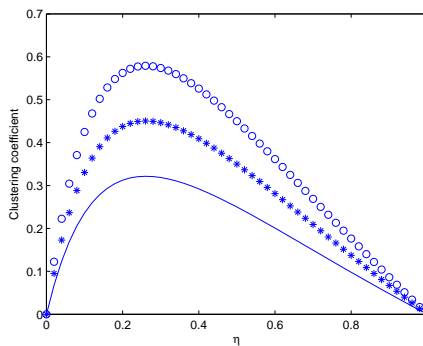


Figure 4.6: Clustering coefficient in the Grindrod random network. The change in the average clustering coefficient in range-dependent random networks developed by Grindrod, with the change in the parameter η for three different average degrees: continuous line ($\bar{k} = 2.5$), line with stars ($\bar{k} = 3.5$) and line with circles ($\bar{k} = 2.5$).

4.4 Nonrandom Long-Range Interactions

4.4.1 The Jackson and Wolinsky Model (JWM)

Jackson and Wolinsky [69] studied the stability and efficiency of social and economic networks, where individuals can form or delete links [70]. The goal of their work was to begin to understand which networks are stable when individuals choose to form new links or deleting existing links. Their analysis was designed to give us some predictions concerning which networks are likely to form, and this depends on productive and redistributive structures. In particular, they examined the relationship between the set of networks which are productively efficient, and those which are stable. To capture the notion of total productivity and how this is allocated among the individual nodes they introduced the notion of a value function and an allocation function.

The Network

Let $\mathcal{N} = \{1, \dots, n\}$ be the finite set of players who are connected in some network relationship. The network relationships are reciprocal and the network is thus modelled as a non-directed graph. We write the complete graph of subsets of \mathcal{N} of size 2 by \mathcal{G}^n and the set of all possible graphs on \mathcal{N} is then $\Xi = \{G | G \subset \mathcal{G}^n\}$. The network obtained by adding a link (i, j) to an existing network G is denoted $G + (i, j)$ and the network obtained by deleting link (i, j) from an existing network G is denoted $G - (i, j)$. For any network G , let $N(G) = \{i | \exists j \text{ such that } (i, j) \in G\}$ be the set of players who have at least one link in the network G .

Value Function and Efficiency

Different network configurations lead to different values of overall production or overall utility to players. These various possible valuations are represented via a value function. A value function is a function $v : \Xi \rightarrow \mathbb{R}$. The set of all possible value functions is $\mathcal{V} = \{v | v : \Xi \rightarrow \mathbb{R}\}$. In some applications the value functions are aggregate of individual utilities and production, i.e.

$$v(G) = \sum_i u_i(G), \quad (4.10)$$

where $u_i \in \mathcal{V}$.

In evaluating societal welfare, we may take various perspectives. A network G is Pareto efficient relative to \mathcal{V} and Y if there does not exist any $G_0 \in \mathcal{G}^n$ such that $Y_i(G_0, \mathcal{V}) \geq Y_i(G, \mathcal{V})$ for all i with strict inequality for some i . This definition of efficiency of a network takes Y as fixed, and hence can be thought of as applying to situations where no intervention is possible. A graph G is said to be strongly efficient if $v(G) \geq v(G')$ for all $G' \in \mathcal{G}^n$. This is a strong notion of efficiency as it takes the perspective that value is fully transferable.

Allocation Rule

A value function only keeps track of how the total societal value varies across different networks. We also wish to keep track of how that value is allocated or distributed among the players forming a network. An allocation function/rule $\mathcal{Y} : \Xi \times \mathcal{V} \rightarrow \mathbb{R}^n$ describes how the value associated with each network is distributed to the individual players. The expression $\mathcal{Y}_i(G, \mathcal{V})$ is the payoff of player i from the graph G under the value function \mathcal{V} . It is important to note that an allocation rule depends on both G and v . This allows an allocation rule to take

full account of player i 's role in the network. This includes not only what the network configuration is, but also and how the value generated depends on the overall network structure.

Pairwise Stability

The main interest is to understand which networks are likely to arise in various contexts, so we need to define a notion which captures the stability of a network. A stable network embodies the idea that players have the discretion to form or delete links. The formation of a link requires the consent of both parties involved, but severance can be done unilaterally. A simple way to analyse the networks that one might expect to emerge in the long run is to examine a sort of equilibrium requirement that agents not benefit from altering the structure of the network. A weak version of such a condition is the pairwise stability notion defined by Jackson and Wolinsky. A network is pairwise stable if no player benefits from severing one of their links and no other two players benefit from adding a link between them, with one benefiting strictly and the other at least weakly.

Definition 4.4.1 *The Network G is pairwise stable with respect to \mathcal{V} and \mathcal{Y} if*

1. *for all links $(i, j) \in E(G)$, $\mathcal{Y}_i(G, \mathcal{V}) \geq \mathcal{Y}_i(G - (i, j), \mathcal{V})$ and $\mathcal{Y}_i(G, \mathcal{V}) \geq \mathcal{Y}_i(G + (i, j), \mathcal{V})$*

and

2. *for all links $(i, j) \notin E(G)$ if $\mathcal{Y}_i(G, \mathcal{V}) < \mathcal{Y}_i(G + (i, j), \mathcal{V})$ then $\mathcal{Y}_j(G, \mathcal{V}) > \mathcal{Y}_j(G + (i, j), \mathcal{V})$*

Let us say that G' is adjacent to G if $G' = G + (i, j)$ or $G' = G - (i, j)$ for some (i, j) . A network G' defeats G if either $G' = G - (i, j)$ and $\mathcal{Y}_i(G', \mathcal{V}) \geq \mathcal{Y}_i(G, \mathcal{V})$,

or if $G' = G + (i, j)$ with $\mathcal{Y}_i(G', \mathcal{V}) \geq \mathcal{Y}_i(G, \mathcal{V})$ and $Y_j(G', \mathcal{V}) \geq Y_j(G, \mathcal{V})$ with at least one inequality holding strictly. Pairwise stability is equivalent to saying that a network is pairwise stable if it is not defeated by another (necessarily adjacent) network. In words, graph G is pairwise when

- for any link (i, j) in G both i and j prefer not to remove the link
- for any link (i, j) not in G both i and j prefer not to add the link.

Therefore the pairwise stability presumes that actors can unilaterally break links, while pairs of actors can add links.

4.4.2 Example 1: The Connections Model

This model models the social communication among individuals. Individuals directly communicate with those to whom they are linked (short contacts) to exchange, for example, some information. Through these links or short contacts they also benefit from indirect communication (long-range contacts) from those to whom their adjacent nodes are linked, and so on. Let $w_{ij} \geq 0$ denote the intrinsic value of individual j to individual i and c_{ij} denote the cost to i of maintaining the link (i, j) . If individual i is connected to player j , by a path of t_{ij} links, then player i receives a payoff of $\delta^{t_{ij}} w_{ij}$ from his indirect connection with individual j . It is assumed that $0 < \delta < 1$, and so the payoff $\delta^{t_{ij}} w_{ij}$ decreases as the path connecting individual i and j increases; thus information that travels a long distance becomes diluted and is less valuable than information obtained from a closer neighbour. The parameter $0 < \delta < 1$ captures the idea that the value that i derives from being connected to j is proportional to the proximity (concepts of proximity will be briefly described in the next chapter) of j to i . The value of communication obtained from other nodes depends on the distance to those nodes. Communica-

tion is costly so that individuals must weigh the benefits of a link against its cost. Each direct link (i, j) results in a cost $c_{ij} = c_{ji} = c$ for both i and j . The cost can have different meanings, it can be interpreted as the time an individual must spend with another in order to maintain a direct link. Less distant connections are more valuable than distant ones, but direct connections are costly. The payoff/utility of each player i from graph G is formally given by:

$$u_i(G) = w_{ii} + \sum_{j \neq i} \delta^{t_{ij}} w_{ij} - \sum_{j \in (i,j)} c_{ij}. \quad (4.11)$$

The value of the graph is given by:

$$\mathcal{V} = \sum_i u_i. \quad (4.12)$$

If we assume that $w_{ii} = 0$ and $w_{ij} = 1$ and $c_{ij} = c$ then the payoff function (4.11) reads:

$$u_i(G) = \sum_{j \neq i} \delta^{t_{ij}} - d_i c_{ij}, \quad (4.13)$$

where d_i is the number of links held by individual i .

4.4.3 Example 2: The Co-author Model

In this case, nodes can be considered as researchers who spend time writing papers [70]. Each node's productivity is a function of its links. A link represent a collaboration between two researchers. The amount of time a researcher spends on any given project is inversely related to the number of projects that researcher is involved in. Therefore, in contrast to the connection model, here the indirect connections will enter the utility/payoff in a negative way as they detract from one's co-author's time. The fundamental utility or productivity of player i given

the network G is

$$u_i(G) = \sum_{j \in (i,j)} w_i(n_i, j, n_j) - c(n_i), \quad (4.14)$$

where $w_i(n_i, j, n_j)$ is the utility derived by i from a direct contact with j when i and j are involved in n_i and n_j projects, respectively, and $c(n_i)$ is the cost to i of maintaining n_i links. A specific version of this utility function is given by the following expression. For $n_i > 0$

$$\begin{aligned} u_i(G) &= \sum_{j \in (i,j)} \left[\frac{1}{n_i} + \frac{1}{n_j} + \frac{1}{n_i n_j} \right] \\ &= 1 + \left(1 + \frac{1}{n_i} \right) \sum_{j \in (i,j)} \frac{1}{n_j} \end{aligned} \quad (4.15)$$

and for $n_i = 0$ and $u_i(G) = 0$. This form assumes that each researcher has units of time which they allocate equally across their projects. The output of each project depends on the total time invested in it by the two collaborators, $1/n_i + 1/n_j$, and on some synergy in the production process captured by the interaction term $1/n_i n_j$. The interaction term is inversely proportional to the number of projects each author is involved with. Here, there is no direct cost of connection. The cost of connecting with a new author is that the new link decreases the strength of the interaction term with the existing link.

Example 3: Pairwise Stability in the Connection Model

To illustrate the pairwise stability condition, we return to the connection model, fixing the set of actors $\mathcal{N} = \{1, 2, 3, 4, 5\}$ and the parameter values $\delta = 0.5$ and $c = 0.55$. Let us consider the star graph $G = \{(1, 2), (1, 3), (1, 4), (1, 5)\}$. It is easy to see that this star graph is not pairwise stable. The payoff for actor 1 (who is

the centre of the star) is (we use formula (4.13))

$$u_1(G) = -d_1c + 4\delta = 4(\delta - c) = -0.2,$$

where $d_1 = 4$ is the degree of node 1. By severing any existing links (say link 12), actor 1's payoff rises to

$$u_1(G - 12) = 3(\delta - c) = -0.15$$

and thus the graph G is not pairwise stable. Intuitively, given our maintained assumption that $c > \delta$, the cost of maintaining a link exceeds the benefits of a direct connection, and thus no individual would be willing to serve as the centre of a star graph. In contrast, the cycle graph $G = \{(1, 2), (2, 3), (3, 4), (4, 5), (5, 1)\}$ is pairwise stable for the assumed parameter values. In this graph, all actors hold similar positions, and payoffs are

$$u_i(G) = 2\delta + 2\delta^2 - 2c = 0.4 \quad \forall i.$$

To establish the pairwise stability of this graph, we must first show that no actor would want to sever an existing link. For instance, suppose link $(1, 2)$ was removed from G . This implies

$$u_1(G - (1, 2)) = u_2(G - (1, 2)) = \delta + \delta^2 + \delta^3 + \delta^4 - c = 0.3875$$

and hence neither actor 1 or 2 would prefer to break this link. Given that the removal of any other edge (i, j) in G has the same consequence for actors i and j , we see that no actor wishes to sever an existing link. Secondly, we must show that no pair of actors would want to add a link. For instance, suppose that link $(1, 3)$

was added to G . This implies

$$u_1(G + (1, 3)) = u_3(g + (1, 3)) = 3\delta + \delta^2 - 3c = 0.1$$

and hence both actors 1 and 3 would prefer not to add this link. Given that the addition of any new link (i, j) to the cycle graph would have the same consequences for actors i and j , we see that no pair of actors would prefer to add a new link. Thus, the graph G is pairwise stable. Note that a single violation of the pairwise stability condition is sufficient to demonstrate the negative result that G is not pairwise stable. Moving beyond these two graphs, Jackson and Wolinsky [69] provide the following characterisation of pairwise stable graphs in the connections model. For $c < \delta - \delta^2$, the complete graph (with links between every pair of actors) is the unique pairwise stable network. For $\delta - \delta^2 < c < \delta$, the star graph is pairwise stable, but is not always the unique pairwise stable graph. Finally, for $c > \delta$, the star graph is not pairwise stable. Intuitively, as c becomes very large, no actor is ever willing to maintain links, and only the empty graph is pairwise stable. Usually it takes more work to establish that a graph is pairwise stable. This result might suggest the possibility for “side payments” from actors on the periphery of the star to the actor in the centre. See Jackson and Wolinsky [69] for development of the connections model with transferable utility.

The model of Jackson and Wolinsky [69] as well as the one by Bala and Goyal [11] are mainly concerned with stability and efficiency of the network resulting from different dynamic updating rules. As we have seen the model of Jackson and Wolinsky study the pairwise stability when agents can only update a link at a time (either delete it or create it), while Bala and Goyal allow agents to rearrange all their connections at once. The updating is deterministic in both models, and a

new configuration is accepted only if it increases the utility of the agent.

Carvalho and Iori [31] combine the physics structure of networks and the economics approach of [69] and [11] by introducing a stochastic network formation mechanism inspired by the utility maximisation models which naturally extends the well known physicists' preferential attachment rule. Their approach can be reduced to two main points:

1. They studied how the average utility depends on the underlying network topology
2. They gained insight into specific network growth mechanisms and network topologies. They studied the preferential attachment mechanism by node utility.

They focus on one particular case in which they set $w_{ij} = 1$, $w_{ii} = 0$ and $c_{ij} = c$ and rewrote the payoff/utility of a node as:

$$u_i = \sum_{l=1}^{l_{max}^{(i)}} \sum_{\{k|d_{ik}=l\}} \delta^l - \sum_{j \in (i,j)} c = \sum_{l=1}^{l_{max}^{(i)}} \delta^l z_l^i - cz_1^i, \quad (4.16)$$

where the sum in l is over all the shortest paths of length l from node i , the sum in k is over all nodes whose shortest path from i is $d_{ik} = l$, $l_{max}^{(i)}$ is the path length of the node the furthest away from node i , and z_l^i is the number of l th-nearest neighbours of node i .

The average utility in a star network is given by:

$$\bar{u}_*(\delta) = \delta z_1 \left(1 + \delta \frac{n-2}{2} \right), \quad (4.17)$$

where $z_1 = 2(n-1)/n$. For large n , $z_1 \sim 2$ and $\bar{u}_*(\delta) \sim n\delta^2$. The average utility

in a generic network is obtained by averaging (4.16)

$$\bar{u}(\delta) = \sum_{l=1}^{\bar{l}} \delta^l z^l - cz_1, \quad (4.18)$$

where z_l is the average number of l th neighbours of a node and \bar{l} is the average path length. Without loss of generality they set $c = 0$ and we get

$$\bar{u}(\delta) = \sum_{l=1}^{\bar{l}} \delta^l z^l. \quad (4.19)$$

By comparing the average utility in different network topologies with the same size and the same average degree, they show that scale-free networks are more efficient than Poisson random networks (even though less efficient than for the star graph). By more efficient we mean of course a network whose structure maximises the total of the average utility.

The high average utility of scale-free networks compared to random networks suggests a new mechanism of growth model. The authors extended the preferential attachment mechanism by introducing a growing process inspired by the work of Jackson and Wolinsky. Thus, the probability that a new node j will be connected to an existing node i depends on the utility of i , such that

$$\prod_i = \frac{u_i}{\sum_{k=1}^n u_k}. \quad (4.20)$$

For $\delta = 0$ and $\delta = 1$ the utility of all nodes is given by:

$$u_i = \begin{cases} 0 & \forall i \text{ when } \delta = 0, \\ N & \forall i \text{ when } \delta = 1, \end{cases} \quad (4.21)$$

so in this case attachment happens randomly and we recover an exponential distribution of node degree. The preferential attachment (4.20) is invariant up to multiplicative factors in (4.16) and so for $\delta \neq 0$ the qualitative behaviour of the model remains unchanged if we define the utility as

$$u'_i = \frac{u_i}{\delta} = k_i + \sum_{l=2}^{l_{max}^{(i)}} \sum_{\{k|d_{ik}=l\}} \delta^l, \quad (4.22)$$

where k_i is the degree of node i . Thus, as $\delta \rightarrow 0$ the model of Corvhallo and Iori converges to the Barabási-Albert model and the network becomes scale-free. They also show that for small values of δ their model based on utility retains a scale-free structure that is nonetheless destroyed when δ increases.

A Nonrandom Network Model to account for Short and Long-Range Connections

Cohen et al. [35] developed a network model for the spread of tuberculosis to account for both close and casual contacts among individuals.

Network Description

The network consisted of individuals placed randomly on a square patch at a constant average density. Contacts between individuals are drawn as edges connecting nodes. These edges represent sufficient contacts for the transmission of TB. It is specified that the chance of a link between two individuals decreases as the distance between them increases such that infection is transmitted preferentially to individuals in the proximity of a case of infection. (The idea of proximity will be briefly presented in the next chapters). We can think of individuals located nearest to each other on the network as family members, while those slightly farther

away may be neighbours, friends or others social contacts. The fact that links between individuals are assigned with a probability related to their distance from each other allows that some long-distance contact will exist in the network. They considered a parameter D that controls the relative probability of creating shorter-versus longer-distance connections in a network. Given two vertices separated by a distance d , they defined a probability of an edge linking them by

$$p = \frac{n}{2\pi D^2} e^{-\frac{d^2}{2D^2}}, \quad (4.23)$$

where n is the average number of contacts and D is the desired length-scale. As can

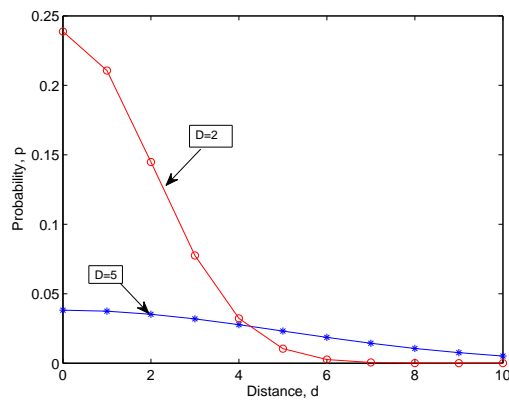


Figure 4.7: Probability p of an edge linking two vertices as a function of the distance d separating these two vertices in the Cohen et al. model

be seen in Figure 4.7, if the parameter D is small, individuals separated at short distances are preferentially linked; when D is large, the long-range interactions are favoured. Adjustment of this single parameter allows us to calibrate the extent of clustering. A network with lower D is dominated by high clustering and a network with larger D is dominated by long-range connections. It is remarkable that the number of casual social contacts is considered to be a product of these long-range interactions. Their results demonstrate that in large communities with low TB

incidences, non-random mixing of the population allows re-infection to play a larger role in disease dynamics than previously recognised. The authors have claimed that “in areas where a substantial proportion of transmission is due to ‘casual’ contacts, a network with higher D value would better represent the contact structure.” That is, casual contacts are proportional to long-range interactions among nodes in a network. In the work of Cohen et al., however, the proximity between individuals is considered to be the Euclidean distance between nodes placed randomly on a plane, which in some way tries to capture their “geographical” separation. We need to provide some of the empirical evidence about the interrelation existing between geographic and social proximity.

Chapter 5

Social Contacts: Close and Casual Contacts. Empirical Evidence

In this chapter we are going to give a group of close and casual contacts in social networks relevant to the transmission of epidemics. Based on this evidence we will elaborate a network model in the next chapter to account for both types of contacts.

5.1 Social Networks

A social network is a social structure made up of individuals (or organisations) called "nodes", which are tied (connected) by one or more specific types of interdependency, such as friendship, kinship, common interest, financial exchange, dislike, sexual relationships, or relationships of beliefs, knowledge or prestige. Social network analysis (SNA) views social relationships in terms of network theory consisting of nodes and ties (also called edges, links, or connections). Nodes are the individual actors within the networks, and ties are the relationships between the actors. The resulting graph-based structures are often very complex. There

can be many kinds of ties between the nodes. Research in a number of academic fields has shown that social networks operate on many levels, from families up to the level of nations, and play a critical role in determining the way problems are solved, organisations are run, and the degree to which individuals succeed in achieving their goals.

In its simplest form, a social network is a map of specified ties, such as friendship, between the nodes being studied. The nodes to which an individual is thus connected are the *social contacts* of that individual. The network can also be used to measure social capital, the value that an individual gets from the social network. These concepts are often displayed in a social network diagram, where nodes are the points and ties are the lines. Social contacts include *close contacts* and *casual contacts*. In the case of epidemic transmission for example, these types of contacts can be defined or characterised as follows:

Nomenclature

- Index case: A suspected or confirmed case of a certain infection on an individual, let say for instance tuberculosis TB or pandemic influenza.
- Casual contact: A person who has shared air with the index case.
- Close contact: A person who has prolonged, frequent, or intense contact with an index case during the case's period of infectiousness. Whether a person is a close contact also depends on:
 - Physical proximity to the index case.
 - The environment in which exposure to the index case occurs.

Examples of close contacts include, but are not limited to, persons who

carpool with the index case several days per week or share the same house or room as the index case or spend time with the index case frequently or share air in small, enclosed spaces with little natural or mechanical ventilation.

- Casual contact: A person who has less prolonged, intense, or frequent contact with the index case than close contacts. Examples of casual contacts include, but are not limited to, persons who visited the index case occasionally or visited the index case weekly for a short time.

5.2 Relevance of Social Network Interactions for the Spread of Infections

The pattern of human interactions in social networks has important implications for the spread and management of infectious diseases [72, 91]. As we have seen in the previous chapters on epidemic spreading in networks, the usual approach to epidemic spreading imposes a number of assumptions [18, 93] that make analytic and numerical treatment relatively straightforward (see Chapter 3); however, at least in some cases, that approach may cause a departure from reality. One such assumption is uniform mixing, whereby the individuals of a population are assumed to come in contact with equal probability, independent of their location. In order to relax this assumption, we observe that contact processes, such as disease transmission, are well localised in space and require that the two or more individuals be no farther apart than some typical distance characteristic of the disease transmission process. In heavily populated urban areas, disease is usually transmitted within such locations as buildings and mass transit areas (waiting areas and mass transit cars). The identification of individuals with a large number of interactions forms the basis of many sexually transmitted disease control policies.

For example the emergence of HIV/AIDS in the 1980s, has led to many attempts for quantifying the structure of sexual interactions [45]. In the case of sexually transmitted diseases or computer viruses, the determination of social contacts can be done in an effective way. However, in other scenarios, such as in the transmission of airborne or close contact infections, the pattern of human interactions produced by encounters between individuals is harder to define [35, 45].

Only recently, some studies have been conducted that shed some light on the patterns of these social contacts. Mossong et al. [91], studied the combination of both close and casual contacts among individuals to account for those social interactions, which include physical and non-physical contacts occurring at different environments (home, work, school, transport, leisure, etc.) for periods of time that range between a few minutes and several hours. These authors studied 97,904 contacts among 7,290 participants in 8 European countries. They recorded the age, sex, location, duration, frequency, and occurrence of physical contact. As they study the occurrence of these social contacts in places like home, work, school, leisure, transport, and others as well as the combination of them, this study accounts for both close and casual contacts among individuals. Information on social contacts was obtained using cross-sectional surveys conducted by different commercial companies or public health institutes in Belgium (BE), Germany (DE), Finland (FI), Great Britain (GB), Italy (IT), Luxembourg (LU), The Netherlands (NL), and Poland (PL). The recruitment and data collection were organised at the country level according to a common agreed quota sampling methodology and diary design. The surveys were conducted between May 2005 and September 2006 with the oral informed consent of participants and approval of national institutional review boards following a small pilot study to test the feasibility of the diary design and recruitment.

Each participant in that study was given the following instructions when filling in the diary [91]:

- Record in the diary every person that you have contact with on your assigned day.
- A contact is defined as:
 - Either a two-way conversation with three or more words in the physical presence of another person,
 - Or physical skin-to-skin contact (for example a handshake, hug, kiss or contact sports).
- Write down every person that you contact during the day, regardless of whether the contact was long or short, and whether you know the person or not.
- Contacts made exclusively by telephone or mobile phone should not be recorded.
- If you contact the same person several times in the course of the day, only record him/her once, and record the total time you spent with that person over the entire day. So each person you meet during the day and have contact with should only have one line in the diary: one person, one line.
- Please provide information on your contact, namely:
 - Age.
 - Gender.
 - How long the contact with the person was over the entire day.

- Places where contact(s) occurred (you may indicate several locations).
 - How often you contact this person in general.
 - Whether there was skin-to-skin contact.
- If you don't know the exact age, give an estimate of the age range (e.g. 40 – 45) and try to make it as narrow as possible.
 - Estimate the total duration of time spent in the presence of the contact person that day. Example: 5 – 15 minutes for a contact in a shop or 1 – 4 hours for longer contact caring for a child at home.
 - After you have finished recording the diary, we suggest that you double check the diary entries by trying to remember all of your activities to make sure you have not missed any contact persons.
 - The order in which you write down your contact persons is not important. The easiest is to use a chronological order according to when you met the person for the first time during your assigned day and then add anyone else that you might remember as you go through your daily activities.
 - For the purposes of this study, the day starts at 5 a.m. on the morning of the day assigned, and ends at 5 a.m. the next morning.

In order to simulate the initial phase of an epidemic, these authors partition the population into 5 years age bands, and group all individuals aged 70 years and older together. The focus is on the generic features of epidemic spreading along the transmission route that is specified by physical and non-physical contacts as defined here. This process results in 15 age classes. Let α_{ij} be the number of at-risk contacts of an individual in age class j with individuals in age class i . The number α_{ij} is also proportional to the observed number of contacts (both physical and

non-physical) that a respondent in age band j makes with other individuals in age band i . The matrix $\mathbf{\Lambda} = (k_{ij})$ is known as the next generation matrix and it can be used to calculate the distribution of numbers of new cases in each generation of infection from any arbitrary initial number of introduced infections. If \mathbf{x}_0 is the vector of the initial number of infected in generation 0, then the expected numbers of new cases in the i th generation is given by:

$$\mathbf{x}_i = \mathbf{\Lambda}^i \mathbf{x}_0. \quad (5.1)$$

The incidence of new infections per age band is obtained by dividing the expected number of new cases per age class by the number of individuals in each age class. To facilitate comparison among countries, the distribution of incidence over age classes is normalised in such a way that for each country the age-specific incidences sum to one.

Sample Description

A total of 7,290 diaries covering all contacts made by respondents during a full day were collected in eight countries ranging from 267 in NL to 1,328 in DE. 37.6% of participants in the survey were under 20 years of age, 12.4% of participants were over 60 years of age, and the medians were 28 years in BE (the lowest) to 33 years in DE (the highest). Returns of diaries by female participants showed a slight excess in all countries (ranging from 50.8% in FI to 55.7% in DE). In all countries except DE, single-person households were under-represented in the sample. This can be partially explained by the fact that children and adolescents were deliberately oversampled, and they are more likely to live in larger households.

Overall, 35.3% of the participants were in full-time education, 32.64% em-

ployed, 11% retired, 6.1% home-makers, 3.6% unemployed or seeking employment, whereas 8.6% recorded other and 2.8% failed to record their occupation. The proportion employed or in full-time education was fairly consistent across the eight countries; the other categories differed somewhat between countries. The analysis of the total number of reported contacts using a multiple regression model shows a consistent pattern of contact in children, a peak among 10 to 19 years old, followed by a fall to a lower plateau in adults until the age of 50 and a sharp decrease after that age [91].

These authors used different ways to measure the frequency, intensity and location of contacts and these measures seem to be highly correlated with each other (see Figure 5.1 for pooled data from all countries). As it can be seen from Figure 5.1, contacts of long duration or of daily frequency were much more likely to involve physical contact. In fact, approximately 70% of contacts made on a daily basis last in excess of an hour, whereas approximately 75% of contacts made with individuals who have never been contacted before lasted for less than 15 minutes. Approximately 75% of contacts at home and 50% of school and leisure contacts were physical, whereas only a third of contacts recorded in other settings were physical; approximately two-thirds of the persons contacted in multiple settings involved a contact at home, and so a high proportion were physical.

Based on association rules of maximum length 3 on the frequency, duration and type of contacts, they show that 75% of the contacts lasting 4 hours or more involved physical contact and occurred on a daily basis (83%), while 83% of the first-time contacts lasting less than 5 minutes were non-physical. First time and occasional contacts mostly lasted less than 15 minutes (lift values 3.3 and 1.8, respectively) and, when non-physical, this association was intensified (lift values 3.6 and 2.6, respectively). Whether contacts were physical or not did not influence

the association between contacts lasting at least 4 hours and occurring on a daily basis nor did it influence the association between contacts lasting from 5 minutes up to one hour and occurring on a weekly or monthly basis. Overall, 67% of all physical contacts lasted for at least 1, while 56% of all physical contacts occurred on a daily basis. Due to the high degree of correlation between physical contact and other measures of intimate contact, physical contacts were used as a proxy measure for high intensity contacts.

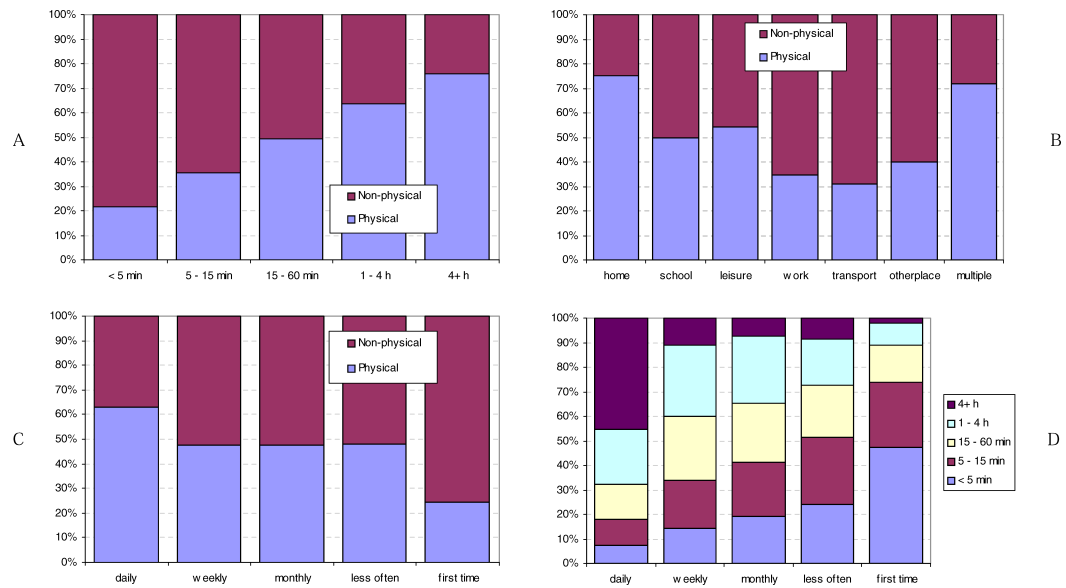


Figure 5.1: Graphs show data by (A) duration, (B) location, and (C) frequency of contact; the correlation between duration and frequency of contact is shown in (D). All correlations are highly significant ($p < 0.001$, χ^2 -test). The figures are based on pooled contact data from all eight countries and weighted according to sampling weights as explained in the methods (based on household size and age). Figure reproduced from [91] with the permission of the authors.

Findings of Mossong et al.

These authors found that mixing patterns and contact characteristics were remarkably similar across different European countries (see Figure 5.2 A and Figure 5.3 B for all numbers of contacts reported and physical contacts only respectively).

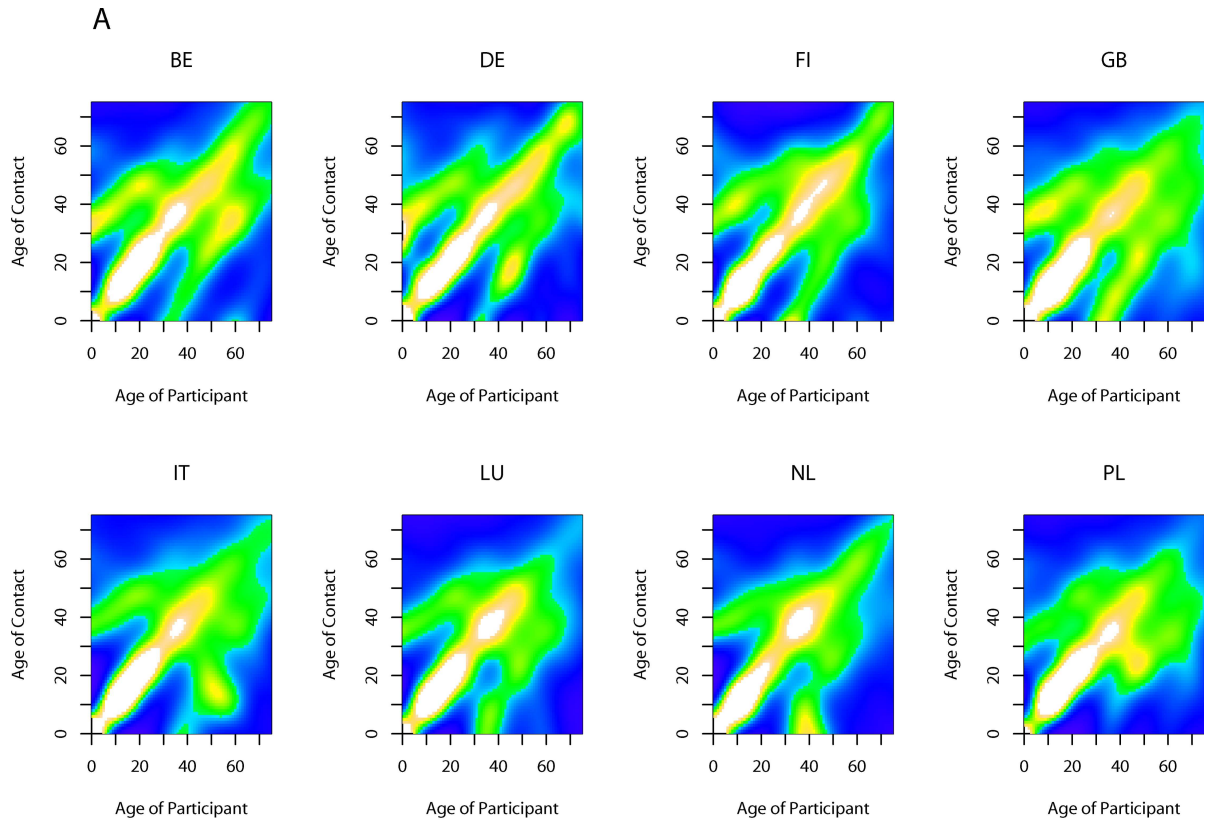


Figure 5.2: Smoothed contacts matrices for each country based on all reported contacts occurring in the home setting. White indicates high contact rates, green intermediate contact rates, and blue low contact rates. Figure reproduced from [91] with the permission of the authors.

Apart from that similarity, the authors have made a remarkable finding from the study. They discovered that the social contacts among individuals occur preferentially among those of similar ages. This pattern is particularly pronounced among children and youngsters in the age range between 5 and 24 years. This can be seen on the main diagonal for almost all countries where the colour white indicates high contact rates. This kind of age assortativity is also observed for adults of about 40 years. This is shown in the figures by two parallel secondary diagonals starting at roughly 30 – 35 years for both contacts and participants. It is well known that children, teenagers, and youngsters develop friendship relationships

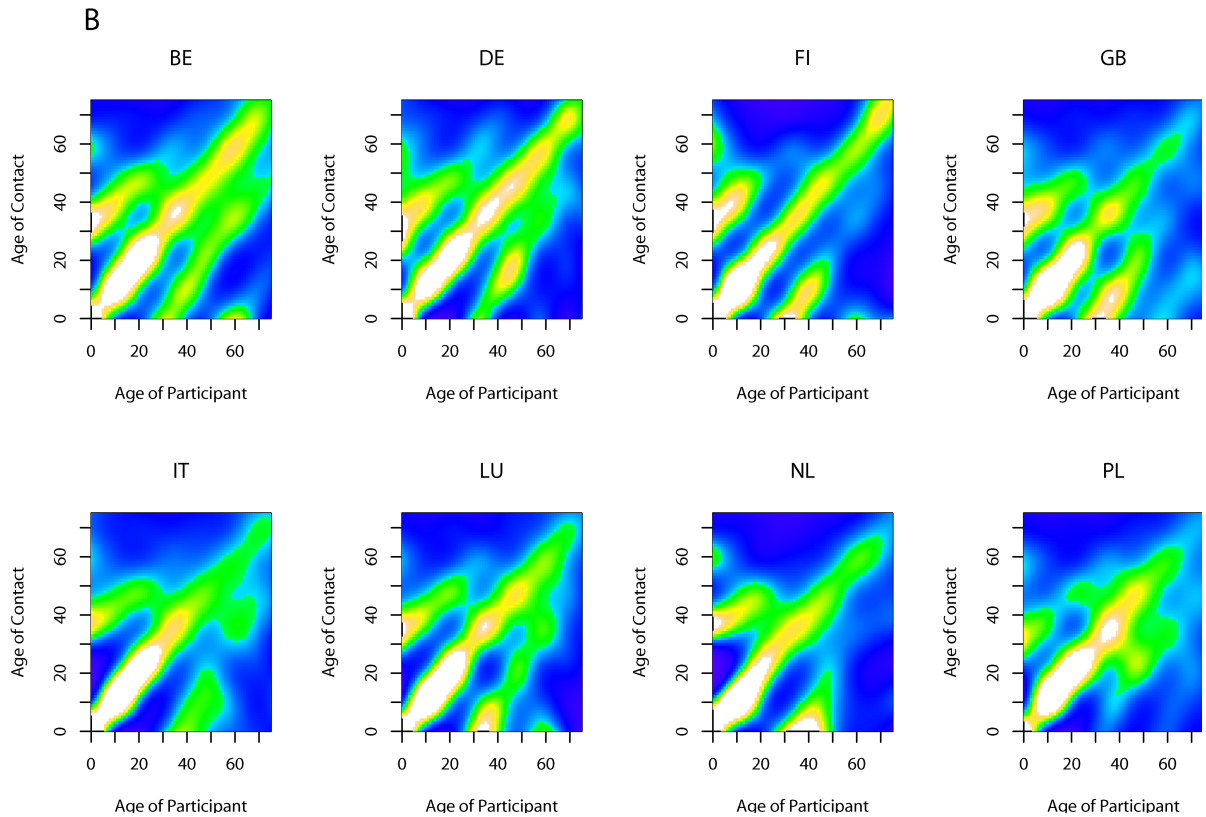


Figure 5.3: Smoothed contacts matrices for each country based on physical contacts only occurring in the work setting. White indicates high contact rates, green intermediate contact rates, and blue low contact rates. Figure reproduced from [91] with the permission of the authors.

preferentially among them, observing some kind of age assortativity in their social ties. This pattern is responsible for why children and teenagers are and have been an important conduit for the initial spread of close contact interactions in the case of influenza for example. Middle-aged adults are also preferentially tied to other individuals of similar ages by means of working relationships or other social ties.

The findings of these authors is particularly interesting because of the fact that it permits us to assess and quantify the risk of transmission in different settings. They have included different measures of “closeness of contact” such as duration and frequency of contact and whether skin-to-skin contact occurred. These measures

correlated highly with each other, such that the longer-duration contacts tended to be frequent and to involve physical contact (and vice versa). More intimate contacts are likely to carry a greater risk of transmission. Furthermore, these types of contact tend to occur in distinct social settings: the most intimate contacts occur at home or in leisure settings, whereas the least intimate tend to occur while travelling. Thus, the risk of infection in these settings varies. This variation has important implications for contact tracing during outbreaks of a new infection. Their results suggest that if efforts concentrate on locating contacts in the home, school, workplace, and leisure settings, on average more than 80% of all contacts would be found. The extent to which individuals preferentially mix with people of the same age (assortativeness) is a key heterogeneity that is now routinely included in models and attempts have also been made to further represent the underlying structure of contact patterns by partitioning the population into household and workplace compartments [68].

Peter Horby et al. [68] have done a similar study to that of Mossong et al. for developing countries despite the fact of the almost complete absence of data from developing countries. They sought to address this knowledge gap by conducting a household based social contact diary in rural Vietnam. The instructions given to participants for this study were similar to those for European countries but adapted to the local context. A diary based survey of social contact patterns was conducted in a household-structured community cohort in North Vietnam in 2011. They used generalised estimating equations (GEE) to model the number of contacts while taking into account the household sampling design, and used weighting to balance the household size and age distribution towards the Vietnamese population. They recorded 6675 contacts from 865 participants in 264 different households and found that mixing patterns were assortative by age but were more homogeneous than

observed in the recent European study [91].

There are similarities in the results found by Peter Horby et al. in comparison to the results of Mossong et al. By using the same definition of a contact and comparable methodology to a large European study, they have identified both similarities and potentially important differences in their study site in Vietnam. Similarities with the European data include significant over dispersion in the distribution of contacts and no gender differences in reported contact frequency. They also observe a peak in contact frequency in school age children, but in contrast to the European data, they also observed a second peak in adults aged 40 – 60 years. Another similarity with the European study was that prolonged and frequent contacts, and contacts occurring at home were much more likely to be physical in nature. However, there were important differences in the total number of contacts, and the duration and intimacy of contacts.

Overall they recorded a mean of 7.7 contacts per participant per day versus 13.4 in the study by Mossong et al. The lower number of daily contacts they recorded may be a feature of the particular community studied or may reflect a recall bias introduced by the retrospective nature of the study design compared to the prospective design of the European study. Over 80% of contacts that occurred on a daily basis in the Vietnam study were more than 4 hours, compared to only around 45% in the study by Mossong et al. Physical contact was more common in the European study, with 75% of home contacts being physical compared to around 45% in their study, and over 60% of daily contacts being physical compared to around 40% in their study. The importance of these differences to disease patterns depends on the relative importance of duration of contact versus intimacy of contact on the probability of successful transmission.

The contact patterns in their study were more homogeneous than that reported

elsewhere. They observed smaller differences between age groups in contact frequency and no significant differences between household sizes. They saw similar patterns of age dependent mixing to those reported by Mossong et al, with pronounced assortative mixing seen as a high intensity diagonal, signals of parent-child mixing, and a ‘plateau’ of mixing of adults with one another. They also observed no significant differences in contact frequency by day of the week, whereas significantly more contacts in Europe were recorded on weekdays compared to weekends. This may be because weekends are not generally observed as a special rest period in rural Vietnam to the extent they are in Europe. They also saw fewer contacts in ‘leisure’ settings (1% vs 16%), which may reflect true differences in the amount of time devoted to leisure, cultural differences in the conceptual separation between work, family and leisure activities, or limitations of the survey method in distinguishing leisure from other activities.

5.3 Role of Assortativity in Social Networks and its Implications on Long-Range Interactions

The role of assortativity in social relationships has been well documented. In social science it is also known as “homophily” and refers to the observed fact that “similarity breeds connections” or that “birds of a feather flock together.” There are many dimensions of homophily that include race and ethnicity, sex and gender, age, religion, education, occupation and social class. An excellent compendium on homophily in social networks is the work of McPherson et al. [84]. To review some of the results described in [84], it has been found in studies of close friendship that homophily (assortativity) by age is the strongest dimension controlling the relationships, with only the exception of race. For instance, about

38% of close friends among men in Detroit were found to be within two years of age and 72% within eight years. This assortativity is less marked in the people in the 60+ age group, which has been the only group for which there was significant outbreeding [84]. These results on social friendship, or close contacts, reproduce very well those obtained for the social contacts, which include both close and causal contacts, in the work of Mossong et al. [91] and of Horby et al. [68].

Consequently, the assortativity relationship between social contacts (close and casual) and age is indicative of the relationship between social distance between individuals and social contacts. By social distance we mean the shortest path distance between two individuals in their social network. That is, two teenagers who are not friends are closer to each other than they are to some middle-aged strangers. The probability that these two teenagers frequent the same place, e.g., concerts, cinema, school, etc., is larger than that for the social contact among the teenager and the adult.

By social network we understand here the social interaction between individuals that can be considered to be of relevance for epidemiological studies and which excludes those contacts that do not correlate with transmission opportunities for infections, such as links by means of only letters, telephone, emails, etc. Unfortunately, we have not found studies that provide empirical evidence of other types of homophily in the casual contacts among individuals. However, it is highly probable that individuals with similar ethnicity, religion, education, occupation, social class, etc., who have been found to be closer in their social networks [84], live in similar geographic locations, use similar transportation, and visit similar places for leisure than individuals with less similarities, confirming the hypothesis of a correlation between casual contacts and social distance. Homophily/Assortativity is the principle that a contact between similar people occurs at a higher rate than

among dissimilar people.

The pervasive fact of homophily means that cultural, behavioural, genetic or material information that flows through networks will tend to be localised. Homophily implies that distance in terms of social characteristics translates into network distance, the number of relationships through which a piece of information must travel to connect two individuals. It also implies that any social entity that depends to a substantial degree on networks for its transmission will tend to be localised in social space and will obey certain fundamental dynamics as it interacts with other social entities in an ecology of social forms.

We are aware of the lack of empirical data about casual contacts in real social systems. Even the empirical study of Mossong et al. [91] and Horby et al. [68] does not include social contacts among individuals in a confined space or in close physical proximity in which the individuals are not talking to each other, e.g., crowds at concerts. Then, we look for some empirical evidence that allows us to model casual social contacts. In some cases these casual encounters between individuals have been modelled by considering that they occur at random [13, 14, 44, 79, 91].

The concept of proximity is widely used in social sciences, in particular in innovation studies, organisation science, and regional science [76]. In many cases “proximity” refers to “geographical proximity,” such as territorial, spatial, local, or physical proximity. Therefore, different types of proximity facilitate the performance and survival of organisations. There are however some others dimensions of proximity such as ‘institutional proximity’, ‘organisational proximity’, ‘cultural proximity’, ‘social proximity’ and ‘technological proximity’. Social proximity in particular refers to actors that belong to the same space of social relations [76]. Social proximity is sometimes denoted as personal proximity or as relational prox-

imity. In some cases it has been observed that geographical proximity is subordinate to the social one. For instance, for the transmission of knowledge Agrawal et al. [2] have concluded that “geographical proximity matters most in the absence of social proximity that may otherwise facilitate access to knowledge”. However, it is difficult in many cases to disentangle social and geographical proximities. In fact, it has been stated that the dichotomy between spatial and aspatial indices is somewhat a false one, since both types of measures incorporate implicit notions of social distance” [112]. We then assume here that in general the concept of social proximity encloses important information about other types of proximities, such as the geographical and cultural ones. Geographical proximity is the most frequent used dimension of proximity in the literature and is sometimes called territorial, spatial, local or physical proximity. It can be also considered as the absolute distance that separates actors. The relevance of geographical proximity in social networks rely on the fact that small geographical distances facilitate face-to-face interactions and, therefore, fosters knowledge transfer and innovation. The main reasoning behind these effect is that short geographical distances bring organisations (or individuals) together, favour interactions with a high level of information richness and facilitate the exchange of, especially tacit, knowledge between actors. The larger the distance between actors, the more difficult it is to transfer these tacit forms of knowledge. All of these concepts of proximity refer to the idea of “being close to something measured on a certain dimension”.

5.4 Attempts for Accounting for all Close Contacts

There have been several studies made on the relationship between human mobility and the spread of infections. Human travel is responsible for the geographical spread of human infectious disease. D. Brockmann et al. [30] made a study on human mobility that can help to understand the spread of diseases when closed and casual contact are considered. They reported on a solid and quantitative assessment of human travelling statistics by analysing the circulation of bank notes in the United States, using a comprehensive data set of over a million individual's displacements. The central aim of their work was to use data collected at online bill-tracking websites (which monitor the world-wide dispersal of large numbers of individual bank notes) to infer the statistical properties of human dispersal with very high spatio-temporal precision.

Analysis Description

In order to track and analysis human movement, the authors obtained trajectories of 464,670 dollar bills from the bill-tracking system www.wheresgeorge.com. They studied the dispersal of bank notes in the U.S., excluding Alaska and Hawaii. The data consisted of 1,033,095 reports to the bill-tracking website. From the reports, they then calculated the geographical displacements $r = |x_2 - x_1|$ between a first (x_1) and secondary (x_2) report location of a bank note and the elapsed time T between successive reports. The qualitative features of bank note trajectories are illustrated by short-time trajectories ($T < 14$ days) originating from three major U.S. cities: Seattle, New York and Jacksonville. After their initial entry into the tracking system, most bank notes are next reported in the vicinity of

the initial entry location, that is $|x_2 - x_1| < 10$ km (Seattle, 52.7%; New York, 57.7%; Jacksonville, 71.4%). However, a small but considerable fraction is reported beyond a distance of 800 km (Seattle, 7.8%; New York, 7.4%; Jacksonville, 2.9%).

From a total of 20,540 short-time trajectories originating across the U.S., they measured the probability $P(r)$ of traversing a distance r in a time interval δT of 14 days. 71% of secondary reports occurred outside a short-range radius $L_{\min} = 10$ km. Between L_{\min} and the approximate average East-West extension of the United States, $L_{\max} < 3,200$ km, the kernel shows power-law behaviour $P(r) \sim r^{-1+\beta}$ with an exponent $\beta = 0.59 \pm 0.02$. They shown that for $r < L_{\min}$, $P(r)$ increases linearly with r , and implies that displacements are distributed uniformly inside the disk $|x_2 - x_1| < L_{\min}$. The probability $P(r)$ was measured for three classes of initial entry locations: highly populated metropolitan areas (191 sites, local population $N_{loc} > 120,000$), cities of intermediate size (1,544 sites, local population $120,000 > N_{loc} > 22,000$) and small towns (23,640 sites, local population $N_{loc} < 22,000$), comprising 35.7%, 29.1% and 25.2% of the entire population of the United States, respectively. Despite systematic deviations for short distances, they shown that all distributions $P(r)$ show an algebraic tail with the same exponent $\beta < 0.6$, which confirms that the observed power-law is an intrinsic and universal property of dispersal. In summary these authors found the following:

- Travelling distances distribution of bank notes decays as a power law, showing that trajectories of bank notes are reminiscent of scale-free random walks i.e. ‘Levy flights’. A Levy flight is a random walk for which the step size Δr follows a power-law distribution, i.e.

$$P(\Delta r) \sim (\Delta r)^{-1+\beta}$$

where the displacement exponent β is such that $\beta < 2$.

- The probability of remaining in a small spatially confined region for a time T is dominated by algebraically long tails that attenuate the super-diffusive spread. They show that human travelling behaviour can be described mathematically on many spatio-temporal scales by a two-parameter continuous-time random walk model to a surprising accuracy, and conclude that human travel on geographical scales is an ambivalent and effectively superdiffusive process.

Given that money is carried by individuals, bank note dispersal is a proxy for human movement, suggesting that human trajectories are best modelled as a continuous-time random walk with fat-tailed displacements and waiting-time distributions. A particle following a Levy flight has a significant probability to travel very long distances in a single step which seems to be consistent with human travel patterns: most of the time we travel only over short distances, between home and work, whereas occasionally we take longer trips. Each consecutive sighting of a bank note reflects the composite motion of two or more individuals who owned the bill between two reported sightings. Thus, it is not clear whether the observed distribution reflects the motion of individual users or some previously unknown convolution between population-based heterogeneities and individual human trajectories. Owing to that fact, a similar study has been done by Marta C. Gonzalez et al. [65]. They studied instead the trajectory of 100,000 mobile phone users by detecting their position during the period of a half year. Contrary to bank notes, mobile phones are carried by the same individual during his/her daily routine, offering the best proxy to capture individual human trajectories.

Marta C. Gonzalez et al. used two different data sets for exploring the mobility pattern of individuals. The first data set (D_1) consisted of the mobility patterns

recorded over a six-month period for 100,000 individuals selected randomly from a sample of more than 6 million anonymous mobile phone users. The location of the tower routing the communication was recorded at each time a user initiated or received a call or a text message, allowing them to reconstruct the user's time-resolved trajectory. The time between consecutive calls followed a 'bursty' pattern, indicating that although most consecutive calls are placed soon after a previous call, occasionally there are long periods without any call activity. To make sure that the obtained results were not affected by the irregular call pattern, they also studied a second data set (D_2) that captured the location of 206 mobile phone users, recorded every two hours for an entire week. In both data sets, the spatial resolution was determined by the local density of the more than 104 mobile towers, registering movement only when the user moved between areas serviced by different towers. The average service area of each tower was approximately 3 km^2 , and over 30% of the towers covered an area of 1 km^2 or less. The authors explored the statistical properties of the populations mobility patterns, they measured the distance between users positions at consecutive calls, capturing 16,264,308 displacements for the D_1 and 10,407 displacements for the D_2 data set. It has been found that the distribution of displacements over all users is well approximated by a truncated power-law:

$$P(\Delta r) = (\Delta r + \Delta r_0)^{-\beta} \exp(-\Delta r/\kappa) \quad (5.2)$$

where $\beta = 1.75 \pm 0.15$, $\Delta r_0 = 1.5 \text{ km}$ and cut-off values $\kappa|_{D_1} = 400 \text{ km}$, and $\kappa|_{D_2} = 80 \text{ km}$.

In summary these authors have found the following:

- They found that, in contrast to the results found by D. Brockmann et al.

(the random trajectories predicted by the prevailing Levy flight and random walk models), human trajectories show a high degree of temporal and spatial regularity, each individual being characterised by a time-independent characteristic travel distance and a significant probability to return to a few highly frequented locations.

- The individual travel patterns collapse into a single spatial probability distribution, indicating that, despite the diversity of their travel history, humans follow simple reproducible patterns. This inherent similarity in travel patterns could impact all phenomena driven by human mobility from epidemic prevention to emergency response, urban planning and agent-based modelling.

Finally, there is a group of empirical evidence that is important for the development of the current approach. This refers to the way in which individuals establish their links in social networks. We remark that the number of close and casual contacts among individuals has been claimed to be proportional to the probability of creating links among them [35]. This probability has been considered to be proportional to the gain that these two individuals will obtain from the new link [69]. Similarly, Sorenson and his co-authors have assumed that the new social links are created on the basis of the “expectations of the value” of those relationships [114]. An illuminating piece of evidence for the use of a “value motivation” for the establishment of social relations was obtained by Manson [81] in the study of the primates rhesus macaques. Manson [81] observed that “a young female may gain by investing in a friendship with a low-ranking male who

1. is not presently sought by many females as a friend and,
2. will stay in the group and achieve high rank and thus have high protective

ability in the future.”

So far, it is evident that the creation of new social ties is seen as an investment in which the “future value” of the relation is more important than the “present value” that the establishment of this link represents.

Summary

We have seen that there is empirical evidence that support the following claims:

1. Social contacts among individuals are somewhat determined by their social distance. They account for an amalgam of proximities including social and geographical ones.
2. The number of close and casual contacts is somewhat determined by the probability of linking pairs of individuals by means of short-range and long-range interactions.
3. The probability of linking pairs of individuals in a network depends on the future value that such a new link will bring to both individuals.

Part II

Results and Discussions

Chapter 6

Accounting for Close and Casual Contacts in Complex Networks

In Chapter 3 of the first part we have analysed and described the spreading of disease in a population and complex networks. Models studied in that chapter are characterised by the fact that an infected node can only transmit infections to its close neighbours or close contacts along the edges of the network conceptualised by its adjacency matrix. There are many things we can consider on a social network and it is difficult to capture all the information which is relevant to the disease spreading. The adjacency matrix that represent the network is then an approximation to represent only close contact among individuals. In this chapter we aim to combine the empirical evidence analysed in Chapter 5 of the first part and summarised in the three points at the end of it (see page 193) into a mathematical model. That is we are going to construct a network model that will account for close and casual contacts via short contacts and long-range contacts. Our aim is to account for the probability that two individuals have social contacts that are relevant for the transmission of an infection. Most of the material in this Chapter,

Chapter 5 and all the following chapters are based on our paper [56].

6.1 The Network

6.1.1 Probability of establishing Short/Direct-Contacts

We start by considering the existence of a social network among a group of individuals that is represented by a graph $G = (V, E)$. We assume that the social relationship between node i and node j in a network, which is represented by $(i, j) \in E$, corresponds to one that conveys close contacts of relevance to the transmission of the type of infection under consideration. In doing so we are assuming that if $(i, j) \in E$, the probability ε_{ij} that the two nodes have close social contacts is equal to 1, i.e., $\varepsilon_{ij} \equiv 1$. Our next assumption is that if $(i, j) \notin E$, then the probability that both nodes have social contacts is not necessarily equal to zero, but is such that $0 < \varepsilon_{ij} < 1$. This means that both nodes can “eventually meet” in the same place and time by means of some kind of casual contacts, such as in transport, leisure, the supermarket, etc. Using empirical evidence points (1) and (2) at the end of Chapter 5 on the page 193, we will assume that this probability is determined by the structure of the social network, in particular by the probability of establishing a new link between both nodes.

6.1.2 Probability of establishing Long-Range Contacts

Now we are going to use point (3) of the summary on page 193 from Chapter 5 to determine the probability ε_{ij} for non-nearest neighbours (or for long-range contacts). That is, we assume that if two nodes are not directly connected, they will have casual contacts in a way that is proportional to the establishment of a new link between them. They will see the establishment of this new link as an invest-

ment in which its future value will determine their decision to form a new tie. We consider such a process like the one in which the time value of money, in particular the future value of a growing annuity is determined in quantitative finance [22].

6.1.3 Future Value (FV) of a piece of Information

Assume that we have a piece of information with a value of 1.00 now and we want to invest it to earn r interest. After one period, we will have the value of 1.00 plus the interest earned on the 1.00. Let FV be the future value of information and r be the annual interest rate. Then,

$$FV = 1 + r. \quad (6.1)$$

Repeating the process, at time 2 we will have

$$FV = (1 + r) + r(1 + r) = (1 + r)^2 \quad (6.2)$$

and the future value of the piece of information with value 1.00 invested for n periods is

$$FV = (1 + r)^n. \quad (6.3)$$

If for example $r = 0.10$ and $n = 2$, we have

$$FV = (1 + r)^n = (1.10)^2 = 1.21.$$

If instead of starting with a piece of information with 1.00 we start with a piece of information having present value, PV , of 50, the value at time 2 is

$$\begin{aligned} FV &= PV(1+r)^n \\ &= 50(1.10)^2 = 60.50. \end{aligned} \tag{6.4}$$

With a 0.10 interest rate, the value 50 grows to 55 at time 1. The value 55 grows to 60.50 at time 2. Equation (6.4) is the standard compound interest formula. The term $(1+r)^n$ is called the accumulation factor. The power of compounding (earning interest on interest) is dramatic. It can be illustrated by computing how long it takes to double the value of an investment.

6.1.4 Present Value (PV) of a piece of Information

Starting with Equation (6.4), we have

$$PV = \frac{FV}{(1+r)^n}. \tag{6.5}$$

Using C_n to denote the future value of information at the end of period n and r to denote the time value of that information, the present value, PV , of C_n is given by:

$$PV = \frac{C_n}{(1+r)^n} \tag{6.6}$$

or, equivalently,

$$PV = C_n(1+r)^{-n}, \tag{6.7}$$

where $(1+r)^{-n}$ is the present value of the piece of information with value 1 to be received at the end of period n when the time value of information is r . The term $(1+r)^{-n}$ is called the present value factor.

Example 6.1.1 • *What is the present value of a piece of information with value 1.00 to be received three time periods from now if the time value of the information is 0.10 per period? We have that $C_n = 1\$$, $n = 3$ and $r = 0.10$. Using (6.7) we get $PV = (1 + 0.10)^{-3} = 0.7513$.*

- *The present value of a piece of information with value 100.00 to be received three time periods from now if the time value of the information is 0.10 is given by $PV = 1000(1 + 0.10)^{-3} = 75.13$.*

Now lets come back to networks and instead of money we generalise the process by considering that a node lends a piece of information to another node. This information has a future value FV that is determined, according to the quantitative finance theory, by its present value PV , the interest rate r , and the number of time periods t at which the information is lent [21]. Here we assume that if the node i lends some information to node j , the information flows through the shortest path connecting both nodes (or one of them if more than one exists) according to empirical evidence point (2) of the summary on the page 193. The information is passed using a discrete time in which every step in the path is considered to have a unit time. That is, the number of periods for which the information is borrowed is assumed here to be equal to the shortest path separation of the two nodes.

Let us consider the shortest paths between the two nodes as a directed chain from the lender to the borrower. We assume that the chain has length l and that the nodes are numbered in consecutive order starting with 1. In a process of lending information from node v_1 to node v_{l+1} , the information is first transferred to node v_2 with a value A and an interest rate r . The present value of the information in the hands of node v_2 is

$$\frac{A}{(1 + r)}. \quad (6.8)$$

Then node v_2 enriched this information by a given value g , which we will designate as the *growth rate* of the information [21]. When node v_2 lends this information to node v_3 with the same interest and growth rates, the information will have a value

$$\frac{A(1+g)}{(1+r)^2}, \quad (6.9)$$

in the hands of node v_3 . As every node in the chain lends the information to its nearest neighbour with interest r and growth rate g , the information in the hands of borrower node v_{l+1} will have a value of

$$\frac{A(1+g)^{l-1}}{(1+r)^l}. \quad (6.10)$$

The cumulative present value of the information in this process is given by the sum of all the values at the nodes of the chain [21]:

$$PV = \frac{A}{(1+r)} + \frac{A(1+g)}{(1+r)^2} + \dots + \frac{A(1+g)^{l-1}}{(1+r)^l}. \quad (6.11)$$

If the growth and interest rates are the same, i.e., $g = r$, the present value of the information is simplified to

$$PV = \frac{Al}{1+r}. \quad (6.12)$$

Then, the future value of the information is given as [21]

$$FV = Al(1+r)^{l-1}. \quad (6.13)$$

We will consider here that $A \equiv 1$ for the sake of simplicity. Then, because in a connected network any two nodes i and j are separated by a shortest-path distance d_{ij} , the expression for the future value of the information transmitted from i to j

is given by

$$FV = d_{ij}x^{d_{ij}-1}, \quad (6.14)$$

where $x = 1 + r = 1 + g$. We consider here that lending information is carried out with a negative gain g . That is, every node will appropriate some part of the information they receive before lending to its nearest neighbour. Due to this, a node prefers to lend information to its closest neighbours than to far strangers. We also consider that the maximum benefit that a node can have is by lending information to its nearest neighbour. As a consequence, the values of the parameter x are bounded as $0 \leq x < 0.5$. The value $x = 0$ presents the situation in which no long-range transmission is allowed, which corresponds to the case in which only close contacts take place (as considered in Chapter 3). When $x \rightarrow 0.5$, the nodes are allowed to transmit information directly to their non-nearest neighbours (long-range contacts). This situation represents scenarios in which a substantial proportion of transmission is due to casual contacts. To avoid the future value of nodes separated at distance 2 becoming equal to unity, equation (7.16) must satisfy the inequality

$$d_{ij}x^{d_{ij}-1} < 1. \quad (6.15)$$

So when $d_{ij} = 2$, the parameter x should be such that

$$0 \leq x < 0.5. \quad (6.16)$$

In closing, the probability to establish long-range contacts in our model is given by:

$$\varepsilon_{ij} = FV = d_{ij}x^{d_{ij}-1}, \quad (6.17)$$

which means that the maximum social contacts is obtained for the nearest neighbours and it decreases with the increase of the social distance between the two nodes. This simple model agrees with the three groups of empirical evidence analysed in summary page 193 of Chapter 5. In addition it also agrees with the empirical observation that most of the transmission usually occurs through close contacts rather than through casual ones [35]. At this point it is straightforward to propose a matrix representation \mathbf{M} for the social contacts (close and casual) among all nodes in a network. The entries of this matrix, that represents the network, are defined as follows:

1. $\mathbf{M}(i, j) = 1$ if individuals i and j are directly connected, that is, this entry accounts for direct contact or close contacts in the network,
2. $\mathbf{M}(i, j) = d_{ij}x^{d_{ij}-1}$ if individuals i and j are not directly connected in the network and are separated by a distance d_{ij} , that is, this entry accounts for long-range contacts or casual contacts between i and j , decreasing when the distance separating nodes increases,
3. $\mathbf{M}(i, j) = 0$ otherwise.

The matrix representation \mathbf{M} is exactly the ‘generalised graph matrix’ introduced in [50] to describe a more general network structure. Properties of this matrix will be described in the next section.

6.2 Generalised Topological Index and the Generalised Graph Matrix

Generalised Topological Indices have been introduced by E. Estrada [50] by means of the vector-matrix-vector multiplication (VMV) and the Generalised Graph Ma-

trix of a graph G , $\mathbf{\Gamma}(G, x, p)$ which gives a unified expression from which classical topological indices can be obtained. The generalised graph matrix $\mathbf{\Gamma}(G, x, p)$ introduced was shown to describe a more general network structure under which, not only different topological indices of chemical properties can be obtained, but also encompasses the classical network information as a particular case [50]. In this sense, the Generalised Graph Matrix allows, for instance, to consider long-range interactions in a performing network and to defined the generalised centralities measures [94].

6.2.1 Mathematical Definition

Let $G = (V, E)$ be a network with $|V| = n$ vertices and $|E| = m$ edges. Let d_{ij} denote the geodesic distance between vertices $i \neq j$ in G . The generalised graph matrix $\mathbf{\Gamma}(G, x, p)$ is a $n \times n$ symmetric matrix whose elements g_{ij} are defined as

$$g_{ij} = \begin{cases} 1 & \text{if } i \sim j \\ (d_{ij}x^{d_{ij}-1})^p & \text{if } i \neq j \text{ and } i \not\sim j, \\ 0 & \text{if } i = j. \end{cases} \quad (6.18)$$

From this matrix $\mathbf{\Gamma}(G, x, p)$, the most important graph matrices can be obtained as particular cases for different values of x and p . Thus, for instance, $\mathbf{\Gamma}(G, 0, 1) = \mathbf{A}(G)$, the adjacency matrix of the graph G , and $\mathbf{\Gamma}(G, 1, 1) = \mathbf{D}(G)$, the topological distance matrix of the graph G . In this thesis we will consider the case when $p = 1$ and simply write the generalised graph matrix as $\mathbf{\Gamma}(G, x)$ which corresponds to the matrix \mathbf{M} introduced at the end of the previous section.

The parameter x can have several interpretations according to the field of study. From now on, in this thesis, we will call the parameter x the ‘conductance’

as it controls the way in which casual contacts are allowed in a network. In a zero conductance network only close contacts are allowed, which can be the case for the transmission of sexually transmitted diseases or computer viruses. As an example,

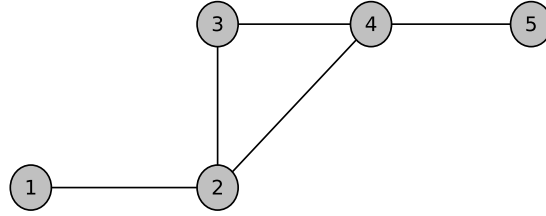


Figure 6.1: $G = (V, E)$, with $|V| = 5$ vertices and $|E| = 5$ edges

for the graph G in Figure 6.1 we obtain the following generalised graph matrix

$$\mathbf{\Gamma}(G, x, p = 1) = \begin{pmatrix} 0 & 1 & 2x & 2x & 3x^2 \\ 1 & 0 & 1 & 1 & 2x \\ 2x & 1 & 0 & 1 & 2x \\ 2x & 1 & 1 & 0 & 1 \\ 3x^2 & 2x & 2x & 1 & 0 \end{pmatrix} \quad (6.19)$$

which, for the particular value

$$\mathbf{\Gamma}(G, x = 0) = \begin{pmatrix} 0 & 1 & 0 & 0 & 0 \\ 1 & 0 & 1 & 1 & 0 \\ 0 & 1 & 0 & 1 & 0 \\ 0 & 1 & 1 & 0 & 1 \\ 0 & 0 & 0 & 1 & 0 \end{pmatrix} = \mathbf{A}(G), \quad \mathbf{\Gamma}(G, x = 1) = \begin{pmatrix} 0 & 1 & 2 & 2 & 3 \\ 1 & 0 & 1 & 1 & 2 \\ 2 & 1 & 0 & 1 & 2 \\ 2 & 1 & 1 & 0 & 1 \\ 3 & 2 & 2 & 1 & 0 \end{pmatrix} = \mathbf{D}(G).$$

A generalised topological index GTI [50] associated to a graph G is defined as a

generalised vector-matrix-vector invariant through the generalised graph matrix

$$GTI[G] = K\mathbf{u}^T(y, \vec{w}, q)\mathbf{\Gamma}(x, p)\mathbf{v}(z, \vec{s}, r),$$

where K is a constant and $\mathbf{u}(y, \vec{w}, q)$ and $\mathbf{v}(z, \vec{s}, r)$ are column vectors whose components are given by

$$u_i(y, \vec{w}, q) = (\omega_i + \sum_{j=1}^n g_{ij}(y, 1))^q$$

and

$$v_i(z, \vec{s}, r) = (s_i + \sum_{j=1}^n g_{ij}(z, 1))^r.$$

6.2.2 Properties of the Matrix $\mathbf{\Gamma}(G, x)$

We consider only undirected networks, so that the matrix $\mathbf{\Gamma}(G, x)$ is symmetric. The first observation concerning the matrix $\mathbf{\Gamma}(x)$ is that it represents a weighted complete graph in which the weights of the non-adjacent nodes are given by $w_{ij} = d_{ij}x^{d_{ij}-1}$. Let \mathbf{P}_k be the k -path matrix of the network, whose entries are defined as follows:

$$(\mathbf{P}_k)_{ij} = \begin{cases} 1 & \text{if there is a path of length } k \text{ between node } i \text{ and } j, \\ 0 & \text{otherwise.} \end{cases} \quad (6.20)$$

Note that $\mathbf{P}_1 = \mathbf{A}$. Then, the matrix $\mathbf{\Gamma}(G, x)$ can be represented as a polynomial-matrix also known as a λ -matrix

$$\mathbf{\Gamma}(G, x) = \mathbf{A} + 2x\mathbf{P}_2 + 3x^2\mathbf{P}_3 + \cdots + Dx^{D-1}\mathbf{P}_D, \quad (6.21)$$

where D is the diameter of the network. In this sense the generalised network matrix can be represented by a multi-layered network as illustrated in Figure 6.2.

Lambda-Matrix

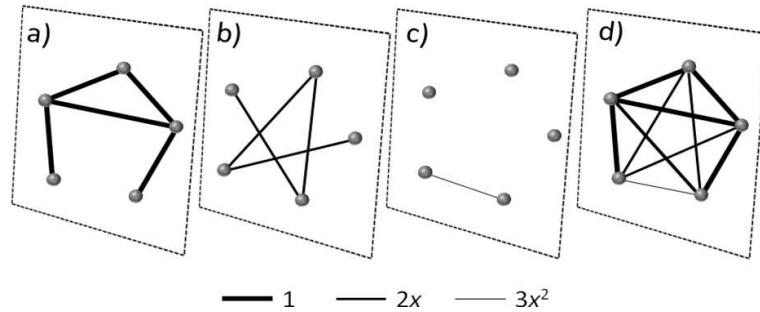


Figure 6.2: Multilayer representation of the $\Gamma(G, x)$. In (a) a social network with 5 nodes and 5 social connections is represented. In layers (b) and (c) the eventual proximity interactions between nodes are represented. Eventual proximity of nodes in (b) and (c) are given by $2x$ and $3x^2$, respectively. Layer (d) represents the superposition of the three previous layers and accounts for both direct and LR transmission of an infection by superposing the social and proximity networks.

A λ -matrix is a $m \times n$ matrix whose elements are polynomials in the scalar λ ; the coefficient of the polynomials may be complex numbers. Such a matrix may obviously be considered as a polynomial in λ whose coefficients are constant $m \times n$ matrices. In the case of the generalised graph matrix $\Gamma(G, x)$ we have that $\lambda = x$.

The derivative of the matrix $\Gamma(G, x)$ with respect to x is defined as the matrix whose elements are the first derivative of the elements of the same matrix.

Therefore

$$\frac{d\Gamma(G, x)}{dx} = 2\mathbf{P}_2 + 6x\mathbf{P}_3 + \dots + (D - 1)Dx^{D-2}\mathbf{P}_D,$$

and if $\Gamma_1(G, x)$ and $\Gamma_2(G, x)$ are two x -matrices then we have:

$$\frac{d}{dx}[\Gamma_1(G, x) + \Gamma_2(G, x)] = \frac{d\Gamma_1(G, x)}{dx} + \frac{d\Gamma_2(G, x)}{dx}$$

and

$$\frac{d}{dx}(\mathbf{\Gamma}_1(G, x)\mathbf{\Gamma}_2(G, x)) = \frac{d\mathbf{\Gamma}_1(G, x)}{dx}\mathbf{\Gamma}_2(G, x) + \mathbf{\Gamma}_1(G, x)\frac{d\mathbf{\Gamma}_2(G, x)}{dx}.$$

It is important to note that the order of the factors must always be preserved.

This implies that in general

$$\frac{d}{d\lambda}(\mathbf{\Gamma}^n(G, x)) \neq n\mathbf{\Gamma}^{n-1}(G, x)\frac{d\mathbf{\Gamma}(G, x)}{dx}$$

for integers $n > 1$, as one might hope, but that

$$\frac{d}{d\lambda}(\mathbf{\Gamma}^n(G, x)) = \sum_{i=1}^n \mathbf{\Gamma}^{i-1}(G, x)\frac{d\mathbf{\Gamma}(G, x)}{dx}\mathbf{\Gamma}^{n-i}(G, x).$$

For non-singular matrices we have

$$\mathbf{\Gamma}^{-n}(G, x)\mathbf{\Gamma}^n(G, x) = \mathbf{I},$$

Where \mathbf{I} is the identity matrix. Therefore we have

$$\frac{d\mathbf{\Gamma}^{-n}(G, x)}{dx}\mathbf{\Gamma}^n(G, x) + \mathbf{\Gamma}^{-n}(G, x)\frac{d\mathbf{\Gamma}^n(G, x)}{dx} = \mathbf{0}.$$

Thus the derivative of a negative integer power of $\mathbf{\Gamma}(G, x)$ is given by

$$\frac{d\mathbf{\Gamma}^{-n}(G, x)}{dx} = -\mathbf{\Gamma}^{-n}(G, x)\frac{d\mathbf{\Gamma}^{-n}(G, x)}{dx}\mathbf{\Gamma}^{-n}(G, x). \quad (6.22)$$

The integral of $\mathbf{\Gamma}(G, x)$ with respect to x is simply defined as the matrix whose

elements are the corresponding integrals of the elements of $\mathbf{\Gamma}(G, x)$, that is

$$\begin{aligned} \int \mathbf{\Gamma}(G, x) dx &= \mathbf{A} \int dx + 2\mathbf{P}_2 \int x dx + 3\mathbf{P}_3 \int x^3 dx + \cdots + D\mathbf{P}_D \int x^{D-1} dx \\ &= x\mathbf{A} + x^2\mathbf{P}_2 + \frac{3}{4}x^4\mathbf{P}_3 + \cdots + \mathbf{P}_D + \mathbf{C}, \end{aligned}$$

where \mathbf{C} is a constant matrix. There is a relation between the Jackson and Wolinsky model presented in Chapter 4 and the generalised network matrix $\mathbf{\Gamma}(G, x)$ introduced in this section. This relationship will be analysed later.

In general the determinant of the matrix $\mathbf{\Gamma}(G, x)$, $|\mathbf{\Gamma}(G, x)|$ depends on x and we call the values of x for which $|\mathbf{\Gamma}(G, x)| = 0$ the latent roots of $\mathbf{\Gamma}(G, x)$. If x_i is any such root, then the sets of homogeneous equations

$$\mathbf{\Gamma}(G, x = x_i)\mathbf{u} = \mathbf{0} \quad \text{and} \quad \mathbf{v}'\mathbf{\Gamma}(G, x = x_i) = \mathbf{0} \quad (6.23)$$

have at least one non-trivial solution for \mathbf{u} and \mathbf{v} respectively. Any non-trivial solutions of (6.23) are known as right or left latent vectors of $\mathbf{\Gamma}(G, x)$, respectively. The number of linearly independent solutions of either set is equal to the degeneracy of $\mathbf{\Gamma}(G, x)$. If $\mathbf{\Gamma}(G, x)$ has degeneracy α_i , then there are α_i linearly independent right latent vectors (solutions) associated with the latent root x_i , and similarly for the left latent vectors. As $\mathbf{\Gamma}(G, x)$ is a symmetric matrix, then the subspace of right and left latent vectors associated with a particular root coincide. Latent roots and vectors are only defined for matrices dependent on a parameter.

6.3 Generalised Degree

For a given node, the generalised degree is given by a polynomial of the form:

$$k_i(x) = \sum_j \mathbf{A}_{ij} + 2x \sum_j (\mathbf{P}_2)_{ij} + \cdots + Dx^{D-1} \sum_j (\mathbf{P}_D)_{ij}, \quad (6.24)$$

which clearly is the ‘classical degree’ of the node when $x = 0$. The analogous result of the Handshaking Lemma 0.5.10 of the introduction page 21 for the generalised network matrix reads as follow:

$$\sum_{i=1}^n k_i(x) = 2(|\mathbf{P}_1| + 2x|\mathbf{P}_2| + 3x^2|\mathbf{P}_3| + \cdots + Dx^{D-1}|\mathbf{P}_D|), \quad (6.25)$$

where $|\mathbf{P}_k|$ stands for the number of paths of length k in the network, and $|\mathbf{P}_1| = m$ is the number of links. Indeed the generalised degree of a node is the sum of the weights of the edges adjacent to it and every edge of weight one or $d_{ij}x^{d_{ij}-1}$ connects two vertices. Therefore the sum of generalised degree must be the double of the sum of the weights of all the edges. We can also generalise all concepts on networks on the basis of the generalised graph matrix, such as degree distribution, average path length, clustering coefficient, degree centrality [93, 94], eigenvalue centrality [94], betweenness centrality [94], communicability centrality [54], subgraph centrality [57], the Estrada Index [49] etc. For instance the generalised degree distribution of a given network can be obtained by plotting the probability $p(k, x)$ of finding a node of degree k for a certain value of the parameter x , versus the generalised degree $k(x)$, where

$$p(k, x) = \frac{n(k, x)}{n}, \quad (6.26)$$

in which $n(k, x)$ is the number of nodes having generalised degree $k(x)$. We recall that the procedure is quite similar to what is done for the ‘strength distribution’

in weighted networks [38]. However, in the current case the distribution converges to the degree distribution of the network when $x \rightarrow 0$. Also, because $k(x)$ is not an integer it is customary to use ranges of values of the generalised degree in order to obtain $n(k, x)$. In the next section we will analyse an interesting effect that takes place when the generalised degree distribution is studied for heterogeneous networks for different values of the parameter x .

6.3.1 Generalised Degree for Some Special Networks

Path Network, P_n

A path network contains only vertices of degree 1, also called terminals, and vertices of degree 2. If the nodes are labelled from 1 to n starting from an endpoint, the degree distribution of the path for $x = 0$, consists of two peaks at $k_1 = 1$ and at $k_n = 1$ with probability $p(k_1) = p(k_n) = \frac{2}{n}$ and peaks at $k_i = 2$ ($i = 2, \dots, n - 1$) with probability $p(k_i) = \frac{n-2}{n}$. Now, when $x \neq 0$ the generalised degrees for terminals are given by:

$$k_1(x) = k_n(x) = \sum_{\alpha}^D \alpha x^{\alpha} \quad \forall x, \quad (6.27)$$

where D is the diameter of the network. For any other vertex of degree 2 the generalised degree is given by

$$k_i(x) = 1 + \sum_{\alpha=1}^{\epsilon_i} \alpha x^{\alpha} \quad \forall x, \quad (6.28)$$

where ϵ_i is the greatest geodesic distance (also known as the eccentricity) between node i and any other vertex.

Cycle Network, C_n

In a cycle network every vertex has degree 2. For $x = 0$ the degree distribution of a cycle network consists of one peak at $k_i = 2$ with probability $p(k_i) = \frac{1}{n}$. When

$x \neq 0$ the generalised degree of every vertex is given by:

$$k_i(x) = 2 \sum_{\alpha}^D \alpha x^{\alpha} \quad \forall x, \quad (6.29)$$

where D is the diameter of the network.

Star Network, S_n

The star network is a very simplified network in which a central node has $n - 1$ nearest neighbours and all the other nodes are only connected to the central one. Then, it can be considered as a simple example of a network with ‘heterogeneous’ degree distribution [51]. The degree distribution of the star for $x = 0$ consists of two peaks, one at $k_i = 1$ with probability $p(k_i) = (n - 1)/n$ and another at $k_j = n - 1$ with probability $1/n$, which indeed is a very skew distribution. Now, when $x \neq 0$ the generalised degrees of the two nodes are given by:

$$k_i(x) = 1 + (n + 1)x \quad \forall x, \quad (6.30)$$

and

$$k_j(x) = n - 1, \quad \forall x. \quad (6.31)$$

Consequently, when

$$x \rightarrow \frac{n - 2}{n(n - 1)} \quad (6.32)$$

in the star graph both types of nodes have exactly the same generalised degree, i.e., $k_i = k_j = n - 1$, which means that the generalised degree distribution consists of only one peak at $k = n - 1$ with unit probability. This distribution is identical to those of regular networks, indicating that the ‘degree heterogeneity’ of the star graph has disappeared as a consequence of the consideration of LR interactions among its nodes. The same situation occurred when we analysed the generalised

degree distribution of networks with power-law degree distributions obtained for instance with the BA model.

Complete Network, K_n

In a complete network each pair of vertices is connected by an edge. The complete network with n vertices has $\binom{n}{2} = n(n-1)/2$ (the triangular numbers) undirected edges. The degree distribution of a complete network for $x = 0$ consists of one peak at $k_i = n - 1$ with probability $p(k_i) = \frac{1}{n}$. For $x \neq 0$ the generalised degree of every vertex is given by:

$$k_i(x) = n - 1, \quad \forall x. \quad (6.33)$$

6.3.2 Connection with Jackson and Wolinsky Model

If we consider the Jackson and Wolinsky model of Chapter 4 in which $\delta = x$ for a network in which $w_{ii} = 0 \forall i \in V$, $w_{ij} = 1$ and $c_{ij} = 0 \forall i, j \in E$, the utility function of a node i introduced by Jackson and Wolinsky can be written as:

$$u_i = \int k_i(x) dx \quad (6.34)$$

which indicates that the utility is the area under the curve defined by the polynomial representing the generalised degree of a node. The probabilities introduced by Carvalho and Iori [31] are then expressed as,

$$\pi(u) = \frac{\int k_i(x)}{\sum_i \int k_i(x)}. \quad (6.35)$$

These probabilities do not recover in the limit the Barabási-Albert [17] ones, i.e. $p(u) = k_i/2m$ and consequently this model cannot be seen as a generalisation of the BA preferential attachment. However, the following simple modification based on the generalised network matrix model immediately recovers the BA model in

the limit when $x \rightarrow 0$. This modification simply consists of the use of the following probability instead of the one given by (6.35):

$$\pi(k(x)) = \frac{k_i(x)}{\sum_i k_i(x)} \quad (6.36)$$

6.3.3 The Study of the Generalised Degree for BA Network

An interesting effect takes place when the generalised degree distribution is studied for networks with ‘heterogeneous’ degree distributions. In this section we are going to study how the generalised degree of a BA network changes with the values of the parameter x . We want to answer the question: what happens to the generalised degree of each node when the value of x increases? In Figures 6.3 and 6.4 we

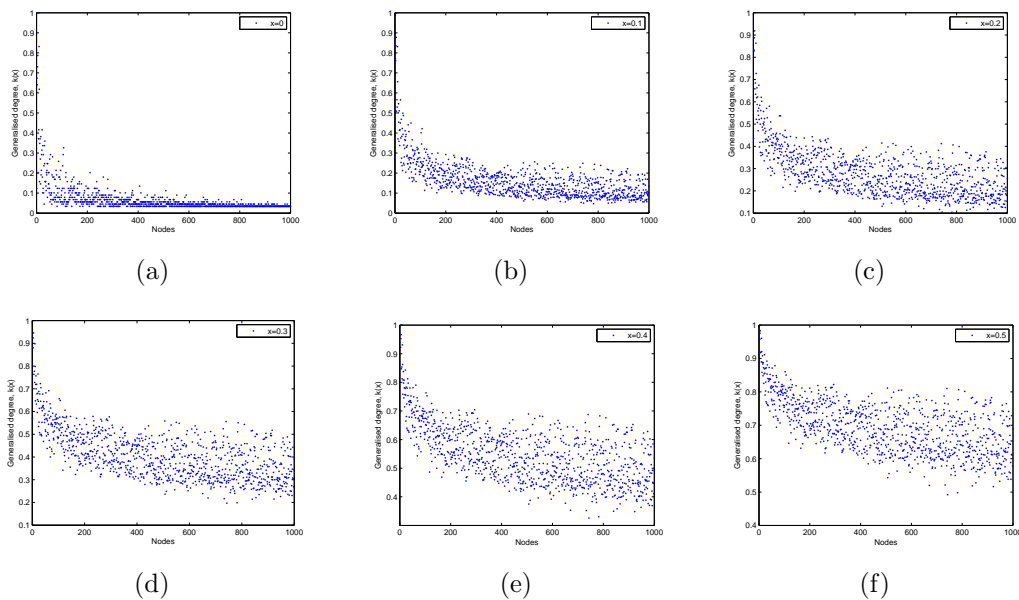


Figure 6.3: Illustration of the evolution of the degree of the nodes in a network created with the BA model as the values of the conductance change. Here for a BA network with $n = 1000$ and $\bar{k} \approx 6$ we represent the values of the generalised degree $k(x)$ for every node for different values of $0 \leq x \leq 0.5$. Notice that there is an inversion of the centrality of the nodes as the values of the conductance increases.

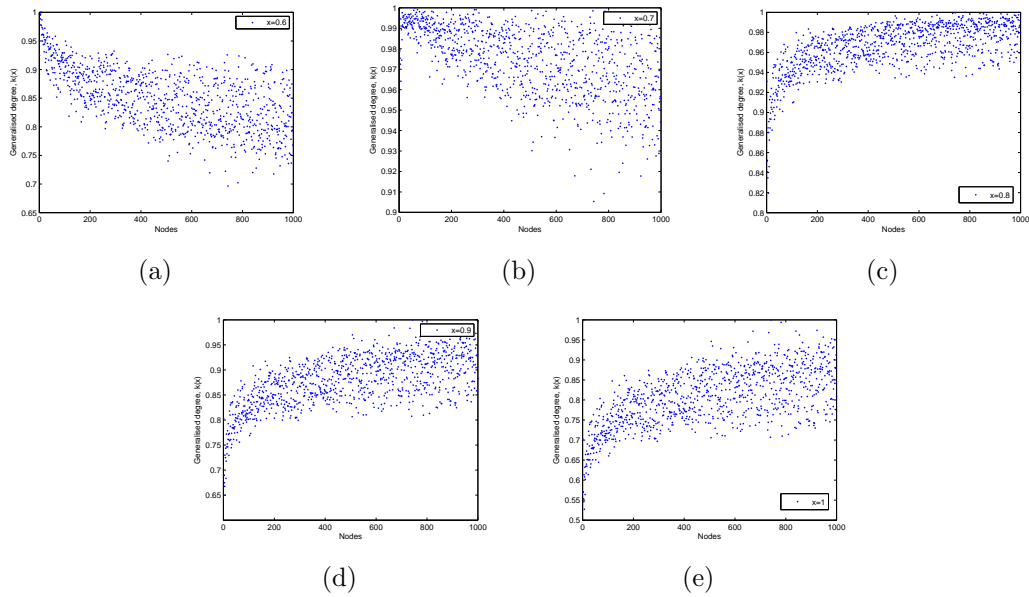


Figure 6.4: Illustration of the evolution of the degree of the nodes in a network created with the BA model as the values of the conductance change. Here for a BA network with $n = 1000$ and $\bar{k} \approx 6$ we represent the values of the generalised degree $k(x)$ for every node for different values of $0.6 \leq x \leq 1$. Notice that there is an inversion of the centrality of the nodes as the values of the conductance increases.

illustrate the typical values for a BA network in which we simply represent the nodes in the abscissa and generalised degree of the nodes in the ordinate. In Figure 6.3 (a) we illustrate the case for $x = 0$. This plot looks like any typical distribution of the degrees in a SF network, with very few nodes of high degree and many of low degree. Now, if we explore what happens when the value of x increase, the results are very appealing see Figure 6.3 (b)-(f) and Figure 6.4 (a)-(e). As can be seen, there is an inversion in the population of high and low degree nodes in the network. After a certain value of x the original hubs of the network become the poorest connected ones in terms of the generalised degree $k_i(x) = \sum_{j=1}^n \Gamma_{ij}(G, x)$. We allow for a while that x takes values up to 1. At the same time all nodes with low degree $k(x = 0)$ are now among the most central ones in the network according to $k(x = 1)$. This inversion is a direct consequence

of the fact that $k_i(x = 1) = \sum_{j=1}^n d_{ij}$ is the sum of all distances from node i to the rest of the nodes in the network. Then, in Figure 6.4 (e) (in which $x = 1$) we observe the distribution of the distance-sum for every node in the network.

6.3.4 The Study of the Generalised Degree for ER Network

We wish also to study what happen to the generalised degree of the nodes in an ER network. As we can see from the Figure 6.5 and Figure 6.6 all the node degrees for different values of x such that $0 \leq x \leq 0.5$ are localised in a band which have almost the same value, reflecting the homogeneity in the node degree for a Poissonian network.

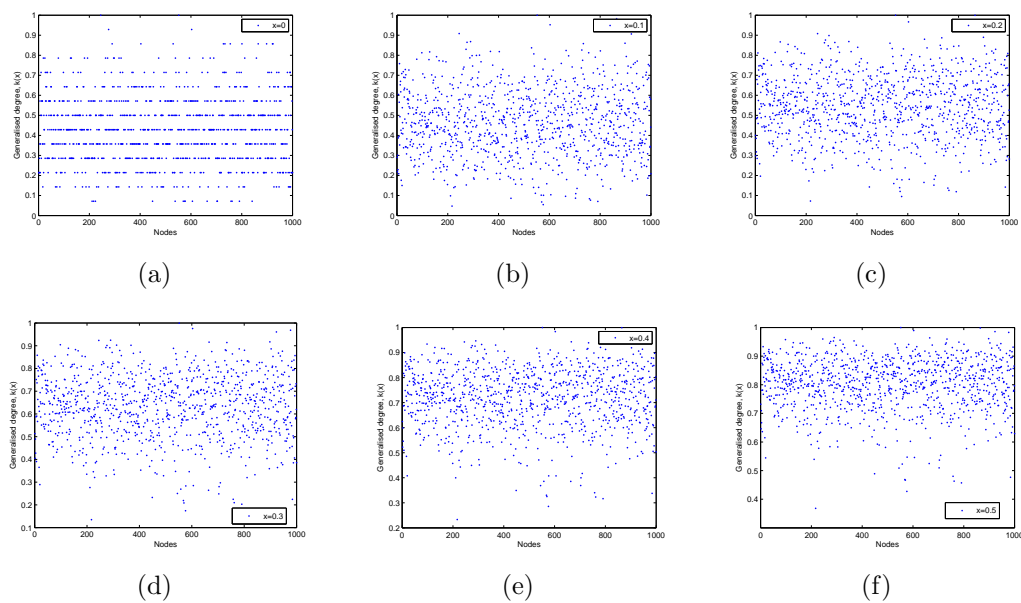


Figure 6.5: Illustration of the evolution of the degree of the nodes in a network created with the ER model as the values of the conductance change. Here for a ER network with $n = 1000$ and $\bar{k} \approx 6$ we represent the values of the generalised degree $k(x)$ for every node for different values of x such that $0 \leq x \leq 0.5$.

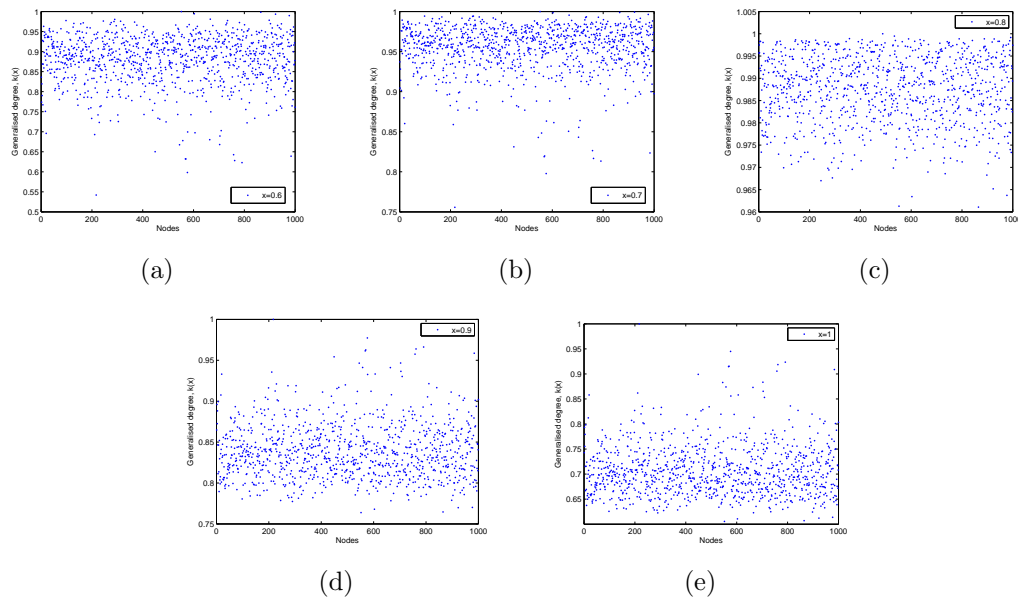


Figure 6.6: Illustration of the evolution of the degree of the nodes in a network created with the ER model as the values of the conductance change. Here for a ER network with $n = 1000$ and $\bar{k} \approx 6$ we represent the values of the generalised degree $k(x)$ for every node for different values of x such that $0.6 \leq x \leq 1$.

6.3.5 Relationship between Degree and Generalised Degree

In this section we want to compare the node degree ($x = 0$) and the generalised degree ($x \neq 0$) when x is increasing. One way to do this is to compute the rank correlation coefficients, between degree and generalised degree. Rank correlation coefficients such as Spearman's rank correlation coefficient (ρ) or Kendall's rank correlation coefficient (τ) [125] measure the extent to which, as one variable increases, the other variable tends to increase, without requiring that increase to be represented by a linear relationship. If, as one variable increases, the other decreases, the rank correlation coefficients will be negative. They are used to measure the association between two measured quantities. The ρ and τ test are a non-parametric hypothesis test which uses the coefficient to test for statistical

dependence. They assess how well the relationship between two variables can be described using a monotonic function. If there are no repeated data values, a perfect Spearman correlation of $+1$ or -1 occurs when each of the variables is a perfect monotone function of the other. Without going into much detail, the Kendall rank correlation coefficients can be mathematically formulated as follow:

Kendall rank correlation

Let $(x_1, y_1), (x_2, y_2), \dots, (x_n, y_n)$ be a set of joint observations from two random variables X and Y respectively, such that all the values of (x_i) and (y_i) are unique. Any pair of observations (x_i, y_i) and (x_j, y_j) are said to be concordant if the ranks for both elements agree: that is, if both $x_i > x_j$ and $y_i > y_j$ or if both $x_i < x_j$ and $y_i < y_j$. They are said to be discordant, if $x_i > x_j$ and $y_i < y_j$ or if $x_i < x_j$ and $y_i > y_j$. If $x_i = x_j$ or $y_i = y_j$, the pair is neither concordant nor discordant. The Kendall τ coefficient is defined as:

$$\tau = \frac{(\text{number of concordant pairs}) - (\text{number of discordant pairs})}{\frac{1}{2}n(n-1)} \quad (6.37)$$

Spearman rank correlation

The Spearman correlation coefficient is defined as the Pearson correlation coefficient between the ranked variables. For a sample of size n , the n raw scores X_i, Y_i are converted to ranks x_i, y_i , and ρ is computed from these:

$$\rho = \frac{\sum_i (x_i - \bar{x})(y_i - \bar{y})}{\sqrt{\sum_i (x_i - \bar{x})^2 \sum_i (y_i - \bar{y})^2}} \quad (6.38)$$

Tied values are assigned a rank equal to the average of their positions in the ascending order of the values. In applications where ties are known to be absent, a simpler procedure can be used to calculate ρ . Differences $d_i = x_i - y_i$ between the ranks of each observation on the two variables are calculated, and ρ is given

by:

$$\rho = 1 - \frac{6 \sum_i d_i^2}{n(n^2 - 1)} \quad (6.39)$$

We will be interested here only in the Kendall τ measure. Figure 6.7 shows an illustration of the Kendall rank correlation coefficient between the degree and the generalised degree for BA and ER networks. As can be seen when the conductance increases, there is an inversion in the rank correlation coefficient going from positive values to negative values for BA and ER networks. The inversion point in the rank correlation coefficient appears earlier in BA networks than in ER networks.

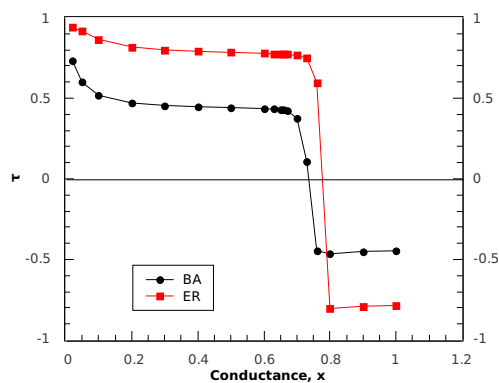


Figure 6.7: Illustration of the Kendall rank correlation coefficient τ between the degree ($x = 0$) and the generalised degree ($x \neq 0$) for BA and ER networks having both $n = 1000$ nodes and average degree $\bar{k} \approx 6$.

6.4 Extension of the concepts of Subgraph Centrality, Closeness, and Betweenness Centrality

In a social network, a centrality measure is used to characterise the importance of a node or a group of nodes in the network. In this section we are going to extend the definitions of some of those measures that will be relevant for the next chapters

of this thesis. Several measures have been introduced and details on centrality measures can be found in [52].

6.4.1 Subgraph Centrality in terms of the Generalised Graph

Matrix $\mathbf{\Gamma}(G, x)$

The subgraph centrality (SC) measure measures the participation of each node in all subgraphs in a network. This measure was introduced in 2005 by E. Estrada [57] who has shown that the subgraph centrality measure can be obtained from the spectra of the adjacency matrix of the network. The aim of this section is to extend this concept when the generalised graph matrix of the network $\mathbf{\Gamma}(G, x)$ is used. We will also extend the concept of closeness and betweenness centralities measure in the framework of the generalised graph matrix $\mathbf{\Gamma}(G, x)$. Subgraph centrality as introduced in [57] is defined in terms of the adjacency matrix \mathbf{A} of the network. Let G be a simple graph of order n as shown in [57] subgraph centrality of a vertex i is defined to be the sum of the closed walks of different lengths in the network starting and ending at vertex i . In this sum all subgraphs are considered. Here, we are going to extend subgraph centrality in terms of the generalised graph matrix $\mathbf{\Gamma}(G, x)$. The key concept behind subgraph centrality is the characterisation of the importance of a node by considering its participation in all closed walks starting and ending at it. In terms of the matrix $\mathbf{\Gamma}(G, x)$, and for a given value of x , a closed walk of length k , starting and ending at node i denoted by $\mu_k(i, x) \in \mathbb{R}$ is given by the i th diagonal entry of the k th power of the matrix $\mathbf{\Gamma}(G, x)$, that is,

$$\mu_k(i, x) = (\mathbf{\Gamma}^k(G, x))_{ii}, \quad 0 \leq x \leq 1, \quad (6.40)$$

where $(\mathbf{\Gamma}(G, x))_{ii}^k = (\mathbf{\Gamma}^k(G, x))_{ii}$ for simplicity. We notice that $\mu_k(i, x)$ is also the number of closed walks of length k starting and ending at node i . This number of walks $\mu_k(i, x)$ is a real number instead of an integer as it was in the case when the adjacency matrix is considered. Following [57] the generalised subgraph centrality $SC(i, x)$ for a vertex i and for a given conductance x can be written as:

$$SC(i, x) = \sum_{k=0}^{\infty} \mu_k(i, x). \quad (6.41)$$

As the sum in (6.41) is divergent we need to scale the contribution of closed walks

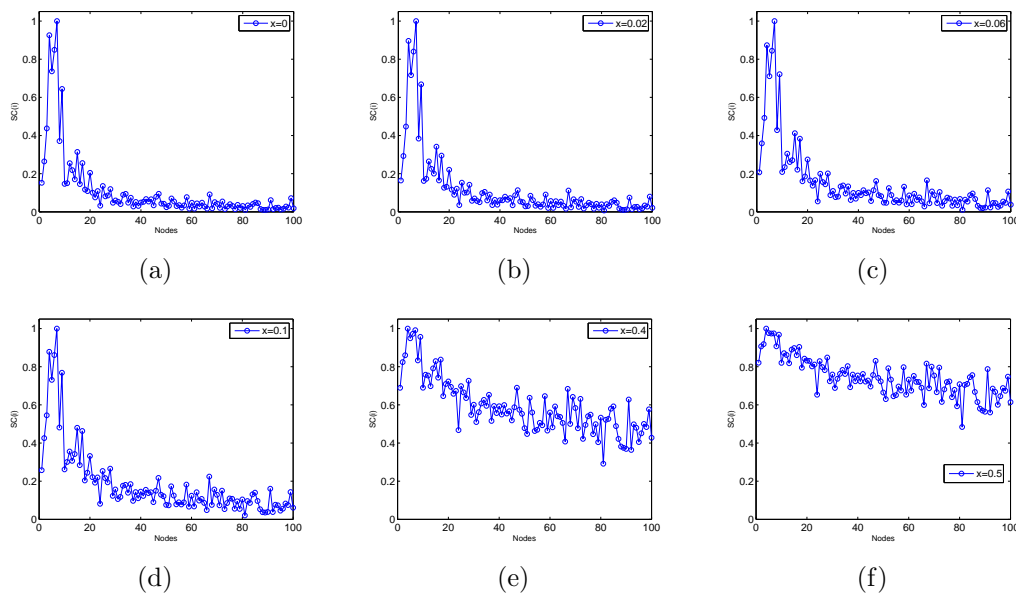


Figure 6.8: Generalised subgraphs centrality measures in the BA network having 100 nodes and average degree $\bar{k} \approx 6$ and for different values of the conductance x .

to the centrality of the vertex i by the factorial of the order of the spectral moment and rewrite (6.41) as follows:

$$SC(i, x) = \sum_{k=0}^{\infty} \frac{\mu_k(i, x)}{k!}. \quad (6.42)$$

If $\lambda_m(x)$ is an eigenvalue of the matrix $\mathbf{\Gamma}(G, x)$ corresponding to the eigenvector $v_m(x)$, then we have:

$$\mathbf{\Gamma}(G, x)v_m(x) = \lambda_m(x)v_m(x) \quad m = 1, \dots, n \quad (6.43)$$

Letting $\lambda_{1,\mathbf{\Gamma}}(x)$ be the largest eigenvalue of $\mathbf{\Gamma}(G, x)$, we have

$$(\mathbf{\Gamma}(G, x))_{ii}(v_m(x))_i = \lambda_m(x)(v_m(x))_i \leq \lambda_{1,\mathbf{\Gamma}}(x)(v_m(x))_i, \quad (6.44)$$

and

$$((\mathbf{\Gamma}(G, x))_{ii})^k \leq (\lambda_{1,\mathbf{\Gamma}}(x))^k, \quad (6.45)$$

therefore

$$\mu_k(i, x) \leq \lambda_{1,\mathbf{\Gamma}}^k(x), \quad i = 1, \dots, n \quad (6.46)$$

and we can show that the series (6.42) of non-negative terms converges

$$\sum_{k=0}^{\infty} \frac{\mu_k(i, x)}{k!} \leq \sum_{k=0}^{\infty} \frac{\lambda_{1,\mathbf{\Gamma}}^k(x)}{k!} = e^{\lambda_{1,\mathbf{\Gamma}}(x)}. \quad (6.47)$$

Thus, the subgraph centrality for every vertex i and for a given x is bounded above by:

$$SC(i, x) \leq e^{\lambda_{1,\mathbf{\Gamma}}(x)}. \quad (6.48)$$

Theorem 6.4.1 *Let $G = (V, E)$ be a simple graph of order n . Let v_1, v_2, \dots, v_n be an orthonormal basis of \mathbb{R}^N composed from the eigenvectors of the matrix $\mathbf{\Gamma}(x)$ associated to the eigenvalues $\lambda_1(x), \lambda_2(x), \dots, \lambda_N(x)$. Let $v_j^i(x)$ be the i component*

of v_j . For all $i \in V$, the generalised subgraph centrality $SC(i, x)$ is given by:

$$SC(i, x) = \sum_{j=1}^N (v_j^i(x))^2 e^{\lambda_j(x)} \quad i = 1, \dots, N. \quad (6.49)$$

proof 6.4.2 We can write (6.40) as follow,

$$\mu_k(i) = (\mathbf{\Gamma}^k(x))_{ii} = \left\langle \mathbf{\Gamma}^k(x)e_i, e_i \right\rangle = \left\langle \mathbf{\Gamma}^k(x) \sum_{j=1}^N p_j(e_i), \sum_{j=1}^N p_j e_i \right\rangle = \sum_{j=1}^N \lambda_j^k(x) (v_j^i(x))^2, \quad (6.50)$$

where $p_j(e_i)$ is the orthogonal projection of the unit vector e_i , the i th vector of the canonical basis of \mathbb{R}^N on v_j . Using expression (6.42), we obtain,

$$SC(i, x) = \sum_{k=0}^{\infty} \left(\sum_j^N \frac{\lambda_j^k(x) (v_j^i(x))^2}{k!} \right). \quad (6.51)$$

Reordering the terms of the series of (6.51), we obtain the absolute convergent series

$$SC(i, x) = \sum_j^N \left(\sum_{k=0}^{\infty} (v_j^i(x))^2 \frac{\lambda_j^k(x)}{k!} \right), \quad (6.52)$$

and this finishes the proof.

An alternative way of computing the subgraph centrality of node i is to take the ii th entry of the exponential matrix \expm of the generalised graph matrix $\mathbf{\Gamma}(G, x)$, that is

$$SC(i, x) = (\exp(\mathbf{\Gamma}(G, x)))_{ii}. \quad (6.53)$$

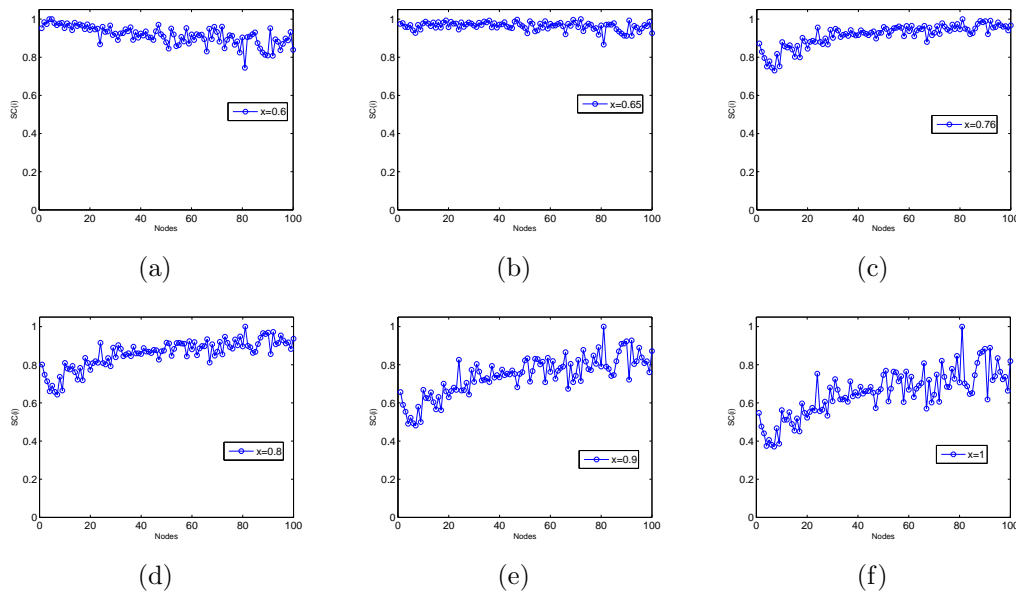


Figure 6.9: Generalised subgraphs centrality measures in the BA network having 100 nodes and average degree $\bar{k} \approx 6$ and for different values of the conductance x .

6.4.2 Communicability in terms of the Generalised Graph

Matrix $\Gamma(G, x)$

Communicability between a pair of nodes in a network is assumed to depend on all routes that connect two nodes. The shortest path being one of those routes makes the most important contribution as it is the most 'optimal' way of connecting two nodes in a network. The new concept of communicability in networks introduced in [54] is expressed in terms of the adjacency matrix of the network \mathbf{A} . As we did for the subgraph centrality, we are also going to extend this new concept of communicability measure in the framework of the generalised graph matrix $\Gamma(x)$. Following [54] the communicability between pairs of nodes p and q uses the same strategy making longer walks have small contributions to the communicability function than shorter ones. If P_{pq}^s is the number of the shortest paths between the nodes p and q having length s and $W_{pq}^{(k)}$ is the number of walks connecting p and

q of length $k > s$, the communicability between nodes p and q can be written as:

$$G_{pq} = \frac{1}{s!} P_{pq}^s + \sum_{k>s} \frac{1}{k!} W_{pq}^{(k)}. \quad (6.54)$$

The communicability between a pair of nodes in a network is usually considered as the shortest path connecting both nodes. However, the expression (6.54) for the communicability between a pair of nodes (p, q) accounts not only for the shortest paths communicating them but also for all the other walks that permit for a “particle” or a piece of information to travel from one to the other. The strategy in (6.54) is to make longer walks have lower contributions to the communicability function than shorter ones. In the framework of the generalised graph matrix $\mathbf{\Gamma}(x)$, the quantities G_{pq} , P_{pq}^s and $W_{pq}^{(k)}$ will be functions of the conductance of the medium x . Taking into account the conductance of the medium, expression (6.54) can be generalised in the following way:

$$G_{pq}(x) = \frac{1}{s!} P_{pq}^s(x) + \sum_{k>s} \frac{1}{k!} W_{pq}^{(k)}(x). \quad (6.55)$$

In term of the power of the generalised graph matrix $\mathbf{\Gamma}(x)$, the generalised communicability between nodes p and q may be formally determined by:

$$G_{pq}(x) = \sum_{k=0}^{\infty} \frac{(\mathbf{\Gamma}(x))^k}{k!} = e^{\mathbf{\Gamma}(x)}, \quad (6.56)$$

where $0 \leq x \leq 1$. Using the graph spectrum of $\mathbf{\Gamma}(x)$ we can rewrite ((6.56)) in the following form:

$$G_{pq}(x) = \sum_{j=1}^n \phi_j^p(x) \phi_j^q(x) e^{\lambda_j(x)}, \quad (6.57)$$

where $\phi_j^p(x)$ is the p th element of the j th orthonormal eigenvector of the generalised matrix $\Gamma(x)$ associated with the eigenvalue $\lambda_j(x)$.

6.4.3 Closeness Centrality in terms of the Generalised Graph

Matrix $\Gamma(G, x)$

Sometimes it is important to look not for the nodes of high degree, but for those which are relatively close to all other nodes in the network. An appropriate measurement of the centrality of a node for a connected network $G = (V, E)$ having n vertices and m edges, is defined as the inverse of the sum of shortest path distances from the node in question to all other nodes in the network. This centrality measure is known as closeness centrality [52], which is expressed by:

$$CC(i) = \frac{1}{\sum_{j \in V(G)} d_{ij}}. \quad (6.58)$$

Closeness centrality of a vertex i is also defined as the geodesic mean from vertex i to all other nodes in the network. Let us assume that a piece of information is carried from one node to another in the network. In the framework of the generalised graph matrix the closeness centrality of a node i is defined this time as the inverse of the sum of the future values $\varepsilon_{ij} = FV = d_{ij}x^{d_{ij}-1}$ (see Chapter 6) of the information transmitted from a node i to nearest and non nearest neighbours nodes j that is:

$$CC_i(x) = \frac{1}{\sum_{j \in V(G)} \varepsilon_{ij}}. \quad (6.59)$$

When $x = 1$ we recover the closeness centrality of the node i and when $x = 0$, $CC_i(x)$ is the inverse of the degree centrality [52] of the node i .

6.4.4 Betweenness Centrality in terms of the Generalised Graph Matrix

Apart from the closeness centrality we can consider the relative importance of a node in the communication between other pairs of nodes. These nodes facilitate or inhibit the communication between other nodes in the network. Betweenness centrality measure accounts for the proportion of information that passes through a given node in communicating other pairs of nodes in the network. Following [52], we are going to define the betweenness centrality in the framework of the generalised graph matrix matrix. Let us assume that information is going from one node to another through the shortest paths connecting those nodes. Then for a given conductance, if $\rho(i, j, x)$ is the number of these shortest paths from node i to node j , and $\rho(i, k, j, x)$ is the number of these shortest paths that pass through node k in the network for a conductance x , the betweenness centrality of node k in this framework is given by:

$$BC(k)(x) = \sum_i \sum_j \frac{\rho(i, k, j, x)}{\rho(i, j, x)}, \quad i \neq j \neq k. \quad (6.60)$$

It is known that communication between pairs of nodes in complex networks does not always take place through the shortest paths connecting pairs of nodes. In many real-world situations such communication occurs by using some or even all of the available channels to go from one place to another in the network. Several measures have been proposed to account for the betweenness of a node when communication takes place by using such other alternative ways. These measures include for instance the communicability betweenness centrality [54], the flow betweenness centrality, and the random walk betweenness centrality. The details about these measures can be found in [52].

6.4.5 Influence of the Conductance on Centrality Measures

In this section we want to analyse what happens to the generalised subgraph centrality, closeness centrality, communicability or betweenness centrality when we increase the conductance of the medium. We will only restricted here to the generalised subgraph centrality and closeness centrality. The impact of this effect will be exploited later when we will study the spreading of infection in networks. We consider the Barabási-Albert and the Erdős-Rényi networks having both a small number $n = 100$ nodes for simplicity and average degree $\bar{k} \approx 6$. We shall also consider real-world networks; the network of corporate directors of the 500 top corporations in the USA and the jazz musicians network. In this section we will allow x to vary between 0 and 1. In order to have a clear idea of the results reported

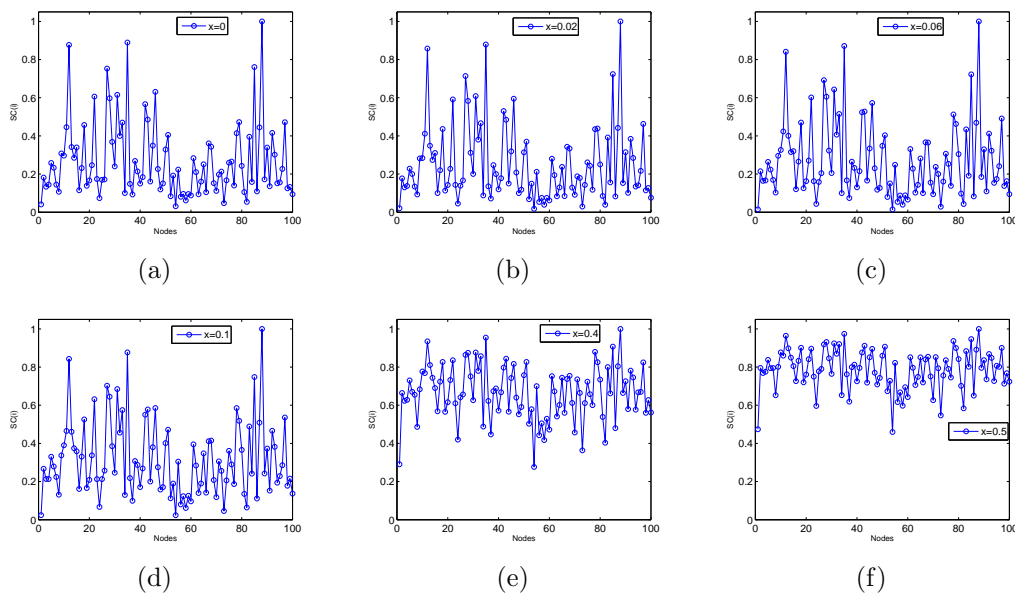


Figure 6.10: Generalised subgraphs centrality measures in the ER network having 100 nodes and average degree $\bar{k} \approx 6$ and for different values of the conductance x

in Figure 6.8, 6.9, 6.10 and 6.12, we report in Figure 6.11 the mean subgraph centrality value and the variance for different value of the conductance. As can be seen from the Figure 6.11 the mean subgraph centrality value is increasing as

the conductance increases. As the reported variance is very small (less than 0.2), there is no large variability in the node subgraph centralities as the conductance increases. There is a kind of transition in the subgraph centralities corresponding to a particular value of the conductance where the mean subgraph centrality value reaches its maximum associated to the lowest value of the variance. Then after this critical point, the mean centrality value decreases and keeps a very small value of the variance.

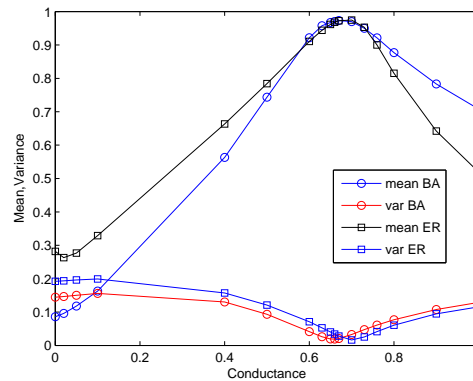


Figure 6.11: Illustrations of the mean subgraph centrality and variance for different values of the conductance in the BA and ER networks having both 100 nodes and average degree $\bar{k} \approx 6$.

In Figure 6.8 and Figure 6.9 we are plotting the subgraph centralities measures of nodes for the Barabási-Albert (BA) graph and in Figure 6.10 and Figure 6.12 we show the nodes subgraph centralities for the Erdős-Rényi (ER) random graph and for different values of the conductance x . The first thing that we can see from these plots is that the centralities of nodes are changing as the value of the conductance increases. To see how the values of nodes centralities are affected by the conductance, we have reported in Table 6.1 and Table 6.2 the first ten most central nodes and the first ten less central nodes for the Barabási-Albert graph and in Table 6.3 we present the first ten central nodes only for Erdős-Rényi network and for different values of x . In both cases it can be seen that the most central nodes

are becoming the less central nodes as the value of the conductance x is increasing (Table 6.1 and Table 6.2 for BA and for ER (Table 6.3). There is an inversion in the nodes subgraph centralities. Centralities show a power-law distribution for small values of x ($x \leq 0.1$) for the BA graph and a certain homogeneity for the ER graph. For instance for the BA graph this fact is similar to what we observed earlier in the generalised degrees of nodes when increasing the conductance, see page 213.

It is known that from expression (6.42) the subgraph centrality of the vertex i is defined as the sum of closed walks of different length in the network starting and ending at vertex i , with shorter closed walks being more important than longer closed walks. When $x = 0$ there is no influence of the term $d_{ij}x^{d_{ij}-1}$ and smaller

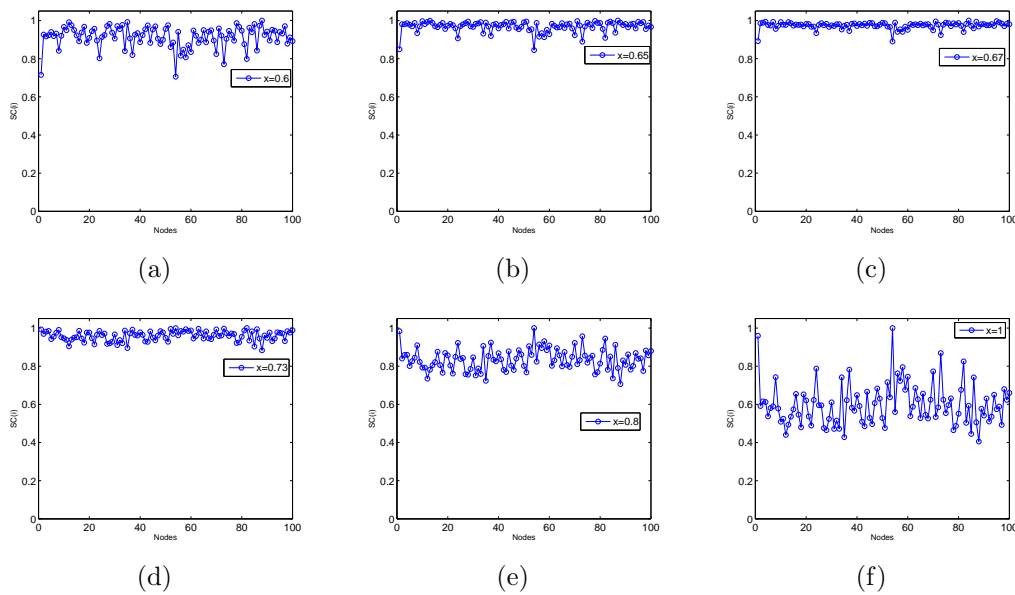


Figure 6.12: Generalised subgraphs centrality measures in the ER network having 100 nodes and average degree $\bar{k} \approx 6$ and for different values of the conductance x

distance means that nodes of high degree (hubs) in BA or ER graphs participate in a large number of smaller subgraphs of length two and contribute more to the subgraph centralities for these nodes. Longer walks having weight close to zero.

That is why we see that nodes of high degree in BA networks having larger subgraph centrality when $x = 0$ and showing a power-law distribution (for $x \leq 0.1$). In ER networks most of the nodes have the same degree and also participate in the same large number of small subgraphs of length two when $x = 0$ giving more contribution to the centrality of nodes showing certain homogeneity in the node centrality. When $x \neq 0$, the term $d_{ij}x^{d_{ij}-1}$ influence directly the generalised subgraph centralities of nodes. Let us consider the quantity $\bar{d}(k)x^{\bar{d}(k)-1}$ where $\bar{d}(k)$ is the average shortest path distance for nodes having degree k . When x increases, the term $\bar{d}(k)x^{\bar{d}(k)-1}$ is larger for nodes of high degree (for example the hubs in a BA network) which means that these nodes participate in a small number of subgraphs of length two having the weight $d_{ij}x^{d_{ij}-1}$ than in subgraphs of length two having weight one. At the same time the term $\bar{d}(k)x^{\bar{d}(k)-1}$ is smaller for nodes of low degree which means that these nodes participate in a very large number of subgraphs of length two having weight $d_{ij}x^{d_{ij}-1}$ than in subgraphs of length two having weight one.

In short, when x increases nodes of low degree participate in a large number of subgraphs (closed walks) of length two having a weight greater than one, but nodes of high degree participate in a large number of smaller subgraphs (closed walks) of length two having weight one than in subgraphs of length two having weight more than one. This fact explains why central nodes i.e. nodes having high centrality in BA or ER networks are becoming less central nodes, i.e. nodes of low centrality as the value of the conductance increases. These are the scenarios we are observing in Figure 6.8 and Figure 6.9, Figure 6.10 and Figure 6.12 or in Table 6.1, Table 6.2 and Table 6.3 when centralities is changing with x showing nodes of larger centrality becoming nodes of small centrality when x increases and vice-versa. In Figure 6.19 we illustrate the generalised closeness centrality for

Table 6.1: First 10 most central nodes (left to right) for different values of x for a BA network having $n = 100$ nodes and average degree $\bar{k} \approx 6$.

x	nodes									
0.00	6	3	5	4	8	2	7	14	1	16
0.02	6	3	5	4	8	2	7	14	16	1
0.06	6	3	5	8	4	2	7	14	16	1
0.1	6	3	5	8	4	2	7	14	16	1
0.4	3	6	5	8	4	2	16	7	14	1
0.5	3	4	6	5	8	2	7	1	16	14
0.6	4	3	1	13	8	5	10	7	2	18
0.63	46	18	71	10	68	13	4	1	15	35
0.65	71	46	68	18	90	35	57	51	33	45
0.66	71	68	46	90	35	45	18	98	57	51
0.67	71	68	90	46	98	45	35	63	55	33
0.70	55	63	60	96	98	97	71	45	73	74
0.73	87	91	94	89	72	55	60	76	88	86
0.76	80	91	87	89	88	94	72	86	78	76
0.8	80	91	89	87	88	94	78	72	86	99
0.9	80	91	89	88	87	78	94	72	99	86
1	80	91	89	88	87	78	94	72	99	86

each node in a BA network having $n = 100$ nodes and average degree $\bar{k} \approx 6$. As can be seen, there is an inversion in the generalised closeness centrality of nodes as the conductance x increases. This fact can be explained by a similar argument as for the generalised subgraph centrality of each node. Indeed when $x = 0$ nodes of high degree show larger closeness centrality. When x increases, the term $d_{ij}x^{d_{ij}-1}$ is increasing for nodes of high degree result in a lower generalised closeness centrality.

Relation Between Subgraph Centrality and Generalised Subgraph Centrality

The results obtained in the previous section indicate that if we compute the rank correlation coefficient between centralities ($x = 0$) and generalised centralities ($x \neq 0$) we will also observe a point where the initial positive correlation becomes negative (as this was the case for the degree and the generalised degree of Section 6.3.5). In Figure 6.13 and Figure 6.14 we plot the rank correlations of nodes

subgraph centralities for a BA graph.

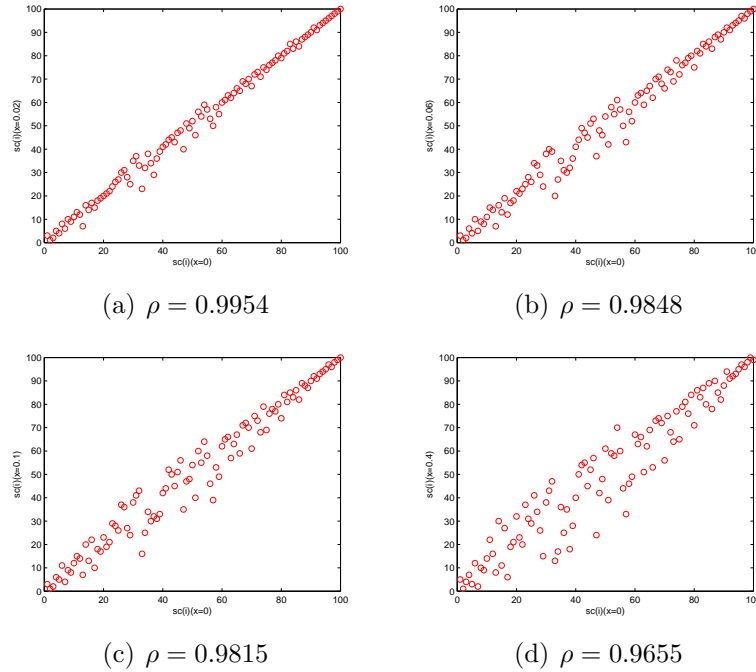


Figure 6.13: Rank correlations between subgraph centrality and generalised subgraph centrality for a BA network having $n = 100$ nodes and average degree $\bar{k} \approx 6$ and for different values of x .

In Figure 6.13 and Figure 6.14 we only compute the Spearman's rank correlation coefficient (ρ) for the BA network having $n = 100$ and average degree $\bar{k} \approx 6$. In Figure 6.15 and Figure 6.16 we plot the Spearman's rank correlation for ER network with same number on nodes and average degree. For values of x much larger than zero, the correlation coefficient is close to zero showing no correlation between rank centralities of nodes as seen in Figure 6.17. For a certain range of values of x this correlation is negative showing inverse correlation between ranks of nodes centralities and generalised centralities.

The same effects on subgraph centrality can also be formulated for the communicability centrality and betweenness centrality.

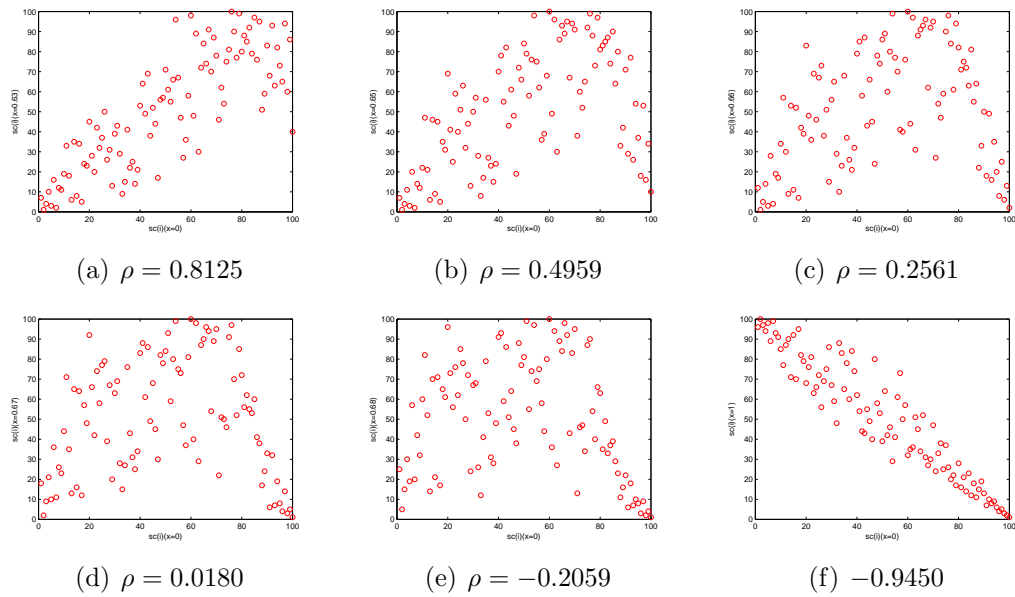


Figure 6.14: Rank correlations between subgraph centrality and generalised subgraph centrality for a BA network having $n = 100$ nodes and average degree $\bar{k} \approx 6$ and for different values of x .

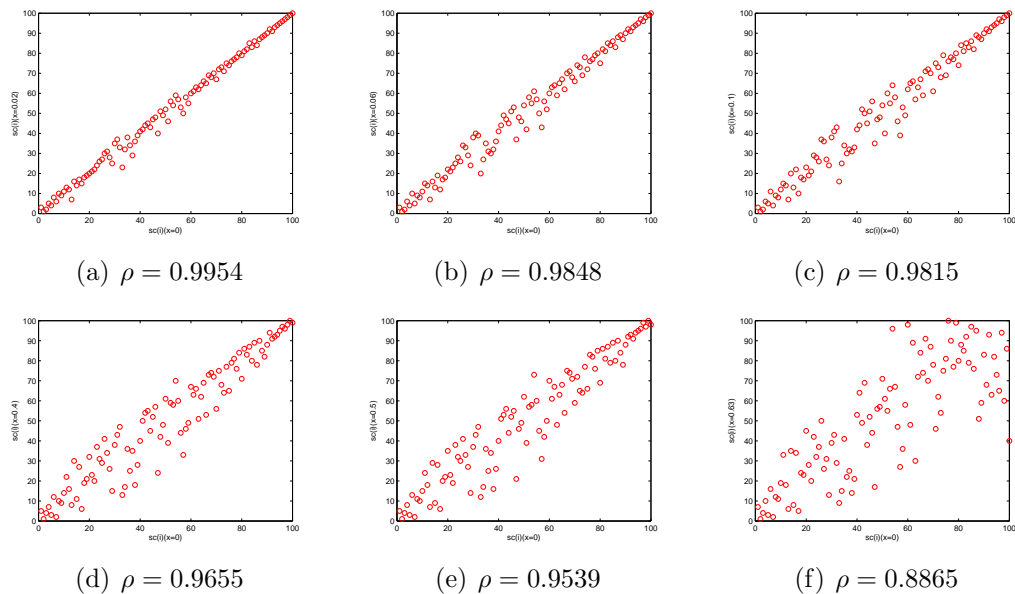


Figure 6.15: Rank correlations between subgraph centrality and generalised subgraph centrality for an ER network having $n = 100$ nodes and average degree $\bar{k} \approx 6$ and for different values of x .

We can do the same analysis for real-world networks. For instance the network of corporate directors of the top 500 corporations in the USA and the network of

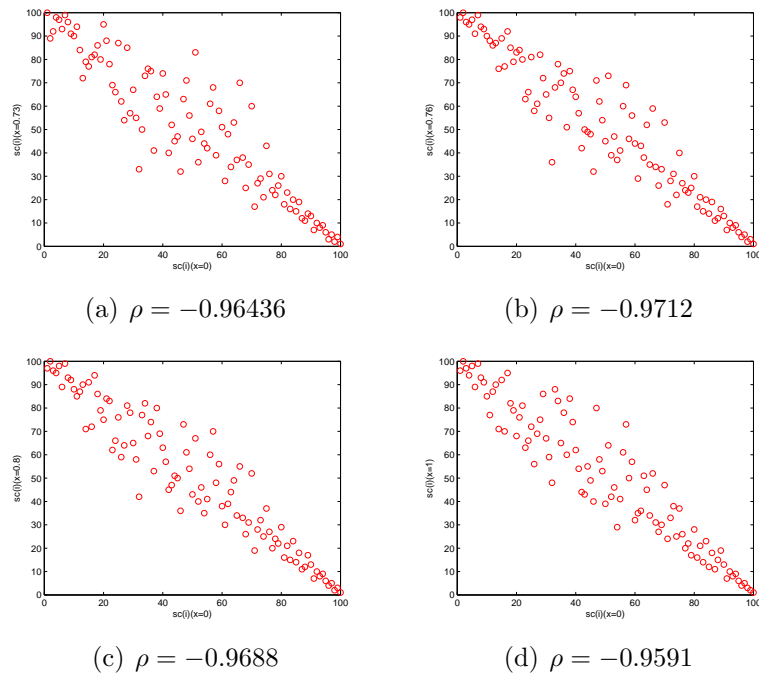


Figure 6.16: Rank correlations between subgraph centrality and generalised subgraph centrality for a ER network having $n = 100$ nodes and average degree $\bar{k} \approx 6$ and for different values of x .

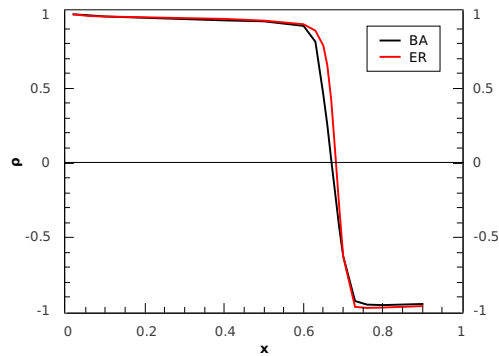


Figure 6.17: Evolution of the rank correlation coefficient ρ as a function of the conductance for BA and ER networks. The inversion point in the centrality measure is pretty much the same for both BA and ER networks, but in BA network this inversion point is reached much earlier than in ER network.

jazz musicians. Due to the memory limitation of computers, it becomes impossible to compute the subgraph centrality (or communicability centrality) of the vertex i for large networks when the value of x is increasing and when the generalised

Table 6.2: First 10 less central nodes (left to right) for different values of x for a BA network having $n = 100$ nodes and average degree $\bar{k} \approx 6$.

x	nodes									
0.00	87	80	88	94	89	76	91	72	86	95
0.02	80	88	87	89	94	91	65	76	86	72
0.06	80	88	87	89	91	94	65	86	72	76
0.1	80	88	87	91	89	94	65	86	72	78
0.4	80	91	89	88	87	78	94	65	86	72
0.5	80	91	89	88	87	78	65	94	99	86
0.6	80	91	89	88	78	87	65	94	99	50
0.63	80	91	89	88	78	65	87	99	50	94
0.65	80	91	89	88	78	65	87	50	99	6
0.66	80	6	89	91	88	5	78	8	65	50
0.67	6	80	5	8	3	16	14	2	88	89
0.70	6	5	8	3	4	2	16	14	7	19
0.73	6	5	8	3	4	2	16	14	7	1
0.76	6	5	3	8	4	2	16	14	7	1
0.8	6	5	3	8	4	2	16	14	7	1
0.9	6	3	5	8	4	2	16	14	7	1
1	6	3	5	8	4	2	16	14	7	1

graph matrix $\mathbf{\Gamma}(x)$ is considered. To overcome this difficulty we use the relation

$$\exp(\mathbf{\Gamma}(x) - r\mathbf{I}) = \exp(-r) \exp(\mathbf{\Gamma}(x)). \quad (6.61)$$

This means that if we simply use $(\exp(\mathbf{\Gamma}(x) - r\mathbf{I}))_{ii}$ as the subgraph centralities we will obtain values which are linearly correlated with those of $(\exp(\mathbf{\Gamma}(x)))_{ii}$ but having smaller values. This technique has been used for the corporate directors and jazz musicians networks. As for theoretical networks we have also provided in Figure 6.20 and Figure 6.21 plots for rank correlations of nodes centralities for the networks of corporate directors and jazz musicians showing also and inversion of nodes centralities when x increases.

Table 6.3: Top 10 most central nodes (left to right) for different values of x for an ER network having $n = 100$ nodes and average degree $\bar{k} \approx 6$

x	nodes									
0.00	87	34	11	84	26	45	30	21	27	41
0.02	87	34	11	84	26	30	45	21	27	41
0.06	87	34	11	84	26	30	27	21	45	42
0.1	87	34	11	84	26	30	27	21	45	77
0.4	87	34	11	84	77	30	27	26	32	42
0.5	87	34	11	84	77	27	30	32	26	42
0.6	87	34	11	77	27	84	32	50	12	42
0.63	77	87	11	34	27	12	86	50	42	32
0.65	86	12	77	70	9	50	83	27	45	42
0.66	83	86	70	12	94	9	77	6	50	45
0.67	83	94	70	86	3	6	9	12	95	2
0.70	83	3	62	94	2	99	6	15	51	95
0.73	81	53	72	62	51	85	57	69	0	36
0.76	53	0	72	81	57	69	36	85	23	51
0.8	53	0	72	81	57	36	69	23	55	85
0.9	53	0	72	81	57	23	36	69	55	85
1.	53	0	72	81	57	23	36	69	55	59

6.5 Age-Assortativity and the Modification of Watt-Strogatz Model

Based on the empirical evidence provided in Chapter 5 we have set up in Section 6.1 a network model that accounts for close and casual contacts relevant to the transmission of epidemics. In this section we are going to show that our model is able to reproduce the age-assortativity/homophily as observed in the work of Mossong et al. [91]. Epidemics are usually modelled on small-world networks [28]. That is, individuals are placed at the nodes of a regular lattice whose links represent close contacts along which the infection may spread to others. Then, an infection proceeds either locally (through close contacts), within a prescribed neighbourhood, or through casual contacts established at random between any two individuals [28, 89, 95, 119]. That is, in this case the long-range interactions among individu-

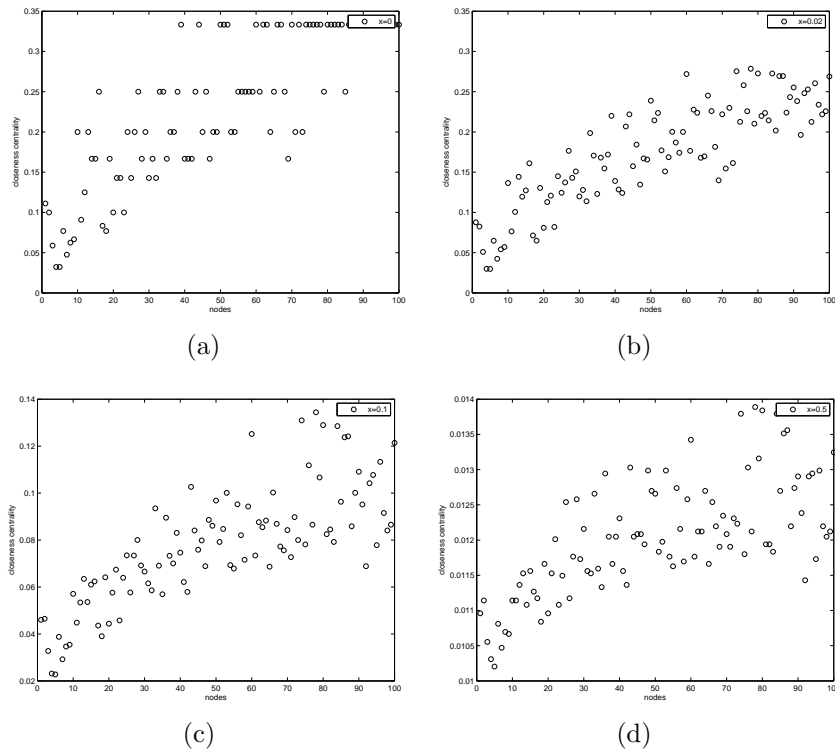


Figure 6.18: Generalised closeness centrality measures for each node in a BA network having $n = 100$ nodes and average degree $\bar{k} \approx 6$ and for different values of the conductance x .

als are considered to be at random and not to depend at all on the social distance between individuals in the network.

6.5.1 Random Rewiring and Age Homophily

In this section we are going to illustrate the lack of age homophily when casual contacts are considered as random. For this, we modify the Watts-Strogatz (WS) model [123] in order to account for the age of individuals. For simplicity, we start from a cycle graph of 100 nodes, and then we connect every node to its second nearest neighbours as shown in Figure 6.22 (a). This lattice, which is a circulant graph, is known as the *WS*-graph for rewiring probability $p = 0.0$. We then assign an age to every node starting from the node labelled as 1. The ages are

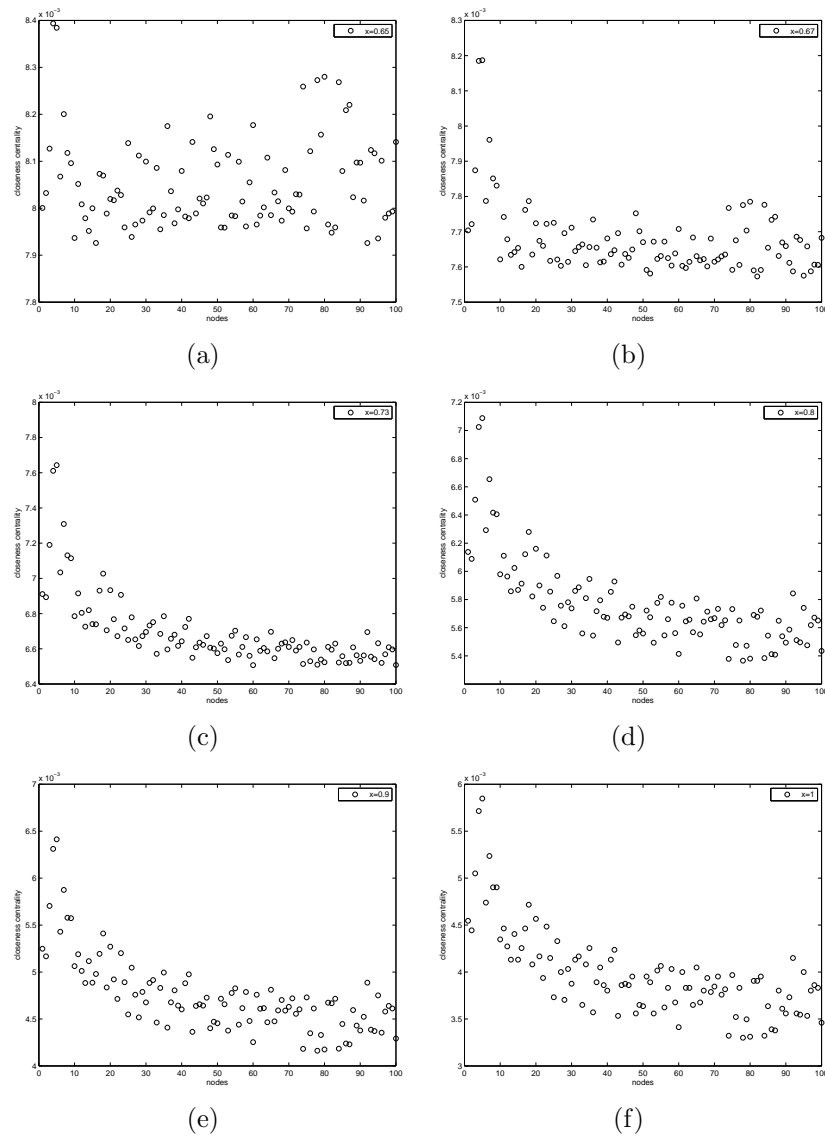


Figure 6.19: Generalised closeness centrality measures for each node in a BA network having $n = 100$ nodes and average degree $\bar{k} \approx 6$ and for different values of the conductance x .

assigned starting from 0 years with a clockwise increment of 0.757 years. The node labelled as 100 is then 75 years old. Thus, the nearest neighbours have similar ages, reproducing the observed age homophily in real social networks [68, 72, 84, 91]. In addition, the youngest and older nodes are also linked together as a consequence of the circular nature of the lattice. This characteristic has also been observed

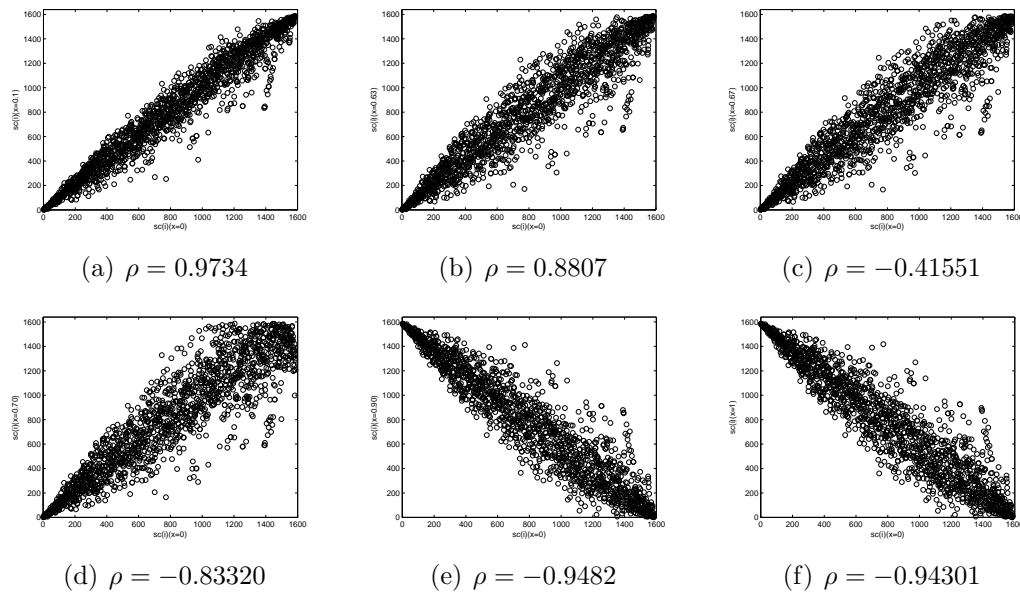


Figure 6.20: Rank correlations for the network of corporate directors of the top 500 corporations in the USA for different values of x .

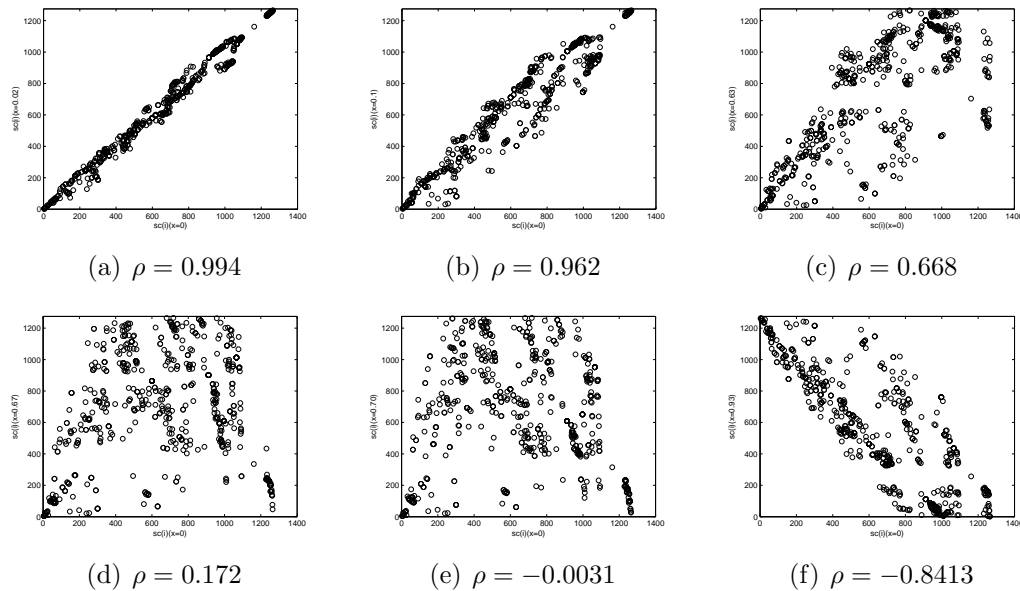


Figure 6.21: Rank correlations for the network measures for the jazz musicians for different values of x .

in real-world social relationships [68, 72, 84, 91]. We shall call this modified WS-graph/model the aged-WS model. For the aged-WS graph we proceed with the typical rewiring of links with probability $p > 0.0$ as illustrated in Figure 6.22 (b) in

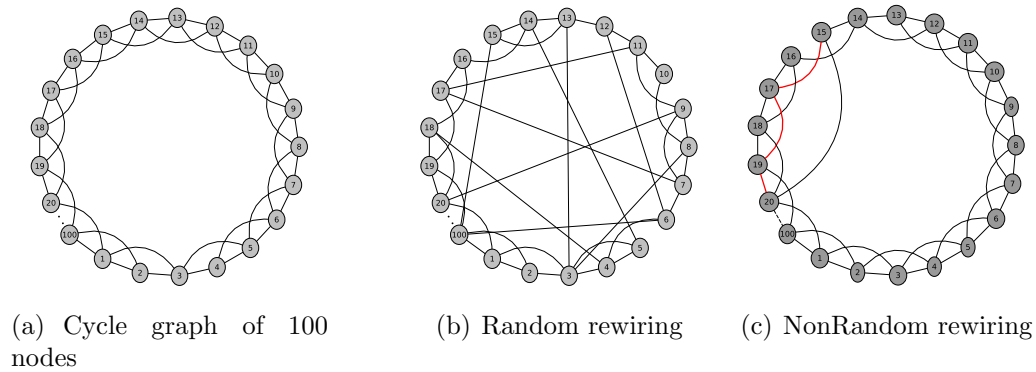


Figure 6.22: In (a) individuals are places on a WS-model starting from node labelled 1 to node labelled 100. Individual 1 has age 0, individual 2 has 0.757 and individual 100 has age 75. In (b) we are rewiring some edges at random. For example link (16, 15) has been rewired at random to link (15, 100) and link (10, 9) has been rewired at random to link (9, 20) and so on. In (c) the rewiring is not random, but depends on the distance between nodes. For instance the link (15, 16) is rewired to the link (15, 20) but taking into account the distance between the node 15 and 20 represented in red.

which few links have been rewired completely at random. Then, we calculate the average age of the nearest neighbours of each node for a given rewiring probability and report the average for the groups of ages 0 – 5, 5 – 10, 10 – 15, 15 – 20, 20 – 30, 30 – 40, 40 – 50, 50 – 60, 60 – 70, and 70+ as in the work of Mossong et al. [91].

The results are also illustrated in Figure 6.23. As can be seen in Figure 6.23 the classical WS model is unable to reproduce the age assortativity observed in social contacts. As $p \rightarrow 1.0$, all nodes tend to have neighbours of the same average age. The age assortativity disappears even for small values of p . For instance, for nodes in the group 10 – 15, which are known to display high age homophily in real networks [91], the average age of nearest neighbours is almost doubled from 12.5 for $p = 0.0$ to 22.8 for $p = 0.4$. For the nodes with ages between 5 and 24 for which Mossong et al. [91] have found strong age assortativity, the average age of nearest neighbours is almost duplicated for $p = 0.5$ when a random rewiring is used in the

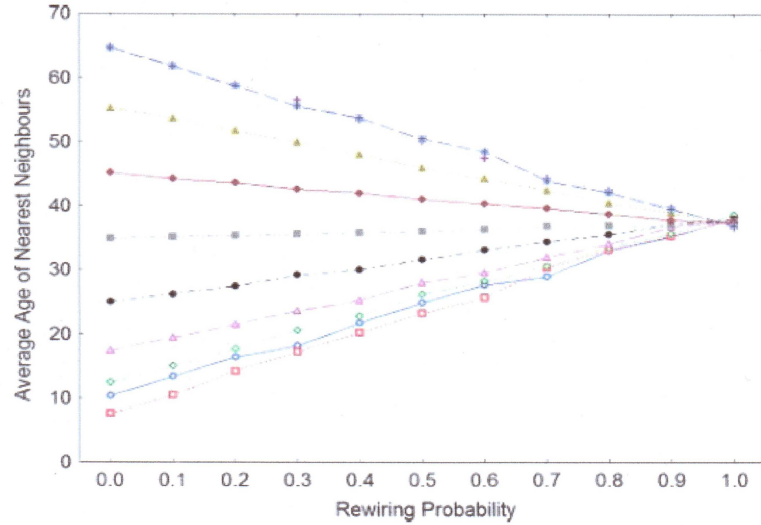


Figure 6.23: Average age of the nearest neighbour nodes in different age groups (see text) by using the WS model with node ages and a random rewiring of links. The ages are organised from top to bottom at probability 0.0 in the following groups: 0–5, 5–10, 10–15, 15–20, 20–30, 30–40, 40–50, 50–60, 60–70, and 70+.

age-WS model. In closing, the randomness of casual contacts is not able to explain the age assortativity observed by Mossong et al. [91] and other possibly existing homophilies in the social contacts among individuals in eight different European countries.

6.5.2 Deterministic Rewiring and Age Homophily

One of the main characteristics of the current model (see Section 6.1) is that it reproduces the age assortativity observed by Mossong et al. [91] in the social contacts in real networks. We consider the modification of the age-WS model used in the previous section in which casual contacts depend this time on the social distance between individuals. Then, instead of considering a random rewiring such as in the age-WS model we consider that for nodes i and j , with $d_{ij} > 1$,

the probability that i has a link with j is given by $p_{ij} = d_{ij}x^{d_{ij}-1}$. That is, the rewiring is carried out here on the basis of the “social distance” that separates two individuals (the social distance between two individuals being the shortest path length between them). That is a link, lets say (i, j) , is rewired to the link (i, k) not just at random, but this rewiring depends on the distance between i and k and the rewiring probability is given by $p_{ik} = d_{ik}x^{d_{ik}-1}$. That is why here we call this kind of rewiring deterministic as opposed to the completely random one of the previous section. Using exactly the same age assignation to nodes as in the previous section (see Figure 6.22 (a)). As can be seen, from Figure 6.24, the aged-WS

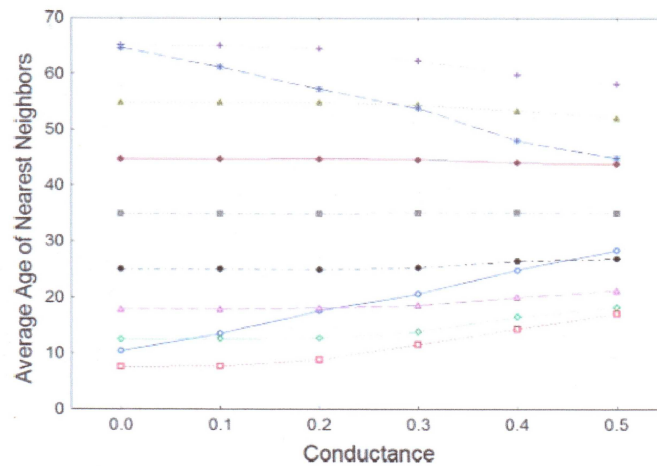


Figure 6.24: Average age of the nearest neighbour nodes in different age groups (see text) by using the WS model with node ages in which the rewiring probability depends explicitly on the inter node distance. The ages are organised in groups as in Figure 6.23.

model with distance-based rewiring displays strong age assortativity for all values of the conductance. In the case of the two extreme age groups, i.e., 0–5 and 70+, there is a larger difference in the average age of the nearest neighbours between $x = 0.0$ and $x = 0.5$, which is about 18 years. We remark again that in these groups it has been observed “experimentally” that there is a larger outbreeding

than in the rest of age groups [91]. For the nodes in each of the other groups of ages analysed in the previous section the increase of age does not exceed 10 years even for a high conductivity of $x = 0.5$, in complete agreement with the empirical evidence provided by the work of Mossong et al. [91]. For instance, for the same age group analysed previously (10 – 15 years), the average age of nearest neighbours changes from 12.5 at $x = 0.0$ to 18.1 at $x = 0.5$. For the nodes with ages between 5 and 24 years analysed by Mossong et al. [91] the average age of nearest neighbours changed only by 6 years when the conductance changed from 0.0 to 0.5. These results clearly point out the fact that the consideration of social distance as a director for casual social contacts is of relevance for studying the spread of infections in the real-world. *This characteristic has not long been reproduced by existing models that account for casual contacts as random long-range interactions among individuals.*

Average Path Length and Average Clustering Coefficient

In Figure 6.25 we plot the characteristic average path length and average clustering coefficient for Aged-WS model with deterministic rewiring of links. As can be seen the average clustering coefficient is decreasing as x is increased. The average path

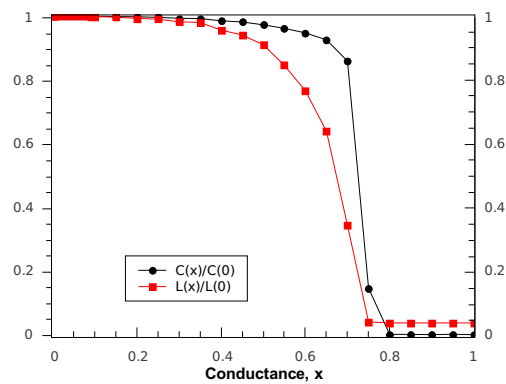


Figure 6.25: Characteristic average path length and average clustering coefficients in age-WS model with deterministic rewiring.

length is also decreasing but still high compared to the average path length in the

random rewiring of the Watts-Strogatz model. In this strategy it is not possible to have a small world characteristic. That is, having at the same time high clustering coefficient and low average path length for a certain value of the conductance.

Age-Assortativity Measure

In order to compare the variability in the age of nodes in the random and deterministic rewiring, we introduce a measure for the age-assortativity defined as follow:

1. Random rewiring. In this case the age assortativity measure $A(p)$ given by:

$$A(p) = \sum_{i \neq j} (\text{age}(i)(p) - \text{age}(j)(p))^2, \quad (6.62)$$

where $\text{age}(i)(p)$ is the age of individual i for probability p .

2. Deterministic rewiring. For this case the age assortativity measure $A(x)$ is defined as:

$$A(x) = \sum_{i \neq j} (\text{age}(i)(x) - \text{age}(j)(x))^2, \quad (6.63)$$

where $\text{age}(i)(x)$ is the age of node i and $\text{age}(j)(x)$ is the age of node j for a given conductance x . In Figure 6.26 we plot both $A(p)$ and $A(x)$ for the same values of the probability p , and the conductance x . As can be seen, the age assortativity measure $A(p)$ in the random rewiring is always large than the age assortativity measure $A(x)$ in the deterministic rewiring. This is telling us that there is less age variability in the deterministic rewiring than in the random rewiring. This fact is also in agreement with the age homophily observed in the work of Mossong et al. [91].

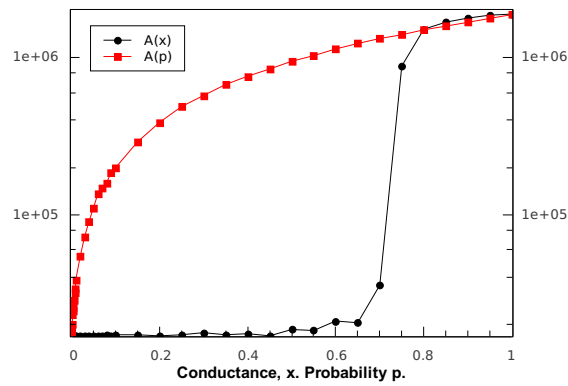


Figure 6.26: Age assortativity measure $A(x)$ in the deterministic rewiring and $A(p)$ in the random rewiring. As can be seen the assortativity measure in random rewiring is larger than the age assortativity measure in the deterministic rewiring. There is less variability in the age of nodes in deterministic rewiring than in random rewiring. This fact is in agreement with the age homophily observed by Mossong et al. [13]

Chapter 7

Non-Linear Dynamical System (NLDS)

In Chapter 3 we studied the epidemics in complex networks and we presented various equations that described the spread of epidemics in different scenarios. Most of those equations were continuous in time or were seen as continuous dynamical systems. Several assumptions were made that allowed us to get simpler approximate equations which were straightforward to solve. For example, the homogeneous assumption was used in the case of SIS, SIR models on populations. In the case of epidemics on networks, the assumption of statistical equivalence of all nodes of the same degree were made to make things easy and in some cases the degree correlation was completely ignored. We have seen that there is no unified framework to study and analyse the spread of epidemics. Each model was specific to a particular case and cannot be used to tackle all cases. In this chapter we are going to present a probabilistic framework for epidemic spreading in complex networks which is a discrete-time formulation of the problem of contact-based epidemic spreading in networks. This model has the advantage of being network

free, that is it does not depend on the type of the network under consideration. It works fine in most of the cases considered. This approach consists of a model independently developed by Chakrabarti et al. [32] and Gómez et al. [63, 64] on the basis of susceptible-infected-susceptible (SIS) epidemic models. The model so far considered was first developed by Chakrabarti et al. [32] as a Non-Linear Dynamical System (NLDS) in order to explain the propagation of viruses in computer networks. More recently, Gómez et al. [63, 64] have proposed a similar Microscopic Markov-Chain Approach (MMCA), which uses the same principles as in NLDS, but concentrates on the probability of infection of individuals rather than on the common heterogeneous mean-field approach. We clarify beforehand that our interest here, as in the precedent papers [63, 64], is in networks of very large size, with any kind of topology. For obvious reasons we propose to call this model NLDS/MMCA. The framework introduced separately by these authors will play an important role in the next chapter of this thesis. All the future development of the thesis will be based on that framework. Before going into the development of the NLDS/MMCA let us briefly summarise the propagation of viruses in computer networks. We begin by a quick overview of the Kephart and White (KW) model.

7.1 Propagation of Computer Viruses

Kephart and White were the first to propose an epidemiology-based model to study and analyse the propagation of computer viruses [73]. Their model falls into the general class of the so called homogeneous epidemiological models described in Chapter 4, that is each individual has equal contact to others in the population and the rate of infection is principally determined by the density of the infected population.

Description of the Kephart-White Model

In the Kephart-White Model (KWM) the communication among individuals is modelled as a directed graph: a directed edge from node i to node j means that i can directly infect node j . A rate of infection, the birth rate β is associated with each edge. A virus death rate δ is associated with each infected node.

Mathematical description of KWM

The mathematical formulation of the SIS model based on the KW assumption will be derived for a random graph with n nodes and edge probability p . Let $\eta(t)$ be the total number of the infected population at time t and let $i(t) = \frac{\eta(t)}{N}$ be the fraction of infected nodes in the population. Given n nodes and edge probability p , the expected number of edges in the graph is

$$E = pn(n - 1). \quad (7.1)$$

Now, if we consider a particular infected node, then the expected number of edges emanating from that node (also called the connectivity) is

$$\bar{k} = E/n = p(n - 1). \quad (7.2)$$

The fraction of neighbours of the infected node that are susceptible to infection is

$$f(t) = 1 - i(t) = 1 - \frac{\eta(t)}{n}.$$

The expected number of nodes that can be infected is

$$\bar{k} \left(1 - \frac{\eta(t)}{n} \right).$$

Therefore the total system-wide rate at which infected nodes infect uninfected nodes is

$$r(t) = \beta \bar{k} \eta(t) (1 - i(t))$$

where $\beta \bar{k}$ is the average total rate at which a node attempts to infect its neighbours. The system-wide rate at which nodes are cured is $\delta \eta(t)$. The equation of evolution of $i(t)$ is

$$\frac{di(t)}{dt} = \beta \bar{k} i(t) (1 - i(t)) - \delta i(t). \quad (7.3)$$

Since $i(t) = \frac{\eta(t)}{n}$ we have also

$$\frac{d\eta(t)}{dt} = \beta \bar{k} \eta(t) \left(1 - \frac{\eta(t)}{N}\right) - \delta \eta(t). \quad (7.4)$$

The solution to (7.4) is given by:

$$\eta(t) = \frac{\eta_0 \left(1 - \frac{\delta}{\beta \bar{k}}\right)}{\frac{\eta_0}{n} + \left(1 - \frac{\eta_0}{n} - \frac{\delta}{\beta \bar{k}}\right) e^{-(\beta \bar{k} - \delta)t}} \quad (7.5)$$

where $\eta_0 = \eta(t = 0)$ is the initial number of infected nodes in the population (network). The steady state solution of (7.4) is given by:

$$\eta = n \left(1 - \frac{\delta}{\beta \bar{k}}\right). \quad (7.6)$$

Equation (7.5) gives the evolution in time of the number of infected nodes in the network. From equation (7.5) we can see that:

- if $\delta/\beta > \bar{k}$ then $\eta(t) \rightarrow 0$ as $t \rightarrow \infty$ and the infection dies out, and
- if $\delta/\beta < \bar{k}$ then $\eta(t) \rightarrow n(1 - \frac{\delta}{\beta \bar{k}})$ and the infection survives and becomes an epidemic.

From this fact, we can draw the following conclusion: The epidemic threshold in the KW model is given by:

$$\tau_{KW} = \frac{1}{k}. \quad (7.7)$$

Limitations of KW Model

This model was designed for the epidemiology approach in the case of computer viruses and assumes a directed network. In the real world, transmission of infections can go in two directions and therefore the model cannot perform very well for undirected networks. Moreover, this approach uses the homogeneous assumption. There is no need for all nodes to have the same average degree. NLDS/MMCA goes beyond these limitations, by considering not only the case of computer networks but any real or random network and also removes the assumption of degree homogeneity by considering a network with any degree distribution.

7.2 Model definition of NLDS

As mentioned in the previous chapters, a node or an individual in SIS can only be in two different states either susceptible or infected. For graphs having n nodes, the process of viruses spreading is described by a Markov chain having 2^n possible states. Each state of the Markov chain corresponds to one particular configuration of n nodes. It becomes almost impossible to solve this Markov chain for large networks. In Chapter 4 several assumptions were made to simplify the equations so they can be easily and straightforwardly solved. Chakrabarti et al. developed a mathematical model for the *SIS* method of viral infection, which is applicable to any undirected graph G . Their model assumes very small discrete time-steps of size Δt , where $\Delta t \rightarrow 0$. Their results can also be applied equally well to continuous systems, though they focus on discrete systems for ease of exposition. In the NLDS

model [32], a node i remains healthy at time t in a network if it does not receive infection from its nearest neighbours at a previous time step, $t - 1$. In addition, if the node has been infected, it can recover and become healthy again with a certain probability. The probability $1 - p_{i,t}$ that the node remains healthy in the network is given by:

$$1 - p_{i,t} = (1 - p_{i,t-1})\xi_{i,t} + \delta p_{i,t-1}\xi_{i,t}, \quad (7.8)$$

where $p_{i,t}$ is the probability that node i is infected at time t , $\xi_{i,t}$ is the probability that it does not receive infection from its nearest neighbours at time t and δ is the rate at which it can recover from infection. The probability that a node does not receive infection from its nearest neighbours is assumed to be determined by the product of individual probabilities (independence assumption), which are determined by $p_{j,t-1}$ for all nearest-neighbours of i and by the universal birth rate of the infection β [32]. That is,

$$\xi_{i,t} = \prod_{j \sim i} (1 - \beta p_{j,t-1}), \quad (7.9)$$

where $j \sim i$ indicates that j is directly connected to i . The size of the infected population in the network is given by:

$$\eta(t) = \sum_{i=1}^n p_{i,t}. \quad (7.10)$$

The quantity $\xi_{i,t}$ depends on the universal birth rate of the infection β and the network topology around i . In this model, within a Δt time interval, an infected node i tries to infect its neighbours with probability β . At the same time, i may be cured with probability δ .

Independence Assumption

This assumption appears for the first time here in this model. It says that the states of the nearest neighbours of a given node i are independent from each other, that is in relation (7.9) the probabilities $p_{j,t-1}$ are independent from each other. This assumption places no constraints on network topology; and the method works with any arbitrary finite graph. Also, this assumption is far less constrained than the mean field assumption. In fact, Chakrabarti et al. showed experimentally that the number of infected nodes over time under the independence assumption is very close to that without any assumptions, for a wide range of datasets. The hypothesis of independence assumption turns out to be valid for many cases of complex networks because the inherent topological disorder makes dynamical correlations not persistent [63, 64]. Equation (7.8) can be written as follows:

$$\mathbf{p}_t = F(\mathbf{p}_{t-1}), \quad (7.11)$$

where

$$F : \mathbb{R}^n \rightarrow \mathbb{R}^n, \quad \mathbf{p}_{t=t_0} = \mathbf{p}_0 \quad (7.12)$$

and

$$F^i(\mathbf{p}_{t-1}) = 1 - (1 - p_{i,t-1})\xi_i(t) + \delta p_{i,t-1}\xi_{i,t} \quad (7.13)$$

$$(\mathbf{p}_t)_i = p_{i,t} \quad (7.14)$$

and $F_i(\cdot)$ and $(\mathbf{p}_t)_i$ are respectively the i th element of the function F and \mathbf{p}_t . The equivalent equations (7.8) and (7.12) can be seen as a multidimensional non linear discrete dynamical system as introduced and reviewed previously in Chapter 2. Let us suppose that the dynamical system has a steady-state equilibrium, $\bar{\mathbf{p}}$. Namely,

$\exists \bar{\mathbf{p}} \in \mathbf{R}^n$ such that:

$$\bar{\mathbf{p}} = F(\bar{\mathbf{p}}). \quad (7.15)$$

A Taylor expansion of the i^{th} equation of (7.12), $p_{i,t} = F^i(\mathbf{p}_{t-1})$, around the steady-state value, $\bar{\mathbf{p}}$, yields

$$p_{i,t} = F^i(\mathbf{p}_{t-1}) = F^i(\bar{\mathbf{p}}) + \sum_{j=1}^n F_j^i(\bar{\mathbf{p}})(p_{j,t-1} - \bar{p}_j) + \cdots + R_n, \quad (7.16)$$

where

$$F_j^i(\bar{\mathbf{p}}) = \frac{\partial F^i(\mathbf{p}_{t-1})}{\partial p_{j,t-1}}(\bar{\mathbf{p}}) = \begin{cases} \beta & \text{for } j \neq i, \\ 1 - \delta & \text{for } j = i. \end{cases} \quad (7.17)$$

We can show that $\bar{\mathbf{p}} = \mathbf{0}$ is a fixed point for the system, that is

$$F(\mathbf{0}) = \mathbf{0}. \quad (7.18)$$

In fact the infection dies out when $p_i(t) = 0$ for all i . We have

$$F_i(\mathbf{0}) = 1 - \xi_i(t). \quad (7.19)$$

The other solutions can be founded iteratively by solving:

$$(\bar{\mathbf{p}})_{i,t} = 1 - (1 - (\bar{\mathbf{p}})_{i,t})\xi_{i,t} - \delta(\bar{\mathbf{p}})_{i,t}\xi_{i,t}. \quad (7.20)$$

Thus, using (7.16) the linearised equation (an approximation) around the steady state $\bar{\mathbf{p}} = \mathbf{0}$ is given by:

$$p_{i,t} \approx (1 - \delta)p_{i,t-1} + \beta \sum_{j \sim i}^n p_{j,t-1}, \quad (7.21)$$

which can be expressed in matrix form as

$$\mathbf{p}_t \approx (\beta \mathbf{A} + (1 - \delta) \mathbf{I}) \mathbf{p}_{t-1}, \quad (7.22)$$

where \mathbf{p}_t is a vector whose i th entry is $p_{i,t}$, \mathbf{A} is the adjacency matrix of the network and \mathbf{I} is the identity matrix. The first term in brackets represents the probability that a node is infected from the nearest neighbours and the second is the probability that it recovers from infection. We notice that the linear approximation (7.21) is satisfied only in the vicinity of the steady state solution $\bar{\mathbf{p}} = \mathbf{0}$.

7.3 The Epidemic Threshold under NLDS

Theorem 7.3.1 *In NLDS, the epidemic threshold τ_{NLDS} for an undirected graph $G = (V, E)$ is [32]*

$$\tau_{NLDS} = \frac{1}{\lambda_{1,\mathbf{A}}}, \quad (7.23)$$

where $\lambda_{1,\mathbf{A}}$ is the largest eigenvalues of the adjacency matrix \mathbf{A} of the graph.

The epidemic threshold τ_{NLDS} for NLDS is a value such that

- if $\beta/\delta < \tau_{NLDS}$ then the infection dies out over time, i.e. $p_i(t) \rightarrow 0$ as $t \rightarrow \infty$ $\forall i$.
- if $\beta/\delta > \tau_{NLDS}$ then the infection survives and becomes an epidemic.

Chakrabarti et al. [32] have proved that in order to ensure that over time the infection probability of each node in the graph goes to zero (that is, the epidemic dies out), it is necessary to have:

$$\beta/\delta < \tau_{NLDS} \quad (7.24)$$

and if (sufficient condition)

$$\beta/\delta < \tau_{NLDS} \quad (7.25)$$

then the epidemic will die out over time (the infection probabilities will go to zero), irrespective of the size of the initial outbreak of infection.

7.4 Numerical Experiment on NLDS

In this section we are going to illustrate the propagation of infection in theoretical and real networks by using the NLDS. We are going to consider the cases of, the path graph P_n , the cycle graph C_n , the star graph S_n , the complete graph K_n , the Erdős-Rényi (ER) random graph, the Barabási-Albert Graph and the graph of jazz musicians and the top 500 corporate directors in the USA.

Path Graph

We are considering a path graph P_n having $n = 200$ nodes in two different cases. In the first case the values of the parameters are $\beta = 0.35$ with two different values of δ , namely $\delta = 0.02$ and $\delta = 0.075$ (see Figure 7.1). In the second scenario, we keep the same number of nodes but this time $\beta = 10^{-5}$ and $\delta = 0.024$ and $\delta = 0.038$ (see Figure 7.2). In both cases we start the simulations with a small number of randomly infected nodes $n_0 = 10$. The largest eigenvalue of the adjacency matrix \mathbf{A} for a path graph P_n is given by (see Chapter 1)

$$\lambda_{1,\mathbf{A}} = 2 \cos \left(\frac{\pi}{n+1} \right). \quad (7.26)$$

Then, according to NLDS the epidemic threshold for this case is given by:

$$\tau = \frac{1}{2 \cos\left(\frac{\pi}{n+1}\right)}. \quad (7.27)$$

For instance, for $n = 200$ and $\tau = 0.5$.

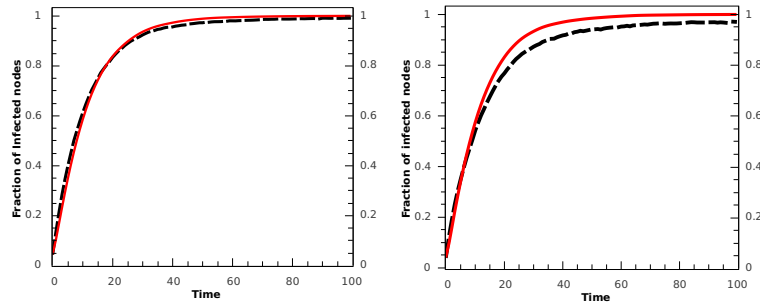


Figure 7.1: Results for the simulations (dashed lines) and the NLDS (solid lines) for a path graph having $n = 200$ nodes. In both cases $\beta = 0.035$ and $\delta = 0.02$ (left) and $\delta = 0.075$ (right). As $\beta/\delta > \tau = 0.5$ (left plot) and also $\beta/\delta > \tau = 0.5$ (right plot), we see that the infection is growing and becomes an epidemic. The simulations are the averages of just 10 realisations.

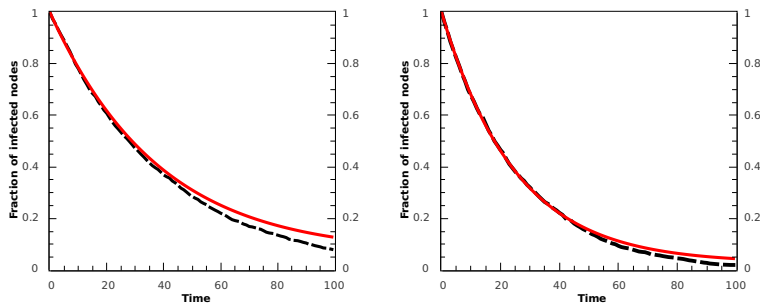


Figure 7.2: Results for the simulations (dashed lines) and the NLDS (solid lines) for a path graph having $n = 200$ nodes. In both cases $\beta = 10^{-5}$ and $\delta = 0.024$ (left) and $\delta = 0.038$ (right). As $\beta/\delta < \tau = 0.5$ (left plot) and also $\beta/\delta < \tau = 0.5$ (right plot), we see that the infection dies out and as time is increasing the infection is going to zero.

Cycle Graph

We are considering a cycle graph P_n having $n = 200$ nodes in two different cases. In the first case the value of the parameters are $\beta = 0.35$ and $\delta = 0.02$ (see Figure 7.3 (left)). In the second scenario, we keep the same number of nodes but with this time $\beta = 10^{-5}$ and $\delta = 0.024$ (see Figure 7.3 (right)). In both cases the simulations start with a small number of randomly infected nodes, $n_0 = 10$. The results are similar to those of the path graph having the same parameters. This may be explained by the fact that a cycle is a version of a path graph in which the two terminals are joined. The largest eigenvalue of the adjacency matrix \mathbf{A} for a cycle graph C_n is given by

$$\lambda_{1,\mathbf{A}} = 2 \cos \left(\frac{2\pi}{n} \right), \quad (7.28)$$

then according to NLDS the epidemic threshold in this case is given by:

$$\tau = \frac{1}{2 \cos \left(\frac{2\pi}{n} \right)}. \quad (7.29)$$

For instance, for $n = 200$, $\tau = 0.5$.

Star Graph

Here we consider a star graph having $n = 1000$ nodes. In the first two scenarios we infect all nodes (see Figure 7.4 (a) and (b)) and the values of the parameters are $\beta = 0.002$ and $\delta = 0.316$ and $\delta = 0.158$. In the second scenario (see Figure 7.4 (c) and (d)) we start with a very small number of infected nodes, 5 in this case, and the values of the parameters are $\beta = 0.2$ and $\delta = 0.24$ and $\delta = 0.09$. We can see that the simulations and NLDS match. According to Chapter 3 the largest

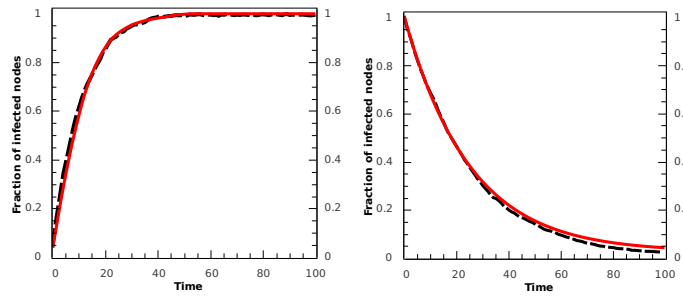


Figure 7.3: Results for the simulations (dashed lines) and the NLDS (solid lines) for a cycle graph having $n = 200$ nodes. In the first case $\beta = 0.35$ and $\delta = 0.024$ (left) and in the second case $\beta = 10^{-5}$ and $\delta = 0.038$ (right). As $\beta/\delta < \tau = 0.5$ (left plot) the infection is growing and never dies out and as $\beta/\delta < \tau = 0.5$ (right plot), we see that the infection dies out and as time is increasing the number of infected nodes is going to zero.

eigenvalue of the adjacency matrix \mathbf{A} for a star graph is given by:

$$\lambda_{1,\mathbf{A}} = \frac{1}{\sqrt{n-1}}, \quad (7.30)$$

then according to NLDS the epidemic threshold in this case is given by:

$$\tau = \frac{1}{\lambda_{1,\mathbf{A}}} \quad (7.31)$$

$$= \frac{1}{\sqrt{n-1}} \quad (7.32)$$

Complete Graph

We consider a complete graph K_n having $n = 200$ in two different cases. In the first case $\beta = 0.0023$ and $\delta = 0.001$ (see Figure 7.5 (left)). In the second case $\beta = 10^{-6}$ and $\delta = 10^{-1}$. The largest eigenvalue of the adjacency matrix \mathbf{A} for a complete graph K_n is $\lambda_{1,\mathbf{A}} = 1$ and the epidemic threshold is $\tau = 1$. In the first scenario (Figure 7.5 (left)) the infection survives and becomes an epidemic.

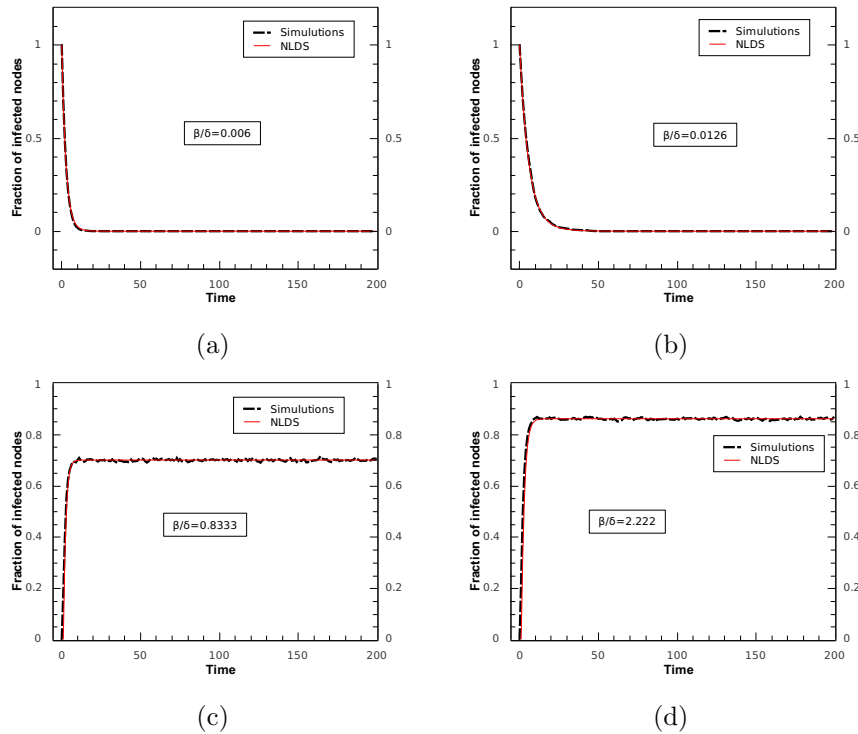


Figure 7.4: Results for the simulations (dashed lines) and the NLDS (solid lines) for a star graph having $n = 1000$ nodes. In (a) and (b) we start with all nodes infected. As $\beta/\delta < \tau = 1/999$ we see that the infection dies out and as time is increasing the number of infected nodes is going to zero. In (c) and (d) we start with a small number of infected nodes, in this case 5, and as $\beta/\delta > \tau = 1/999$ we see that the epidemic is growing and never dies out and becomes an epidemic. The results are the average of just 15 realisations.

We can see that in the complete graph the infection is propagating a lot faster than in any other network. For very small values of the parameters almost all the nodes are infected. This may be explained by the fact that in a complete graph every node is connected to all other nodes and an infected node may infect all other nodes resulting in a high increase in the infected population. In the second scenario (Figure 7.5 (left)) we start with all nodes infected. As can be seen, it is very hard to eradicate the infection in this case. We need a very small value of β and a large value of δ .

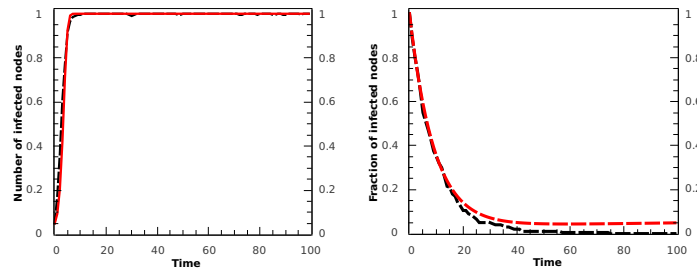


Figure 7.5: Results for the simulations (dashed lines) and the NLDS (solid lines) for a complete graph having $n = 200$ nodes. In the left plot we start with 10 infected nodes and $\beta = 0.0023$ and $\delta = 0.001$. As $\beta/\delta > \tau$ we see that the infection is growing and never dies out and becomes an epidemic. In the right plot we have $\beta = 10^{-6}$ and $\delta = 10^{-1}$ and we see that the infection dies out and as time is increasing the number of infected nodes is going to zero. The results are the average of just 10 realisations.

Complete Bipartite Graph

We consider here a bipartite graph with $n_1 = 100$ and $n_2 = 100$ and keeping the same values of parameters as for the complete graph of the previous section. The largest eigenvalue of the adjacency matrix \mathbf{A} for a complete bipartite graph K_{n_1, n_2} is

$$\lambda_{1, \mathbf{A}} = \sqrt{n_1 n_2}, \quad (7.33)$$

and the epidemic threshold is

$$\tau = \frac{1}{\sqrt{n_1 n_2}}. \quad (7.34)$$

For $n_1 = 100$ and $n_2 = 100$, $\tau = 0.032$.

Erdős-Rényi (ER) random graph and Barabási-Albert BA graph.

We illustrate in Figure 7.7 the results of simulations and NLDS for the ER random graph (a) and (c) ($\beta = 0.2$ and $\delta = 0.12$ and $\delta = 0.24$) having $n = 1000$ and for a

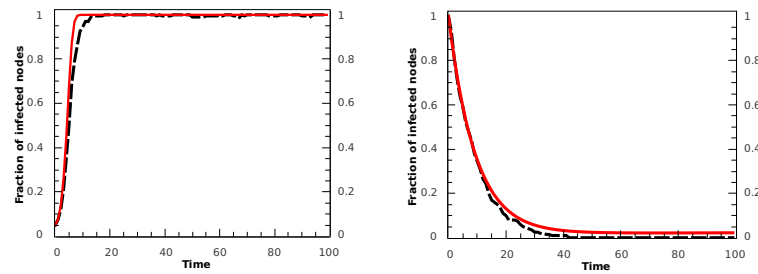


Figure 7.6: Results for the simulations (dashed lines) and the NLDS (solid lines) for a complete bipartite graph having $n_1 = 100$ and $n_2 = 100$. In the left plot we start with 10 infected and $\beta = 0.0023$ and $\delta = 0.001$. As $\beta/\delta > \tau$ we see that the epidemic is growing and never dies out and becomes an epidemic. In the right plot we have $\beta = 10^{-6}$ and $\delta = 10^{-1}$ and we see that the infection dies out and as time is increasing the number of infected nodes is going to zero. The results are the average of just 10 realisations.

BA network (b) and (d) with the same values of parameters. The largest eigenvalue of the adjacency matrix \mathbf{A} for a ER network having $n = 1000$ nodes and average degree $\bar{k} \approx 6$ is $\lambda_{1,\mathbf{A}} \approx 15.18$. As $\beta/\delta > 1/\lambda_{1,\mathbf{A}} = 0.066$, the infection survives and becomes an epidemic (see Figure 7.7 (a) and (c)). For the BA graph with the same number of nodes and the same average degree, the largest eigenvalue of the adjacency matrix is $\lambda_{1,\mathbf{A}} \approx 13.17$. Also in this case as $\beta/\delta > 1/\lambda_{1,\mathbf{A}} = 0.076$, the infection survives and becomes an epidemic (see Figure 7.7 (b) and (d)).

Network of Jazz musicians and for the network of top 500 corporate directors in the USA

The Jazz musicians network has 1265 nodes/individuals and 32358 links and the second network has 1586 corporate directors and 11540 links or collaborations between them. The largest eigenvalues of the adjacency matrices \mathbf{A}_1 and \mathbf{A}_2 of the Network of Jazz musicians and for the top 500 corporate directors are respectively $\lambda_{1,\mathbf{A}_1} \approx 171.5$ and $\lambda_{1,\mathbf{A}_2} \approx 23.23$. As $\beta/\delta > \lambda_{1,\mathbf{A}_1}$ and $\beta/\delta > \lambda_{1,\mathbf{A}_2}$

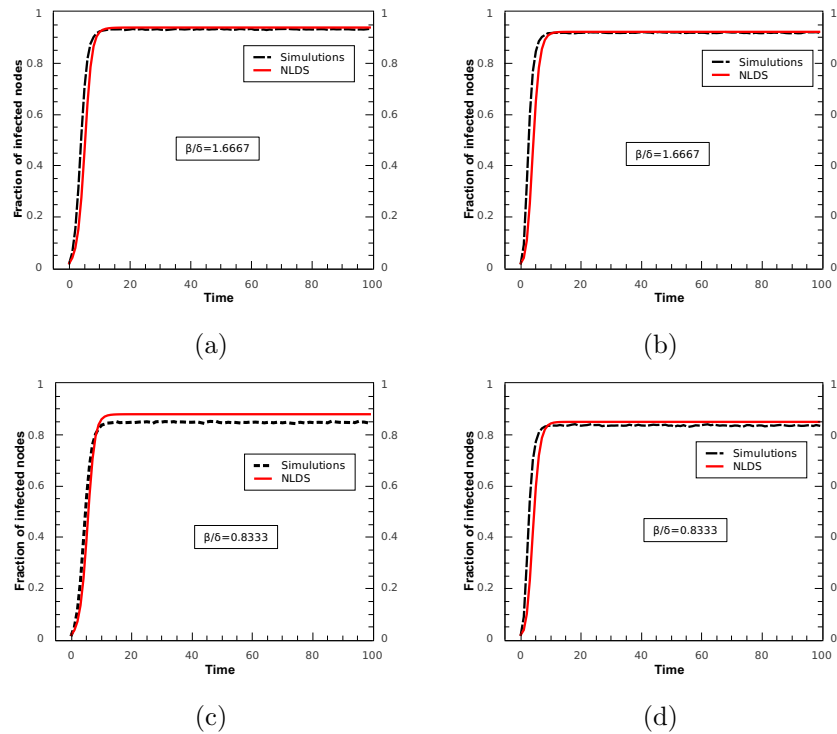


Figure 7.7: Results for the simulations (dashed lines) and the NLDS (solid lines) for an ER network having $n = 1000$ nodes (a) and (c) (β is fixed and δ varies) and for a BA network (b) and (d) (β is fixed and δ varies) having the same number of nodes. Both networks have the same average degree $\bar{k} \approx 6$. In the two cases the simulations start with a small number of randomly infected nodes, here 20.

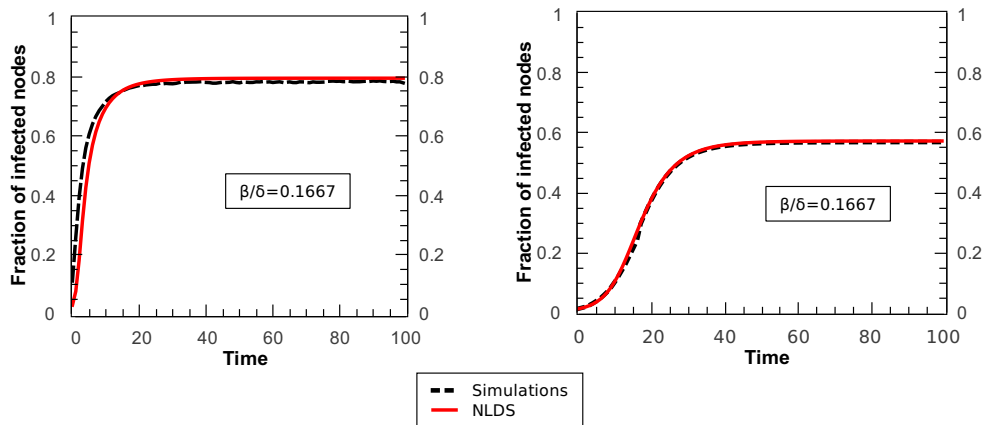


Figure 7.8: Results of the simulations (dashed lines) and NLDS (solid lines) for the Jazz musicians network (left) and for top 500 corporate directors in the USA (right). The results are averages of 100 realisations and $\beta = 0.02$, $\delta = 0.12$

in both cases the infection survives and becomes an epidemic. We can see that the spread of infection in the Jazz musicians is much faster than in the top 500 corporate directors in the USA.

Limitations of NLDS

In Chapter 6 we have seen that a node in a network can also interact with nodes that are not directly connected to it. We have illustrated this fact by providing a lot of empirical evidence. In Chapter 5 we have given a huge amount of empirical evidence about close and casual contact in networks. NLDS is limited in the sense that it can only model the spreading of infections that involve only close contacts conceptualised by the adjacency matrix. This is for instance the case of sexual transmitted diseases, or computer viruses. The adjacency matrix is just an approximation that represents contacts in a network and it cannot represent every thing or all the information relevant to the transmission of infection. As a consequence of these facts, NLDS cannot be used to model long-range transmission of diseases due to casual contacts. In Chapter 6 we have provided a model of a network that can be used to model the spreading of epidemics involving long-range interactions. We now need to extend NLDS to a generalised model, called here the Generalised Non Linear Dynamical System (GNLDS), that accounts for direct and indirect contacts. This generalised dynamic will be developed in the next chapter.

Chapter 8

Generalised Non-Linear Dynamical System (GNLDS)

8.1 Model definition of GNLDS

In this chapter we are interested in considering the case in which an infection is transmitted from one infected node to its close and casual contacts with a certain probability. Obviously, the nearest neighbours, representing close contacts in the social network of that infected node are at the highest risk to be infected. However, we consider here that every node in that network can be infected directly from that infected node as they can be casually proximal to it at a certain stage. Our assumption is that these casual contacts depend on the shortest-path distance which these nodes are from the infected node. Then, the generalised graph matrix $\Gamma(G, x)$ introduced in Chapter 6 is a natural substitution for the adjacency matrix in NLDS-MMCA, which transforms this model into a generalised one (GNLDS-MMCA), where the probability $1 - p_{i,t}$ that node i remains healthy in the network

is given by

$$1 - p_{i,t} = (1 - p_{i,t-1})\xi_{i,t}^G + \delta p_{i,t-1}\xi_{i,t}^G, \quad (8.1)$$

and now the generalised probability that node i does not receive an infection at time t , $\xi_{i,t}^G$, is given by

$$\xi_{i,t}^G = \prod_{j \sim i} (1 - \beta p_{j,t-1}) \prod_{j \not\sim i} (1 - d_{ij} x^{d_{ij}-1} \beta p_{j,t-1}). \quad (8.2)$$

The first term in this expression, which corresponds to $\xi_{i,t}$, represents the probability that a node is not infected by close contacts in the social network. The second term accounts for the probability that a node does not receive an infection from its casual contacts. Obviously, as $x \rightarrow 0$, $\xi_{i,t}^G \rightarrow \xi_{i,t}$ and $\mathbf{\Gamma}(G, x = 0) \rightarrow \mathbf{A}(G)$, which means that GNLDS-MMCA is reduced to the NLDS-MMCA model. In this context, the parameter x controls the feasibility that an infected node can transmit an infection in only one step to others that are not its close contacts. When $x = 0$ we recover the particular case of NLDS of Chapter 7. In this general case, we also make use of the independence assumption, that is probabilities $p_{j,t-1}$ are assumed to be independent from each other.

Theorem 8.1.1 Epidemic threshold under GLNDS

Let G be a connected undirected network with generalised matrix $\mathbf{\Gamma}(G, x)$. Let $\lambda_1(x) \geq \lambda_2(x) \geq \dots \geq \lambda_n(x)$ be the eigenvalues of $\mathbf{\Gamma}(G, x)$. Then, the epidemic threshold for this network by considering a conductance equal to x ($0 < x \leq 0.5$) is uniquely determined by

$$\tau = \frac{1}{\lambda_1(x)}. \quad (8.3)$$

proof 8.1.2 Equation (8.1) can be expressed as

$$\mathbf{p}_t = F(\mathbf{p}_{t-1}), \quad F : \mathbb{R}^n \rightarrow \mathbb{R}^n, \quad (8.4)$$

and where

$$F_i(\mathbf{p}_{t-1}) = 1 - (1 - p_i(t-1))\xi_{i,t}^G + \delta p_{i,t-1}\xi_{i,t}^G. \quad (8.5)$$

The infection dies out when $p_i = 0$ for all i . If $p_{i,t-1} = 0$ for all i , it follows from (8.1) and (8.2) that $p_{i,t} = 0$ and therefore $\mathbf{p} = \mathbf{0}$ is a fixed point of the system (8.5). Thus, we need to see if $\mathbf{p} = \mathbf{0}$ is an asymptotically stable fixed point in the dynamical system (8.5) and, proceeding as in [32]. According to Theorem 2.2.12, the system (8.5) is asymptotically stable at $\mathbf{p} = \mathbf{0}$ if the eigenvalues of the Jacobian $\nabla F(\mathbf{0})$ matrix (evaluated at $\mathbf{p} = \mathbf{0}$) are less than 1 in absolute value, where

$$[\nabla F(\mathbf{0})]_{i,j} = \left. \frac{\partial F_i}{\partial p_j} \right|_{\mathbf{p}=\mathbf{0}}.$$

By combining equation (8.2) and equation (8.5) we have

$$\nabla F(\mathbf{0}) = \begin{cases} \beta & \text{if } d_{ij} = 1, \\ \beta d_{ij} x^{d_{ij}-1} & \text{if } i \neq j \text{ and } d_{ij} \neq 1, \\ 1 - \delta & \text{if } d_{ij} = 1, \end{cases} \quad (8.6)$$

and by the definition of the generalised network matrix $\mathbf{\Gamma}(G, x)$ in Chapter 6 we can write,

$$\nabla F(\mathbf{0}) = \begin{cases} \beta \mathbf{\Gamma}_{ij} & \text{if } j \neq i, \\ 1 - \delta & \text{if } j = i. \end{cases} \quad (8.7)$$

Thus, we can obtain the system matrix $\mathbf{S}(x)$ of the non linear system (8.5) as

$$\mathbf{S}(x) = \nabla F(\mathbf{0}) = (1 - \delta)\mathbf{I} + \beta \mathbf{\Gamma}(G, x), \quad (8.8)$$

which describes the behaviour of the virus when it is about to die. If $\mathbf{u}_i(x)$ is an eigenvector of the generalised network matrix $\mathbf{\Gamma}(G, x)$ associated with the eigenvalue $\lambda_i(x)$ then we have

$$\begin{aligned}
 \mathbf{S}\mathbf{u}_i(x) &= [(1 - \delta)\mathbf{I} + \beta\mathbf{\Gamma}(G, x)] \mathbf{u}_i(x) \\
 &= (1 - \delta)\mathbf{u}_i(x) + \beta\mathbf{\Gamma}(G, x)\mathbf{u}_i(x) \\
 &= (1 - \delta)\mathbf{u}_i(x) + \beta\lambda_i(x)\mathbf{u}_i(x) \\
 &= (1 - \delta + \beta\lambda_i(x))\mathbf{u}_i(x).
 \end{aligned} \tag{8.9}$$

Thus

$$\lambda_{i,\mathbf{S}(x)} = 1 - \delta + \beta\lambda_i(x) \tag{8.10}$$

is an eigenvalue of the system matrix $\mathbf{S}(x)$ and where $\lambda_i(x) \equiv \lambda_{i,\mathbf{\Gamma}(x)}$ denotes the eigenvalue of $\mathbf{\Gamma}(G, x)$ and the eigenvectors of $\mathbf{S}(x)$ are the same as those for $\mathbf{\Gamma}(G, x)$. Hence, by Theorem 2.2.12 the system is asymptotically stable when

$$|\lambda_{i,\mathbf{S}(x)}| < 1 \quad \forall i, \forall x. \tag{8.11}$$

Now, since $\mathbf{\Gamma}(G, x)$ is a real symmetric matrix, (Chapter 6) its eigenvalues are real, and by (8.10), the eigenvalues of $\mathbf{S}(x)$ are real too. Also, since the network G is connected, $\mathbf{\Gamma}(G, x)$ represents the adjacency matrix of a weighted complete undirected graph, and therefore it is irreducible. Thus, $\mathbf{\Gamma}(G, x)$ is a real, symmetric, non-negative, irreducible, and square matrix. Under these conditions, the Perron-Frobenius Theorem [97] states that the largest eigenvalue $\lambda_{1,\mathbf{\Gamma}(x)}$, also called the Perron root of $\mathbf{\Gamma}(G, x)$, is positive and simple. Thus

$$\lambda_{1,\mathbf{\Gamma}(x)} = |\lambda_{1,\mathbf{\Gamma}(x)}| > \lambda_{i,\mathbf{\Gamma}(x)} \quad \forall i > 1, \forall x, \tag{8.12}$$

and

$$\lambda_{1,\mathbf{s}(x)} = |\lambda_{1,\mathbf{s}(x)}| > \lambda_{i,\mathbf{s}(x)} \quad \forall i > 1 \quad \forall x. \quad (8.13)$$

Using (8.10) and (8.11) we have

$$\lambda_{1,\mathbf{s}(x)} = 1 - \delta + \beta\lambda_{1,\mathbf{\Gamma}(x)} < 1. \quad (8.14)$$

Thus, if the epidemic dies out, we must have

$$\frac{\beta}{\delta} < \tau = \frac{1}{\lambda_{1,\mathbf{\Gamma}(x)}}. \quad (8.15)$$

In order to complete the proof of Theorem 1, we need to see that if

$$\frac{\beta}{\delta} < \tau = \frac{1}{\lambda_{1,\mathbf{\Gamma}(x)}}, \quad (8.16)$$

then the epidemic will die out over time (sufficiency of epidemic threshold).

In (8.2), since all terms β , $p_{j,t-1}$, and $d_{ij}x^{d_{ij}-1}$ are non-negative and not greater than 1,

$$\prod_{j \sim i} (1 - \beta p_{j,t-1}) \geq 1 - \beta \sum_{j \sim i} p_{j,t-1}$$

and

$$\prod_{j \not\sim i} (1 - d_{ij}x^{d_{ij}-1}\beta p_{j,t-1}) \geq 1 - \beta \sum_{j \sim i} d_{ij}x^{d_{ij}-1}p_{j,t-1}.$$

Thus,

$$\begin{aligned}\xi_{i,t}^G &\geq \left(1 - \beta \sum_{j \sim i} p_{j,t-1}\right) \left(1 - \beta \sum_{j \not\sim i} d_{ij} x^{d_{ij}-1} p_{j,t-1}\right) \\ &= 1 - \beta \sum_{j \sim i} p_{j,t-1} - \beta \sum_{j \not\sim i} d_{ij} x^{d_{ij}-1} p_{j,t-1} + \\ &+ \beta^2 \left(\sum_{j \sim i} p_{j,t-1}\right) \left(\sum_{j \not\sim i} d_{ij} x^{d_{ij}-1} p_{j,t-1}\right),\end{aligned}$$

and since

$$\beta^2 \left(\sum_{j \sim i} p_{j,t-1}\right) \left(\sum_{j \not\sim i} d_{ij} x^{d_{ij}-1} p_{j,t-1}\right) \geq 0,$$

$$\begin{aligned}\xi_{i,t}^G &\geq 1 - \beta \sum_{j \sim i} p_{j,t-1} - \beta \sum_{j \not\sim i} d_{ij} x^{d_{ij}-1} p_{j,t-1} \\ &= 1 - \beta \left(\sum_{j \sim i} p_{j,t-1} + \sum_{j \not\sim i} d_{ij} x^{d_{ij}-1} p_{j,t-1}\right) \\ &= 1 - \beta \sum_j \Gamma_{ij} p_{j,t-1}.\end{aligned}$$

Thus, from (8.1)

$$\begin{aligned}1 - p_{i,t} &= (1 - p_{i,t-1})\xi_{i,t}^G + \delta p_{i,t-1}\xi_{i,t}^G \geq \\ &\geq (1 - (1 - \delta)p_{i,t-1}) \left(1 - \beta \sum_j \Gamma_{ij} p_{j,t-1}\right) \\ &= 1 - (1 - \delta)p_{i,t-1} - \beta \sum_j \Gamma_{ij} p_{j,t-1} + \\ &+ (1 - \delta)p_{i,t-1}\beta \sum_j \Gamma_{ij} p_{j,t-1},\end{aligned}$$

and then

$$\begin{aligned}
 p_{i,t} &\leq (1 - \delta)p_{i,t-1} + \beta \sum_j \Gamma_{ij} p_{j,t-1} - \cdots \\
 &\quad - (1 - \delta)p_{i,t-1} \beta \sum_j \Gamma_{ij} p_{j,t-1}, \\
 &\leq (1 - \delta)p_{i,t-1} + \beta \sum_j \Gamma_{ij} p_{j,t-1},
 \end{aligned}$$

which can be expressed in matrix form as

$$\mathbf{p}_t \leq [(1 - \delta)\mathbf{I} + \beta\mathbf{\Gamma}(G, x)] \mathbf{p}_{t-1}, \quad (8.17)$$

which uses the same system matrix as (8.8),

$$\begin{aligned}
 \mathbf{p}_t &\leq \mathbf{S}(x)\mathbf{p}_{t-1} \leq \mathbf{S}^2(x)\mathbf{p}_{t-1} \leq \cdots \leq \mathbf{S}^t(x)\mathbf{p}_0 \\
 &\leq \sum_i \lambda_{i,\mathbf{S}(x)}^t \mathbf{u}_{i,\mathbf{S}(x)} \mathbf{u}'_{i,\mathbf{S}(x)} \mathbf{p}_0,
 \end{aligned}$$

where the last inequality is the spectral decomposition of $\mathbf{S}^t(x)$ and $\mathbf{u}'_{i,\mathbf{S}(x)}$ is the transpose of $\mathbf{u}_{i,\mathbf{S}(x)}$. By (8.10), when

$$\frac{\beta}{\delta} < \frac{1}{\lambda_{1,\mathbf{\Gamma}(x)}},$$

then

$$\lambda_{i,\mathbf{S}(x)} < 1 \quad \text{and} \quad \lambda_{i,\mathbf{S}(x)}^t \approx 0$$

for all i and large t , which makes $p_t \approx 0$ as t increases, implying that the infection dies out over time. We will make use of the following theorem which states the monotonicity property of the Perron root for non-negative and irreducible square matrices (see Theorem 1.3 in [5]).

Theorem 8.1.3 *Let \mathbf{A} and \mathbf{B} be non-negative matrices of order $n \geq 1$. If $\mathbf{A} \leq \mathbf{B}$, then the Perron roots of \mathbf{A} and \mathbf{B} satisfy the inequality*

$$\lambda_{1,\mathbf{A}} \leq \lambda_{1,\mathbf{B}}. \quad (8.18)$$

Furthermore, if \mathbf{B} is irreducible and $\mathbf{A} = \mathbf{B}$, then the inequality holds strictly:

$$\lambda_{1,\mathbf{A}} < \lambda_{1,\mathbf{B}}. \quad (8.19)$$

Corollary 8.1.4 *If $\beta/\delta > \lambda_{1,\Gamma(x_c)}$, then the infection survives and becomes an epidemic for any $x \geq x_c$ and if $\beta/\delta < \lambda_{1,\Gamma(x_c)}$, then the infection dies out for any value of the conductance $x \leq x_c$.*

proof 8.1.5 *Let $0 \leq x_1 \leq x_2$. If $d_{ij} = 1$, then $\Gamma_{ij}(x_1) = \Gamma_{ij}(x_2) = 1$, and if $d_{ij} > 1$, then*

$$\Gamma_{ij}(x_1) = d_{ij}x_1^{d_{ij}-1} < \Gamma_{ij}(x_2) = d_{ij}x_2^{d_{ij}-1}.$$

Thus

$$\Gamma_{ij}(x_1) \leq \Gamma_{ij}(x_2)$$

and the result is a direct consequence of Theorem 8.1.3.

8.2 Applications of the GNLDS-MMCA Model

8.2.1 Networks Generation

We start by analysing the accuracy of the GNLDS-MMCA model by comparing it with the results obtained from simulations in random networks. We generate random networks with Poisson degree distribution using the Erdős-Rényi (ER)

model as well as random networks with power-law degree distributions according to the Barabási-Albert (BA) model. These networks were generated by using NetworkX [9] in Python. In addition, we also generate scale-free networks having power-law degree distribution of the form $p(k) \sim k^\gamma$ for a given power exponent $1.894 \leq \gamma \leq 3$, which were generated using the algorithm described in [120].

8.2.2 Simulations

For the simulations we use the average of at least 100 individual runs that begins with a set of randomly chosen infected nodes (usually between 2.0% and 2.5% of the total number of nodes) and fixed values of the parameters β and δ and the conductance x . Simulations evolve in steps of one time unit. During each step, an infected node i attempts to infect its nearest neighbours j with probability β and also nodes that are far away with probability $d_{ij}x^{d_{ij}-1}\beta$. Every infected node is cured with probability δ . An infection attempt on an already infected node has no effect. Simulations as well as GNLDS-MMCA were implemented in C and PYTHON, and the programs are available on request.

8.2.3 Simulations and GNLDS Tests on a Path and Cycle Networks

We consider here a path and a cycle network having both the same number of nodes $n = 100$. The values of the parameters are $\beta = 0.35$ and $\delta = 0.023$ and the values of the conductance are $x = 0, 0.1, 0.2$. In Figure 8.1 we show the results of the simulations (dashed lines) and the GNLDS (solid lines) for the path network (left) and for the cycle network (right). The effect of GNLDS can be seen in the earlier stage of the epidemic and when the time increases the infection reaches the

saturation faster. The lower effect of the GNLDS in these cases can be explained by the fact that in a path network, for example, a terminal can only infect a node at shorter distances and as the distance increases the chance to infect nodes that are far away reduces. We can see here that some shortest path distances are very long and reduce the effect of long-range interactions and therefore of GNLDS. We observe the same thing in the cycle network. In fact the cycle network is just a version of a path network. For this reason there are not many differences in the results of the simulations and GNLDS for the two networks as can be seen in Figure 8.1. We now going to analyse the case of a star network.

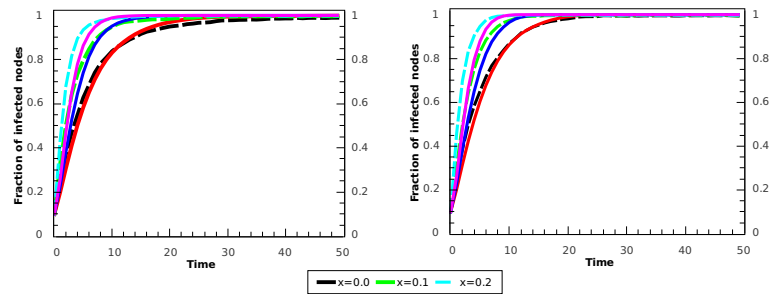


Figure 8.1: Results of the simulations (dashed lines) and the exact GNLDS-MMCA (solid lines) for a path graph (left) and cycle graph (right) with $n = 100$ nodes, where $\tau(0) = 0.5$ for both of them. Parameters in both plots are $\beta = 0.35$, $\delta = 0.0023$ and starting with about 10% of the nodes infected; since $\beta/\delta > \tau(0)$, the infection will become an epidemic for any value of the conductance x . The results are the average of 150 realizations. The values of the conductivity parameter are, from bottom to top, $x = 0, 0.1$ and 0.2 .

8.2.4 Simulations and GNLDS Tests on a Star Network

We consider now a star graph having $n = 1000$ nodes in two different cases.

- **Case 1** In this case the simulations start with a very small number of infected nodes (0.2%) and the values of the parameters are $\beta = 0.002$ and $\delta = 0.01$ with different values of the conductance x .

- **Case 2** In this case the simulations start with all the node infected (100%) and the values of the parameters are $\beta = 0.0002$ and $\delta = 0.024$ with the same values of the conductance x as in Case 1.

We have illustrated the dependence of the epidemic threshold on the conductance in Figure 8.3 for a network with a star topology. In the case of a star network we have

$$\begin{aligned}\lambda_1(x) &= x(n-1) + \sqrt{x^2(n-2)^2 + (n-1)} \\ &\geq \sqrt{n-1} = \lambda_{1,\mathbf{A}} = \lambda_1(0).\end{aligned}\tag{8.20}$$

From Figure 8.3 and from Case 1 we can see that $\beta/\delta > \tau(x)$ for all x and the epidemic survives for all conductance and becomes an epidemic. This is illustrated in Figure 8.2 (left) showing the progress of the infection. In Case 2 and from Figure 8.3 we can see that $\beta/\delta = 0.0083 < \tau(x)$ for all x and the epidemic dies out over time for any value of the conductance smaller than 0.5 as shown in Figure 8.2 (right). Note that for any $0 \leq x \leq 0.5$, we have $\mathbf{\Gamma}(G, x) \geq \mathbf{\Gamma}(G, 0) = \mathbf{A}$, and from (8.20) we can see that as the conductance parameter is increased, the network is more resistant to the elimination of the infection. That is, when there is no conductance, about 10% of the nodes remain infected at time $t = 100$. However, for $x = 0.13$ this percentage is about 30%. In summary, by Corollary 8.1.4 when $\beta/\delta > 1/\lambda_1(x = 0)$, the infection survives for any value of the conductance $x > 0$ and the number of infected nodes saturates for relatively small times as $x \rightarrow 0.5$ (Figure 8.3 left). On the other hand, when $\beta/\delta < 1/\lambda_1(x = 0.5)$ the infection dies out for any value of the conductance $x < 0.5$ (Figure 8.3 right).

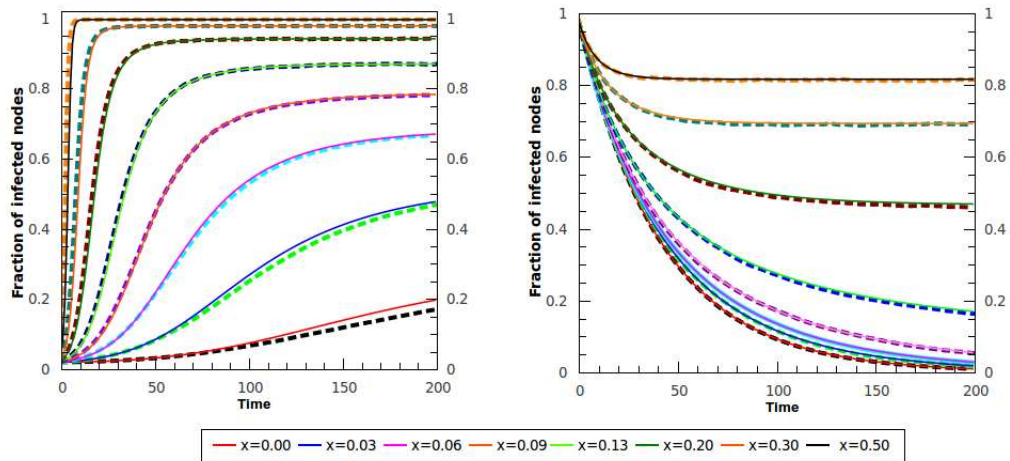


Figure 8.2: Results of the simulations (dashed lines) and the exact GNLDS-MMCA (solid lines) for a star graph with $n = 1000$ nodes, where $\tau = 1/999 \approx 0.0316$. Parameters in the left plot are $\beta = 0.002$, $\delta = 0.01$ and starting with about 20% of the nodes infected; since $\beta/\delta = 0.2 > \tau$, the infection will become an epidemic for any value of the conductance x . Parameters in the right plot are $\beta = 0.0002$ and $\delta = 0.024$; thus $\beta/\delta = 0.0083 < \tau$, and even when starting with all nodes infected, the epidemic dies out for all values of the parameter x . The results are the average of 100 realizations. The values of the conductivity parameter are, from bottom to top, 0.0, 0.03, 0.06, 0.09, 0.13, 0.20, 0.30, and 0.50.

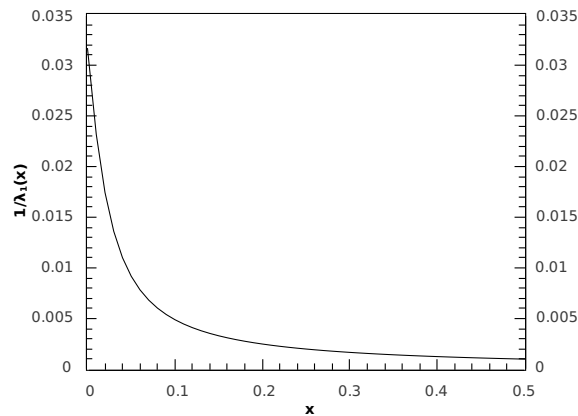


Figure 8.3: Dependence of the epidemic threshold with the conductance for a star graph having $n = 1000$ nodes.

8.3 Simulations and GNLDS Tests on ER and BA Random Networks

In the first experiment we consider an ER and a BA random network having the same number of nodes $n = 1000$ and the same average degree $\bar{k} = 6$. The values of parameters are $\beta = 0.02$ and $\delta = 0.12$ and we have to consider different values of the conductance, $x = 0.00$, $x = 0.03$, $x = 0.06$, $x = 0.09$ and $x = 0.13$. In Figure 8.4 we illustrate the results of the exact GNLDS-MMCA and the simulations for the ER and BA random networks for different values of the conductance. First

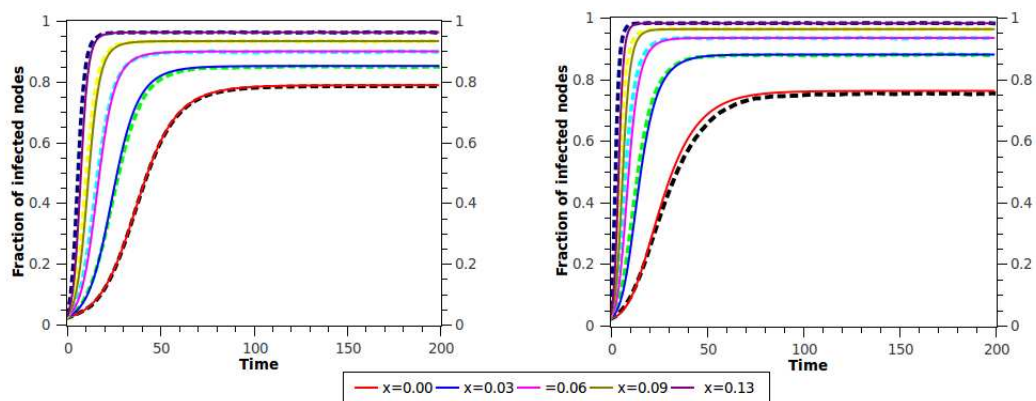


Figure 8.4: Results of the simulations (dashed lines) and the exact GNLDS-MMCA (solid lines) for (left) ER and (right) BA networks having $n = 1000$ nodes, $\bar{k} \approx 6$, with $\beta = 0.02$ and $\delta = 0.12$, and for different values of the parameter x . The results are the average of 250 realisations. The values of the conductivity parameters are, from bottom to top, 0.0, 0.03, 0.06, 0.09, and 0.13.

of all, it can be seen that the GNLDS-MMCA reproduces the results obtained by simulating the infection spread in both types of networks very well. In Table 8.1 we show the values of the largest eigenvalues $\lambda_1(x)$ and the epidemic thresholds $1/\lambda_1(x)$ for different value of the conductance for both ER and BA networks. As for both cases $\beta/\delta > 1/\lambda_1(x)$ for all x , the epidemic survives and becomes an epidemic for all x . In Figure 8.5 we illustrate a snapshot of the propagation of

ER, $\tau = \beta/\delta = 0.167$			BA, $\tau = \beta/\delta = 0.167$		
x	$\lambda_1(x)$	$1/\lambda_1(x)$	x	$\lambda_1(x)$	$1/\lambda_1(x)$
0.00	7.18	0.139	0.00	13.16	0.075
0.03	10.27	0.097	0.03	19.77	0.051
0.06	14.75	0.068	0.06	28.69	0.035
0.09	20.93	0.048	0.09	40.18	0.025
0.13	32.44	0.031	0.13	59.97	0.017

Table 8.1: Conductance x , largest eigenvalues $\lambda_1(x)$ and epidemic thresholds $1/\lambda_1(x)$ for the ER and BA random networks having $n = 1000$, $\bar{k} = 6$, $\beta = 0.02$ and $\delta = 0.12$. The threshold in the ER model is almost the double of the threshold in the BA model.

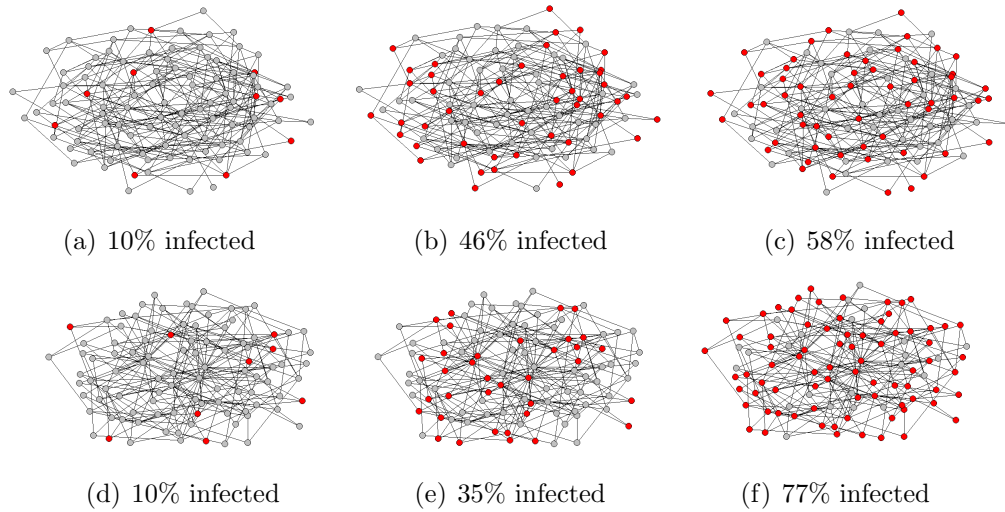


Figure 8.5: Illustration of the progress of an infection in an ER (first row) and a BA (second row) network. The first column represents the initial stage in which only 10% of the nodes are infected (marked in red) in ER and BA. In the second column we illustrate the progress of the infection for time $t = 25$ when only direct transmission is considered for both ER and BA. The last column represents the progress of the infection at the same time as before ($t = 25$) but now considering both direct and LR transmissions of the infection. Both networks have the same size ($n = 100$) and average degree ($\bar{k} = 12$). The value of the conductance for this snapshot is $x = 0.03$.

an infection in both ER (first row) and BA (second row) networks. By starting in both at $t = 0$ with 10% of randomly infected nodes (first column), at $t = 25$ there is no significant difference in the percentage of infected nodes when only

direct transmissions are considered (second column). However, as soon as LR interactions are allowed the percentage of infected nodes in the scale-free network overpasses that in the Poissonian one by about 20% at $t = 25$ (third column). We will explain in the next section why epidemics in general spread faster in BA than in ER networks.

8.3.1 Why epidemics spread faster in a BA than in an ER random networks as the conductance increases?

We will answer this question in different stages. Apart from the fact that the simulations and the GNLDS match perfectly for the values of parameters chosen, the second, and more important observation, is related to the relationship between the structure of these networks and the dynamics of the epidemic spreading. By keeping all other topological parameters identical, we can compare the effect of the degree distribution of a network on the propagation of an infection. It can be seen that the initial rate of propagation is faster in scale-free BA networks than in Poissonian ER ones. This is true for any value of the conductance. In fact, let $t_{1/2}$ be the time needed by an infection to infect 50% of the population in a given network. In Table 8.2 we show the $t_{1/2}$ for a BA and an ER network for different values of the conductance x . As can be seen, for $x = 0$, $t_{1/2} \approx 48.44$ for ER networks with 1000 nodes and average degree $\bar{k} = 6$, while it is only $t_{1/2} \approx 34.45$ for BA networks of the same size and average degree. As soon as we allow for casual contacts, that is the long-range interactions, the time needed to infect 50% of the population reduces dramatically, and it continues to be smaller for BA than for ER networks as shown in Table 8.2 or in Figure 8.6 showing the evolution of $t_{1/2}$ as a function of the conductance x . For instance, a very small increase in the conductance to $x = 0.03$ drops this time to $t_{1/2} \approx 28.36$ in ER networks and to

ER, $\tau = \beta/\delta = 0.167$		BA, $\tau = \beta/\delta = 0.167$	
x	$t_{1/2}$	x	$t_{1/2}$
0.00	48.44	0.00	34.45
0.03	28.36	0.03	16.67
0.06	18.3	0.06	13.22
0.09	13.87	0.09	7.76
0.13	8.29	0.13	5.09

Table 8.2: Time needed by an infection to infection 50% of the population for different values of the conductance, for an ER and a BA network having both $n = 1000$ nodes and $\bar{k} = 6$, $\beta = 0.02$ and $\delta = 0.12$.

$t_{1/2} \approx 15$ in BA ones. As $x \rightarrow 0.5$, the number of infected nodes in both networks tends to saturation.

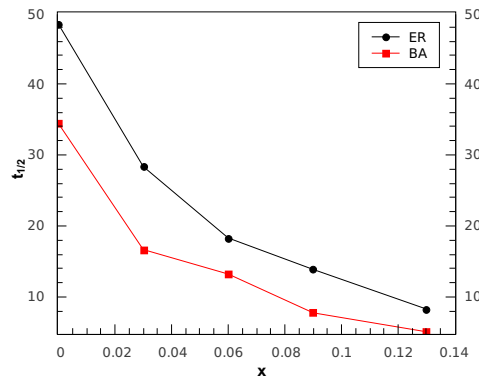


Figure 8.6: Illustration of the evolution of $t_{1/2}$ as a function of the conductance in ER and BA random networks ($n = 1000$ nodes, $\bar{k} = 6$, $\beta = 0.02$ and $\delta = 0.12$).

8.3.2 GNLDS on Regular Networks

In this section we are going to study the effect of long-range interactions on regular networks. In a regular network each node has the same number of neighbours, that is every node has the same degree. For simplicity we are going to consider regular networks having $n = 10$ nodes in which every node has degree 3. There are in total 19 regular networks with that condition (see Figure 8.7 and 8.8). The values of the

parameters are $\beta = 0.3$ and $\delta = 0.0001$. Simulations start with only one randomly infected node and were averaged over 100 realisations. As $\beta/\delta > 1/\lambda_1(0) = 3$ the infection grows and never dies out. As can be seen in Figure 8.9 and Figure 8.10, GNLDS has an effect only for short period of time and as time increases, the infection quickly reaches the saturation and GNLDS has no effect for large period of time.

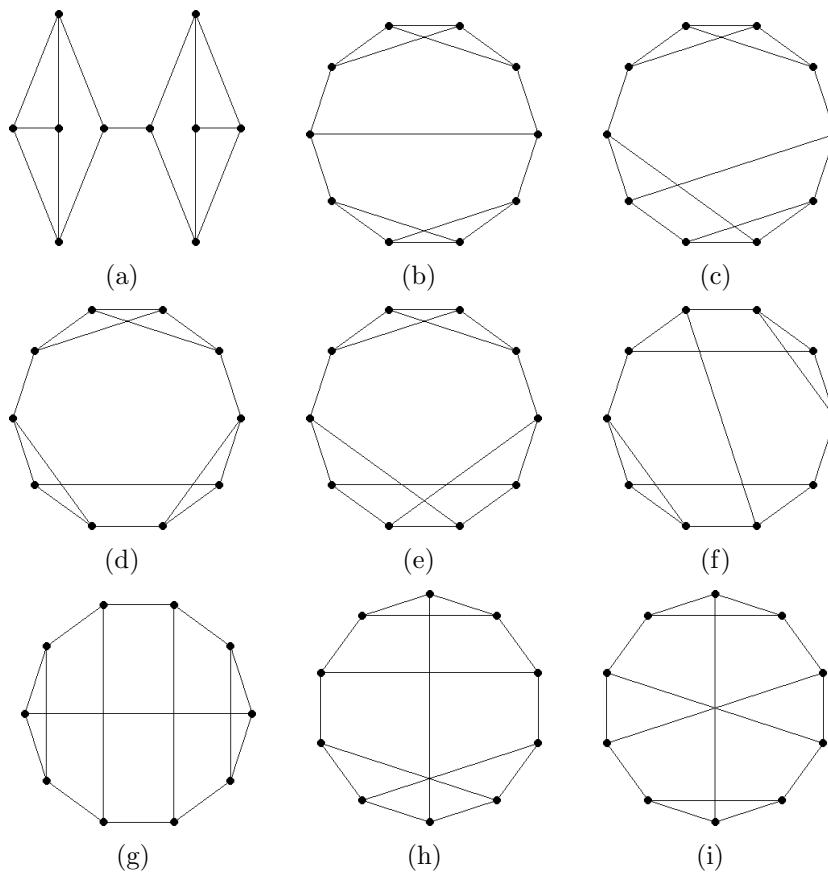


Figure 8.7: Regular Networks having $n = 10$ nodes where each node has degree 3

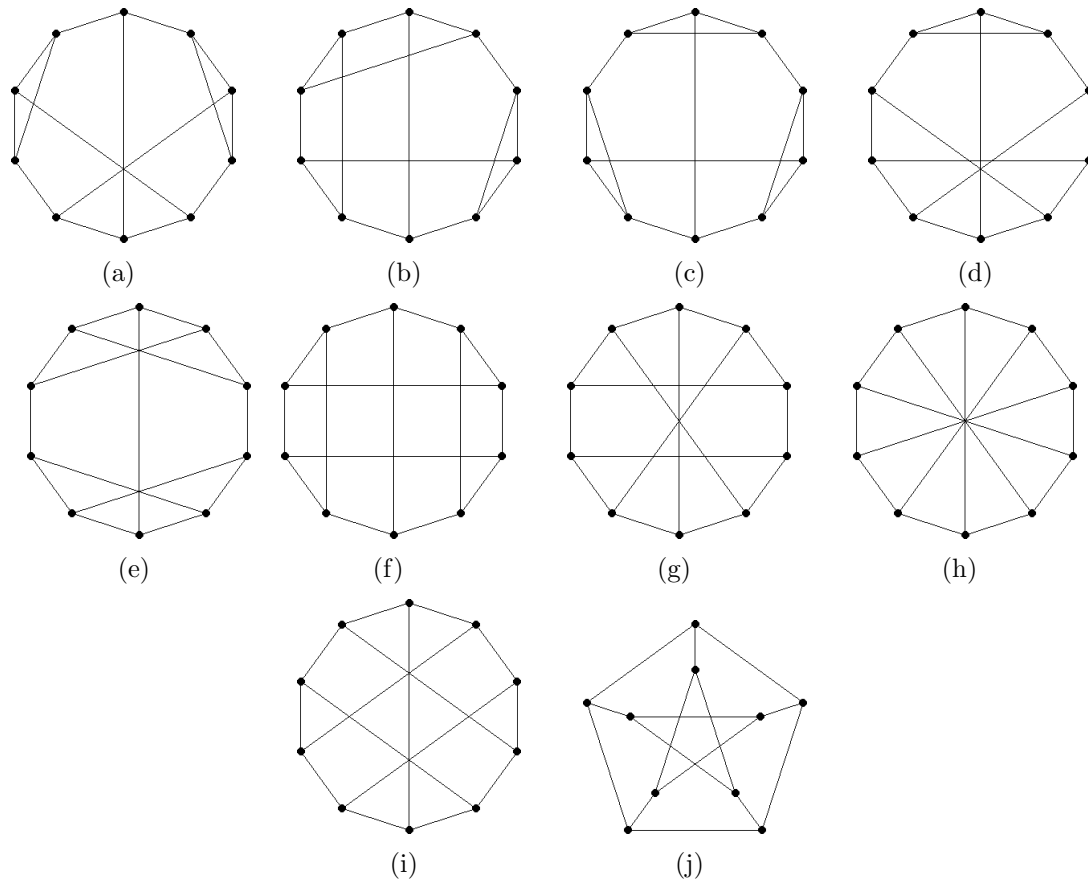


Figure 8.8: Regular Networks having $n = 10$ nodes where each node has degree 3

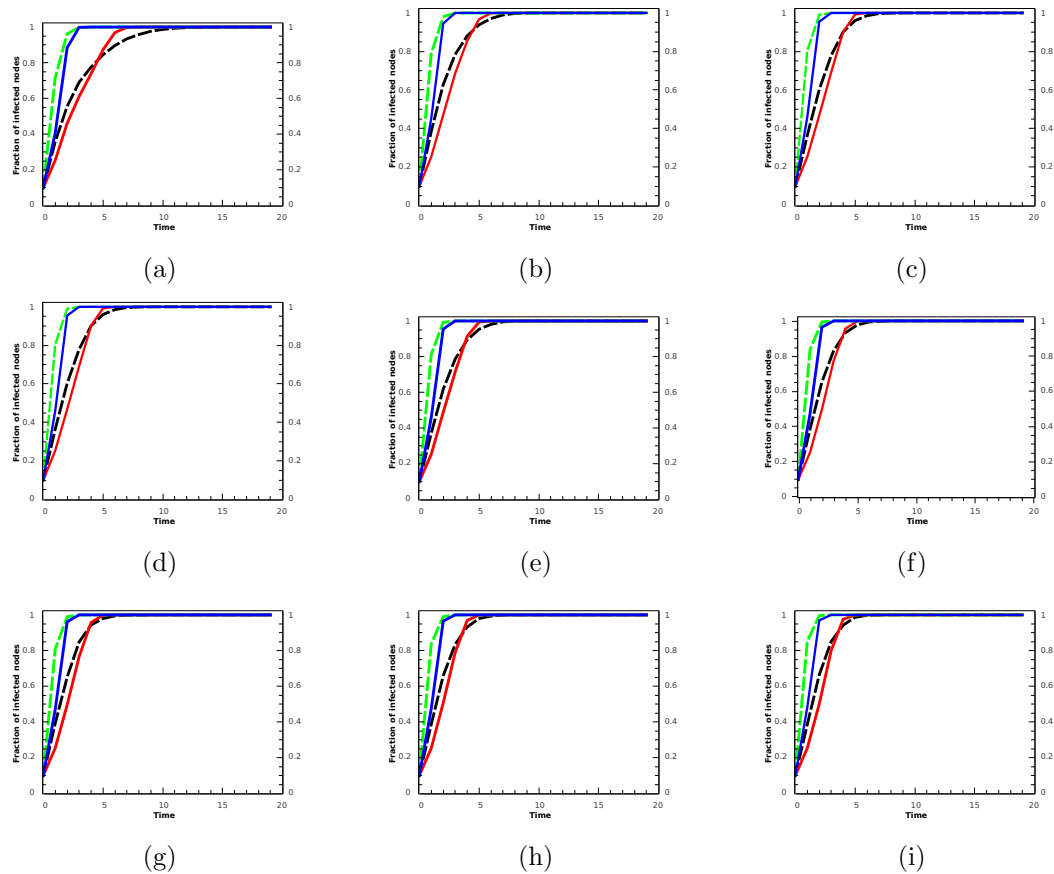


Figure 8.9: Results of the simulations (dashed lines) and the exact GNLDS-MMCA (solid lines) for the first nine regular networks of Figure 8.7 which all have $n = 10$ nodes which each have degree 3, $\beta = 0.3$ and $\delta = 0.0001$. The values of conductance parameter are, from bottom to top, 0.0, 0.3. Simulations start with only one randomly infected node and are the average of 100 realisations.

8.3.3 Influence of the Network Heterogeneity on the Spreading of Infections

In this section, we turn our attention to the influence of the network heterogeneity on the rate of epidemic spreading. Concretely, we consider the variation of the power-law exponent in the degree distribution of scale-free networks. That is, we consider networks with 1000 nodes having power-law degree distribution of the form $p(k) \sim k^{-\gamma}$, $1.89 \leq \gamma \leq 3$. In Figure 8.11 we illustrate the results obtained for

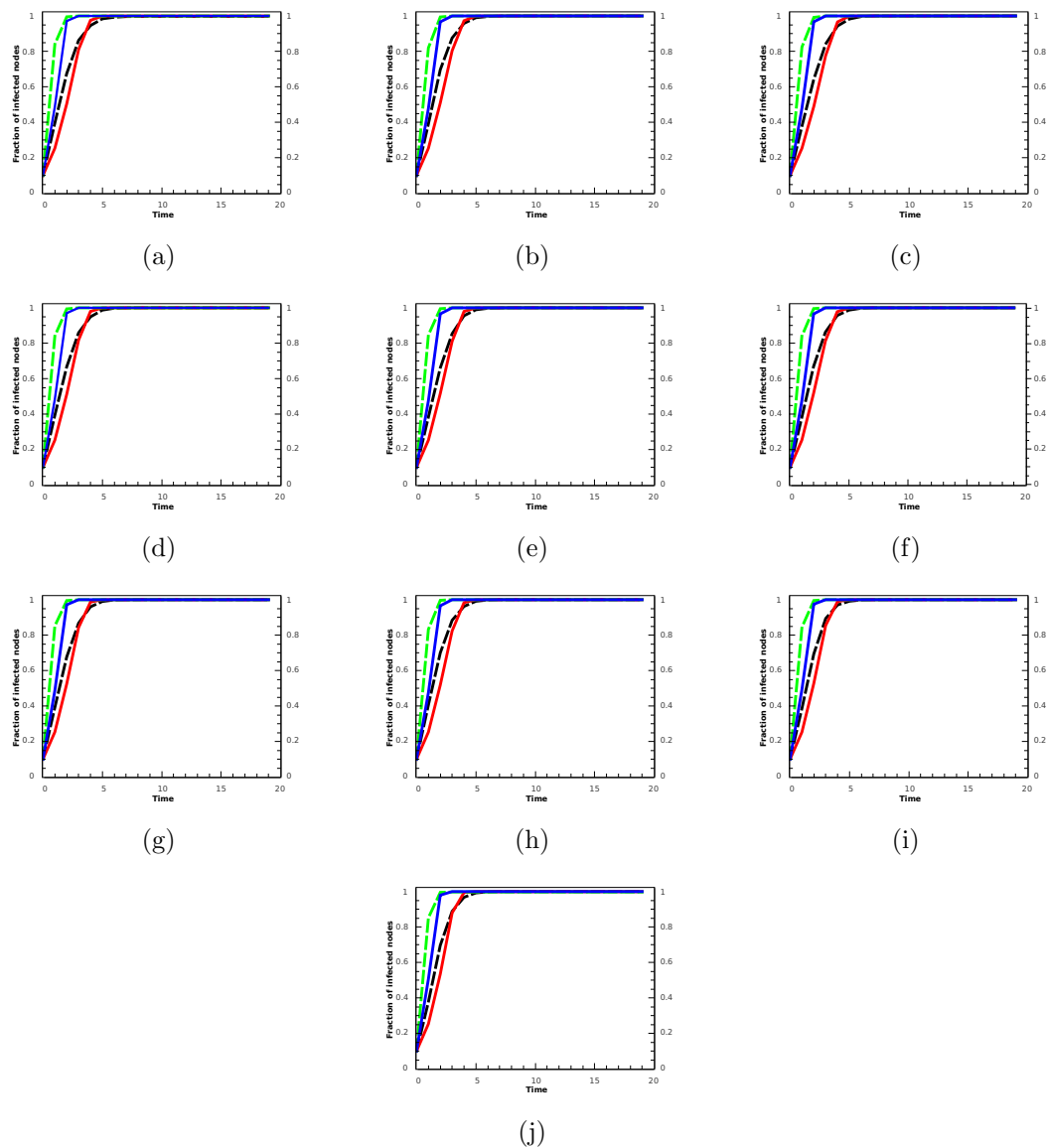


Figure 8.10: Results of the simulations (dashed lines) and the exact GNLDS-MMCA (solid lines) for the last ten regular networks of Figure 8.7 which each have $n = 10$ nodes which each have degree 3, $\beta = 0.3$ and $\delta = 0.0001$ and for two different values of the conductance. The values of the conductivity parameter are, from bottom to top, 0.0, 0.3. Simulations start with only one randomly infected node and are the average of 100 realisations.

two of these networks having $\gamma = 1.89$ and $\gamma = 1.98$. We explore different values of the conductance parameter, both by using our simulation strategy and by using the GNLDS model. In Table 8.3 we have reported the largest eigenvalues, and the

$\gamma = 1.89, \tau = \beta/\delta = 0.167$			$\gamma = 1.98, \tau = \beta/\delta = 0.167$		
x	$\lambda_1(x)$	$1/\lambda_1(x)$	x	$\lambda_1(x)$	$1/\lambda_1(x)$
0.00	46.93	0.021	0.00	39.58	0.025
0.03	65.78	0.015	0.03	55.25	0.018
0.06	96.22	0.010	0.06	78.68	0.013
0.09	132.44	0.0076	0.09	106.98	0.0093
0.13	185.90	0.0054	0.13	150.22	0.0067
0.15	214.36	0.0047	0.15	173.93	0.0057
0.20	290.038	0.0034	0.20	239.18	0.0042

Table 8.3: Conductance x , largest eigenvalues $\lambda_1(x)$, and epidemic threshold $1/\lambda_1(x)$ for two power-law distributions with $\gamma = 1.89$ and $\gamma = 1.98$, $\bar{k} = 6$, $\beta = 0.02$ and $\delta = 0.12$. The threshold for $\gamma = 1.89$ is always smaller than for $\gamma = 1.98$.

thresholds for two power-law networks having the same number of nodes $n = 1000$ and $\gamma = 1.89$, $\gamma = 1.98$ respectively and with different values of the conductance x . As $\beta/\delta > \tau = 1/\lambda_1(x)$ for all x , the infection will survive and become an epidemic. As can be seen for $x = 0$, there are no significant differences between the epidemic spreading in both networks. However, even for relatively low values of the conductance the differences between the spreading in both kinds of networks are quite significant. For instance, the networks with power-law coefficient $\gamma = 1.98$ have about 20% more nodes infected for $x = 0.03$ than when $x = 0$. A small drop of the power-law exponent to $\gamma = 1.89$ almost doubles the percentage of infected nodes for $x = 0.03$ in comparison with the network having $\gamma = 1.98$. As before we also compute the time $t_{1/2}$ needed by the epidemic to infect 50% of the population. In Figure 8.12 we have illustrated in three dimensions $t_{1/2}$ as a function of the conduction x and the power-law exponent between $1.89 \leq \gamma \leq 3$. In general, as can be seen in Figure 8.12, the rate of epidemic spreading as measured by $t_{1/2}$ increases very fast with the increase of the power-law exponent γ and decreases as the conductance x increases. Using STATISTICA, the value of $t_{1/2}$ scales as a negative exponential of the parameter x and as a power law of the exponent γ :

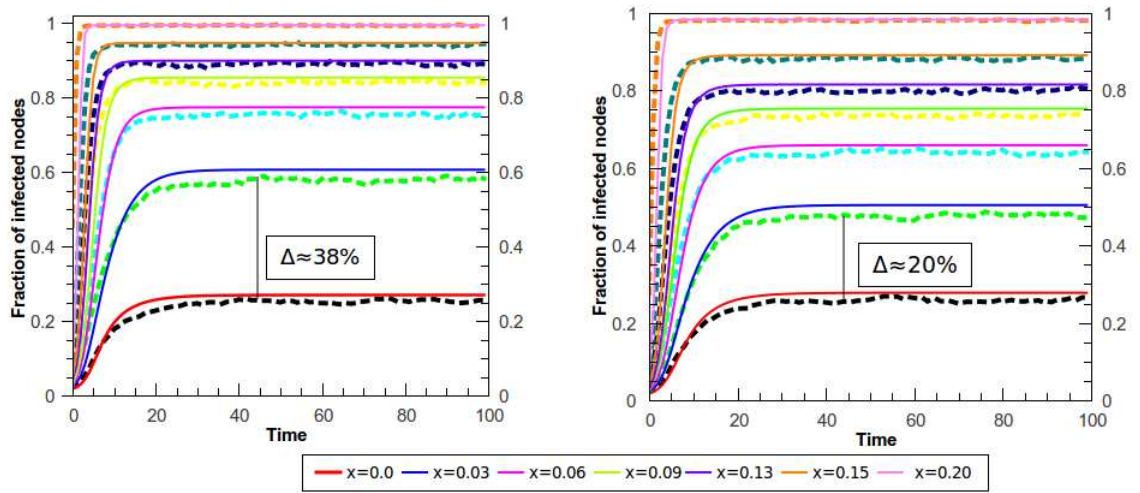


Figure 8.11: Results of the simulations (dashed lines) and the exact GNLDS-MMCA (solid lines) for networks with power-law degree distributions $p(k) \sim k^{-\gamma}$ with (left) $\gamma = 1.89$ and (right) $\gamma = 1.98$. The results are the average of 100 realisations for networks with $n = 1000$ nodes, $\beta = 0.02$, and $\delta = 0.12$ and for different values of the parameter x . The values of the conductivity parameter are, from bottom to top, 0.0, 0.03, 0.06, 0.09, 0.13, 0.15, and 0.20.

that is

$$t_{1/2}(x, \gamma) \approx 24.36 \exp(-13.58x) - 0.44\gamma^{3.38} - 10.56. \quad (8.21)$$

In other words, an epidemic spreads much faster in a network with high heterogeneous degree distribution than in one with more regularity, i.e., for small values of γ . This rate of spreading is significantly increased if casual contacts (LR interactions) are present, in which case the rate of spreading is exponentially affected by small variations of the conductance parameter.

8.4 Influence of the force of infection $d_{ij}x^{d_{ij}-1}$ in BA and ER random networks

The term $d_{ij}x^{d_{ij}-1}$ influences directly the probability with which an infection spreads through casual contacts in a network. In order to understand the basic

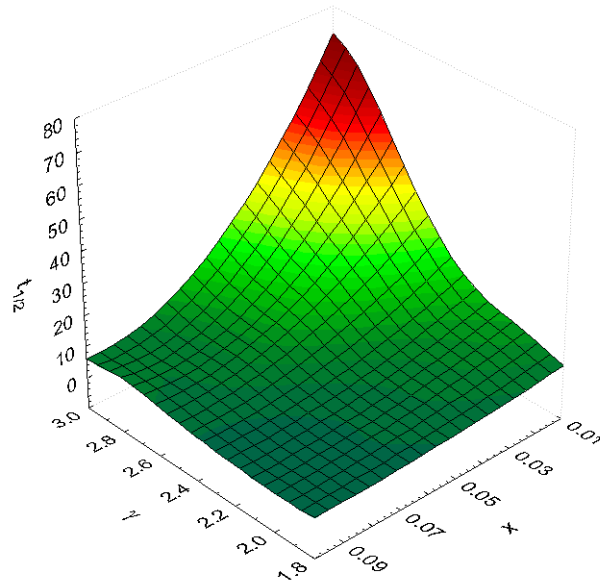


Figure 8.12: Rate of epidemic spreading measured by $t_{1/2}$, i.e., the time needed to infect 50% of the whole population, for different values of the power-law exponent γ and for different values of the conductance x .

differences between the consideration of casual contacts in the spread of epidemics in networks with Poissonian and scale-free degree distributions we start by considering how distances are distributed in both types of networks as a function of the node degrees. In Figure 8.13 we illustrate the plot of the probability of infection (infectability) $\bar{d}(k)x^{\bar{d}(k)-1}\beta$ versus k for networks with Poissonian and scale-free degree distributions. Here $\bar{d}(k)$ is the average shortest-path distance for nodes having degree k , and we use a fixed value of the parameter β . Nodes with large degree tend to have small average shortest-path distance, which means that they are closer to the rest of the nodes than nodes with low degree. Then, for a given value of $0 < x < 0.5$ the term $\bar{d}(k)x^{\bar{d}(k)-1}\beta$ is larger for smaller distances and decreases as the distance separating a pair of nodes increases. According to Section 6.4.5 of Chapter 6 these nodes of high degree participate in a large number of subgraphs of length two and they are having high subgraph centrality and high closeness centrality and high communicability centrality. Consequently, the most

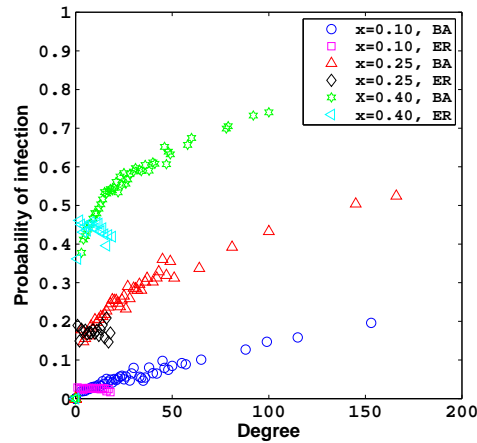


Figure 8.13: Probability of infection $\bar{d}(k)x^{\bar{d}(k)-1}$ for different values of the conductance x for BA and ER networks having the same number of nodes, $n = 1000$, and the same average degree.

connected nodes in the network display the largest infectability, which means that the probability that they are infected through casual contacts is very high. In networks with power-law degree distributions there are nodes with much higher degree than in Poissonian networks of the same size and density. Thus, these nodes are very susceptible to being infected through casual encounter transmission, and once they are infected, they can spread the infection in a very effective way, both by close and casual contact transmission. As the value of the conductance increases, the infectability is also increased as seen in Figure 8.13, which explains why in scale-free networks the infection spreads so fast when the conductance increases.

The situation occurring here in BA networks was illustrated in Chapter 6, Section 6.3.3 (Figure 6.3 (a)-(f) and Figure 6.3 (a)-(e)) where we plotted the generalised degrees of each node for different values of the conductance x . We learnt that as x increases from zero to one, at a certain point there is an inversion in the generalised degree, that is nodes of high degree become nodes of low degree and vice versa. In [80], it is pointed out that the node-node distribution of distances in SF networks have Poisson-like shapes. In fact in Figure 8.14 and Figure 8.15 we

plot the cumulative generalised degree distributions for a BA network, and as can be seen as soon as we depart from the value of $x = 0$, the distributions become Poisson-like even for small values of the conductance.

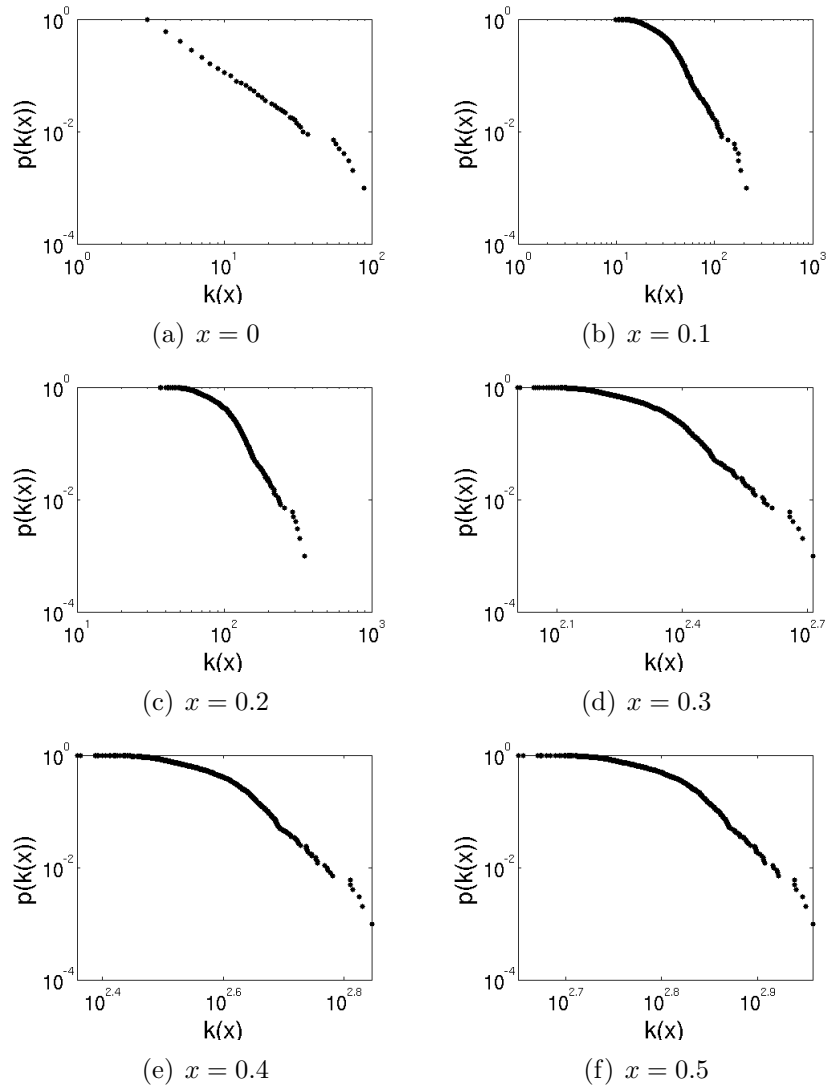


Figure 8.14: Illustration of the evolution of the cumulative degree distribution of the nodes for the network studied in Figure 6.3 and Figure 6.4 for $x = 0$, $x = 0.1$, $x = 0.2$, $x = 0.3$, $x = 0.4$ and $x = 0.5$. Notice that there is a change in the distribution from a power law at $x = 0$ to a Poissonian-like distribution as x increases.

The results illustrated in Figure 6.3 and Figure 6.4 of Chapter 6, Section 6.3.3 indicate that if we obtain the rank correlation between $k_i(x = 0)$ versus $k_i(x \neq 0)$

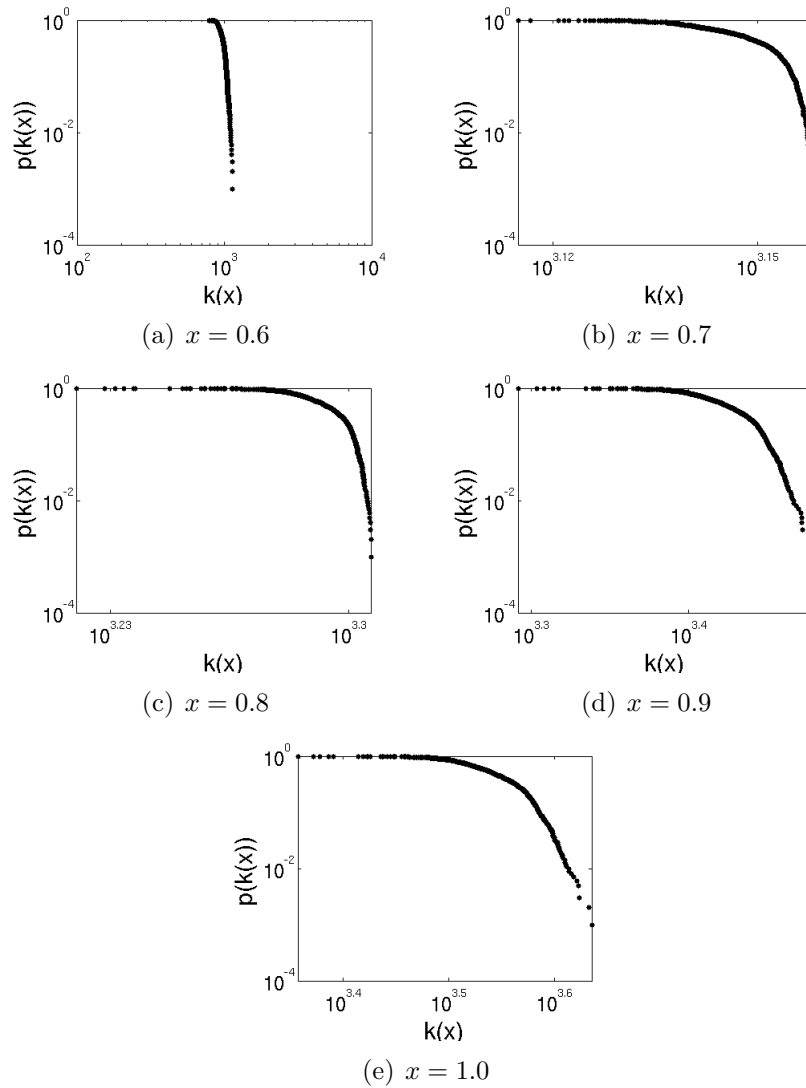


Figure 8.15: Illustration of the evolution of the cumulative degree distribution of the nodes for the network studied in Figure 6.3 and Figure 6.4 for $x = 0.6$, $x = 0.7$, $x = 0.8$, $x = 0.9$ and $x = 1$. Notice that there is a change in the distribution from a power law at $x = 0$ to a Poissonian-like distribution as x increases.

for all nodes i in the network, we will observe a point in which the initially positive correlation becomes negative. This is exactly what we observe in Figure 8.16 (left), where we plot the values of the rank correlation coefficient, measured by the Kendall τ index, versus the values of the conductivity for networks with different values of the power-law exponent γ . It is interesting to note that the value of x

at which the sign inversion occurs increases with the value of γ . That is, the more heterogeneous a network is, then the smaller the value of x at which the inversion point of the rank correlation occurs, compared to a homogeneous network. The

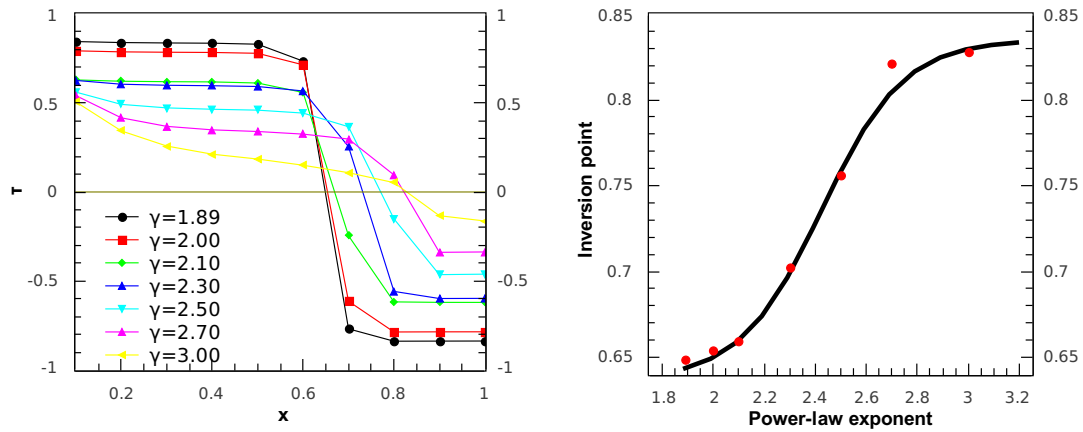


Figure 8.16: (left) Change of the rank correlation between $k_i(x = 0)$ and $k_i(x \neq 0)$ as a function of the conductance x for scale-free (SF) networks with different exponents of the power law. (Right) Scaling of the conductance at which an inversion in the rank correlation occurs as a function of the exponent of the power law in SF networks (see text for explanations).

value of x at which the inversion of the rank correlation occurs (inversion point) changes as a sigmoid function with the power-law exponent Figure 8.16 (b). More exactly, using STATISTICA, it can be expressed as

$$x_{inv} \approx 0.099 \tanh(3.123\gamma + 7.357) + 0.736. \quad (8.22)$$

All in all, these results indicate that heterogeneous networks are very sensitive to changes in the conductivity and consequently when casual contacts are included the spread of infection increases dramatically.

8.5 Epidemics Spreading in Real World Networks

We turn now our attention to the real world, where not only diseases can propagate in a network through close and casual contacts but also attitudes, fads, fashion styles, and tendencies of a different nature can use similar mechanisms of propagation. We consider here a couple of real-world networks from two different scenarios. The first one is a network of collaboration between 1265 jazz musicians in which two nodes are linked if the respective musicians have collaborated in the same band [62]. The total number of such collaborations in this network is 32358. The second network represents 1586 corporate directors of the top 500 corporations in the United States [40]. Here two nodes are connected if the corresponding directors share a position on the board of at least one corporation. In the first scenario we can think about the propagation of musical tendencies and styles in jazz, which can be diffused through the direct collaboration between musicians. In

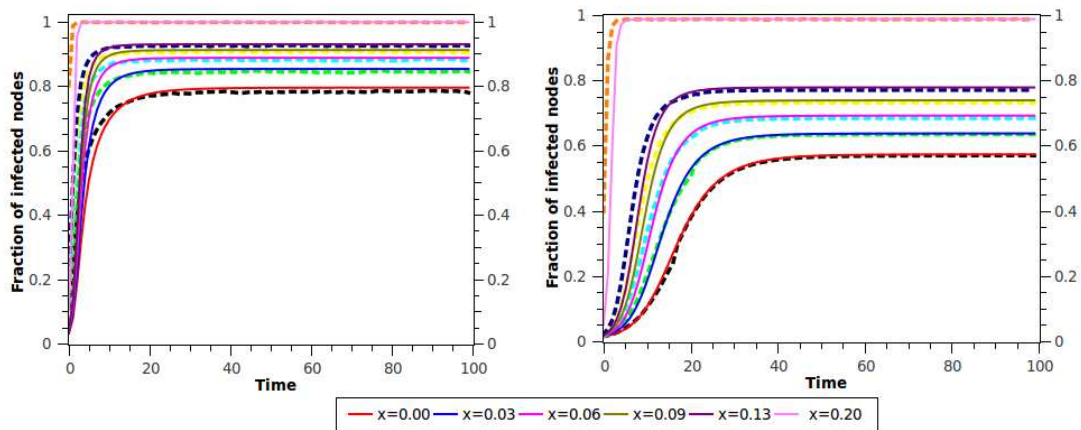


Figure 8.17: Results of the simulations and GNLDS-MMCA for the networks of collaboration among (left) jazz musicians and (right) for the corporate directors of the top 500 corporations in the United States. The results are the average of 250 realisations with $\beta = 0.02$, $\delta = 0.12$ and for different values of the conductance parameter x . The values of the conductivity parameter are, from bottom to top, 0.0, 0.03, 0.06, 0.09, 0.13, and 0.20.

addition, two musicians that have not collaborated directly in a band can influence

each other simply if they have listened to or studied their respective music. In the second scenario we can be interested in the analysis of how strategic decisions taken in one corporation can be adopted by others. Such strategies can be transmitted by those directors who share positions on the board of more than one corporation, but they can also be propagated by casual encounters of the directors. In this case casual contacts can account for the way in which some directors analyse, copy, and adapt what other directors are doing in corporations where the first are not members of the board of directors. For the network of jazz musicians, taking $\beta = 0.02$, $\delta = 0.12$ and null conductance, the infection propagates in a very fast way, infecting about 70% of the whole population for $t \geq 20$. This network has a large average degree, $\bar{k} = 50.6$, and a fat-tail degree distribution. Consequently, an infection propagates through close contacts in a very effective way due to the density of the network and the fact that each time one of the high degree nodes is infected, the infection is able to propagate to a large number of other nodes. The consideration of long-range interactions does not have a big impact on the infection spreading in this network. Here $t_{1/2} < 5$ for $x = 0$, and it is impossible to have a dramatic increase in the rate of propagation due to an increase in the conductance. However, as can be seen in Figure 8.17, the consideration of a conductance of $x = 0.13$ increases the percentage of the population infected to about 90%, and saturation is reached with small increases of this parameter. The situation is quite different for the network of the US corporate elite. First of all, the time at which 50% of the population is infected drops from $t_{1/2} \approx 40$ for $x = 0$ to $t_{1/2} \approx 7$ for $x = 0.13$. This represents a dramatic increase in the rate of propagation of attitudes among directors of the corporate elite in the United States if relatively small chances for casual contacts are allowed. In fact, the increase of the conductance up to $x = 0.13$ produces an increase of about 30% in the infected

population in comparison with the consideration of direct contagion only.

8.6 Statistical Mechanics Interpretation of the Epidemic Threshold in the GNLDS Model

Generalising the results published in [53, 54] we can have the following interpretation for the epidemic threshold in the GNLDS model. We may define the Estrada index [52] in terms of the generalised graph matrix $\mathbf{\Gamma}(x)$ in the form:

$$EE(x) = EE(G, x) = \sum_{r=0}^{\infty} \sum_{j=1}^N \lambda_j^k(x) = \sum_{j=1}^N e^{\lambda_j(x)}, \quad (8.23)$$

where $EE(G, x)$ is the generalised Estrada index. Let us consider a network in which every pair of vertices is weighted by a parameter β . Let $\mathbf{B}(x)$ be the adjacency matrix of this network. It is obvious that $\mathbf{B}(x) = \beta\mathbf{\Gamma}(x)$ and

$$\mu_r(\mathbf{B}(x)) = Tr(\mathbf{B}^r(x)) = \beta^r Tr(\mathbf{\Gamma}^r(x)) = \beta^r \mu_r(x), \quad (8.24)$$

where $Tr(\mathbf{A})$ denotes the trace of the matrix \mathbf{A} . The subgraph centrality can be generalised in the following way:

$$EE(G, \beta, x) = \sum_{r=0}^{\infty} \frac{\beta^r \mu_r(x)}{r!} = \sum_{j=1}^N e^{\beta \lambda_j(x)}. \quad (8.25)$$

Alternatively, we can write $EE(G, \beta, x)$ as follows:

$$EE(G, \beta, x) = Tr \left(\sum_{r=0}^{\infty} \frac{\beta^r \mathbf{\Gamma}^r(x)}{r!} \right) = Tr(e^{\beta \mathbf{\Gamma}(x)}). \quad (8.26)$$

Let us consider that the network is submerged into a thermal bath of temperature T . The sum of all closed walks in the network having generalised graph matrix $\Gamma(x)$ is given by:

$$Z(G, \beta, x) = Tr \left(\sum_{r=0}^{\infty} \frac{\beta^r [\Gamma(x)]^r}{r!} \right) = Tr(e^{\beta\Gamma(x)}). \quad (8.27)$$

It is straightforward to realise that this is the partition function of the complex network, where the generalised Hamiltonian is $\mathbf{H} = -\Gamma(x)$ [53, 54] and β can be considered here as the ‘strength’ of infection along the adges of the network between an infected nodes and a susceptible one and assuming that this strength is the same for all edges of the network. In term of statistical mechanics, the strength of the infection β can be related to the temperature T by the expression:

$$\beta = 1/(K_B T). \quad (8.28)$$

As we can see from Equation (8.28) the lowest the temperature the strongest the strength of infection between an infected node and a susceptible one and in this case the spreading of the infection across the network is favoured. At very large temperatures, $\beta \rightarrow 0$, the strength of the infection along edges decreases to zero and the spreading is unfavoured.

We can now define the probability p_j that the system occupies a microstate j as follows:

$$p_j(x) = \frac{e^{\beta\lambda_j(x)}}{\sum_j \beta\lambda_j(x)} = \frac{\beta\lambda_j(x)}{Z(G, \beta, z)}. \quad (8.29)$$

Based on equation (8.29) we can also define the information theoretic entropy for

the network using the Shannon expression:

$$S(G, \beta, x) = -k_B \sum_j [p_j(x)(\beta\lambda_j(x) - \ln Z)], \quad (8.30)$$

where we wrote $Z(G, \beta, x) = Z$. This expression can be written in the following equivalent way:

$$S(G, \beta, x) = -k_B\beta \sum_j \lambda_j(x)p_j(x) + k_B \ln Z \sum_j p_j(x), \quad (8.31)$$

which, by using the standard relation $F = H - TS$, immediately suggests the expressions for the total energy $H(G)$ and the Helmholtz free energy $F(G)$ of the network:

$$\begin{aligned} H(G, \beta, x) &= -\frac{1}{Z} \sum_{j=1}^n (\lambda_j(x) e^{\beta\lambda_j(x)}) \\ &= -\frac{1}{Z} \text{Tr}(\mathbf{\Gamma}(x) e^{\beta\mathbf{\Gamma}(x)}) \\ &= -\sum_{j=1}^n \lambda_j(x) p_j(x), \end{aligned} \quad (8.32)$$

and $F(G, \beta, x) = -\beta^{-1} \ln Z$. Now, let us consider the low temperature limit. The principal eigenvalue dominates the r th spectral moment of the $\mathbf{\Gamma}(x)$ matrix for large r [39]:

$$\mu_r \approx [\lambda_1(x)]^r = e^{r \ln \lambda_1(x)} \quad (r \rightarrow \infty). \quad (8.33)$$

Then, in the zero temperature limit we approximate the value of the partition function as

$$Z \approx \sum_{r=0}^{\infty} \frac{\beta^r e^{r \ln \lambda_1(x)}}{r!}, \quad (8.34)$$

for large β , or as $T \rightarrow 0$. This expression indicates that in the zero temperature

limit the system is “frozen” at the ground state configuration which has the interaction energy $-\lambda_1(x)$. Then, the total energy and Helmholtz free energy are simply reduced to the interaction energy of the network:

$$H(G, T \rightarrow 0, x) = F(G, T \rightarrow 0, x) = -\lambda_1(x). \quad (8.35)$$

Consequently, we have $S(G, T \rightarrow 0, x) = 0$ because the system is completely localised at the ground state with $p_1 \cong 1$.

As a consequence of this result we have the following interpretation of the epidemic threshold in the GNLDS model:

Theorem 8.6.1 *The epidemic threshold is the negative of the inverse of the free energy of the network when the system is frozen at extremely low temperatures, i.e.*

$$\tau = \frac{1}{\lambda_1(x)} = -\frac{1}{F(G, T \rightarrow 0, x)}. \quad (8.36)$$

8.7 Programs Developed

In this section we give some programs developed to producing some of the results in this thesis. Most of the programs developed were written in Python, C or Matlab. Most of the analysis of network structure and disease dynamics were written in Python using NetworkX or Igraph (the python version and R version). Some simulations for the NLDS and GNLDS were written in C while Matlab was used for curve fitting, solving non linear equations, plotting etc.

Python is a general-purpose, high-level programming language whose design philosophy emphasises code readability. Python claims to combine “remarkable power with very clear syntax”, and its standard library is large and comprehensive.

NetworkX (<http://networkx.lanl.gov/>) [9] is a Python language software

package for the creation, manipulation, and study of the structure, dynamics, and functions of complex networks. Igraph is another Python language software package similar to NetworkX. Igraph comes in three different versions, the Python version, the C version and the R version. I have contributed the subgraph centrality and communicability algorithms (<http://networkx.lanl.gov/reference/credits.html>) used to produce some results in section 6.4.

Python comes with many Linux machines. Apart from Python one needs to install some packages such as Scipy (scientific python equivalent to Matlab), Numpy (Numerical Python), Matplotlib (a tool for visualisation) and NetworkX and Igraph packages. For programs in C one needs to have a C compiler such as gcc or g++ or Cywin depending on whether we are under Linux or Windows.

Programs developed to produce results in Chapter 3

Program used to compute the characteristic path length and clustering coefficient in the Watt-Strogatz model. See Figure 4.2 on page 151. This program is called WS.py

WS.py

```
# This python program computes the characteristic average
# path length and average clustering coefficient in the
# Watt-Strogatz model.
# Franck KM.

from __future__ import division

import networkx as nx

import pylab as pb

N=1000
```

```
k=10
probability=[0,0.00025,0.000375,0.0005,0.000625,0.00075,0.000875,0.001,\
0.002,0.003,0.004,0.005,0.006,0.007,0.008,0.009,0.01,0.02,0.03,0.04,0.05\
,0.06,0.07,0.08,0.09,0.1,0.15,0.2,0.25,0.3,0.35,0.4,0.45,0.5,0.55,0.6,0.65,\
0.70,0.75,0.8,0.85,0.9,0.95,1]
C=[]
L=[]
niter=50 # number of iteration.
for p in prob:
    s1=0
    s2=0
    for j in range(niter):
        g2=nx.connected_watts_strogatz_graph(N, k, p)
        av=nx.average_clustering(g2)
        ap=nx.average_shortest_path_length(g2)
        s1=s1+av/niter
        s2=s2+ap/niter
    C.append(s1)
    L.append(s2)
Cp=[n/C[0] for n in C]
Lp=[n1/L[0] for n1 in L]
pb.figure(2)
pb.semilogx(prob,Cp,'s')
pb.semilogx(prob,Lp,'o')
pb.xlabel('p')
pb.show()
```

Programs developed to produce results in Chapter 6

Program developed to compute the generalised degree shown in Figure 6.3 and Figure 6.3 page 213 and page 214 and in Figure 6.5 and Figure 6.6 on page 215 and page 216. The same program can be used to compute the generalised graph matrix of any network. This program is called `gendegree.py`

`gendegree.py`

```
# This python program computes the generalised
# degree of each node for different values of the conductance.
# Franck KM.

from __future__ import division
from networkx import *
import pylab as p
import scipy

p.rcParams['legend.loc'] = 'best'
numN=1000 # number of nodes
nodes=list(range(numN)) # list of nodes

#create the barabasi albert network with n=1000 nodes and m0=3.
Gb=barabasi_albert_graph(numN,3)
# or create the Erdos-Renyi network with
# n=1000 and p=0.014 (average degree 6).
#G=gnp_random_graph(numN,0.014)
#while is_connected(G)==False:
#    G=gnp_rando_graph(numN,0.014)
#nodes=list(range(numN))
```

```

all_ones=scipy.ones((1,numN)) #column vector of 1
conductance=[0,0.02,0.05,0.1,0.4,0.5,0.6,0.63,0.65\
,0.66,0.67,0.70,0.73,0.76,0.8,0.9,1]
# setting up the Generalised Graph Matrix GGM
weigth=shortest_path_length(Gb) # single source shortest path length.
# assigning a weight  $d_{ij} * x^{(d_{ij})}$  to every edge (i,j) in G.
for x in conductance:
    weighted_edges=[] #initialise the list of edges and their weight.
    for i in range(numN):
        for j in range(numN):
            if i==j: # no loops
                continue
            weighted_edges.append((i,j,weigth[i][j]*x**(weigth[i][j]-1)))
GGM=Graph()# generalised graph matrix with no vertex and no edges
# adding to GGM weighted_edges
GGM.add_weighted_edges_from(weighted_edges) #GGN is here.
# compute the adjacency A matrix of GGM
A=adj_matrix(GGM)
# do the dot multiplication of A and
#the transpose of the vector all_ones
gendegree=scipy.dot(A,scipy.transpose(all_ones))
# plot the vector gendegree against the list of nodes
p.figure(conductance.index(x))
p.plot(nodes,gendegree,'.')
#visualise the plots.
p.show()

```

Program used to do the random rewiring and the deterministic rewiring and compute the age assortativity measure in both cases to produce Figure 6.25 and Figure 6.26 on page 243 and page 245. This program is called `assorm.py`

assorm.py

```
# This program does the deterministic rewiring in PART 1.
# It is a modification of the random rewiring of
# the Watts-Strogatz model, see program WS.py
# In PART2 for random rewiring we just use the function
# connected_watts_strogatz_graph(n,k,p) provided
# by the package NETWORKX in PYTHON.
# Franck KM

from __future__ import division

import random

import scipy

import pylab as plb

import networkx as nx

import itertools

pb.rcParams['legend.loc'] = 'best'

Num=1000 # number of node

nodes=list(range(Num)) # list of node

k=4

ninter =20 # number of iterations

# generating a regular ring of 1000 nodes each
# having 4 nearest neighbours

G=nx.connected_watts_strogatz_graph(Num,k,0)
```

```
#####
# PART 1 deterministic rewiring
#####
# setting up the age list between 0 and 75.
age=scipy.zeros((Num,1)) # all_zeros vector
age[0]=0 # first node is assigned age 0
for i in nodes:
    age[i]=age[i-1]+(75/(Num-1)) # age of node i
age=age.ravel() # one dimensional age vector
# assign node attributes, i.e. assign to each node i of G its age
for i in nodes:
    G.node[i]['age']=int(age[i])
Cx=[] # initialising average clustering coefficient list
Lx=[] # initialising average shortest path length list
Ax=[] # initialising age assortativity measure list
conductance =[0,0.1,0.2,0.3,0.4,0.5,0.6,0.7,0.8,0.9,1]
for x in conductance:
    s1=0
    s2=0
    s3=0
    for r in range(niter):
        H=G.copy() # make a copy of G for each iteration
        for j in range(1, k// 2+1):
            targets = nodes[j:]+nodes[0:j]
            for u,v in zip(nodes,targets): # for every edge (u,v) in G
                w=random.choice(nodes) # choose a random node
```

```

d=nx.shortest_path_length(H,source=u,target=w)
if d==0 or d==1:
    continue
if random.random() < d*x**(d-1):
    H.add_edge(u,w)
    H.remove_edge(u,v)
av=nx.average_clustering(H)
ap=nx.average_shortest_path_length(H)
s2=s2+av/niter
s3=s3+ap/niter
# computing the age assortativity measure
for e in H.edges_iter():
    s1=s1+((H.node[e[0]]['age']- H.node[e[1]]['age'])**2)/niter
Ax.append(s1)
Cx.append(s2)
Lx.append(s3)
Cxn=[n/Cx[0] for n in Cx] # normalising
Lxn=[n/Lx[0] for n in Lx] # normalising
#####
# PART2 RANDOM REWIRING
#####
Cp=[] # initialising average clustering coefficient list
Lp=[] # initialising average shortest path length list
Ap=[] # initialising age assortativity measure list
probability =[0,0.1,0.2,0.3,0.4,0.5,0.6,0.7,0.8,0.9,1]
for p in probability:

```

```

s1p=0
s2p=0
s3p=0
for r in range(niter):
    Gp=nx.connected_watts_strogatz_graph(Num,k,p)
    av1=nx.average_clustering(Gp)
    ap1=nx.average_shortest_path_length(Gp)
    s2p=s2p+av1/niter
    s3p=s3p+ap1/niter
    # computing the age assortativity measure
    for e in Gp.edges_iter():
        s1p=s1p+((Gp.node[e[0]]['age']- Gp.node[e[1]]['age'])**2)/niter
    Ap.append(s1p)
    Cp.append(s2p)
    Lp.append(s3p)
Cpn=[n/Cp[0] for n in Cp] # normalising
Lpn=[n/Lp[0] for n in Lp] # normalising
plb.plot(prob,Cpn,'o-',prob,Lxn,'s-')
plb.plot(conductance,Ax,'o-',prob,Ap,'s-')
pb.show() # visualise

```

Programs developed to produce results in Chapter 7

Program developed for the NLDS and GNLDS in Python used for the simulation of the spread of disease in networks. This program is called GNLDS.py

GNLDS.py

```
# This program does the simulation
# and computes the results of the
# GNLDS. Both results of the
# GNLDS and simulation are written
# to a file GNLDS-SIMUL.txt
# and the program does plot the
# results. When x=0 this program
# is simply the NLDS.
# Franck KM

from __future__ import division
from numpy import array as ar
from networkx import *
import pylab as p
import random as rd
import scipy
import numpy as np

p.rcParams['legend.loc'] = 'best'
kate=file('GNLDS-SIMUL.txt','w')

DODYN=1

Num=1000

m0=3

beta=0.35

delta=0.023

T=100

niter=60
```

```
conductance=[0,0.1,0.2]

nodes=list(range(numN)) # list of nodes

G=barabasi_albert_graph(numN,m0) # BA graph

ininf =10 # initial number of infected nodes

# we start with a small number of infected.
# if state = '0' then we only infected few
# nodes and if state = '1' then we infect all nodes.

state ='0' # we infect only a few nodes randomly

# setting up the Generalised Gamma Matrix GGM
# as in the program assorm.py
weight=shortest_path_length(G1)
weighted_edges=[]

for i in range(numN):
    for j in range(numN):
        if i==j:
            continue
        weighted_edges.append((i,j,weight[i][j]))

GGM=Graph()

GGM.add_weighted_edges_from(weighted_edges) # Gamma Matrix.

# this function initialises the state of each node,
# infected (set to 1) or susceptible (set to 0)

def initialisation():

    global N, pit, nodes, ininf
```

```
pit=scipy.zeros((1,numN)).ravel()
N=scipy.zeros((1,numN)).ravel()
if state == '0': #infect few nodes
    infected=0
    infected_node=[]
    for i in range(ininf):
        w=rd.choice(nodes)
        while w in infected_node:
            w=rd.choice(nodes)
        infected_node.append(w)
        N[w]=1
        pit[w]=1
        infected = infected+1
else:
    for i in nodes: # infected all nodes
        N[i] = 1
        pit[i] = 1
    infected = numN
return infected
for x in conductance:
    SUMSIMUL=scipy.zeros((1,T)).ravel() # initialise simulation cumul to 0
    SUMGNLDS=scipy.zeros((1,T)).ravel() # initialise GNLDS cumul to 0
    for r in range(niter):
        SIMUL=scipy.zeros((1,T)).ravel()
        GNLDS=scipy.zeros((1,T)).ravel()
        if DODYN:
```

```

numinf = initialisation()
SIMUL[0]=GNLDS[0]=numinf
if DODYN:
    zeta=scipy.ones((1,numN)).ravel()
for t in range(1,T):
    if(numinf==0 and DODYN==0):
        print t, numinf
        continue
    if numinf:
        for i in range(numN):
            if (N[i]!=0) and (rd.random() < delta):
                N[i]=0
                numinf=numinf-1
        for n in nodes:
            if G[n].keys()==[]:
                continue
            for v in G[n].keys():
                if DODYN:
                    d=G[n][v]['weight']
                    zeta[n]=(1-d*x**(d-1)*beta*pit[v])*zeta[n]
                    zeta[v]=(1-d*x**(d-1)*beta*pit[n])*zeta[v]
            if numinf:
                if(N[n]-N[v]==0):
                    continue
                if rd.random() < d*x**(d-1)*beta:
                    if(N[n]):

```

```

                                N[v]=1
                                else:
                                N[n]=1
                                numinf=numinf+1

                                SIMUL[t]=numinf
                                if DODYN:
                                    expinf=0
                                    for i in range(numN):
                                        pit[i]=1-(1-(1-delta)*pit[i])*zeta[i]
                                        expinf=expinf+pit[i]

                                GNLDS[t]=expinf

                                SUMSIMUL=SUMSIMUL+SIMUL/niter
                                SUMGNLDS=SUMGNLDS+GNLDS/niter

                                for i in range(T):
                                    print >> kate, SUMSIMUL[i]/numN,# print simulations to file GNLDS-SIMUL
                                print >> kate, ''
                                for i in range(T):
                                    print >> kate, SUMGNLDS[i]/numN,# print GNLDS to file GNLDS-SIMUL
                                print >> kate, ''
                                p.plot(range(T),SUMSIMUL/numN,'.-',range(T),SUMGNLDS/numN,'*-')
                                p.ylim(0,1.04)
                                p.show()
                                kate.close()

```

Often simulations under python take more time to complete for large networks, here is the equivalent of GNLDS.py written in C. The program is called GNLDS.c

GNLDS.c

```
#include <stdio.h>
#include <stdlib.h>
#include <math.h>
#include <time.h>
#include <sys/time.h>
#include <iostream>
#include <algorithm>
#define DO_DYN_SYSTEM 1
using namespace std;
int numN;
FILE *fp;
int *N;
int T;
double b,d;
double *pit, *zeta, *SIMUL, *SUMSIMUL, *GNLDS, *SUMGNLDS,*p;
// conductance array having 5 elements
double conductance[5]={0.0,0.03,0.06,0.09,0.13};
int nn=5;
float SIMULRESULTS[100][6];
float GNLDSRESULTS[100][6];
int niter=2; // number of iterations
int NN=100; // number of nodes
int state=0;
// if state = 0 we infecte only few node
// if state = 1 we infecte all the nodes
```

```
int ininf=15; // initial number of infected node
main(int argc, char **argv){
int t,i,j,k,m,from,to,seed,numinf,node;
double tmp,expinf,x;
float weight;
int *p;
//double time_start = get_time();

if(argc != 6){
printf("Usage: %s <numnodes> <edgefile> <timesteps> <beta> <delta>\n",argv[0]);
printf("Graph is considered undirected\n");
exit(1);
}
numN = atoi(argv[1]);
if(!(fp=fopen(argv[2],"r"))){ fprintf(stderr,"Cannot open %s\n",argv[2]);exit(1);}
T = atoi(argv[3]);
b = atof(argv[4]);
d = atof(argv[5]);
srand(seed);
srand ( time(NULL) );

for(i=0;i<T;i++){SIMULRESULTS[i][0]=(float)i;GNLDSRESULTS[i][0]=(float)i;}

for(k=0;k<nn;k++){
x=conductance[k];
//cout <<x<<"\n";
```

```
SUMSIMUL=(double*)calloc(T, sizeof(double));
SUMGNLDS=(double*)calloc(T, sizeof(double));

int *p;

for(m=1;m<=niter;m++){
SIMUL=(double*)calloc(T, sizeof(double));
GNLDS=(double*)calloc(T, sizeof(double));
zeta=(double*)calloc(numN, sizeof(double));
N = (int*)calloc(numN, sizeof(int));
pit = (double*)calloc(numN, sizeof(double));

if (state==0){
numinf= 0;

int index[15]={};
for(i=0;i<15;i++){index[i]=-1;}

for(i=0;i<15;i++){
node=rand() % NN;
p = find(index,index+15,node);
if (p == index+15){
index[i] = node;
N[index[i]]=1;
pit[index[i]]=1;
numinf=numinf+1;
}
```

```
}  
else --i;  
}  
}  
  
else{  
for(i=1;i<=NN;i++){  
N[i]=1;  
pit[i]=1;  
numinf = NN;  
}  
}  
  
SIMUL[0]=(float)numinf;  
GNLDS[0]=(float)numinf;  
  
for(t=1;t<T;t++){  
if(!numinf && !DO_DYN_SYSTEM){  
printf("%d %d\n",t,numinf);  
continue;  
}  
if(numinf){  
for(i=0;i<numN;i++){  
if(N[i] && 1.0*rand()/(RAND_MAX+1.0)<d){  
N[i]=0; numinf--;  
}  
}
```

```

}
}
if(DO_DYN_SYSTEM)
for(i=0;i<numN;i++) {
zeta[i] = 1.0;
//cout<<zeta[i]<<endl;
}
fseek(fp,0,SEEK_SET);
while(fscanf(fp,"%d %d %g",&from,&to,&weight) == 3){
if(DO_DYN_SYSTEM){
if((x==0.0) && (weight==1)){
zeta[from] *= (1-b*pit[to]);
zeta[to] *= (1-b*pit[from]);}
if((x!=0.0) && (weight >=1)){
zeta[from] *= (1-weight*pow(x,weight-1)*b*pit[to]);
zeta[to] *= (1-weight*pow(x,weight-1)*b*pit[from]);}
}
}
if(numinf){
    if((x==0.0) && (weight==1)){
if(N[from]-N[to] == 0) continue; /* both inf/uninf */
if((double)rand()/((double)RAND_MAX+1) < b){
if(N[from]) N[to] = 1;
else N[from] = 1;
numinf++;
}
}
}

```

```
}  
}  
if(numinf){  
  
    if((x!=0.0) && (weight >=1)){  
        if(N[from]-N[to] == 0) continue; /* both inf/uninf */  
        if((double)rand()/((double)RAND_MAX+1) < weight*pow(x,weight-1)*b){  
            if(N[from]) N[to] = 1;  
            else N[from] = 1;  
            numinf++;  
        }  
    }  
}  
}  
}  
if(DO_DYN_SYSTEM){  
    expinf = 0.0;  
    for(i=0;i<numN;i++){  
        pit[i] = 1-(1-(1-d)*pit[i])*zeta[i];  
        expinf += pit[i];  
    }  
}  
SIMUL[t]=numinf;  
GNLDS[t]=expinf;  
}  
for (t=0;t<T;t++)  
{SUMSIMUL[t]=SUMSIMUL[t]+SIMUL[t]/niter;
```

```
SUMGNLDS[t]=SUMGNLDS[t]+GNLDS[t]/niter;
}
}
for(t=0;t<T;t++){
SIMULRESULTS[t][k+1]=SUMSIMUL[t]/NN;
GNLDSRESULTS[t][k+1]=SUMGNLDS[t]/NN;
}

}
for(i=0;i<T;i++){
for(j=0;j<nn+1;j++){
printf("%g ",SIMULRESULTS[i][j]);
}
printf("\n");
}

for(i=0;i<T;i++){
for(j=0;j<nn+1;j++){
printf("%g ",GNLDSRESULTS[i][j]);
}
printf("\n");
}

//double time_end = get_time();
//printf("Code took %f seconds.\n", time_end - time_start);
}
```

Programs developed to compute the generalised closeness centralities of nodes in Chapter 6

The program is named closenessx.py

8.7.1 closenessx.py

```
# This python program computes
# the closeness centrality of
# each node for different
# values of the conductance.
# Franck KM.

from __future__ import division
from numpy import array as ar
from networkx import *
import pylab as p
import random as rd
import scipy
import numpy as np

p.rcParams['legend.loc'] = 'best'
numN=100

G1=barabasi_albert_graph(numN,3)
#or for an Erdos-Renyi random graph
#issue the following commands
#G=gnp_random_graph(1000,0.014)
#while is_connected(G)==False:
#    G=gnp_rando_graph(1000,0.014)
```

```
d=scipy.ones((1,numN))# all one column vector
conductance=[0,0.02,0.05,0.1,0.4,0.5,0.6,0.63,0.65,\
             0.66,0.67,0.70,0.73,0.76,0.8,0.9,1]
nodes=list(range(numN))
weight=shortest_path_length(G1)
for x in conductance:
    weighted_edges=[]
    for i in range(numN):
        for j in range(numN):
            if i==j:
                continue
            weighted_edges.append((i,j,weight[i][j]*x**(weight[i][j]-1)))
G=Graph()
G.add_weighted_edges_from(weighted_edges)
A=adj_matrix(G)
cl=scipy.dot(A,scipy.transpose(d))
clr=scipy.array(cl)
clrn=1/f1 # closeness
p.figure(conducx.index(x))
p.plot(range(numN),clrn,'o')
p.show()
```

Chapter 9

Conclusion

We have proposed a way for accounting for the social contacts among individuals by considering that casual contacts can be inferred from the network of close contacts. We based our model on a series of empirical observations made in the epidemiological and social science literature. We model such casual contacts by means of the probability that two nonconnected individuals in a close contact social network have of creating a new link between them. Then, we use the principle that new social ties are created on the basis of the future value of this relationship to infer the casual contacts among individuals. In this model, casual contacts are created on the basis of long-range interactions as a function of the social distance between two individuals, while close contacts are assumed to be determined by the links in the social network. This approach is then integrated in an epidemic spreading model such as the NLDS-MMCA model. In this case we observe that there are two main factors influencing the rate of propagation of an epidemic in a complex network when both close and casual interactions are considered. The first one is the conductance parameter, which controls how feasible casual contacts are by means of LR interactions. If this conductance is set to zero, there is no possibil-

ity of contagion through casual contacts, and everything happens only by means of the close contacts among individuals, such as in the case of sexually transmitted diseases or computer viruses. As the conductance parameter increases, the rate of propagation increases dramatically, and the infection is less likely to die out. In these cases the number of infected nodes saturates in relatively short times after the initiation of the propagation. The second factor influencing the propagation is the heterogeneity of the network. It has been observed that epidemics are propagated much faster in scale-free networks than in more regular ones. Furthermore, in scale-free networks the influence of the conductance parameter on the propagation is significantly more marked than in networks with Poissonian degree distributions. All in all, an infection propagates very quickly in heterogeneous networks when the number of casual contacts is large, making the infections easily become epidemics with high resistance to dying out. As we have shown here, GNLDs-MMCA can be a useful tool for understanding important problems in modern societies, ranging from viral epidemics to the propagation of attitudes and consumer styles.

We have extended several key concepts of graph theory in the framework of the generalised graph matrix and studied the influence of the conductance on these concepts too. These include, for instance, the generalised degree or the generalised centrality. We have shown that the generalised centrality increases with the conductance of the medium. We observed an inversion in the degree centrality of nodes as the conductance increases. Nodes of high degree becoming nodes of low degree and vice-versa. That is, there is a point (the inversion point) where the rank correlation coefficients between centrality and generalised centrality change sign going from positive values to negative values as the conductance increases. The inversion point is reached earlier in the heterogeneous networks than in homogeneous networks with the same number of nodes and same average degree. In

power-law networks, the inversion point is increasing with the conductance. The same kind of inversion was observed when studying the effect or the influence of the conductance on the closeness centrality, subgraph centrality, communicability centrality and betweenness centrality. Extending the Estrada Index in the framework of the generalised network matrix, and using its statistical mechanical interpretation we established at the very end of this thesis that the epidemic threshold in the GNLDs is the negative inverse of the free energy of the network when it is frozen at extremely low temperature.

We have developed several codes in this thesis and we have provided at the end of Chapter 8 some of the most important codes that we used to produce some of the results in this thesis. These codes can be copied and used free of charge.

9.1 Future Work

The results in this thesis provide a strong foundation for future work. A number of chapters provide several research directions. The concept of long range interactions outlined and developed in this thesis can be extended to other areas of complex networks, such as the consensus process [98], the synchronisation process [8], the diffusion process [93], random walks on networks [93] and the resistance network [52], etc.

In the second part of the thesis we extended concepts of centrality measures in the framework of the generalised graph matrix. We have studied the influence of the conductance of the medium on those measures. Physical interpretations, both classical and quantum, of various communicability functions have been gained in [55], by considering a network as a system of coupled oscillators. A new line of research will be the generalisation of concepts in [55] by the use of the generalised

graph matrix.

In Chapter 8 we have introduced a connection between the epidemic threshold in GNLDS and statistical mechanical functions. The epidemic threshold is seen as the negative inverse of the free energy of the network when it is frozen at a very low temperature. We have not yet established the connection between the GNLDS and statistical mechanics. Another line of research will be the interpretation of the GNLDS (or the NLDS when $x = 0$) in terms of statistical mechanical functions.

Bibliography

- [1] J. Abello, A. Buchsbaum, and J. Westbrook. A functional approach to external graph algorithms. *Lect. Notes Comput. Sci.*, 1461:332–343, 1998.
- [2] A. Agrawal, D. Kapur, and J. McHale. How do spatial and social proximity influence knowledge flows? evidence from patent data. *J. Urban Econ.*, 64:258–269, 2008.
- [3] R. Albert and A.-L. Barabási. Statistical mechanics of complex networks. *Rev. Mod. Phys.*, 74:47–97, 2002.
- [4] R. Albert, H. Jeong, and A.-L. Barabási. Error and attack tolerance in complex networks. *Nature*, 406:378, 2000.
- [5] Y. Alpin and L. Kolotilina. The generalized monotonicity property of the perron root. *J. Math. Sci.*, 141:1576–1585, 2007. 10.1007/s10958-007-0066-9.
- [6] R. M. Anderson and R. M. May. *Infectious diseases of humans: Dynamics and control*. Oxford University Press, Oxford, 2002.
- [7] H. Anton. *Elementary Linear Algebra*. John Wiley and Sons, Inc., USA, 7th edition, 1994.
- [8] A. Arenas, A. Daz-Guilera, J. Kurths, Y. Moreno, and C. Zhou. Synchronization in complex networks. *Physics Reports*, 469(3):93 – 153, 2008.

- [9] A. H. Aric, A. S. Daniel, and J. S. Pieter. *Exploring Network Structure, Dynamics, and Function using NetworkX*. Proceedings of the 7th Python in Science Conference (SciPy2008), Gel Varoquaux, Travis Vaught, and Jarrod Millman (Eds), Pasadena, CA USA, 2008.
- [10] N. Bailey. *The mathematical Theory of Infectious Diseases and its Applications*. Griffin, London, 1975.
- [11] V. Bala and S. Goyal. A noncooperative model of network formation. *The Econometric Society*, 68(5):1181 – 1229, 2000.
- [12] D. Balcan, V. Colizza, B. Goncalves, H. Hu, J. Ramasco, and A. Vespignani. Multiscale mobility networks and the spatial spreading of infectious diseases. *Proc. Natl. Acad. Sci.*, 106:21484–21489, 2009.
- [13] F. Ball and P. Neal. A general model for stochastic SIR epidemics with two levels of mixing. *Math. Biosc.*, 180:73–102, 2002.
- [14] F. Ball and P. Neal. Network epidemic models with two levels of mixing. *Math. Biosci.*, 212:69–87, 2008.
- [15] B. Ballobás. *Random graphs*. Academic Press, New York, 2nd edition, 2001.
- [16] A. L. Barabási and R. Albert. Emergence of scaling in random networks. *Science*, 286:509–512, 1999.
- [17] A.-L. Barabási and R. Albert. Statistical mechanics of complex networks. *Science*, 286:509–512, 1999.
- [18] A. Barrat, M. Barthélemy, and Vespignani A. *Dynamical Processes on Complex Networks*. Cambridge University Press, New York, NY, USA, 1st edition, 2008.

- [19] A. Barrat and M. Weigt. On the properties of small-world network models. *Eur. Phys. J. B*, 13:547–560, 2000.
- [20] M. Barthélemy, A. Barrat, R. Pastor-Satorras, and A. Vespignani. Velocity and hierarchical spread of epidemic outbreaks in scale-free networks. *Phys. Rev. Lett.*, 92:178701, Apr 2004.
- [21] H. Bierman Jr. *An Introduction to Accounting and Managerial Finance: A Merger of Equals*. World Scientific, Singapore, 2010.
- [22] H. Bierman Jr. *An Introduction to Accounting and Managerial Finance: A Merger of Equals*. World Scientific, Singapore, 2010.
- [23] D. G. Blanchflower, A. J. Oswald, and B. Landeghem. Imitative obesity and relative utility. *J. Eur. Econ. Assoc.*, 7:528–538, 2009.
- [24] M. Boguñá and R. Pastor-Satorras. Epidemic spreading in correlated complex networks. *Phys. Rev. E*, 66:047104, 2002.
- [25] B. Bollobás and O. Riardon. The diameter of a scale-free random graph. *Combinatorica*, 25:5–34, 2004.
- [26] B. Bollobás and O. Riordan. Robustness and vulnerability of scale-free random graphs. *Internet Math*, 1:1–35, 2003.
- [27] J. A. Bondy and U. S. R. Murty. *Graph Theory with applications*. The MacMillan Press LTD, London, 1st edition, 1976.
- [28] M. Boots and A. Sasaki. ‘small worlds’ and the evolution of virulence: infection occurs locally and at a distance. *Proc. R. Soc. Lond. B*, 266:1933–1938, 1999.

- [29] L. P. Boss. Epidemic hysteria: a review of the published literature. *Epidemiol. Rev.*, 19:233–243, 1997.
- [30] D. Brockmann, L. Hufnagel, and T. Geisel. The scaling laws of human travel. *Nature*, 439:462–465, 2006.
- [31] R. Carvalho and G. Iori. Socioeconomic networks with long-range interactions. *Phys. Rev. E*, 78(1):016110, Jul 2008.
- [32] D. Chakrabarti, Y. Wang, C. Wang, J. Leskovec, and C. Faloutsos. Epidemic thresholds in real networks. *ACM Trans. Inf. Syst. Sec.*, 10:13, 2002.
- [33] N. A. Christakis and J. H. Fowler. The spread of obesity in a large social network over 32 years. *New Engl. J. Med.*, 357(9):370–379, 2007.
- [34] A. Clauset, C. R. Shalizi, and M. E. J. Newman. Power-law distributions in empirical data. *SIAM Rev.*, 51(4):661–703, November 2009.
- [35] T. Cohen, C. Colijn, B. Finklea, and M. Murray. Exogenous re-infection and the dynamics of tuberculosis epidemics: local effects in a network model of transmission. *J. R. Soc. Interface*, 4(14):523–531, 2007.
- [36] E. Cohen-Cole and J. M. Fletcher. Is obesity contagious? social networks vs. environmental factors in the obesity epidemic. *J. Health Econ.*, 27:1382–1387, 2008.
- [37] V. Colizza, A. Barrat, M. Barthelemy, and A. Vespignani. The modeling of global epidemics: stochastic dynamics and predictability. *Bull. Math. Biol.*, 68:1893–1921, 2006.

- [38] V. Colizza, A. Barrat, M. Barthelemy, and A. Vespignani. The role of the airline transportation network in the prediction and predictability of global epidemics. *Proc. Natl. Acad. Sci.*, 103:2015–2020, 2006.
- [39] D. Cvetkovic and P. Rowlinson. The largest eigenvalue of a graph—a survey. *Algebra*, pages 3–33, 1990.
- [40] G. F. Davis, M. Yoo, and W. E. Baker. The small world of the american corporate elite. *Strategic Org.*, 1:301–326, 2003.
- [41] G. F. Davis, M. Yoo, and W. E. Baker. The small world of the corporate elite. *Strategic Organization*, 1:301–326, 2003.
- [42] S. N. Dorogovtsev. *Lectures on Complex Networks*. Oxford University Press, Oxford, 2nd edition, 2010.
- [43] S. N. Dorogovtsev, J. F. F. Mendes, and A. N. Samakhin. Structure of growing networks with preferential linking. *Phys. Rev. Lett.*, 85:4633–4636, 2000.
- [44] H.-P. Duerr, M. Schwehm, C. C. Leary, S. J. De Vlas, and M. Eichner. An algorithm for identifying “who transmits to whom” in outbreaks of interhuman transmitted infectious agents. *Epidemiol. Infect.*, 135:1124–1132, 2007.
- [45] K. T. D. Eames, J. M. Read, and W. J. Edmunds. Dynamic social networks and the implications for the spread of infectious disease. *J. R. Soc. Interface*, 5(26):1001–1007, 2008.
- [46] P. Erdős and A. Rényi. On random graphs. *Publ. Math. (Debrecen)*, 6:290–297, 1959.

- [47] P. Erdős and A. Rényi. On the evolution of random graphs. *Publicationes Mathematicae*, 6:290–297, 1959.
- [48] P. Erdős and A. Rényi. On the evolution of random graphs. *Bull. Inst. Int Stat*, 38:343, 1961.
- [49] E. Estrada. Characterization of 3d molecular structure. *Chem. Phys. Lett.*, 319:713–718, 2000.
- [50] E. Estrada. Generalization of topological indices. *Chem Phys Lett*, 336:248–252., 2001.
- [51] E. Estrada. Quantifying network heterogeneity. *Phys. Rev. E*, 82:066102, 2010.
- [52] E. Estrada. *The Structure of Complex Network: Theory and Applications*. Oxford University Press, Oxford, 1st edition, 2011.
- [53] E. Estrada and N. Hatano. Statistical-mechanical approach to subgraph centrality in complex networks. *Chem. Phys. Lett.*, 439:247–251, 2007.
- [54] E. Estrada and N. Hatano. Communicability in complex networks. *Phys. Rev. E*, 77(3):036111, 2008.
- [55] E. Estrada, N. Hatano, and M. Benzi. The physics of communicability in complex networks. *CoRR*, abs/1109.2950, 2011.
- [56] E. Estrada, F. Kalala-Mutombo, and A. Valverde-Colmeiro. Epidemic spreading in networks with nonrandom long-range interactions. *Phys. Rev. E*, 84:036110, 2011.
- [57] E. Estrada and J. A. Rodríguez-Velázquez. Subgraph centrality in complex networks. *Phys. Rev. E*, 71(5):056103, 2005.

- [58] S. Eubank, H. Guclu, V. S. Anil Kumar, M. V. Marathe, A. Srinivasan, Z. Toroczkai, and N. Wang. Modelling disease outbreaks in realistic urban social networks. *Nature*, 429:180–184, 2004.
- [59] M. Faloutsos, P. Faloutsos, and C. Faloutsos. On power-law relationship of the internet topology. *ACM SIGCOM*, 1999.
- [60] A. Fronczak, P. Fronczak, and J. A. Holyst. Average path length in random networks. *Phys. Rev. E.*, 70:056110, 2004.
- [61] O. Galor. Introduction to stability analysis of discrete dynamical systems. (0409011), 2004.
- [62] P. Gleiser and L. Danon. Community structure in jazz. *Adv. Compl. Syst.*, 6:565–573, 2003.
- [63] S. Gómez, A. Arenas, J. Borge-Holthoefer, S. Meloni, and Y. Moreno. Probabilistic framework for epidemic spreading in complex network. *Int. J. Complex Systems in Sciences*, 89:38009, 2010.
- [64] S. Gómez, A. Arenas, J. Borge-Holthoefer, S. Meloni, and Y. Moreno. Discrete-time markov chain approach to contact-based disease spreading in complex networks. *Europhys. Lett.*, 1:47–54, 2011.
- [65] M. C. González, C. A. Hidalgo, and A.-L. Barabási. Understanding individual human mobility patterns. *Nature*, 543:779–782, 2008.
- [66] G. R. Grimmett and D. R. Stirzaker. *Probability and random processes*. The Clarendon Press Oxford University Press, New York, second edition, 1992.
- [67] P. Grindrod. Range-dependent random graphs and their application to modeling large small-world proteome datasets. *Phys. Rev. E.*, 66:066702, 2002.

- [68] P. Horby, Q. T. Pham, N. Hens, Q. M. Nguyen, T. T. Le, D. T. Dang, M. L. Nguyen, T. H. Nguyen, N. Alexander, W. J. Edmunds, N. D. Tran, A. Fox, and T. H. Nguyen. Social contact patterns in vietnam and implications for the control of infectious diseases. *PloS Medicine*, 6:e16965, 2011.
- [69] M. O. Jackson and A. Wolinsky. A strategic model of social and economic networks. *J. Econ. Theor.*, 71:44–74, 1996.
- [70] M. O. Jackson and A. Wolinsky. A strategic model of social and economic networks. *Journal of Economic Theory*, 71(1):44–74, 1996.
- [71] H. Jeong, B. Tomobor, R. Albert, N. Oltvai, and A.-L. Barabási. The large-scale organization of metabolic networks. *Nature*, 470:605, 2000.
- [72] M. J. Keeling and K. T. D. Eames. Networks and epidemic models. *J. R. Soc. Interface*, 2:295–307, 2005.
- [73] J. O. Kephart and S. R. White. Measuring and modelling computer virus prevalence. In *Proceedings of the 1993 IEEE Computer Society Symposium on Research in Security and Privacy*, pages 2–15, 1993.
- [74] J. Kleinberg. The small-world phenomenon: an algorithmic perspective. *Proc. 32nd ACM Symp. Theor. Comput.*, 2000a.
- [75] K. Klemm and V. M. Eguíluz. Growing scale-free networks with small-world behavior. *Phys. Rev. E.*, 65:57102, 2002b.
- [76] J. Knobon and L. A. G. Oerlemans. Proximity and inter-organization: A literature review. *Int. J. Manag. Rev.*, 8:71–89, 2006.

- [77] L. Kocarev and U. Parlitz. Generalized synchronization, predictability, and equivalence of unidirectionally coupled dynamical systems. *Phys. Rev. Lett.*, 76:1816–1819, 1996.
- [78] A. L. Lloyd and Robert M. M. How viruses spread among computers and people. *Science*, 292(520):1316–1317, 2001.
- [79] I. M. Longini Jr., J. S. Koopman, A. S. Monto, and J. P. Fox. Detecting human-to-human transmission of avian influenza a H5N1. *Am. J. Epidemiol*, 115:736–, 1982.
- [80] K. Malarz, J. Karpinska, A. Kardas, and K. Kulakowski. Node-node distance distribution for growing networks. *e-print arXiv:cond-mat/0309255v2*.
- [81] J. H. Manson. Mating patterns, mate choice, and birth season heterosexual relationships in free-ranging rhesus macaques. *Primates*, 35:417–433, 1994.
- [82] M. Marchiori and V. Latora. Harmony in the small-world. *Physica A*, 285, 200.
- [83] M. Marchiori and V. Latora. Efficient behavior of small-world networks. *Phys. rev. lett.*, 87(19), 2001.
- [84] M. McPherson, L. Smith-Lovin, and J. M. Cook. Birds of a feather: Homophily in social networks. *Annu. Rev. Sociol*, 27:415–444, 2001.
- [85] S. Meloni, A. Arenas, and Y. Moreno. Traffic-driven epidemic spreading in finite-size scale-free networks. *Proc. Natl. Acad. Sci.*, 106:16897–16902, 2009.
- [86] Carl D. Meyer. *Matrix analysis and applied linear algebra*. SIAM, USA, 1st edition, 2000.

- [87] S. Milgram. The small world problem. *Psychology Today*, 2, 1967.
- [88] D. Mollison. The structure of epidemic models. In *Epidemic Models: Their Structure and Relation to Data*, pages 17–33. Cambridge University Press, Cambridge, 1975.
- [89] C. Moore and M. E. J. Newman. Epidemics and percolation in small-world networks. *Phys. Rev. E*, 61:5678–5682, 2000.
- [90] Y. Moreno, R. Pastor-Satorras, and Vespignani A. Epidemic outbreaks in complex heterogeneous networks. *Eur. Phys. J.*, 26:521–592, 2010.
- [91] J. Mossong, J. M. Hens, P. Beutels, K. Auranen, R. Mikolajczyk, M. Massari, S. Salmaso, G. Scalia Tomba, J. Wallinga, J. Heijne, M. Sadkowska-Todys, M. Rosinka, and W. J. Edmunds. Social contacts and mixing patterns relevant to the spread of infectious diseases. *PloS Medicine*, 5:e74, 2008.
- [92] M. E. J. Newman. Scientific collaboration networks. II. shortest paths, weighted networks, and centrality. *Phys. Rev. E*, 64:016132, 2001.
- [93] M. E. J. Newman. *Networks: An Introduction*. Oxford University Press, Oxford, 2nd edition, 2011.
- [94] M. E. J. Newman. The structure and function of complex networks. *SIAM Rev.*, 45, 2011.
- [95] M. E. J. Newman, I. Jensen, and R. M. Ziff. Percolation and epidemics in a two-dimensional small world. *Phys. Rev. E*, 65:021904, 2002.
- [96] M. E. J. Newman and D. J. Watts. Scaling and percolation in the small-world network model. *Phys. Rev. E*, 60:7332–7342, 1999.

- [97] F. Ninio. A simple proof of the perron-frobenius theorem for positive symmetric matrices. *J. Phys. A: Math. and Gen.*, 10(7):1259, 1977.
- [98] R. Olfati-Saber and Richard M. Murray. Consensus problems in networks of agents with switching topology and time-delays. *IEEE TRANSACTIONS ON AUTOMATIC CONTROL*, 49, 2004.
- [99] P. Ormerod and G. Wiltshire. 'binge' drinking in the uk: a social network phenomenon. *Mind and Soc.*, 8:135–152, 2009.
- [100] A. Papoulis. *Probability, random variables, and stochastic processes*. McGraw-Hill Series in Electrical Engineering. Communications and Information Theory. McGraw-Hill Book Co., New York, second edition, 1984.
- [101] R. Pastor-Satorras and A. Vespignani. Epidemic spreading in scale-free networks. *Phys. Rev. Lett.*, 86(14):3200–3203, 2001.
- [102] R. Pastor-Satorras and A. Vespignani. *Internet: structure et Evolution*. Belin Editeur., Paris, 2004.
- [103] L. M. Pecora and T. L. Carroll. Synchronization in chaotic systems. *Phys. Rev. Lett.*, 64:821–824, 1990.
- [104] S. Peng, C. Xian-bin, D. Wen-bo, and C. Cai-long. The effect of geographical distance on epidemic spreading. *Physics Procedia*, 3(5):1811–1818, 2010. The International Conference on Complexity and Interdisciplinary Sciences. The 3rd China-Europe Summer School on Complexity Sciences.
- [105] A. Pikovsky, M. Rosenblum, and J. Kurths. Phase synchronization in regular and chaotic systems: a tutorial. *Internat. J. Bifur. Chaos*, 10:2291–2305, 1999.

- [106] B. J. Pettejohn, M. J. Berryman, and M. D. McDonnell. Methods for generating complex networks with selected structural properties for simulations: A review and tutorial for neuroscientists. *Front. Comput. Neurosci.*, 5(00011), 2011.
- [107] D. J. Price. Networks of science papers. *Science*, 149:510–515, 1965.
- [108] A. Rapoport. Spread of information through a population with socio-structural bias i. assumption of transitivity. *Bull. Math. Biophys.*, 15:523–533, 1953.
- [109] A. Rapoport. Spread of information through a population with socio-structural bias ii. various models with partial transitivity. *Bull. Math. Biophys.*, 15:533–546, 1953.
- [110] A. Rapoport. Spread of information through a population with socio-structural bias iii. suggested experimental procedures. *Bull. Math. Biophys.*, 16:75–81, 1954.
- [111] A. Rapoport and W. Horvath. A study of a large sociogram. *Behav. Sci.*, 2:79–91, 1961.
- [112] S. F. Reardon and G. Firebaugh. Measures of multigroup segregation. *Social. Methodology*, 32:33–67, 2002.
- [113] S. Riley. Large-scale transmission model of infectious diseases. *Science*, 68:1298–1301, 2007.
- [114] M. D. Ryall and O. Soreson. Brokers and competitive advantage. *Manag. Sci.*, 53:566, 2007.

- [115] D. M. Skowronski, C. Astell, R. C. Brunham, D. E. Low, M. Petric, R. L. Roper, P. J. Talbot, T. Tam, and L. Babiuk. Severe acute respiratory syndrome SARS: a year in review. *Annu. Rev. Med.*, 56:357–381, 2005.
- [116] S. H. Strogatz. Exploring complex networks. *Nature*, 410:268–276, 2001.
- [117] J. Travers and S. Milgram. An experimental study of the small world problem. *Sociometry*, 32(4):425–443, 1969.
- [118] P. N. V. Tu. *Dynamical Systems*. Springer-Verlag, Berlin, 2nd edition, 1994.
- [119] J. Verdasca. Short and long-term dynamics of childhood diseases on dynamic small-world networks. *In BioMat2005. Proc. Int. Symp. Math. Comput. Biol., Ed. R. P. Mondani and R. Dilo, World Sci. pub. Co., page p. 171., 2006.*
- [120] F. Viger and M. Latapy. *Efficient and simple generation of random simple connected graphs with prescribed degree sequence*. In The Eleventh International Computing and Combinatorics Conference, Springer, Berlin, 2005.
- [121] S. Wasserman and K. Faust. *Social network analysis*. Cambridge University Press, Cambridge, 1194.
- [122] D. J. Watts. Small world: The dynamic of networks between order and randomness. *The American Mathematical Monthly*, 107(7):664–668, 2000.
- [123] D. J. Watts and S. H. Strogatz. Collective dynamic of small-world networks. *Nature*, 393:440–442, 1998.
- [124] H. Yang and S. Zhang. Viruses epidemics of avian influenza based on complex networks. *Journal of System Simulation*, 20:5001–5005, 2008.

- [125] G. U. Yule and M. G. Kendall. *An Introduction to the Theory of Statistics*. Charles Griffin and Co, 14th edition (5th impression 1968) edition, 1950.